Taxonomy and Phylogeny of Cotylea (Platyhelminthes: Polycladida) from Japan

日本産吸盤亜目ヒラムシ類（扁形動物門：多岐腸目）の系統分類学的研究

Aoi Tsuyuki

A Ph.D. dissertation presented

to

Department of Natural History Sciences,

Graduate School of Science,

Hokkaido University,

Sapporo

060-0810

in

March 2023

This dissertation is based on the following papers:

Chapter II-1

1. Tsuyuki A, Oya Y, Kajihara H. 2022b. Reversible shifts between interstitial and epibenthic habitats in evolutionary history: molecular phylogeny of the marine flatworm family Boniniidae (Platyhelminthes: Polycladida: Cotylea) with descriptions of two new species. PLoS ONE 17: e0276847.

Chapter II-3

2. Tsuyuki A, Oya Y, Jimi N, Kajihara H. 2020a. Description of *Pericelis flavomarginata* sp. nov. (Polycladida: Cotylea) and its predatory behavior on a scaleworm. Zootaxa 4894(3): 403–412.

3. Tsuyuki A, Oya Y, Kajihara H. 2022c. Two new species of the marine flatworm *Pericelis* (Platyhelminthes: Polycladida) from southwestern Japan, with an amendment of the generic diagnosis based on phylogenetic inference. Marine Biology Research 17(9–10): 946–959.

Chapter II-4

4. Tsuyuki A, Oya Y, Kajihara H. 2020b. First record of *Stylostomum ellipse* (Dalyell, 1853) (Platyhelminthes, Polycladida) from the Pacific Ocean. Check List 16(3): 773–779.

Chapter II-5

5. Tsuyuki A, Oya Y, Kajihara H. 2019. A new species of *Prosthiostomum* (Platyhelminthes: Polycladida) from Shirahama, Japan. Species Diversity 24(2): 137–143.

6. Tsuyuki A, Kajihara H. 2020. A giant new species of *Enchiridium* (Polycladida, Prosthiostomidae) from southwestern Japan. ZooKeys 918: 15–28.

7. Tsuyuki A, Kohtsuka H, Kajihara H. 2021. Description of a new species of the marine flatworm *Prosthiostomum* (Platyhelminthes: Polycladida) and its three known congeners from Misaki, Japan, with inference of their phylogenetic positions within Prosthiostomidae. Zoological Studies 60(29): 1–20.

Chapter II-6

8. Tsuyuki A, Kohtsuka H, Hookabe N, Kajihara H. 2022a. First record of *Bulaceros porcellanus* Newman & Cannon, 1996 (Platyhelminthes, Polycladida, Cotylea) from Japanese waters, with a revision of the generic diagnosis based on morphology and molecular phylogeny. Plankton and Benthos Research 17(2): 147–155.

ACKNOWLEDGEMENTS

I am deeply grateful to my supervisor Prof. Hiroshi Kajihara for his help and guidance during my master's and doctoral research. Dr. Keiichi Kakui is acknowledged for his useful advice in my research. I also thank Prof. Kazuhiro Kogame, Prof. Hiroshi Kajihara, and Dr. Keiichi Kakui for reviewing this thesis and providing valuable comments.

I deeply thank Dr. Yuki Oya for the helpful guidance and supports of polyclad taxonomy in Japan.

I have been helped by innumerable people in sampling and collecting specimens. I am thankful to Dr. Naoto Jimi, Dr. Yuki Oya, Mr. Hisanori Kohtsuka, Dr. Daisuke Uyeno, Dr. Shinta Fujimoto, Ms. Natsumi Hookabe, Mr. Naohiro Hasegawa, Prof. Toru Miura, Dr. Kohei Ogushi, Dr. Hiroki Kise, Ms. Midori Matsuoka, Dr. Seiji Arakaki, Prof. Mutsunori Tokeshi, Dr. James Reimer, Dr. Gaëlle Quéré, Dr. Angelo Poliseno, Dr. Yuka Kushida, Dr. Guin Yee Soong, Dr. Takuma Fujii, Dr. Shinri Tomioka, Mr. Haruki Ishiyama, Mr. Shoki Shiraki, Prof. Masato Kiyomoto, Dr. Hiroaki Nakano, Ms. Mayuko Nakamura and the staffs at Akkeshi Marine Station, Misaki Marine Biological Station, Noto Marine Laboratory, Oshoro Marine Station, Seto Marine Biological Laboratory, Kuroshio Biology Research Institute, Ishigaki Sensui Do for assistance in sampling.

I am also grateful to Prof. Marco Curini-Galletti, Prof. Sigmer Quiroga, and Dr. Christopher Edward Laumer for providing helpful information. Dr. Carolina Noreña, Dr. Daniel Marquina, Mr. Jorge Rodriguez Monter, Dr. Stephen Keable, Dr. Geoff Thompson, Dr. Mal Bryant, Dr. Sue-Ann Watson, Dr. Robyn Cumming, and Dr. Terry

Miller are acknowledged for arrangement of the histological photomicrographs of the type series.

This study was supported by the Research Institute of Marine Invertebrates (FY 2019), Kuroshio Biology Research Institute (FY 2018 for Aoi Tsuyuki), Japan Science and Technology Agency SPRING (No. JPMJSP2119), and Japan Society for the Promotion of Science (JSPS) under KAKENHI grant number 22J13246, and the Japanese Association for Marine Biology (JAMBIO). I am deeply grateful to financial support by JST and JSPS. Special thanks to my family, friends, and Biodiversity 1 members for kind supports.

TABLE OF CONTENTS

LIST OF FIGURES

LIST OF TABLES

I. GENERAL INTRODUCTION

Order Polycladida

The order Polycladida is a group of free-living dorsoventrally flattened flatworms that are most commonly found in the littoral zone among platyhelminths. Recent phylogenetic analyses support the monophyly of the phylum Platyhelminthes, within which Polycladida is reciprocally monophyletic to another order Prorhynchida (or Lecithoepitheliata) (Egger et al. 2015, Laumer et al. 2015). This clade (Polycladida + Prorhynchida/Lecitoepitheliata) represents the third earliest-branching lineage following the first and second earliest-branching taxa Catenulida and Macrostomorpha; at the same time, it is sister to the rest of the phylum, including Rhabdocoela, Proseriata, Tricladida, Bothrioplanida, and Neodermata (Monogenea, Cestoda, and Trematoda) (Egger et al. 2015, Laumer et al. 2015). Polyclads are characterized by *i*) a dorsoventrally flattened body, *ii*) a plicate pharynx opening into a main intestine with numerous branches radiating to the body margin and spreading all over the body, *iii*) the nervous system with numerous radiating nerve cords, *iv*) numerous ovaries and testis scattered all over the body, *v*) absence of yolk glands, and *vi*) the habitat in almost exclusively sea waters (Hyman 1951). To date, all species are known as simultaneous hermaphrodite.

Currently, Polycladida contains more than 800 species distributed worldwide (Tyler et al. 2006–2022), which are divided into two suborders Acotylea and Cotylea. The two suborders are basically classified by the absence or presence of the ventral adhesive organs located posterior to the female reproductive organ (Faubel 1983, Prudhoe 1985).

Morphology

Body shape and coloration

Polyclads have relatively large size, ranging from 2 mm to 15 cm (Prudhoe 1985). The shape of body is variable depending on taxa, ranging from oval to ribbon-like elongated. Most species have translucent coloration without any pigments on dorsal surface, but in particular taxa such as Pseudocerotidae Lang, 1884 and Euryleptidae Stimpson, 1857, conspicuous color patterns can be observed (Newman and Cannon 1994); some color morphs are considered as warning signals for predators (Ang and Newman 1998) or mimic to nudibranchs (Newman et al. 1994). The ventral surface is usually without any coloration. Some species such as in *Acanthozoon* Collingwood, 1876 and *Thysanozoon* Grube, 1840 in Pseudocerotidae have numerous papillae on the dorsal surface.

Sense organs

Some species have a pair of tentacles being separated into three types: *i*) nuchal tentacles near the cerebral organ on the dorsal surface, *ii*) marginal tentacles extended from anterior sides of the body periphery, and *iii*) pseudotentacles that are formed by folds of anterior margin of the body. In addition, the shape of the pseudotentacles could vary *i*) simple, *ii*) ear-like, *iii*) knobbed, and *iv*) square-shaped among pseudocerotid genera (Newman and Cannon 1996a).

Almost all species have eyespots except for a few bathyal species (cf. Oya and Kajihara 2019). The eyespots are categorized into six types based on their positions: *i*) cerebral eyespots located near the brain, *ii*) marginal or sub-marginal eyespots situated along the body periphery, *iii*) frontal eyespots distributed between cerebral and anterior

marginal ones, *iv*) ventral eyespots on the ventral side, *v*) tentacular eyespots within or beneath tentacles, or, on the assumed place of tentacles when tentacles are absent, and *vi*) pseudotentacular eyespots within pseudotentacles.

Digestive systems

The digestive system is composed of the mouth, the pharynx, and the intestine with numerous branches. The mouth is located generally on body center, but also situated on more anteriorly or posteriorly in several taxa. The pharynx is plicated, muscularized, lying within the pharyngeal chamber. The ruffled or tubular pharynx is observed in polyclads; the difference in the shape is one of the diagnostic characters for some families. Polyclad flatworms capture preys by using pharynx extended from the mouth (e.g., Newman et al. 2000, Merory and Newman 2005).

Copulatory apparatuses

Male and female copulatory apparatuses are usually used as diagnostic characters for superfamily, family, genus, and species. The male copulatory apparatus is basically composed of the sperm ducts, the seminal vesicle, the prostatic vesicle, and the penis papilla or cirrus. The sperm ducts are usually present as a pair, running on both sides of the body midline, connecting into the seminal vesicle independently or via the common sperm duct. The seminal vesicle is a heavily muscularized organ to store sperms before being ejected. The prostatic vesicle is a secretory organ releasing substances that are presumed to maintain sperm activity; in some taxa, this organ is totally lacking or substituted by modified prostatoid organs. The penis papilla is a muscular projection of the ejaculatory duct, which has sometimes a cuticularized stylet. The cirrus is observed

in some acotyleans such as Planoceridae Lang, 1884 and Gnesiocerotidae Du Bois Reymond Marcus and Marcus, 1966. This organ is formed by a muscular bulb of which inner wall is lined with teeth, spines, or other particles. It functions as an intromittent organ by getting everted outside through the male gonopore.

The female copulatory apparatus is basically composed of the oviduct and the vagina. The oviduct is usually present as a pair of tubes, running on both sides of the body midline leading to the vagina; each oviduct possesses uterine vesicle(s) in some cotyleans. When a part of the oviduct is packed with oocytes, that part becomes the uterus. The proximal duct of the vagina after the joints of the oviducts sometimes forms *i*) a Lang's vesicle, *ii*) a ductus vaginalis, or *iii*) a ductus genito-intestinalis. The Lang's vesicle is lined with tall epithelium, varying in shape as bulbous, elongate, crescent, or Y-shaped, which terminates the proximal end of vagina. The ductus vaginalis continues proximally, then either opens to the ventral surface independent of the female gonopore or recurves and enters the vagina. The ductus genito-intestinalis connects to the intestine. The vagina leads to female atrium; in most cotyleans, the female atrium forms cement pouch within which cement glands release their secretion. In some acotyleans, bursa copulatorix is present as a blind muscular sac connecting to the part of vagina before the joint with the oviduct.

Adhesive organs

Some polyclad species have adhesive organs on the ventral surface. The following three types are currently recognized: *i*) the true sucker for most cotyleans, *ii*) the adhesive disc for Boniniidae Bock, 1923 and Cestoplanidae Lang, 1884, and *iii*) the genital sucker for a few species in acotyleans (Prudhoe 1985). The former two organs are

located posterior to the female gonopore whereas the latter one is between the male and female gonopores. The true sucker is composed of specialized epithelium and a thick muscular lamella which might function as retractor muscles. The adhesive disc is a shallow depression covered by the specialized epithelium for adhesion without muscular lamella. The genital sucker is a depression covered by a thickening of the body musculature (Prudhoe 1985).

Habitat

Most polyclad flatworms are known to live in shallow marine waters. The vertical distributions range from intertidal to a depth of 3,232 m (Quiroga et al. 2006). A few species have also been found from brackish waters (Stummer-Traunfels 1902, Kaburaki 1918). Polyclads are almost exclusively benthic except for a few pelagic species (Palombi 1924) and commonly found on undersurfaces of rocks, coral rubbles, sea weeds, and sunken woods in the deep sea; a few tiny species are living among sand particles (e.g., Curini-Galletti et al. 2008). Some species are also known to associate with other invertebrates such as corals (e.g., Rawlinson et al. 2011), gorgonians (e.g., Cannon 1990), hermit crabs (e.g., Lytwyn and McDermott 1976), mantis shrimps (Oya et al. 2022), innkeeper worms (e.g., Anker et al. 2005), gastropods (e.g., Fujiwara et al. 2014), and chitons (Kato 1935).

Most polyclads are carnivorous and attack other invertebrates such as corals (Rawlinson et al. 2011), small crustaceans (e.g., Jie et al. 2013), mollusks (e.g., Lee et al. 2006, Dittmann et al. 2019b), and ascidians (e.g., Newman et al. 2000). Some of them use the deadly neurotoxin tetrodotoxin (TTX) to capture mobile prey (Ritson-Williams et al. 2006).

Reproduction and Development

Mating behavior

Polyclads obligately practice internal fertilization of the primary oocytes. To date, self-fertilization and asexual reproduction have never been known. The insemination can be reciprocal by direct copulation or unilateral by indirect copulation (cf. Rawlinson et al. 2008). In the direct copulation, a flatworm exchanges its sperm with a partner reciprocally. The indirect copulatory behavior is categorized into *i*) dermal impregnation and *ii*) hypodermic insemination. In the dermal impregnation, the animal deposits its spermatophores onto the surface of the partner; the sperms would be absorbed through the epidermis, and then reach the eggs of the partner (Gammoudi et al. 2011). In the hypodermic insemination, the animal injects an armed penis into the partner's body surface; polyclads can take on the male sexual role as only depositing the sperm bundle, the female sexual role as only receiving the sperm bundle, or the both roles (Tong and Ong 2020). Although the 'penis fencing' has been often observed as precopulatory behavior before the hypodermic insemination (Michiels and Newman 1998), a recent study shows that it is not necessary and could be just a mating ritual (Tong and Ong 2020).

Embryonic development

Among platyhelminths, Polycladida is unique in retaining certain developmental characteristics such as entolecithal eggs and spiral cleavage, sharing with other spilarians (cf. Lapraz et al. 2013). Both direct and indirect development have been known in polyclads; the direct development does not involve metamorphosis of the

hatched juveniles, only found in acotyleans; the indirect development involves metamorphosis to the Müller's, Götte's or Kato's larvae, found in cotyleans and a few acotyleans (Gammoudi et al. 2011).

Suborder Cotylea

The suborder Cotylea is an assemblage of polyclad flatworms that is basically characterized by having muscular sucker or adhesive pad. In addition, the pseudotentacles or marginal tentacles as well as the male copulatory apparatus directed forward are exclusively observed in cotyleans. Traditionally, this suborder included the following 14 families: Amyellidae Faubel, 1984; Anonymidae Lang, 1884; Boniniidae; Chromoplanidae Bock, 1922; Dicteroidae Faubel, 1984; Diposthidae Woodworth, 1898; Euryleptidae; Euryleptididae Faubel, 1984; Laidlawiidae Hallez, 1913; Opsthogeniidae Palombi, 1928; Pericelidae Laidlaw, 1902; Prosthiostomidae; Pseudocerotidae Lang, 1884; and Stylochoididae Bock, 1913, based on the presence of a ventral adhesive structure (Faubel 1984). Recent phylogenetic studies (Bahia et al. 2017, Dittmann et al. 2019a, Litvaitis et al. 2019) support that the two families Cestoplanidae and Theamatidae should be transferred into Cotylea from Acotylea based on their phylogenetic positions being nested within other cotylean families. Also, I treat the family Diposthidae as a taxon including all pericelid species in addition to diposthids, and Pericelidae as invalid in accordance with Litvaitis et al. (2019). Therefore, 15 families are currently recognized in this suborder.

Systematics and phylogenetics

The classification within Cotylea is still contradicted between researchers. Traditionally,

according to Faubel (1984), the cotylean families were considered to comprise two superfamilies, Euryleptoidea Stimpson, 1857 and Pseudocerotoidea Lang, 1884, based on the morphology of pharynx (tubular or ruffled). Bahia et al. (2017) conducted a molecular phylogenetic analysis using partial sequences of 28S ribosomal DNA (28S) and showed that these two superfamilies were not monophyletic reciprocally. Bahia et al. (2017) proposed five superfamilies based on the phylogenetic result: Cestoplanoidea Poche, 1926; Periceloidea Laidlaw, 1902; Chromoplanoidea Bock, 1922; Prosthiostomoidea Lang, 1884; Pseudocerotoidea Lang, 1884. Later, Dittmann et al. (2019a) reconstructed phylogenetic trees based on alignment data of 28S as well as a combined dataset using 18S ribosomal DNA (18S) and 28S, involving Anonymiidae in addition to the eight cotylean families included in Bahia et al. (2017). They supported the view of Bahia et al. (2017) in terms of Periceloidea, Cestoplanoidea, and Prosthiostomoidea, but abolished Chromoplanoidea *sensu* Bahia et al. (2017) and established Anonymoidea and Boniniioidea (Table 1). In contrast, based on the phylogenetic results using solely 28S sequences involving Diposthidae in addition to the taxa in Bahia et al. (2017), Litvaitis et al. (2019) did not consider any superfamilies as valid (Table 1). In this paper, I generally follow the taxonomic scheme of Litvaitis et al. (2019). Most of the families seem to be monophyletic based on molecular phylogeny except for Euryleptidae (Bahia et al. 2017, Dittmann et al. 2019a, Litvaitis et al. 2019). To revise the Euryleptidae, Dittmann et al. (2019a) established a new family, Stylostomidae, for a clade composed of *Stylostomum ellipse* (Dalyell, 1853), *Euryleptodes galikias* Noreña et al., 2014, and *Cycloporus gabriellae* Marcus, 1950, which were separated from other euryleptid species of *Maritigrella* Newman and Cannon, 2000 and *Prostheceraeus* Schmarda, 1859, in addition to *Cycloporus*

variegatus Kato, 1934 and *C. japonicus* Kato, 1944, in their results. In this thesis, however, the family Stylostomidae is not employed because it was so unclearly diagnosed that some species cannot be included in this taxon with certainty.

Within each family, the phylogenetic relationships between some genera still remain unclear due to lack of taxon coverage. Of the 10 families included in recent phylogenetic studies, all families except for Theamatidae did not contain all the constituent genera (Bahia et al. 2017, Dittmann et al. 2019a, Litvaitis et al. 2019).

In addition, DNA barcoding is not proceeding in most polyclad species although it is effective to reveal the actual species diversity by making species identifications more easily available, by helping to reveal cryptic species, and by clarifying taxonomic problems of synonyms (Hebert and Gregory 2005). Prior to my study, there were a few studies to evaluate genetic distances between closely related cotylean species (e.g., Litvaitis et al. 2010, Velasquez et al. 2018). For this purpose, these authors employed partial sequences of 28S, which are supposed to have slower evolutionary rate than the standard metazoan barcode of the mitochondrial cytochrome *c* oxidase subunit I (COI) gene (Bucklin et al. 2010). Therefore, it is possible that some cryptic species may have been overlooked in these studies.

Taxonomic studies in Japan

Before I initiated my research, 72 species in 16 genera of cotylean polyclads had been recorded from Japanese waters based on actual specimens; some photograph-based occurrence records in field guidebooks (e.g., Ono 2015) that are not substantiated by voucher specimens are not counted. These were classified in the following eight families: Amyellidae, Boniniidae, Cestoplanidae, Chromoplanidae, Diposthidae,

Euryleptidae, Prosthiostomidae, and Pseudocerotidae.

Stimpson (1855) described five species from the Okinawa Islands and Kikaijima Island for the first time in Japanese waters. Subsequently, Stimpson (1857) described seven species from the Okinawa Islands, Amami Oshima Island, and Hokkaido. Later, Yeri and Kaburaki (1918, 1920) conducted faunal surveys in Kanagawa, Shizuoka, and Wakayama; 11 species were described or redescribed based on the collected specimens. Also, Kaburaki (1923) described one species from Hokkaido. During the same period, Bock (1922, 1923) also described three species from Misaki and the Ogasawara Islands. In the 1930s to 1940s, Kato conducted a comprehensive taxonomic study of Polycladida in Japan based on material from Hokkaido, Aomori, Miyagi, Niigata (Sado Island), Ishikawa (Noto Peninsula), Kanagawa (Miura Peninsula), Shizuoka (Izu Peninsula), Wakayama, and Kumamoto (the Amakusa Islands). He described almost all of the species currently known from Japan in nine papers (Kato 1934, 1937a, b, c, 1938a, b, 1939a, b, 1943a, 1944). Over 70 years later, Oya and Kajihara (2019) described a new species of *Cestoplana* from the bathyal region in Sagami Bay.

Most species originally described from Japan were questionable as to their taxonomic status and required review of their systematic positions although the Japanese coastal region is one of the most well-researched areas in terms of the polyclad fauna. Some morphological key characters for generic assignment are scarcely mentioned in the original descriptions before 1990s. Most of these species have never been recorded since they were originally described. In addition, these species cannot be confirmed based on their name-bearing type specimens because they are entirely non-existent. Stimpson's material is said to have been destroyed during the Great Chicago

Fire in 1871 (e.g., Evans 1967, Deiss and Manning 1981). The material used by Yeri and/or Kaburaki has not been found, likely because it was lost during the Great Kanto Earthquake and a subsequent disastrous fire in 1923 (cf. Kato 2018). Kato's material was destroyed during the Bombing of Tokyo in 1945 (Kawakatsu 2004). Therefore, to precisely understand the polyclad biodiversity and systematics in Japan, morphological and molecular information is needed on these species based on newly collected specimens, preferably from type localities.

There should be still a lot of undescribed/unrecorded species of Cotylea in Japan. Recent papers provided some new records of cotylean species especially in subtidal zone from southern Japan (e.g., Okuno and Naruse 2013). Some photographic evidence also show that the biodiversity is underestimated especially in the families Diposthidae, Euryleptidae, Prosthiostomidae, and Pseudocerotidae (e.g., Ono 2015). However, there have been only sparce descriptions and records of Cotylea (e.g., Hagiya and Gamô 1992, Okuno and Naruse 2013, Oya and Kajihara 2019) since Kato (1944).

Aims of This Thesis

On the basis of the current situation of taxonomic studies of Cotylea in Japan, the purposes of my thesis are four-fold:

1) To reveal the actual biodiversity of Cotylea in Japan by *i*) exploring previously unsurveyed habitats such as the interstitial environment and the subtidal zone, *ii*) providing formal descriptions based on morphology, and *iii*) examining topotypes of several species for confirmation of taxonomic affiliations,
2) To promote DNA barcoding in Cotylea by generating integrated dataset with morphological and molecular information,

3) To review part of the current classification in Cotylea based on phylogenetic results, and
4) To infer the evolutionary history of several features within subgroups in Cotylea based on molecular phylogenetic analyses.

In this thesis, I provide comprehensive studies of cotylean species belonging to six known families from Japan, Boniniidae (Chapter II-1), Cestoplanidae (Chapter II-2), Diposthidae (Chapter II-3), Eurylepidae (Chapter II-4), Prosthiostomidae (Chapter II-5), and Pseudocerotidae (Chapter II-6), in addition to the first recorded family Theamatidae (Chapter II-7).

II. TAXONOMIC AND PHYLOGENETIC STUDIES OF COTYLEA IN JAPAN

II-1. BONINIIDAE BOCK, 1923

Introduction

Animals inhabiting the space between sand and/or gravel grains have attracted the attention of biologists since the 1930s (cf. Remane 1933), primarily due to their miniaturized body size (Noodt 1974, Ax 1984, Westheide 1987, Worsaae and Kristensen 2005, Struck et al. 2015) and ecological importance (Fenchel 1978), although the existence of such tiny animals was recognized by zoologists in the 19th century (e.g., Lovén 1844, Dujardin 1851). To date, interstitial animals have been documented in at least 23 of the ~34 currently recognized metazoan phyla (Cerca et al. 2018), and different evolutionary scenarios have been proposed to explain the existence of such animals (e.g., Westheide 1987). Recent phylogenetic studies have shown that some annelid interstitial taxa had independently derived from larger epibenthic ancestors either by progenesis or stepwise miniaturization depending on the taxa (Struck et al. 2015, Worsaae et al. 2018). Additional research on these evolutionary processes has shed light on other taxa, including Enteropneusta (Hemichordata) (Worsaae et al. 2012), Acochlidiacea (Heterobranchia: Gastropoda) (Jörger et al. 2014), Rhodopemorpha (Heterobranchia: Gastropoda) (Brenzinger et al. 2013), and Ostracoda (Ha 2016); however, the vast majority of relevant animal groups have yet to be studied in this context, including the phylum Platyhelminthes and one of its constituent subtaxa, the order Polycladida.

Among polyclad flatworms, Boniniidae is interesting in terms of the evolutionary shift between noninterstitial and interstitial habitats because it harbors members that live in both environments. However, the phylogenetic inter-relationships within this family are yet to be resolved because of insufficient taxon sampling (Litvaitis et al. 2019). Boniniids are morphologically characterized by having *i*) a narrow and elongate body with a pair of pointed tentacles located at the anterolateral margins, *ii*) a male copulatory apparatus that includes an unarmed penis papilla and one or several prostatoid organ(s) with stylets, *iii*) a female copulatory apparatus with a Lang's vesicle, and *iv*) a ventral adhesive organ located at the posterior end of the body (Prudhoe 1985). Currently, seven named species of boniniids are classified into three genera: *Boninia* Bock, 1923 (5 species), *Paraboninia* Prudhoe, 1944 (1 species), and *Traunfelsia* Laidlaw, 1906 (1 species). To date, only *Boninia neotethydis* Curini-Galletti and Campus, 2007 from the Mediterranean and Red Sea has been described as a permanent interstitial representative based on adult specimens (Curini-Galletti and Campus 2007). In addition to the interstitial one, *Boninia* contains *Boninia antillara* (Hyman, 1955b); *Boninia divae* Du Bois-Reymond Marcus and Marcus, 1968; *Boninia mirabilis* Bock, 1923; and *Boninia oaxaquensis* Ramos-Sánchez et al., 2020. Morphologically, these species are distinguishable from the other two boniniids, namely *Traunfelsia elongata* Laidlaw, 1906 and *Paraboninia caymanensis* Prudhoe, 1944, by having one or more girdle(s) of prostatoid organs opening into the male atrium (Curini-Galletti and Campus 2007). Except *B. neotethydis*, the abovenamed *Boninia* species have been reported as dwellers on undersurfaces of the rocks in fully mature state (Bock 1923, Hyman 1955b, Du Bois Reymond Marcus and Marcus 1968, Ramos-Sánchez et al. 2020).

During my polyclad faunal survey in Japan, I found two undescribed species of *Boninia* on a single beach, with one species collected from an interstitial environment and the other from rock undersurfaces. From these findings, I hypothesized some evolutionary scenarios pertaining to *i*) shifts between interstitial and noninterstitial microhabitats and *ii*) settlement of the two species at the same beach. Of the conceivable hypothetical scenarios, one suggests the two interstitial species of *Boninia* (*B. neotethydis* in the Mediterranean/Red Sea and the undescribed form in Japan) being exclusively monophyletic. This "interstitial monophyly hypothesis" would be supported if adaptation from a noninterstitial to interstitial lifestyle was evolutionarily irreversible and uncommon. In another hypothesis, the last common ancestor of my two species, which could be either interstitial or noninterstitial, settled at the beach, and one of the two species subsequently changed microhabitat. This "*in situ* speciation hypothesis" would be favored if such an event was considered rare that the settlement of two closely related species (i.e., in the same genus) at a single beach happened twice independently.

Overall, the aims of this section were to *i*) provide formal taxonomic descriptions of my two *Boninia* species and *ii*) test the abovementioned hypotheses using ancestral state reconstruction analysis based on a molecular phylogenetic tree of Boniniidae.

Material and Methods

Collection of specimens and morphological observations

Specimens were collected at Nagahama Beach, Okinawa Island, Japan. Gravelly sediment samples near the edge of the water were agitated in tap water to extract

animals. The supernatant was filtered using an about 1-mm meshed dip net, and the residue was subsequently transferred into seawater. In total, six polyclads were extracted from the sediment samples. Other six polyclads crawling on undersurfaces of rocks were also collected at the sandy beach in the intertidal area. All flatworm specimens were anesthetized in a $MgCl_2$ solution prepared with tap water to match the seawater salinity using an IS/Mill-E refractometer (AS ONE, Japan), after which they were photographed using a Nikon D5600 digital camera with external strobe lightning provided by a pair of Morris Hikaru Komachi Di flash units. Each polyclad specimen was fixed and preserved using one of the four protocols shown in Table 2. All specimens were deposited in the Invertebrate Collection of the Hokkaido University Museum (ICHUM), Sapporo, Japan.

For histological examination, tissues were prestained with acid fuchsin, dehydrated in an ethanol series, cleared in xylene, embedded in paraffin wax, and sectioned serially at a thickness of 4 μm using a microtome. Sections were stained using either hematoxylin and eosin (HE) or Mallory's trichrome (MT) methods, mounted on glass slides, and then embedded in Entellan New (Merck, Germany) under cover slips. They were then observed and photographed using a Nikon D5300/5600 digital camera under an Olympus BX51 compound microscope.

DNA extraction, PCR amplification, and sequencing

Total DNA was extracted using a DNeasy Blood & Tissue Kit (Qiagen, Germany) after specimens were kept overnight at 55°C in 180 μl of ATL buffer (Qiagen, Germany) with 20 μl of proteinase K (>700 U/ml; Kanto Chemical, Japan). As a reference for DNA barcoding, a partial sequence (709 bp) of the COI gene was determined. For

phylogenetic inference, fragments of the 18S (1,758 bp) and 28S (1,014–1,015 bp) were sequenced. Amplification of the three gene markers was performed using polymerase chain reaction (PCR) via a 2720 Thermal Cycler (Applied Biosystems, USA); 10-µl reaction volumes were used, each of which contained 1 µl of total DNA template, 1 µl of 10 × ExTaq buffer (Takara Bio, Japan), 2 mM of each dNTP, 1 µM of each primer, and 0.25 U of Takara Ex Taq DNA polymerase (5 U/µl; Takara Bio, Japan) in deionized water. The forward and reverse primer pairs listed in Table 3 were used. The PCR amplification conditions were as follows: 94°C for 5 min; 35 cycles of 94°C for 30 s, 50°C (18S and COI) or 52.5°C (28S) for 30 s, and 72°C for 2 min (18S), 1.5 min (28S), or 1 min (COI); and 72°C for 7 min. PCR products were purified enzymatically using ExoSAP-IT reagent. All nucleotide sequences were determined using direct sequencing with a BigDye Terminator Kit ver. 3.1 and a 3730 Genetic Analyzer (Life Technologies, California, USA) with the primers listed in Table 3. Sequences were checked and edited using MEGA ver. 7.0 (Kumar et al. 2016). All edited sequences have been deposited in DDBJ/EMBL/GenBank (Table 2).

Phylogenetic analyses

For phylogenetic analyses, a concatenated dataset (2,685 bp) comprising partial 18S (1,739 bp) and 28S (946 bp) sequences was prepared. Additional 18S and 28S sequences of four species from Boniniidae, which were available in a public database, were downloaded from GenBank (Table 4). To assess the last common ancestral state of boniniids, its proposed sister groups Amyellidae Faubel, 1984 and Theamatidae Marcus, 1949 (Dittmann et al. 2019a, Litvaitis et al. 2019) were also included in the analysis (Table 4). The three cotylean species *Cestoplana rubrocincta* (Grube, 1840), *Pericelis*

flavomarginata Tsuyuki et al., 2020a, and *Pericelis tectivorum* Dittmann et al., 2019b were used as outgroups (Table 4). Sequences were aligned using MAFFT ver. 7.427 (Katoh et al. 2017), with the L-INS-i strategy selected using the "Auto" option. Ambiguous sites were trimmed using Clipkit ver. 1.0 via the "kpic" option (Steenwyk et al. 2020). The optimal substitution models, selected using PartitionFinder ver. 2.1.1 (Lanfear et al. 2016) according to the Akaike Information Criterion (AIC; Akaike 1974) with the greedy algorithm (Lanfear et al. 2012), were GTR+I+G for both the 18S and 28S partitions. Phylogenetic analysis was performed using the maximum likelihood (ML) method via RAxML ver. 8.2.10 (Stamatakis 2014). Bayesian inference (BI) of the phylogeny was performed using MrBayes ver. 3.2.3 (Ronquist and Huelsenbeck 2003, Altekar et al. 2004) with two independent runs of Metropolis-coupled Markov chain Monte Carlo [$(MC)^3$], each consisting of four chains of 2,000,000 generations. All parameters (*statefreq*, *revmat*, *shape*, and *pinvar*) were unlinked between each position; trees were sampled every 100 generations. The first 25% of the trees were discarded as burn-in before a 50% majority-rule consensus tree was constructed. Convergence was confirmed using an average standard deviation of split frequencies of 0.001989, potential scale reduction factors for all parameters of 1.000–1.002 and effective sample sizes for all parameters of >209. Nodal support within the ML tree was assessed using analysis of 1,000 bootstrap (BS) pseudoreplicates (Felsenstein 1985). ML BS values ≥70% and posterior probability (PP) values ≥0.90 were considered to indicate clade support (here, combined nodal support is indicated as "PP/BS").

Ancestral state reconstruction related to microhabitat

The habitat of each ingroup species was determined from the original description (Table

4). The habitat information of the three unidentified species, *Boninia* sp., *Chromyella* sp., and *Theama* sp., was provided directly by the collector, Christopher Edward Laumer (Table 4). The possible ancestral states were reconstructed using Bayesian Binary Markov chain Monte Carlo (BBM) analysis implemented in RASP ver. 4.2 (Yu et al. 2015, 2020). To take phylogenetic uncertainty into account, 10 trees randomly selected from the post burn-in trees generated by MrBayes ver. 3.2.3 were used as input trees. BBM analysis was then run on a consensus Bayesian tree. The Markov chain Monte Carlo chain was run for 50,000 generations using 10 chains and sampled every 100 generations. A fixed (LC) model that did not allow null root distribution was used to conduct the analysis.

Data treatment

Digital images were edited using Adobe Photoshop CC 20.0.5 (Adobe Systems Inc., USA) as to background cropping, panorama composition, and brightness adjustment. Illustrations were prepared with Adobe Illustrator CC 23.0.3 (Adobe Systems Inc., USA).

Results

Taxonomy

Family Boniniidae Bock, 1923

1. Genus *Boninia* Bock, 1923

1. *Boninia uru* Tsuyuki, Oya, and Kajihara, 2022b
(Figs 1–3)

Boninia uru Tsuyuki, Oya, and Kajihara, 2022b: 7, figs 1–3.

Etymology. The specific name *uru*, an Okinawan dialect meaning “coarse sand,” is derived from the habitat of the species.

Material examined. Holotype: ICHUM 8278, sagittal sections, 3 slides (HE), collected by Y. Oya in Nagahama Beach (26.6242°N, 128.1843°E), Okinawa, Japan, on December 14, 2019. Paratypes (5 specimens): ICHUM 8279, horizontal sections, 2 slides (HE), collection data same as holotype except for the date (December 13, 2019); ICHUM 8280, sagittal sections, 2 slides (HE), collection data same as holotype; ICHUM 8281, unsectioned, preserved in 99.5% ethanol, collection data same as ICHUM 8279; ICHUM 8282, unsectioned, preserved in 99.5% ethanol, collection data same as holotype; ICHUM 8283, horizontal sections, 3 slides (HE), collection data same as holotype except for the date (December 14, 2020).

Type locality. Nagahama Beach, Okinawa, Japan (26.6242°N, 128.1843°E).

Description. Body elongated, tapered posteriorly, 3.0–4.5-mm long (4.5 mm in holotype) and 0.65–0.90-mm wide (0.72 mm in holotype) in anesthetized living state (Fig. 1A, B). Pair of pointed tentacles located at sides of head, 0.08–0.38-mm long (0.38 mm in holotype) (Fig. 1A–C). Dorsal surface smooth, translucent, without any coloration (Fig. 1A). Ventral surface translucent (Fig. 1B).

Tentacular eyespots absent. Pair of two cerebral eyespots (ca. 12 μm in diameter) located at each anterior side of brain; two eyespots in each pair lying close to each other (Fig. 1C). Marginal eyespots (ca. 22 μm in diameter), 21–29 in number (27 in holotype), distributed sparsely in anterior quarter of body along margins on both sides (Fig. 1A–C). Diameter of marginal eyespots twice as large as that of cerebral eyespots

(Fig. 1C).

Intestine highly branched, spreading all over body. Pharynx ruffled, 0.5–1.1-mm long (1.1 mm in holotype), lying on body center (Fig. 1B). Mouth situated in center of pharynx.

Male gonopore situated immediately behind pharynx (Fig. 1D). Male copulatory apparatus consisting of elongated seminal vesicle, interpolated prostatoid vesicle, penis papilla, and 2–4 prostatoid organs (2 in holotype) (Fig. 2A, B). Pair of sperm ducts running on each side of midline, curving at position of posterior end of pharyngeal pouch to separately enter into seminal vesicle (Fig. 2B). Seminal vesicle elongated, lined with flat nucleated epithelium, coated with thin muscle fibers, distally opening into prostatoid vesicle (Fig. 2A). Prostatoid vesicle lined with high epithelium, connecting to penis papilla (Figs 2A, 3A). Penis papilla unarmed, 20-µm long in dorsoventral axis, projecting into male atrium (Figs 2A, 3A). Inner wall of male atrium well ciliated (Fig. 3A, B). Two prostatoid organs present, each located anterior and posterior to male atrium in holotype (Figs 2A, 3A, B) and one of two sectioned paratypes (ICHUM 8280); three or four prostatoid organs radially arranged around male atrium in other sectioned paratypes (ICHUM 8279 and 8283, respectively) (Figs 2B, 3C, D); prostatoid organs arranged into single girdle. Each prostatoid organ oval in shape, 50-µm wide, with sclerotized stylet (37 µm in length), protruding into male atrium (Figs 2A, 3A–D). Extracapsular glands (“prostatoid organ glands”) not well developed (Fig. 3A, B). Muscle fibers surrounding male atrium, prostatoid organs, and prostatoid vesicle (Fig. 3D).

Pair of uterine canals running on both sides of midline, connecting to anterior part of Lang’s vesicle laterally through short branches; each canal with two uterine

vesicles (Figs 2B, 3E–G). Each uterine canal forming uteri at most anterior and posterior dilations; uteri filled with eggs (Figs 2B, 3F). Lang's vesicle elongated (309 μm in its long axis; 63 μm in its short axis), placed between one pair of posterior uteri; inner wall lined with cilia; elongated cilia observed in posterior region (Fig. 3H). Vagina ciliated, leading from Lang's vesicle to cement pouch (Fig. 2A, B). Cement glands numerous, concentrated around female copulatory apparatus and releasing contents into cement pouch (Figs 2A, 3E–H).

Epidermis on dorsal side ciliated, with numerous ovoid rhabdites (Fig. 3A, B). Ventral epidermis ciliated except for adhesive area (Fig. 3A, B, I).

Adhesive organ located at posterior end of body on ventral side (Figs 1B, D, 3I). Subepidermal muscle fibers not well developed in adhesive area, surface of which are covered by thick glandular epithelium (Fig. 3I).

Distribution. To date, known only from the type locality: Nagahama Beach, eastern coast of Okinawa Island, Japan.

Habitat. To date, confirmed only from gravelly habitats in intertidal coarse sediments.

Diagnosis. Body narrow and elongated; one pair of pointed tentacles located at anterolateral margins; four cerebral eyespots and 21–29 marginal eyespots; 2–4 prostatoid organs arranged into single girdle; Lang's vesicle fully ciliated; subepidermal muscle fibers of adhesive area not well developed.

Sequences. See Table 2.

Remarks. The specimens are assigned to *Boninia* because they conform to the generic diagnosis of Curini-Galletti and Campus (2007), i.e., they have two or more prostatoid organs with stylets opening into the male atrium. *Boninia uru* can be easily

distinguished from *B. antillara*, *B. divae*, and *B. mirabilis* by its single girdle of prostatoid organs (Bock 1923, Curini-Galletti and Campus 2007) (Table 5). The other two congeners *B. neotethydis* and *B. oaxaquensis* have a single girdle of prostatoid organs, as in the species herein; however, *B. uru* is distinguishable from these two species by its small number (2–4) of prostatoid organs (10–18 organs in *B. neotethydis* and 16–24 organs in *B. oaxaquensis*). Additionally, the arrangement of eyespots enables discrimination between *B. uru* and its congeners. *Boninia uru* and *B. neotethydis* are distinguished from the other species of *Boninia* by having just four cerebral eyespots (Table 5), and they are distinguished from each other in terms of the number of marginal eyespots (21–29 in *B. uru*; 6–16 in *B. neotethydis*). Also, the uterine canal connecting lateral to Lang's vesicle of *B. uru* is peculiar among the known *Boninia* species except for *B. oaxaquensis* (the relevant morphology is unknown) (Table 5).

Further examination is required to evaluate whether *Boninia* sp. from Samboanga (the Philippine Islands) (Curini-Galletti and Campus 2007) is conspecific with the species described here. *Boninia* sp. was collected from Samboanga and originally identified as *B. mirabilis* by Bock (1923). Later, Curini-Galletti and Campus (2007) re-examined Bock's (1923) voucher specimens and recognized them as an undescribed species based on their internal morphology, including *i*) the very small number (3–7) of prostatoid organs arranged into a single girdle and *ii*) the completely unciliated Lang's vesicle. *Boninia uru* is similar to the specimens from Samboanga in terms of the small number of prostatoid organs and the single girdle, but it differs by its entirely ciliated Lang's vesicle.

2. *Boninia yambarensis* Tsuyuki, Oya, and Kajihara, 2022b

(Figs 4–6)

Boninia yambarensis Tsuyuki, Oya, and Kajihara, 2022b: 12, figs 4–6.

Etymology. The species was named after the region Yambaru, the northern part of Okinawa Island. The type locality, Nagahama Beach, is located in the southeastern Yambaru region.

Material examined. Holotype: ICHUM 8284, sagittal sections of the posterior body, 9 slides (HE), along with the remaining unsectioned body (preserved in 70% ethanol), collected by A. Tsuyuki in Nagahama Beach (26.6242°N, 128.1843°E), Okinawa, Japan on August 9, 2021. Paratypes (5 specimens): ICHUM 8285, horizontal sections of the posterior body, 3 slides (HE), along with the remaining unsectioned body (preserved in 70% ethanol), collection data same as holotype except for the date (March 31, 2021); ICHUM 8286, sagittal sections of the posterior body, 6 slides (HE), along with the remaining unsectioned body (preserved in 70% ethanol), collection data same as ICHUM 8285; ICHUM 8287, sagittal sections of the posterior body, 8 slides (MT), along with the remaining unsectioned body (preserved in 70% ethanol), collection data same as ICHUM 8285; ICHUM 8288, unsectioned, preserved in 70% ethanol, collection data same as holotype; ICHUM 8289, unsectioned, preserved in 10% formaldehyde solution, collection data same as ICHUM 8285.

Description. Body slender and elongated, tapered posteriorly, 13.9–22.4-mm long (22.4 mm in holotype) and 0.93–1.25-mm wide (1.25 mm in holotype) in living state (Fig. 4A). Pair of pointed tentacles located at sides of head (Fig. 4A, B), 0.3–0.6-

mm long (0.63 mm in holotype). Dorsal surface smooth, translucent, without any coloration (Fig. 4A). Ventral surface translucent (Fig. 4C).

Tentacular eyespots absent. Pair of 3–4 cerebral eyespots present (ca. 14 μm in diameter); in each part of pair, two eyespots lying close to each other with one or two eyespot(s) located at distance of about 0.3 mm posterior to frontal two eyespots (Fig. 4D). Marginal eyespots (ca. 8–23 μm in diameter), 19–42 in number (35 in holotype), distributed anteriorly along margins on both sides (Fig. 4B, D).

Intestine highly branched, spreading all over body. Pharynx ruffled, 2.6–6.6-mm long (6.6 mm in holotype), lying on body center (Fig. 4C). Mouth situated in center of pharynx.

Male gonopore situated immediately behind posterior end of pharynx (Fig. 4C). Male copulatory apparatus consisting of seminal vesicle, interpolated prostatoid vesicle, penis papilla, and 21–22 prostatoid organs with stylets (Figs 4E, 5A, B). Pair of sperm ducts running on each side of midline, curving at posterior position of pharyngeal pouch to separately enter seminal vesicle (Figs 4C, 5B). Seminal vesicle spherical, coated with thin muscle fibers, distally opening into prostatoid vesicle (Figs 5A, 6A). Prostatoid vesicle, 44-μm long in dorsoventral axis, lined with high epithelium, connecting to penis papilla (Figs 5A, 6A). Penis papilla unarmed, 45-μm long in dorsoventral axis, projecting into male atrium (Figs 5A, 6A). Inner wall of male atrium well ciliated (Fig. 6B). Individual ducts of 21–22 prostatoid organs (21 in holotype) radially arranged into single girdle around male atrium and prostatoid vesicle (Figs 4E, 5B, 6C), opened into inner area of male atrium. Each prostatoid organ oval in shape, about 21-μm long in its longest axis, bearing sclerotized stylet (53 μm in length) (Figs 5A, 6A, B). Extracapsular glands (“prostatoid organ glands”) producing glandular

secretion into each prostatoid organ (Figs 5A, 6A, B).

Pair of uterine canals running on both sides of midline, connecting to vagina immediately anterior to entrance of Lang's vesicle (Fig. 5B); each canal connected through short side branches to five uterine vesicles (Figs 5B, 6D). Each uterine canal forming uteri at most anterior and posterior dilations; uteri filled with eggs (Figs 5B, 6D). Lang's vesicle elongated (340 μm in its long axis; 219 μm in its short axis); inner wall lined with cilia; elongated cilia observed in posterior region (Figs 5A, B, 6E). Vagina lined with cilia, curving down and leading to cement pouch (Figs 5A, 6E). Cement glands numerous, concentrated around female copulatory apparatus and releasing contents into cement pouch (Fig. 6E). Female atrium opening to exterior through female gonopore.

Epidermis on dorsal side ciliated, with numerous ovoid rhabdites (Fig. 6A, E). Ventral epidermis ciliated except for adhesive area (Fig. 6F).

Adhesive organ located at posterior end of body on ventral side (Figs 4C, 6F). Subepidermal muscle fibers not well developed in adhesive area.

Distribution. The species is known from the type locality, Nagahama Beach, eastern coast of Okinawa Island, Japan.

Habitat. To date, confirmed only from under rocks in the intertidal region. The thin body width (1–2 mm) of this species suggests that it may also be able to inhabit intergravel spaces. However, *B. yambarensis* seems to have a preference for epibenthic habitats over interstitial habitats because *i*) it has yet to be collected from interstitial environments and *ii*) more than 10 individuals of the species were found under rock surfaces independently in my two surveys.

Diagnosis. Body narrow and elongated; pair of pointed tentacles located at

anterolateral margins; 3–4 pairs of cerebral eyespots and 19–42 marginal eyespots; 21–22 prostatoid organs arranged into single girdle; five uterine vesicles present in each oviduct; Lang's vesicle fully ciliated; subepidermal muscle fibers of adhesive area not well developed.

Sequences. See Table 2.

Remarks. The materials examined belong to *Boninia* because they conform to the generic diagnosis, i.e., they have two or more prostatoid organs with stylets opening into the inner area of the male atrium. *Boninia yambarensis* can be separated from *B. antillara*, *B. divae*, and *B. mirabilis* by its single girdle of prostatoid organs (Bock 1923, Curini-Galletti and Campus 2007). *Boninia yambarensis* resembles *B. neotethydis*, *B. oaxaquensis*, and *B. uru* in having a single girdle of prostatoid organs (Table 5); however, it can be distinguished from *B. neotethydis* and *B. uru* by the number of prostatoid organs (21–22 in *B. yambarensis*; 10–18 in *B. neotethydis*; and 2–4 in *B. uru*). The number of prostatoid organs are the same in *B. yambarensis* and *B. oaxaquensis*; however, the species herein can be discriminated from *B. oaxaquensis* by the number of cerebral eyespots (6–7 in *B. yambarensis*; 14–66 in *B. oaxaquensis*).

Molecular phylogeny

The resulting BI and ML trees were identical in terms of topology; all six species of *Boninia* exclusively formed a clade (0.99 PP; 95% BS) (Fig. 7). *Boninia yambarensis* formed a clade with *B. antillara*, *B. divae*, *B. neotethydis*, and *Boninia* sp. with high support (0.99 PP; 98% BS). *Boninia antillara*, *B. divae*, and *Boninia* sp. were monophyletic with high support (1.00 PP; 99% BS). However, the phylogenetic relationship among Boniniidae (represented by the six species), Theamatidae

(represented by *Theama mediterranea* and *Theama* sp. of Laumer and Giribet (2014), and Amyellidae (represented by *Chromyella* sp. of Laumer and Giribet (2014) remains unclear due to low support values (0.76 PP; 64% BS) (Fig. 7).

Ancestral habitats

The ancestral states of habitats reconstructed via BBM analysis are shown in Fig. 8. The last common ancestor (LCA) of all analyzed species, including the outgroups (node 11), was estimated to be epibenthic with a probability of 98.7%. The LCAs of Amyellidae, Boniniidae, and Theamatidae (node 9), and Boniniidae (node 5) appeared to be interstitial, although the estimated probabilities were relatively low (56.1% and 58.2%, respectively). In contrast, the LCA of *Boninia* sp., *B. antillara*, and *B. divae* (node 2) and that of *Boninia* sp. and *B. antillara* (node 1) were epibenthic with high probabilities of 97.5% and 99.8%, respectively. Also, the ancestral states of nodes 3 and 4 were likely to be epibenthic, which was the most favored state (53.4% and 60.3%, respectively).

Discussion

The phylogenetic results suggest the possibility that an unexpected evolutionary scenario occurred in the *Boninia* lineage. *Boninia uru* was sister to a clade composed of the remaining five congeners, in contrast to both the stated hypotheses (see the Introduction), in which *B. uru* would have been sister to the interstitial *B. neotethydis* ("interstitial monophyly hypothesis") or to the sympatric *B. yambarensis* ("*in situ* speciation hypothesis"). Thus, in this section and based on my results, I discuss the most plausible evolutionary hypotheses pertaining to *i*) the shift between interstitial and

noninterstitial microhabitats and *ii*) the settlement of the two species at the same beach.

Reversible evolutionary shifts from interstitial to epibenthic realms in the *Boninia* lineage

The results of my ancestral state reconstruction analysis show that early boniniids likely lived in interstitial microhabitats, with some descendants subsequently having evolved to inhabit epibenthic environments, whereas others remained in the interstitial realm (Fig. 8). The LCA of all analyzed *Boninia* species (node 5) was estimated as interstitial, although this estimation is not supported with high probability (58.2%) (Fig. 8). In contrast, the LCA of all the remaining *Boninia* species except for *B. uru* and *B. yambarensis* (node 3) was estimated as epibenthic with 60.3%. The LCA of *Boninia* sp., *B. antillara*, and *B. divae* (node 2) and that of the former two species (node 1) were estimated to be epibenthic with high support (97.5% and 99.8%, respectively). These results suggest an evolutionary scenario in which the LCA of all analyzed *Boninia* species inhabited an interstitial environment, and where the LCA of all the remaining *Boninia* sp., *B. antillara*, *B. divae*, and *B. neotethydis* subsequently changed to an epibenthic lifestyle.

A prerequisite for this interpretation is that microhabitat preference of adults is species-specific and alternative, i.e., boniniids in the same species do not occur simultaneously in both interstitial and noninterstitial environments at random in their mature state. I consider this assumption to be realistic and applicable based on my observations. In my three independent field surveys, I collected six individuals of *B. uru* only by washing gravel sediments near the highwater limit where rocks were absent. In contrast, on the same beach, I observed >10 individuals of *B. yambarensis* crawling on

undersurfaces of rocks in the lower intertidal zone. These observations indicate a narrow habitat range at least for each species described herein (see also habitat for *B. yambarensis* above). Such a habitat preference would be expected for the other analyzed species *B. antillara*, *B. divae*, and *B. neotethydis* by extrapolating the empirical evidence observed in my two species, although the actual microhabitat for each of the other congeners should be confirmed in additional investigations in the future.

The evolutionary shift from interstitial to noninterstitial habitats is likely uncommon among Animalia. Indeed, irreversible one-way transition from the noninterstitial realm to the interstitial realm seems to be the norm among animalian taxa investigated to date; such interstitial taxa are exclusively monophyletic, e.g., Dinophilidae, Diurodrilidae, Polygordidae, Protodrilidae, Psammodrilidae (Worsaae et al. 2021) (Annelida), Ototyphlonemertidae (Andrade et al. 2012, Leasi et al. 2016) (Nemertea), and Rhodopemorpha (Wilson et al. 2017) (Mollusca), with the notable exception of acochlidean slugs in the clade Hedylopsacea (Jörger et al. 2014). Moreover, even among acochlidian slugs, evolutionary transitions from interstitial to noninterstitial habitats are limited to species living in specialized habitats, such as those exposed to nonmarine salinities (brackish, limnic, and amphibious species) (Jörger et al. 2014) and living in the deep sea (Neusser et al. 2016), whereas almost all other species of acochlidian slugs live in interstitial habitats at shallow depths. My study suggests a habitat shift from the interstitial to noninterstitial marine realm in the evolutionary history of flatworms based on molecular phylogenetic evidence with statistical support.

It remains unclear what makes such unique evolutionary transitions from interstitial to noninterstitial habitats possible in the *Boninia* lineage. The relatively high phenotypic plasticity in adult body size (about >2–10 times) among polyclads (cf.

Tsuyuki and Kajihara 2020) might be related to the evolutionary pathway. As Westheide (1987) stated, body size is one of the most important factors for microhabitat shifts between interstitial and noninterstitial realms. In acochlidians, “secondary gigantism” in body size (see Westheide 1982, 1987) may have contributed to the evolutionary shift from interstitial to epibenthic habitats; secondary gigantism is likely to be a consequence of adaptation to brackish water, freshwater, and terrestrial systems (Jörger et al. 2014) or to limitations of food resources in the deep sea (Neusser et al. 2016). If interstitial boniniids show plasticity in body size, accidental “gigantism” could potentially have led to a lifestyle outside interstitial biotopes, similar to the known example in acochlidians.

Independent colonization of the same beach

The tree topology suggests that *B. uru* and *B. yambarensis* settled at the same beach independently. In the resulting tree, *B. yambarensis* was more closely related to the Caribbean and Lessepsian species (*B. antillara*, *B. divae*, *B. neotethydis*, and *Boninia* sp. of Laumer and Giribet (2014) than to the sympatric species *B. uru* (Fig. 7). Additionally, the two species clearly differ morphologically in their reproductive organs, i.e., the number of prostatoid organs (2–4 in *B. uru*; 21–22 in *B. yambarensis*). Thus, there seems to be deep divergence between the two species, and they may have encountered the collection site after they had been reproductively isolated.

II-2. CESTOPLANIDAE LANG, 1884

Introduction

Polyclad flatworms in the family Cestoplanidae Lang, 1884 are distinguished from others by *i*) the very slender body without tentacles, *ii*) the ruffled pharynx located posterior to the center of the body, *iii*) the male copulatory apparatus directed anteriorly, and *iv*) the adhesive organ located on the posterior end of the body (Faubel 1983, Prudhoe 1985). This family is currently composed of six genera: *Acestoplana* Faubel, 1983; *Cestoplana* Lang, 1884; *Cestoplanella* Faubel, 1983; *Cestoplanides* Faubel, 1983; *Cestoplanoida* Faubel, 1983; and *Eucestoplana* Faubel, 1983 (Faubel 1983).

The genus *Eucestoplana* currently contains two species, *Eucestoplana cuneata* (Sopott-Ehlers and Schmidt, 1975) and *Eucestoplana meridionalis* (Prudhoe, 1982b), which are distinguished from other cestoplanid species by *i*) the presence of a tubular penis stylet housed in the male atrium and *ii*) the absence of a Lang's vesicle (Faubel 1983). To date, these species have been recorded around the Pacific Ocean including the Galápagos Islands, the Fiji Islands, and South Australia (Sopott-Ehlers and Schmidt 1975, Prudhoe 1982b, c, Tajika et al. 1991). During a faunal survey of the present study, I obtained polyclad specimens representing an undescribed species of *Eucestoplana* and *E.* cf. *cuneata* from the Okinawa Islands, Japan. In this section, I provide morphological descriptions of these two species based on the specimens collected in this survey. I also infer the phylogenetic positions of the two species of *Eucestoplana* among other species of Cestoplanidae based on molecular phylogenetic analyses using partial 18S and 28S sequences of all cestoplanid species currently available in public databases.

Material and Methods

Collection of specimens and morphological observations

Specimens were collected in the Okinawa Islands, Japan. Gravel samples (down to about 15 cm from the sediment surface) were collected at depths of about 20 cm from the water surface at low tide. The gravel was then agitated in seawater to extract animals. The supernatant was filtered using a dip net with about 1-mm mesh, and the residue was subsequently transferred into a bottle filled with fresh seawater. Worms were anesthetized, then photographed in the same way as in Chapter II-1. For DNA extraction, a part of the body was cut, fixed, and preserved in 99.5% ethanol. The rest of the body was fixed in Bouin's solution for 24 h and subsequently stored in 70% ethanol. Methods for histological observation was the same as in Chapter II-1. All specimens were deposited in the ICHUM.

DNA extraction, PCR, and sequencing

Total DNA was extracted in the same way of Chapter II-1. As a reference for DNA barcoding, a partial sequence (677 bp) of COI gene and 16S rDNA (16S; 444–445 bp) were determined. For phylogenetic inference, fragments of the 18S (1,735 bp) and 28S (1,006 bp) were sequenced. Amplification of the four gene markers was performed using PCR in the same protocol as in Chapter II-1. I used the primers 16SarL and 16SbrH (Palumbi et al. 1991) for 16S in addition to those listed in Table 3. The PCR amplification procedure for 16S was as follows: 94°C for 1 min; 35 cycles of 94°C for 30 s, 50°C for 30s, and 72°C for 1 min; and 72°C for 7 min. PCR products were purified and all nucleotide sequences were determined in the same way as mentioned in Chapter II-1. Sequences were checked and edited also in the same way as in Chapter II-

1. In addition to the specimens collected in the present study, a 1,735-bp partial sequences of 18S from the holotype of *Cestoplana nopperabo* Oya and Kajihara, 2019 was determined using the same methods described above. All edited sequences have been deposited in DDBJ/EMBL/GenBank.

Molecular phylogenetic analyses

For phylogenetic analyses, a concatenated dataset (2,834 bp) comprising partial 18S (1,735 bp) and 28S (1,099 bp) sequences was prepared (Table 6). Additional 18S and 28S sequences of three cotylean species, *Pericelis flavomarginata*, *Prosthiostomum siphunculus* (Delle Chiaje, 1828), and *Theama mediterranea* Curini-Galletti et al., 2008, were used as outgroups (Table 6). Sequences were aligned using MAFFT ver. 7.427 (Katoh et al. 2017) with the L-INS-i strategy selected using the "Auto" option. Ambiguous sites were trimmed using Clipkit ver. 1.0 via the "kpic" option (Steenwyk et al. 2020). The optimal substitution models selected using PartitionFinder ver. 2.1.1 (Lanfear et al. 2016) according to the AIC (Akaike 1974) with the greedy algorithm (Lanfear et al. 2012), were GTR+I+G for both the 18S and 28S partitions. An ML analysis was performed using RAxML ver. 8.2.10 (Stamatakis 2014). A BI was performed using MrBayes ver. 3.2.6 (Ronquist and Huelsenbeck 2003, Altekar et al. 2004) with two independent runs of $(MC)^3$, each consisting of four chains of 1,000,000 generations. All parameters (*statefreq*, *revmat*, *shape*, and *pinvar*) were unlinked between each position; trees were sampled every 100 generations. The first 25% of the trees were discarded as burn-in before a 50% majority-rule consensus tree was constructed. Convergence was confirmed using an average standard deviation of split frequencies of 0.003111 and potential scale reduction factors for all parameters of

1.000–1.012. Nodal support within the ML tree was assessed using analysis of 1,000 BS pseudoreplicates (Felsenstein 1985). ML BS values ≥70% and PP values ≥0.90 were considered to indicate clade support. Genetic distances were calculated using MEGA ver. X (Kumar et al. 2018).

Data treatment

Same as in Chapter II-1.

Results

Taxonomy

Family Cestoplanidae Lang, 1884

2. Genus *Eucestoplana* Lang, 1884

3. *Eucestoplana* cf. ***cuneata*** (Sopott-Ehlers and Schmidt, 1975)

(Fig. 9)

?*Cestoplana cuneata* Sopott-Ehlers and Schmidt, 1975: 210–212, figs 9, 10; Tajika et al. 1991, 335.

?*Eucestoplana cuneata* (Sopott-Ehlers and Schmidt, 1975): Faubel 1983, 95.

Material examined. ICHUM 8440, sagittal sections, 3 slides (HE), collected by A. Tsuyuki and Y. Oya in Tokei Beach (26.7143°N, 128.0185°E), Kouri Island, the Okinawa Islands, Okinawa, Japan, on August 7, 2021; ICHUM 8441, sagittal sections, 4 slides (HE), same data as above, except for the date (August 11, 2021); ICHUM 8442, sagittal sections, 4 slides (HE), same data as above, except for the date (August 9,

2021).

Description. Body slender and elongated, 24–30 mm long and 0.71–0.82 mm wide in living state (Fig. 9A). Pair of eyespot-clusters, each composed of 11–15 eyespots, distributed along midline in front of brain (Fig. 9B). Male copulatory apparatus composed of true seminal vesicle, interpolated prostatic vesicle, and penis papilla with stylet (Fig. 9C–E). Testicular follicles arranged in two lateral, longitudinal rows, about half length of body, running anteriorly from area in front of pharynx (Fig. 9A). Seminal vesicle antero-posteriorly elongated, posteriorly turning to right at 180° in front of female copulatory apparatus before running forward for short distance and then descending ventrally to lead to ejaculatory duct; thick muscular wall coating seminal vesicle, becoming thinner toward distal portion (Fig. 9D). Ejaculatory duct 942 μm in length, extending from distal end of prostatic vesicle to proximal end of seminal vesicle. Prostatic vesicle oval, with 19-μm-thick muscular wall, lined with thick glandular epithelium (Fig. 9C–E). Penis papilla with wedged, strongly cuticularized stylet (about 60 μm long) (Fig. 9C, D). Penis sheath cone-shaped (Fig. 9C, D). Male atrium lined with cilia (Fig. 9C), opening to exterior via male gonopore with depth of about 67 μm (Fig. 9C, D). Adhesive organ present at posterior end of body.

Sequence. Partial COI (674 bp), 16S (444 bp), 18S (1,757 bp), and 28S (1,006 bp) sequences from three individuals: LC740488 (COI), LC740489 (16S) from ICHUM 8440; LC740486 (COI), LC740491 (18S), and LC740493 (28S) from ICHUM 8441; LC740487 (COI), LC745667 (16S), LC740494 (28S) from ICHUM 8442.

Remarks. I tentatively identified the specimens as *E.* cf. *cuneata*. Sopott-Ehlers and Schmidt (1975) originally described this species based on two specimens collected in the Galápagos Islands. The present specimens from Kouri Island are

consistent with those of *E. cuneata* given by Sopott-Ehlers and Schmidt (1975) in having *i*) eyespots distributed only anterior to the brain, *ii*) the wedged cuticularized stylet, *iii*) an adhesive organ at posterior end of body, *iv*) the conical penis sheath, and *v*) the fully ciliated inner wall of male atrium. However, the specimens are different from the original description of *E. cuneata* because my specimens have *i*) longer body length (10 mm in the original; 24–30 mm in my specimens), *ii*) less number of eyespots (35–40 in the original; 24–25 in my specimens), and *iii*) the longer ejaculatory duct, of which the length between the distal end of prostatic vesicle and the proximal end of seminal vesicle are about 270 μm in the original (from the schematic diagram of fig. 9C in Sopott-Ehlers and Schmidt (1975)) whereas it was about 940 μm in a specimen from Japan. Although the length of ejaculatory duct might be correlated with the body length, my specimens from Japan could be a distinct species from *E. cuneata* considering three morphological differences mentioned above.

To date, *Eucestoplana cuneata* (as *Cestoplana cuneata*) has been confirmed from the Galápagos Islands (Sopott-Ehlers and Schmidt 1975) and Viti Levu, Fiji (Tajika et al. 1991). Whether the present material from the Okinawa Islands, Japan, is actually the same species should be ascertained in future studies.

4. *Eucestoplana* sp.

(Figs 10, 11)

Material examined. ICHUM 8443, sagittal sections, 6 slides (HE), collected by A. Tsuyuki and Y. Oya in Tokei Beach (26.7143°N, 128.0185°E), Kouri Island, the Okinawa Islands, Okinawa, Japan, on August 11, 2021; ICHUM 8444, sagittal sections,

4 slides (HE), same data as above.

Description of ICHUM 8443. Body slender and elongated, 26 mm long and 0.75 mm wide in living state (Fig. 10A); anteriorly rounded, spreading like fan; posteriorly tapered. Dorsal surface smooth, translucent, without any color pattern. Ventral surface translucent. Tentacles absent. Pair of eyespot-clusters, each composed of 12 or 14 eyespots (12 on left; 14 on right), distributed along midline in front of brain (Fig. 10B), spreading out in fan shape anteriorly. Intestine highly branched without anastomosis, spreading throughout body, not reaching body margin. Pharynx ruffled, 1.94 mm long, situated on last fourth of body (Fig. 10A, C). Mouth opening at last third of pharyngeal pouch (Fig. 10C). Male gonopore opening at last ninth of body (Fig. 10A). Female gonopore situated posterior to male gonopore. Male copulatory apparatus consisting of true seminal vesicle, interpolated prostatic vesicle, and penis papilla with stylet (Fig. 11A–D). Testicular follicles arranged in single, lateral, longitudinal row on each side, about half length of body, running anteriorly from area in front of pharynx (Fig. 10A). Pair of sperm ducts separately entering proximal end of seminal vesicle; each duct forming spermiducal vesicle before entering seminal vesicle (Fig. 11A, B). From junction between spermiducal vesicles, seminal vesicle running posteriorly for about 300 µm, turning to right at 180° in front of female copulatory apparatus, running anteriorly for about 400 µm, then turning to left at 90° to lead to ejaculatory duct; seminal vesicle about 700 µm long in total and 90 µm wide at its widest point. Ejaculatory duct curving downward at its distal end to lead to prostatic vesicle; seminal vesicle and ejaculatory duct coated with 19-µm-thick muscular wall (Fig. 11A, B). Prostatic vesicle oval, elongated, with about 18-µm-thick muscular wall, lined with thick glandular epithelium; distal end of prostatic vesicle forming penis papilla (Fig.

11A, C). Penis papilla with wedged, strongly cuticularized stylet (131 μm long), projecting into male gonopore (Fig. 11A, D). Penis sheath dome-shaped, about 184 μm wide at its widest point, housing penis stylet (Fig. 11A, C, D); external epithelium being exposed to male atrium, former being lined with ciliated epithelium (Fig. 11C, D); penis pouch lined with non-ciliated epithelium. Male atrium lined with thin epithelium without cilia (Fig. 11C, D). Male gonopore about 27 μm depth. Female copulatory organ lacking Lang's vesicle. Pair of oviducts running posteriorly, then connecting to proximal end of vagina independently. Vagina narrow, lined with ciliated epithelium, running anterodorsally from its proximal end for sort distance, then curving ventrally and leading to female gonopore via narrow cement pouch (Fig. 11A, E). Numerous cement glands releasing their contents into cement pouch (Fig. 11E). Adhesive organ located at posterior end of body.

Description of ICHUM 8444. Body length/width, and eyespot arrangements unknown, due to lack of anterior part of body. Body coloration same as ICHUM 8443. Pharynx ruffled, 1.27 mm in length; mouth opening at posterior region of pharyngeal pouch. Male copulatory apparatus composed of elongate seminal vesicle, interpolated prostatic vesicle, and penis papilla with wedged stylet; penis stylet slenderer than that of holotype. Penis sheath dome-shaped, with external epithelium ciliated. Male atrium covered with non-ciliated epithelium. Female copulatory apparatus same as ICHUM 8443 except for shape of cement pouch being more expanded than that of ICHUM 8443. Adhesive organs present at posterior end of body (Fig. 11F).

Distribution. To date, only from the Okinawa Islands, Japan.

Sequence. Partial 16S (443 bp; LC740490), 18S (1,757 bp; LC740492), and 28S (1,006 bp; LC740495) sequences from ICHUM 8443.

Remarks. The specimens belong to *Eucestoplana* based on the following characteristics: *i*) the evident cuticularized penis stylet and *ii*) a female copulatory apparatus without any accessory ducts or Lang's vesicle. *Eucestoplana* sp. can be easily distinguished from *E. meridionalis* by *i*) its translucent body, *ii*) the fewer eyespots only distributed anterior to the brain, and *iii*) the presence of the adhesive organ (Table 7). My specimen of *Eucestoplana* sp. is most similar to *E. cuneata* in having *i*) around 30 eyespots distributed only anterior to the brain, *ii*) a wedge-shaped stylet, and *iii*) the adhesive organ located on the posterior end of body. However, the present *Eucestoplana* sp. is separated from *E. cuneata* by *i*) the shape of the penis sheath (dome-shaped in *Eucestoplana* sp.; cone-shaped in *E. cuneata*), *ii*) the arrangement of the cilia in the inner wall of the male atrium (only present along the outside of the penis sheath in *Eucestoplana* sp.; surrounding the whole male atrium in *E. cuneata*), and *iii*) the shallower male gonopore depth (about 27 μm in *Eucestoplana* sp.; ≥50 μm in *E. cuneata*). Therefore, the present *Eucestoplana* sp. highly likely represents an undescribed species.

Molecular analyses

Molecular phylogeny. The resulting ML and BI trees were identical in terms of topology; all examined six species of Cestoplanidae formed a clade with full support (Fig. 12). Within the clade, *Eucestoplana* and *Cestoplana* were reciprocally monophyletic, each with support of 1.00PP/97% BS and 0.94PP/66% BS, respectively. Within *Cestoplana*, *C. nopperabo* was sister to the remaining three, *C. rubrocincta* (Grube, 1840), *C. salar* Marcus, 1949, and *C. techa* Du Bois-Reymond Marcus, 1957, which received full support, while the latter two being sister with support of

0.67PP/62% BS.

Genetic distances between cestoplanid species. The interspecific genetic distances (uncorrected *p*-values) between my specimens representing *E.* cf. *cuneata* and *Eucestoplana* sp. were 3.153–3.378% for 16S and 1.093% for 28S, both of which were greater than the intraspecific ones (0.225% for 16S and 0.000% for 28S) observed within two specimens of *E.* cf. *cuneata*. I failed to amplify the COI sequence of a specimen of *Eucestoplana* sp. using the primer pair Acotylea_COIF and Acotylea_COIR whereas that of *E.* cf. *cuneata* was successfully done with the same primers (LC740486–LC740488). The interspecific genetic distance for COI was 0.000–0.148% within three specimens of *E.* cf. *cuneata*.

The interspecific genetic distances (uncorrected *p*-values) for the 28S sequences among five species of Cestoplanidae of which 28S sequences are available in public database are shown in Table 8. The minimum value was 0.66% between *C. salar* and *C. techa* (both from Brazil) while the maximum value within this family was 6.98% between *C. rubrocincta* from Italy and *Eucestoplana* sp. from Japan; within the same genus, the maximum intraspecific genetic distance was 5.98% between *C. rubrocincta* and *C. nopperabo*.

Discussion

The resulting tree shows that the two *Eucestoplana* species *E.* cf. *cuneata* and *Eucestoplana* sp. were most closely related to each other among cestoplanid species (Fig. 12). The phylogenetic closeness suggests that their unique traits such as *i*) the heavily sclerotized penis stylet, *ii*) the reduced number of eyespots, and *iii*) the preference of gravelly interstitial habitats may be synapomorphic within the lineage of

Cestoplanidae. The phylogenetic position of *Cestoplana nexa* Sopott-Ehlers and Schmidt, 1975, which shares the latter two characteristics, also requires to be inferred in future studies.

The topology shows that the genera *Cestoplana* and *Eucestoplana* are monophyletic, respectively (Fig. 12). To confirm whether this view can be adopted for all known species belonging to the two genera, further phylogenetic analyses are required involving *E. meridionalis*, the other four species of *Cestoplana*, and constituents of the other four genera *Acestoplana*, *Cestoplanella*, *Cestoplanides*, and *Cestoplanoida*.

The genetic distance for the 16S sequences between *Eucestoplana* sp. and *E.* cf. *cuneata* (3.153–3.378%) supports that the two species are likely to be genetically independent because the values are much larger than 1.4%, the maximum intraspecific distance observed among four *Notocomplana* species (Oya and Kajihara 2017). In addition, the *p*-value for the 28S between *Eucestoplana* sp. and *E.* cf. *cuneata* (1.093%) was larger than that between *C. salar* and *C. techa* (0.66%), which are morphologically clearly distinct (Table 8).

II-3. Diposthidae Woodworth, 1898

Introduction

The family Diposthidae is characterized by *i*) an oval to slightly elongated body with paired marginal tentacles bearing eyespots, *ii*) a ruffled pharynx situated at the center of the body, and *iii*) a pair of spermiducal vesicles or a seminal vesicle opening directly into the unarmed penis papilla (Prudhoe 1985, Litvaitis et al. 2019). Currently, the family is considered to contain four genera: *Asthenoceros* Laidlaw, 1903a; *Diposthus* Woodworth, 1898; *Marcusia* Hyman, 1953; and *Pericelis* Laidlaw, 1902 (Litvaitis et al. 2019, Cuadrado et al. 2021).

The genus *Pericelis* is distinguished from the other genera in Diposthidae by *i*) a pair of marginal tentacles formed by folds of the anterior margin of the body, *ii*) the marginal eyespots that completely encircle the periphery of the body, *iii*) a long ruffled pharynx situated at the center of the body, *iv*) a male copulatory apparatus composed of a prominent seminal vesicle and unarmed penis papilla but without distinct prostatic organs, and *v*) a female copulatory apparatus with a pair of uteri bearing uterine vesicles and a definite cement pouch (Prudhoe 1985, Ramos-Sánchez et al. 2020).

The validity of *Marcusia* is problematic in relation to *Pericelis* because there seems to be no evident characteristics that can differentiate the two genera. *Marcusia* was established based on *Marcusia ernesti* Hyman, 1953 in the acotylean flatworm family Cryptocelidae Laidlaw, 1903b. Subsequently, Hyman (1955a) synonymized *Marcusia* with *Pericelis* because she found that *M. ernesti* should belong to the latter cotylean genus based on a reexamination of its type sections. In contrast, Faubel (1984) separated *Marcusia* and *Pericelis*, possibly due to a misconception on his part. He

proposed the presence or absence of a prostatic vesicle as a key trait that could be used to distinguish the two genera; however, the type species of both genera, namely *M. ernesti* and *Pericelis byerleyana* (Collingwood, 1876) (originally *Typhlolepta byerleyana*), do not actually possess a prostatic vesicle (Laidlaw 1902, Meixner 1907, Kato 1943c, Hyman 1953). To avoid systematic confusion, Hyman's (1955a) taxon concept is accepted in the current study, i.e., *Marcusia* is regarded as a junior synonym of *Pericelis*; *M. ernesti* and *Marcusia alba* Cuadrado et al., 2021 should be under *Pericelis*. However, the generic assignment of the nominal species *Marcusia alba* is skeptical because it does not actually conform to the diagnostic character of *Pericelis* in that the marginal eyespots do not encircle the body periphery (Cuadrado et al. 2021).

Apart from '*Marcusia alba*', the genus *Pericelis* currently contains eight species: *P. byerleyana*; *Pericelis cata* Du Bois-Reymond Marcus and Marcus, 1968; *Pericelis ernesti* (Hyman, 1953); *Pericelis hymanae* Poulter, 1974; *Pericelis nazahui* Ramos-Sánchez et al., 2020; *Pericelis orbicularis* (Schmarda, 1859); *Pericelis sigmeri* Ramos-Sánchez et al., 2020; and *Pericelis tectivorum*. To date, these species have been recorded mainly from subtropical and tropical regions, with the exception of *P. tectivorum* that is only found in aquaria (Fig. 13).

In Japanese waters, the species diversity of *Pericelis* remains unclear. There have been just a few reports of *P. byerleyana* from the Ryukyu Islands and the Ogasawara Islands (Okada et al. 1965, Ooishi 1970, Iwase et al. 1990). However, there is some photographic evidence that the biodiversity of *Pericelis* in southern Japan has been underestimated (Ono 2015). During a faunal survey of the present study, I found polyclad specimens of three undescribed species of *Pericelis*. Here, I describe the three species of *Pericelis*, and confirm the generic assignment of '*Marcusia alba*' based on

molecular phylogenetic analyses using partial 18S and 28S rDNA sequences from all *Pericelis* species currently available in public databases.

Material and Methods

Sampling and morphological observation

Polyclad specimens were collected intertidally at the Ogasawara Islands and subtidally from 10–20 m depths using SCUBA at Shizuoka, Kagoshima, and Ishigaki Island, in 2016 and 2018–2020. Worms were anesthetized, photographed alive in the same way as mentioned in Chapter II-1. For DNA extraction, a part of the body was removed and stored in 99.5% ethanol. The rest of the body was fixed in Bouin's solution or 10% formaldehyde seawater solution for 24–72 h and then preserved in 70% ethanol. Serial sagittal sections were made (7 μm in thickness) in the same way as mentioned in Chapter II-1. Sections were stained with HE, mounted on glass slides, and then embedded in Entellan New under cover slips. The slides were observed and photographed in the same way as in Chapter II-1. All specimens were deposited in the ICHUM.

DNA extraction, PCR amplification, and sequencing

Total DNA was extracted in the same way as mentioned in Chapter II-1 or using a silica-based method (Boom et al. 1990) after specimens were homogenized. As a reference for DNA barcoding, partial sequences (712 bp) of the COI gene were determined from eight specimens in three species (Table 9). For phylogenetic inference, fragments of 18S (1,748 bp) and 28S (1,008 bp) were also sequenced. The PCR amplification and direct sequencing were performed using the same way as mentioned

in the Chapter II-1. All sequences determined in this study have been deposited in DDBJ/EMBL/GenBank under the accession numbers listed in Table 8.

Phylogenetic tree construction and genetic distance calculation

For phylogenetic analysis, a concatenated dataset comprised of partial 18S and 28S sequences was prepared. In addition to the sequences determined in the current study, the 18S sequence of *P. tectivorum* and the 28S sequences of seven species from Diposthidae were downloaded from GenBank (Table 10). The three cotylean species *Boninia* sp., *Cestoplana rubrocincta*, and *Theama mediterranea*, were used as outgroups. Alignment of 18S and 28S sequences was completed using MAFFT ver. 7 (Katoh et al. 2017) with the L-INS-i strategy selected via the "Auto" option; ambiguous sites were removed using Gblocks ver. 0.91b (Castresana 2002) with the option for less stringent selection applied. A concatenated dataset (2,934 bp in total length: 1,756-bp 18S and 1,178-bp 28S) was also prepared using MEGA ver. 7.0. The optimal substitution models, selected using PartitionFinder ver. 2.1.1 (Lanfear et al. 2016) under the AIC (Akaike 1974) with the greedy algorithm, were GTR+I+G for both the 18S and 28S partitions. A phylogenetic analysis was performed using the ML method via RAxML ver. 8.2.10 (Stamatakis 2014). BI of the phylogeny was performed using MrBayes ver. 3.2.3 (Ronquist and Huelsenbeck 2003) with two independent runs of $(MC)^3$, each consisting of four chains of 1,000,000 generations. All parameters (*statefreq*, *revmat*, *shape*, and *pinvar*) were unlinked between each position; trees were sampled every 100 generations. The first 25% of the trees were discarded as burn-in before a 50% majority-rule consensus tree was constructed. Convergence was confirmed using an average standard deviation of split frequencies of 0.001427,

potential scale reduction factors for all parameters of 1.000–1.002, and effective sample sizes for all parameters of >547. Nodal support within the ML tree was assessed by analyzing 1,000 bootstrap (BS) pseudoreplicates. ML BS values ≥70% and posterior probability (PP) values ≥0.90 were considered to indicate clade support (here, combined nodal support is indicated as "BS/PP"). Genetic distances were calculated using MEGA ver. 7.0.

Data treatment

Same as in Chapter II-1.

Results

Taxonomy

Family Diposthidae Woodworth, 1898

Amended diagnosis, based on Prudhoe (1985) and Litvaitis et al. (2019). Cotylean flatworms with oval to slightly elongate body shape; pair of marginal tentacles bearing eyespots; ruffled pharynx arranged centrally; sucker behind female gonopore; pair of spermiducal vesicles or single seminal vesicle opening directly into unarmed penis papilla; female reproductive system usually with uterine vesicles.

3. Genus *Pericelis* Laidlaw, 1902

Amended diagnosis. Diposthidae with elongated oval or circular body; pair of marginal tentacles formed by folds of anterior margin of body; cerebral, tentacular, and marginal eyespots present; marginal eyespots completely encircling body margin or distributed

only at anterior margin of body; long pharynx situated on body center; male reproductive system with prominent seminal vesicle and unarmed penis papilla; without distinct prostatic organ; female reproductive system usually with uterine vesicles.

Remarks. I modified the generic diagnosis of *Pericelis* produced by Laidlaw (1902) in relation to the marginal-eyespot distribution (see Discussion). Based on the phylogenetic results, the new combination of *Pericelis alba* was also introduced in Tsuyuki et al. (2022c).

5. *Pericelis flavomarginata* Tsuyuki, Oya, Jimi, and Kajihara, 2020a

[Japanese name: Lemon-perikerisu]

(Figs 14, 15)

Pericelis flavomarginata Tsuyuki, Oya, Jimi, and Kajihara, 2020a: 406–411, figs 2–4 (Shizuoka; Kagoshima; the Ogasawara Islands, Tokyo).

?*Pericelis* sp. 6: Ono (2015), 71 (the Kerama Islands, Okinawa).

Etymology. The specific name *flavomarginata* (*-us*, *-a, -um*) is a compound adjective derived from the Latin *flavus* and *marginatus*, meaning “yellow-margined”. It was named after the dorsal surface of the body fringed with a lemon-yellow line.

Material examined. Holotype: ICHUM 6116, sagittal sections of the reproductive organs, 18 slides (HE), along with the remaining unsectioned body (preserved in 70% ethanol), collected by D. Uyeno at 10–20 m depth off the coast of Kome-jima (or Yone-jima) (31.4343°N, 130.1212°E), Nomaike, Kagoshima, Japan on July 13, 2019. Paratypes (6 specimens): ICHUM 6117, sagittal sections, 16 slides (HE),

collected by Y. Oya at 1–2 m depth of Omura Beach (27.0934°N, 142.1942°E), Chichi-jima Island, the Ogasawara Islands, Tokyo, Japan on September 6, 2016; ICHUM 6118, sagittal sections, 8 slides (HE), collected by Y. Oya and A. Tsuyuki at 10–15 m depth off the coast of Bonomisaki (31.2541°N, 130.2150°E), Bonotsu, Kagoshima, Japan on July 26, 2018; ICHUM 6119, sagittal sections, 14 slides (HE), collected by N. Jimi at 12 m depth of Koganezaki Beach (34.8431°N, 138.7625°E), Koganezaki, Shizuoka, Japan on January 26, 2020; ICHUM 6120, unsectioned, preserved in 70% ethanol, collected in Shiogaura (31.2547°N, 130.2330°E), Bonotsu, Kagoshima, Japan on July 12, 2019; ICHUM 6121, sagittal sections, 9 slides (HE), collection data same as holotype; ICHUM 6122, unsectioned, preserved in 70% ethanol, collected in Shiogaura (31.2547°N, 130.2330°E), Bonotsu, Kagoshima, Japan on July 6, 2019.

Type locality. Off the coast of Kome-jima (or Yone-jima) (31.4343°N, 130.1212°E), Nomaike, Kagoshima, Japan.

Description. Body elongated oval, slightly tapered posteriorly, 30–48 mm long (32.5 mm in holotype) and 12–35 mm maximum wide (15 mm in holotype) in living state (Fig. 14A, B); body margin slightly ruffled. Pair of marginal tentacles apparent; tip of tentacles extending and tapering (Fig. 14C). Dorsal surface smooth, translucent, fringed with lemon-yellow line except for translucent tip of marginal tentacle; narrow brown midline extending from anterior edge of body to posterior end of pharynx. Ventral surface translucent, without color pattern. Cerebral eyespots in two elongated clusters, lateral to middorsal brown band (Fig. 14D, E). Frontal eyespots scattered between tentacles (Fig. 14D, E). Tentacular eyespots abundant at tip, scattered posteriorly (Fig. 14D, E). Marginal eyespots in single band, completely encircling body. Intestine highly branched, not anastomosing. Pharynx ruffled, elongated, half of body

length, situated on body center (Fig. 14B). Male and female gonopores opening in common behind posterior end of pharynx (Fig. 15A, B). Male copulatory apparatus consisting of large seminal vesicle and unarmed penis papilla (Fig. 15A). Pair of sperm ducts entering laterally into seminal vesicle at point being close to proximal end of ejaculatory duct. Spermiducal bulb absent. Seminal vesicle oval, coated with thick muscular wall, narrowing posteriorly and opening into ejaculatory duct (Fig. 15A, C). Without prostatoid organs or prostatic glands. Ejaculatory duct narrow, curving downward before entering penis papilla (Fig. 15A). Penis papilla elongate conical unarmed, protruding into long narrow male atrium; former occupying about half of length of latter; both lined with muscularized epithelium (Fig. 15A, B, D). Male and female atriums opening to short common atrium and to broad common gonopore (Fig. 15A, B). Female copulatory apparatus behind level of male atrium. Cement glands surrounding female copulatory apparatus and extending anterior up to level of seminal vesicle (Fig. 15A–D). Cement pouch apparent (Fig. 15A, B, D). Vagina curving posteriorly, leading to pair of oviducts; each oviduct running anteriorly, with 4–5 uterine vesicles; posterior-most being largest, arranged posterior to female gonopore (Fig. 15E). Lang's vesicle absent. Sucker well developed, situated in posterior to female copulatory apparatus, near distal end of body (Fig. 15F).

Distribution. My materials were distributed in Koganezaki (Shizuoka), Nomaike and Bonotsu (Kagoshima), Chichi-jima Island (Ogasawara, Tokyo). A similar-looking specimen has been confirmed from the Kerama Islands (Okinawa) (Ono 2015).

Habitat. So far confirmed under rocks in the intertidal and subtidal zones down to 20 m depth.

Diagnosis. Body elongated oval; body margin slightly ruffled; pair of marginal

tentacles with tips extending and tapering; dorsal surface translucent, fringed by lemon-yellow line except for tip of tentacles; narrow brown midline running from anterior edge of body to posterior end of pharynx; pair of cerebral-eyespot clusters antero-posteriorly elongated along brown midline; male and female atriums opening to short common atrium and single gonopore; elongate penis papilla half as long as narrow male atrium; 4–5 uterine vesicles in each oviduct.

Sequences. See Table 9.

Remarks. My specimens belong to *Pericelis* because they conform to the generic diagnosis by having *i*) a pair of folded marginal tentacles with eyespots, *ii*) marginal eyespots that encircle the body margin, *iii*) a long, ruffled pharynx situated centrally, and *iv*) a male copulatory apparatus without distinct prostatic organs (Ramos-Sánchez et al. 2020). *Pericelis flavomarginata* is easily distinguished from *P. byerleyana*, *P. cata*, *P. nazahui*, *P. orbicularis*, *P. sigmeri*, and *P. tectivorum* by their brown coloration (Table 11), which is in contrast to the lemon-yellow marginal rim and the dorsal narrow brown midline of *P. flavomarginata*. This species is similar to *P. hymanae* and *P. alba* in that all species have a narrow brown midline in the dorsal surface of the body. However, *P. flavomarginata* can be distinguished from *P. hymanae* and *P. alba* by the dorsal marginal coloration (lemon yellow in *P. flavomarginata vs.* translucent in *P. hymanae* and *P. alba*). In addition, the species is distinguishable from *P. hymanae* by the presence of common gonopore; according to Meixner (1907) and Du Bois-Reymond Marcus and Marcus (1968), the interpretation of whether or not the male and female gonopores are separated may depend on the fixation state. Therefore, this feature should be reexamined based on specimens with or without careful anesthetization. *Pericelis flavomarginata* is also separated from *P. alba* by the marginal-

eyespot arrangement (completely encircling the body periphery in *P. flavomarginata vs.* only anteriorly distributed in *P. alba*) (Table 11).

Pericelis sp. 6 in the Kerama Islands, Okinawa (Ono 2015) may be identified as *P. flavomarginata* in terms of its similar dorsal coloration. However, more examination is required with observation of internal morphology and molecular analyses.

6. *Pericelis lactea* Tsuyuki, Oya, and Kajihara, 2022c

[Japanese name: Rennyu-perikerisu]

(Figs 16, 17)

Pericelis lactea Tsuyuki, Oya, and Kajihara, 2022c: 5–8, figs 2, 3 (Kagoshima).

Etymology. The specific name *lactea* is a Latin adjective meaning “milk-white”. It was named after the body coloration of translucent white without any color pattern on the dorsal surface. The Japanese vernacular name means “milky *Pericelis*”.

Material examined. Holotype: ICHUM 6288, sagittal sections of the reproductive organs, 14 slides (HE), along with the remaining unsectioned body (preserved in 99.5%), collected by A. Tsuyuki and Y. Oya at 10–20 m depth, off the coast of Kannonzaki (31.5458°N, 130.6360°E), Kagoshima Prefecture, Japan, on July 25, 2018. Paratype: ICHUM 6289, sagittal sections of reproductive organs, 14 slides (HE), along with the remaining unsectioned body (preserved in 99.5% ethanol after cleared in xylene), collection data same as holotype.

Type locality. Off the coast of Kannonzaki (31.5458°N, 130.6360°E),

Kagoshima Bay, Kagoshima, Japan.

Description. Body elongated oval in dorsal view, 2.39–3.37 cm in length (3.37 cm in holotype) and 1.27–1.37 cm at its widest point (1.37 cm in holotype) in living state; body margin slightly ruffled (Fig. 16A, B). Pair of marginal tentacles shallowly folded; tip of tentacles not tapered (Fig. 16A). Dorsal surface smooth, translucent, without any color pattern (Fig. 16A). Ventral surface translucent (Fig. 16B). Cerebral eyespots in two elongated clusters, each composed of 66 (left) and 69 (right) eyespots in holotype (Fig. 16C). Frontal eyespots spreading out anteriorly in fan-like shape and leading to marginal and tentacular eyespots. Marginal eyespots in single band, only distributed along anterior margin of body. Tentacular eyespots gathered at tip (Fig. 16C). Intestine highly branched, not anastomosing. Pharynx ruffled and elongated, 1.31–1.56 cm in length (1.56 cm in holotype; about half of body length), situated in body center (Fig. 16B). Male and female gonopores opening separately behind posterior end of pharyngeal pouch. Male copulatory apparatus consisting of seminal vesicle and unarmed penis papilla (Fig. 17A–C). Pair of spermiducal vesicles opening laterally into seminal vesicle (Fig. 17A, B). Seminal vesicle oval, 373 µm long and 141 µm wide, with about 35-µm-thick wall of fine muscle fibers, connected directly to penis papilla (Fig. 17A–C); exterior muscle fibers present around seminal vesicle (Fig. 17A–C). Penis papilla elongate conical, without internal glandular epithelium, protruding into male atrium; penis papilla occupying about three quarters of male atrium (Fig. 17A). Male atrium opening into male gonopore. Female gonopore situated immediately posterior to male gonopore (Fig. 17A, C). Pair of oviducts, each with three uterine vesicles (Fig. 17D), running posteriorly lateral to pharynx, leading to proximal end of vagina. Lang's vesicle absent. Vagina curving down, leading to cement pouch (Fig.

17A, E). Cement glands densely arranged around cement pouch (Fig. 17A, C, E). Female atrium opening to exterior through female gonopore. Sucker situated posterior to female copulatory apparatus (Fig. 17A, C, E).

Distribution. Only from the type locality.

Habitat. Under rocks in the subtidal zone.

Diagnosis. Body elongated oval; body margin slightly ruffled; pair of marginal tentacles without tapered tips; dorsal surface translucent without any color pattern; pair of cerebral-eyespot clusters antero-posteriorly elongated along midline; marginal eyespots distributed at only anterior margin of body; male and female gonopores separated; penis papilla conical in shape, without stylet; three uterine vesicles in each oviduct.

Sequences. See Table 9.

Genetic distances. The genetic distance (uncollected *p*-value) for the 712-bp COI sequences between two specimens was 0.1%. The translated protein sequences were identical.

Remarks. The specimens described here should be included in *Pericelis* based on the following characteristics: *i*) a pair of folded marginal tentacles with eyespots, *ii*) the long ruffled pharynx situated centrally, and *iii*) the male copulatory apparatus without distinct prostatic organs. Among the 10 known *Pericelis* species, this species is unique in terms of its body coloration, i.e., a translucent background without any pattern on the dorsal surface (Fig. 16A); thus, it can easily be distinguished from the other congeners (Table 11). This species is most similar to *P. alba* because both species have marginal eyespots distributed only at the anterior region of the body. However, *P. lactea* is separated from *P. alba* by *i*) the presence of frontal eyespots and *ii*) the separation of

the male and female gonopores, in addition to *iii*) the difference in body coloration and pattern (translucent white without a color pattern in *P. lactea*; ivory white with brownish dots, brushstroke-like lines, and a midline in *P. alba*) (Table 11).

7. *Pericelis maculosa* Tsuyuki, Oya, and Kajihara, 2022c

[Japanese name: Mizutama-perikerisu]

(Figs 18, 19)

Pericelis maculosa Tsuyuki, Oya, and Kajihara, 2022c: 8–11, figs 4, 5 (Ishigaki Island, Okinawa).

?*Pericelis* sp. 5: Ono 2015, 71 (the Kerama Islands, Okinawa).

Etymology. The specific name *maculosa*, a Latin adjective meaning "spotted", is named after the white to light blue spots sparsely distributed all over the dorsal surface of the body. The Japanese vernacular name literally means "drops-of-water *Pericelis*."

Material examined. Holotype: ICHUM 6290, sagittal sections of the reproductive organs, 10 slides (HE), along with the remaining unsectioned body (preserved in 99.5% ethanol after cleared in xylene), collected by A. Tsuyuki and Y. Oya at 10–20 m depth in "Osaki Hanagoi Reef" (24.4240°N, 124.0749°E), off the coast of Osaki Beach, Ishigaki Island, Okinawa, Japan, on March 12, 2020. Paratypes (5 specimens; collection data same as holotype): ICHUM 6291, sagittal sections of reproductive organs, 15 slides (HE), along with the remaining unsectioned body (preserved in 99.5% ethanol after cleared in xylene); ICHUM 6292, sagittal sections of reproductive organs, 9 slides (HE), along with the remaining unsectioned body

(preserved in 70% ethanol); ICHUM 6293, unsectioned, preserved in 70% ethanol; ICHUM 6294, unsectioned, preserved in 70% ethanol.

Type locality. Off the coast of Osaki Beach (24.4240°N, 124.0749°E), Ishigaki Island, Okinawa, Japan.

Description. Body elongated oval, 1.71–2.17 cm long (2.17 cm in holotype) and 0.59–1.02 cm at its widest point (1.02 cm in holotype) in living state; body margin slightly ruffled. Pair of marginal tentacles shallowly folded; tip of tentacle not tapered (Fig. 18A). Dorsal surface smooth, translucent, covered with numerous dots varying from white to light blue; brown speckles scattered along both sides of pharyngeal pouch (Fig. 18A). Ventral surface translucent, without any color pattern (Fig. 18B). Cerebral eyespots in two elongated clusters, each composed of 23–54 (left; 25 in holotype) and 17–46 (right; 28 in holotype) eyespots (Fig. 18C). Frontal eyespots sparsely scattered in front of cerebral eyespots, arranged to form fan-like shape (Fig. 18C). Marginal eyespots in single band, completely encircling body. Tentacular eyespots gathered at tip (Fig. 18C). Intestine highly branched, not anastomosing. Pharynx ruffled and elongated, 0.83–1.38 cm in length (1.10 cm in holotype; about half of body length), situated in body center (Fig. 18B, D). Male and female gonopores opening separately behind posterior end of pharynx (Figs 18D, 19A). Male copulatory apparatus consisting of large seminal vesicle and unarmed penis papilla (Fig. 19A, B). Pair of spermiducal vesicles entering laterally into seminal vesicle (Fig. 19A). Seminal vesicle spherical, 275 μm in diameter, coated with 21-μm-thick muscular wall, opening directly into penis papilla (Fig. 19A, B). Penis papilla elongate and cylindrical (571 μm in length and 55 μm in width) (Fig. 19A, B), without internal glandular epithelium (Fig. 19C), protruding into long, narrow male atrium; length of penis papilla as long as that of male

atrium. Male atrium opening into male gonopore. Female gonopore located at distance of 0.13 mm posterior to male gonopore (Fig. 19A, E). Pair of oviducts, each having two uterine vesicles (Fig. 19F), running posteriorly on both sides of pharynx from level of anterior tip of pharyngeal pouch to proximal end of vagina (Fig. 18B, D). Lang's vesicle absent. Vagina curving down, leading to cement pouch (Fig. 19A, E). Cement glands surrounding copulatory apparatuses, releasing their contents in cement pouch (Fig. 19E). Female atrium opening to exterior through female gonopore. Sucker situated posterior to female copulatory apparatus, near distal end of body (Figs 18D, 19A, D).

Distribution. Ishigaki Island, Okinawa Prefecture, Japan (this study). A similar-looking specimen has been confirmed from the Kerama Islands, about 400 km far from Ishigaki Island (Ono 2015).

Habitat. Under rocks in shallow water reef.

Diagnosis. Body elongated oval; body margin slightly ruffled; pair of marginal tentacles without tapered tips; dorsal surface translucent, covered with numerous dots varying from white to light blue distributed all over body; brown speckles scattered lateral to pharyngeal pouch; pair of cerebral-eyespot clusters antero-posteriorly elongated along midline; marginal eyespots completely encircling body periphery; male and female gonopores separated; cylindrical penis papilla as long as narrow male atrium; two uterine vesicles in each oviduct.

Sequences. See Table 9.

Genetic distances. The genetic distances (uncorrected *p*-values) for the 712-bp COI sequences among three specimens were 0.4–2.2%. The translated protein sequences were identical.

Remarks. The collected specimens belong to *Pericelis* since they possess the

following characteristics: *i*) a pair of folded marginal tentacles with eyespots, *ii*) a central ruffled pharynx occupying half of the body, and *iii*) male copulatory apparatus without distinct prostatic organs. *Pericelis maculosa* has a translucent background in its body; thus, it can be distinguished from *P. byerleyana*, *P. cata*, *P. ernesti*, *P. nazahui*, *P. orbicularis*, *P. sigmeri*, and *P. tectivorum* by the brownish or blackish background of their dorsal surface (Table 11). Additionally, *P. maculosa* can be distinguished from *P. lactea* by the presence of dots that vary from white to light blue and the brown speckles on its dorsal surface. *Pericelis maculosa* has a similar background color to that of *P. alba*, *P. flavomarginata*, and *P. hymanae*, i.e., a translucent white coloration. However, the dorsal color pattern in *P. maculosa*, i.e., sparse brown speckles along both sides of the pharyngeal region and white to light blue dots scattered all over the body, clearly differs from that of *P. alba*, *P. flavomarginata*, and *P. hymanae* (Table 11).

Molecular phylogeny

The resulting ML and BI trees are identical in terms of topology; all nine species of *Pericelis* formed a clade (1.00 PP; 93% BS) (Fig. 20). *Pericelis lactea* was a sister to the other eight species; the monophyly of the eight species was not highly supported (0.72 PP; 79% BS). These eight species were separated into two clades. The first clade (1.00 PP; 98% BS) was formed by (*P. cata*, (*P. tectivorum*, (*P. byerleyana*, *P. orbicularis*))), each supported with 1.00 PP and 77%–100% BS. The second clade (1.00 PP; 96% BS) consisted of (*P. alba*, (*P. maculosa*, (*P. flavomarginata*, *P. hymanae*))); the relationship among these four species remains unclear due to low support values (0.65–0.70 PP; 37%–53% BS) (Fig. 20).

Discussion

My results support Hyman's (1955a) taxon concept that *Marcusia* is a junior synonym of *Pericelis*. In the phylogenetic tree produced here, '*Marcusia alba*' was nested within a clade along with the other eight species of *Pericelis* included in the analysis (Fig. 20); the result supports that this species belongs to *Pericelis*. Cuadrado et al. (2021) considered that *Marcusia* and *Pericelis* were separated genera in accordance with Faubel (1984). *Pericelis alba* was formerly placed in *Marcusia*, based on *i*) the presence of cerebral, frontal, and marginal eyespots; *ii*) the male copulatory organ enclosed in a muscular bulb; *iii*) the absence of a prostatic vesicle; and *iv*) the common male and female atrium (Cuadrado et al. 2021). However, none of these characteristics can, in fact, discriminate *Marcusia* from *Pericelis*. Although their molecular phylogenetic analyses with three species *M. alba*, *P. byerleyana*, and *P. orbicularis* suggested that *Marcusia* (represented by *M. alba*) was independent of other *Pericelis* species (Cuadrado et al. 2021, fig. 8), the resulting tree involving additional five species (*P. flavomarginata*, *P. hymanae*, *P. lactea*, *P. maculosa*, and *P. tectivorum*) disclosed that *Marcusia* was actually completely nested within *Pericelis*. Based on the current morphological and phylogenetical evidence, *M. alba* should be transferred to *Pericelis* as well as *Marcusia* should be a junior synonym of *Pericelis*.

The marginal-eyespot arrangement should not be taken into account as a diagnostic characteristic of *Pericelis*. My results revealed that the seven species with a complete series of marginal eyespots (*P. byerleyana*, *P. cata*, *P. flavomarginata*, *P. hymanae*, *P. maculosa*, *P. orbicularis*, and *P. tectivorum*) were separated into two clades (Fig. 20). This tree topology suggests that the complete series of marginal eyespots would have been either lost or acquired independently at least twice during the

evolution of these lineages. *Pericelis alba* and *P. lactea* have marginal eyespots that are distributed at only the anterior part of the body (Cuadrado et al. 2021; Fig. 16C). However, these two species match the diagnosis of *Pericelis* in terms of other characteristics such as paired marginal tentacles, the long and ruffled pharynx at the center of the body, and the absence of distinct prostatic organs. Given that no apparent traits can discriminate between the subclades within the nine analyzed *Pericelis* species, it is more reasonable to amend the diagnosis of *Pericelis* by removing the character of marginal-eyespot distribution than it is to establish new genera.

This study partially supports the view that the phylogenetic closeness among *Pericelis* species may be reflected by the similarity in their dorsal coloration. Here, the eight *Pericelis* species were separated into three clades (Fig. 20): a patternless species *P. lactea*, a clade of *P. byerleyana*, *P. cata*, *P. hymanae*, *P. orbicularis*, and *P. tectivorum* with a cream or beige background, and a clade of *P. alba*, *P. flavomarginata*, and *P. maculosa* with translucent white to gray background. Of the latter two clades, the species in one clade, i.e., *P. byerleyana*, *P. cata*, *P. orbicularis*, and *P. tectivorum*, can be characterized by having a reticulated brown pattern whereas the species in the other clade, i.e., *P. alba*, *P. flavomarginata*, *P. hymanae*, and *P. maculosa*, could not be characterized by any specific color pattern.

The phylogenetic relationship among *P. byerleyana*, *P. orbicularis*, and *P. tectivorum* is controversial. The branching order was not consistent with the previous result of Dittmann et al. (2019a); *P. byerleyana* was sister to *P. orbicularis* in this study whereas the species was reported to be close to *P. tectivorum* in Dittmann et al. (2019a). This contradiction may be caused by using different dataset (concatenated 18S and 28S sequences in this study; 28S only in Dittmann et al. (2019a)).

II-4. EURYLEPTIDAE Stimpson, 1857

Introduction

The family Eurylepidae is characterized by having *i*) a plicate tubular pharynx, *ii*) pseudotentacles, and *iii*) a single prostatic vesicle. Although this family requires to be revised due to its non-monophyly (Bahia et al. 2017, Dittmann et al. 2019a, Litvaitis et al. 2019), Eurylepidae is supposed to include 17 genera: *Acerotisa* Strand, 1926, *Anciliplana* Heath and McGregor, 1913, *Ascidiophilla* Newman, 2002, *Cycloporus* Lang, 1884, *Eurylepta* Ehrenberg, 1831, *Eurylepodes* Heath and McGregor, 1912, *Leptoteredra* Hallez, 1913, *Maritigrella* Newman and Cannon, 2000, *Katheurylepta* Faubel, 1984, *Oligoclado* Pearse, 1938, *Oligocladus* Lang, 1884, *Parastylostomum* Faubel, 1984, *Pareurylepta* Faubel, 1984, *Praetheceraeus* Faubel, 1984, *Prostheceraeus* Schmarda, 1859, *Stygolepta* Faubel, 1984, and *Stylostomum* Lang, 1884 (Faubel 1984). In Japan, seven eurylepid species were recorded prior to my research.

The eurylepid flatworm genus *Stylostomum* Lang, 1884 *sensu* Holleman (2001) is characterized by *i*) the body being oval in form and small to moderate in size, *ii*) the mouth and the male gonopore opening in common to the exterior, and *iii*) the tentacles reduced to small stumps or wanting. *Stylostomum* consists of nine valid species: *S. ellipse* (Dalyell, 1853); *S. felinum* Marcus, 1954; *S. frigidum* Bock, 1931; *S. hozawai* Kato, 1939b; *S. lentum* Heath and McGregor, 1913; *S. maculatum* Kato, 1944; *S. mixtomaculatum* Pitale and Apte, 2019; *S. sanjuania* Holleman, 1972; and *S. spanis* Holleman, 2001. All but *S. mixtomaculatum* (from west coast of India) (Pitale and Apte 2019) are distributed in the boreal and temperate realms north of latitude 36°N and south of latitude 36°S (Holleman 2001).

Stylostomum ellipse is known to show the most discontinuous distribution among polyclads (Prudhoe 1985). This species has been recorded in both the northeastern and southern parts of the Atlantic: Scandinavia to Mediterranean, South Africa, the Patagonian region, South Georgia, and the Antarctic region (Fig. 21A). In this section, I present the first record of *S. ellipse* from the Pacific.

Material and Methods

Collection of specimens and morphological observations

Eight polyclad specimens were collected subtidally by dredging in the Pacific coast of Hokkaido, northern Japan (Fig. 21B). Worms were photographed, anesthetized, then fixed in the same way of Chapter II-2. The histological observation was done in the same way as in Chapter II-3. All specimens were deposited in the ICHUM.

DNA extraction, PCR amplification, and sequencing

Total DNA of six specimens was extracted using a silica-based method (Boom et al. 1990) after specimens were homogenized. A 979-bp fragment of the 28S was amplified with the primer pair fw1 and rev2 (Sonnenberg et al. 2007). The protocols for PCR amplification and sequencing were same as the way for 28S in Chapter II-1. Sequences were checked and edited in the same way as mentioned in Chapter II-1. 28S uncorrected *p*-distance was calculated using MEGA ver. 7.0 (Kumar et al. 2016). All edited sequences have been deposited in DDBJ/EMBL/GenBank.

Data treatment

Same as in Chapter II-1.

Results

Taxonomy

Euryleptidae Stimpson, 1857

4. Genus *Stylostomum* Lang, 1884

8. *Stylostomum ellipse* (Dalyell, 1853)

(Figs 22–24)

Planaria ellipsis Dalyell, 1853: 101–102, pl. 14, figs 9–16 (Scotland).

Polycelis ellipsis Leuckart, 1859: 183.

Leptoplana ellipsis Diesing, 1862: 542; Johnston 1865, 7; McIntosh 1874, 150; McIntosh 1875, 107.

Stylochus roseus Sars in Jensen, 1878: 75, pl. 8, figs 1–3 (Norway).

Stylostomum ellipse Lang, 1884: 588; Gamble 1893a, 511; Bock 1913, 270–273 (Koster, Sweden; Spitzbergen, Norway; Falkland Islands; Tierra del Fuego; South Africa); Steinböck 1932, 334, 337; Steinböck 1933, 20 (Croatia); Bresslau 1928–1933, 241, fig. 240; Stummer-Traunfels 1933, 3575, fig. 154; Westblad 1952, 9–10 (Falkland Islands; South Georgia; Tierra del Fuego); Crothers 1966, 22 (Wales); Laverack and Blackler 1974, 32; Hendelberg 1974, 15, 17, figs 22–24 (Sweden); Galleni and Puccinelli 1981, 42, pl. VII, figs 1–3 (Britain); Prudhoe 1982a, 68–69, fig. 24A, B (Scotland); Faubel 1984, 223; Prudhoe 1985, 141; Holleman 2001, 227–229; Faubel and Warwick 2005, table 1 (off the Day Mark); Faasse and Ligthart 2007, 44–46, figs 1, 2 (Netherlands); Çinar 2014, 718, table (Turkey); Noreña et al.

2014, 18, fig 7C (Iberian Peninsula); Dittmann et al. 2019a, table 1 (Croatia); Tsuyuki et al. 2020b, 774–777, figs 2–4.

Stylostomum roseum Lang, 1884: 589; Bock 1913, 270.

Stylostomum variabile Lang, 1884: 73, 585–588, pl. 8, figs 3, 4, 6, pl. 30, fig. 14, pl. 36, fig. 22 (Gulf of Naples); Carus 1885, 157; Lo Bianco 1888, 400; Vaillant 1890, 656 (France); Bergendal 1890, 327 (Sweden); Gamble 1893a, 511–513, pl. XXXIX, fig. 1 (Isle of Man); Gamble 1893b, 47 (England); Gamble 1893c, 171, pl. XIV, figs 43–46 (Isle of Man); Hallez 1893, 178–180, pl. 3, fig. 9, pl. 4, figs 9–11; Hallez 1894, 230–233, pl. 2, figs 9–11; Plehn 1896, 172 (Patagonia); Browne et al. 1898, 813 (Ireland); Micoletzky 1910, 180 (Trieste); Bock 1913, 270; Southern in Farran 1915, 36 (Ireland); Southern 1936, 72 (Ireland); Bassindale and Barrett 1957, 251 (Stockholm); Eales 1961, 51.

Stylostomum sanguineum Hallez, 1893: 180, 197, pl. 3, fig. 10, pl. 4, figs 12–14 (southern France); Hallez 1894, 233–235, pl. 2, figs 12–14 (France); Bock 1913, 270, 273.

?*Stylostomum antarcticum* Hallez, 1905: 126 (Antarctica); Hallez 1907, 10–11, pl. 1, fig. 6, pl. 2, figs 5, 6.

?*Stylostomum punctatum* Hallez, 1905: 126–127 (Antarctica); Hallez 1907, 10, pl. 2, figs 1–4.

Material examined. ICHUM 6002, sagittal sections, 4 slides (HE), collected by Y. Oya in Nakanose (43.0061°N, 144.7892°E; depth 6.4–8.4 m), Akkeshi Bay, Hokkaido, Japan, by Research and Training Vessel *Misago-maru* (Akkeshi Marine Station, Hokkaido University), on June 28, 2018; ICHUM 6003, sagittal sections, 8 slides (HE),

collection data same as above; ICHUM 6007, sagittal sections, 10 slides (HE), collection data same as above except for date (June 20, 2019); ICHUM 6000, unsectioned, preserved in 70% ethanol, collection data same as above except for date (June 25, 2017); ICHUM 6001, unsectioned, preserved in 70% ethanol, collection data same as above; ICHUM 6004–6006, unsectioned, preserved in 70% ethanol, collection data same as above except for date (June 20, 2019).

Type locality. Scotland.

Description. Body oval, 4.0–12.3 mm in length, 1.8–5.8 mm in maximum width in living state. Marginal tentacles rudimentary. Dorsal surface smooth, translucent, variably colored (white, orange, and red) depending on gut contents (Figs 22A, 23A–C). Body margin transparent. Intestine highly branched, spreading all over body; median intestinal branches absent in front of pharyngeal pouch. Pair of cerebral-eyespot clusters extending from brain to middle portion of pharyngeal pouch; each cluster consisting of 4–22 eyespots; two large cerebral eyespots, closely set to each other, located at anterior-most region in each cluster (Fig. 22B); additional, single, small cerebral eyespot embedded in parenchyma located closely anterior to large cerebral eyespot on each side (Fig. 23D, indicated by arrowheads), only found in ICHUM 6001, 6003–6006 (Fig. 23A, B); no such additional small cerebral eyespots found in ICHUM 6002, 6007 (Fig. 23C). Marginal and tentacle eyespots spreading around two marginal tentacles (Fig. 22B). Ventral eyespots absent. Plicated pharynx tubular in shape. Male atrium and mouth sharing common pore, opening in front of pharynx (Fig. 24A, B). Male copulatory apparatus consisting of large seminal vesicle, spherical prostatic vesicle, and armed penis papilla, located under pharynx (Fig. 24C). Spermiducal vesicles well developed, forming single row on each side of midline, separately entering

into seminal vesicle. Seminal vesicle oval, coated with thick muscular wall. Prostatic vesicle half as large as seminal vesicle, former situated above latter (Fig. 24A, C). Penis papilla armed with pointed tubular stylet, enclosed in penis pouch, protruding into male atrium. Female reproductive system posterior to pharynx. Female gonopore and sucker situated posterior to male-atrium–mouth common pore (Fig. 24A, D, E). Uterus bending directly downward, splitting into left and right immediately behind cement pouch (Fig. 24D). Uterine vesicle developed when containing eggs. Cement glands numerous, concentrated around vagina and releasing their contents into cement pouch.

Sequences. Partial 28S sequences (979 bp) from four individuals: LC508269 from ICHUM 6002, LC508270 from ICHUM 6003, LC508271 from ICHUM 6004, LC508272 from ICHUM 6006; all were completely identical.

Genetic distance. In terms of partial 28S rDNA sequences, the uncorrected *p*-distance between the overlapping 972 bp of LC508269–508272 (979 bp) from Japan and GenBank MN384704 (1395 bp) from Punat, Adriatic Sea (Dittmann et al. 2019a), was 2.160%.

Remarks. The following morphological characteristics observed in my specimens correspond to the diagnostic characters for *S. ellipse* provided by previous researchers (Lang 1884, Bock 1913, Marcus 1954): *i*) pair of two large cerebral eyespots anterior to smaller ones in each cerebral-eyespot cluster and *ii*) seminal vesicle twice as large as prostatic vesicle.

Stylostomum ellipse has potentially five subjective synonyms: *S. antarcticum* (Antarctica), *S. punctatum* (Antarctica), *S. roseus* (Norway), *S. sanguineum* (southern France), and *S. variabile* (Italy). Lang (1884) suggested that slight morphological differences in the arrangement of the eyespots among *S. ellipse*, *S. roseum*, and *S.*

variabile possibly represented a variation within a single species. Bock (1913) synonymized *S. roseum* and *S. variabile* with *S. ellipse* based on his specimens collected in Sweden, Norway, South America, and South Africa. Bock (1913) also remarked that *S. punctatum*, which was considered to be identical to *S. antarcticum*, and *S. sanguineum* each possibly represented a particular local variety of *S. ellipse*. Likewise, Faubel (1984) regarded *S. roseum*, *S. sanguineum*, and *S. variabile*, as synonymous with *S. ellipse*. In addition, Faubel (1984) uncertainly placed *S. antarcticum* and *S. punctatum* in the synonymy of *S. ellipse* as well.

Discussion

This study represents the first record of *S. ellipse*—or at least its close relative, if not conspecific (see below)—from the Pacific Ocean. *Stylostomum ellipse* in the sense of this thesis shows a cosmopolitan distribution, so far recorded from the Atlantic coasts of Europe (including the Mediterranean Sea), South America, and South Africa; and the Antarctic Sea (Fig. 21A). Being from the sub-boreal zone, the present findings of *S. ellipse* in the Pacific coast of northern Japan (Fig. 21B) accord with what was previously known as to the distribution of the species, which has been mostly in the cold-temperate provinces (Holleman 2001).

While the present specimens are morphologically identifiable as *S. ellipse*, there remains a possibility that this morphospecies is comprised of two or more cryptic species, as the present genetic data suggest: the 28S uncorrected *p*-distance between Hokkaido and Punat, 2.16%, was much greater than a maximum intraspecific distance, 0.543%, observed within the Caribbean population of the pseudocerotid cotylean *Pseudoceros bicolor* Verrill, 1901 (Litvaitis et al. 2010). In addition, the partial 28S

sequences of the two distinct geographical populations (South Florida *vs.* the Great Barrier Reef) of *Pseudoceros splendidus* (Lang, 1884) have been reported to be identical (Litvaitis et al. 2019), even though the two distributions are over 10,000 km far apart. It suggests that the intraspecific genetic variation in a cotylean cosmopolitan species be limited like as in a sympatric species. Without morphological data of the Punat material (Dittmann et al. 2019a) and molecular data from the type locality (St. Andrews, Scotland), the possibility cannot be ruled out that even the Punat specimen may not represent *S. ellipse* s.str. To firmly establish the taxonomic identity of *S. ellipse*, further studies are necessary by careful morphological and molecular comparison among the populations around the northeastern and south Atlantic including the type locality. Likewise, confirmation of the validity pertaining to the five potentially subjective synonyms *S. antarcticum*, *S. punctatum*, *S. roseum*, *S. sanguineumi*, and *S. variabile* necessitates genetic and morphological examination of material from each type locality.

II-5. PROSTHIOSTOMIDAE LANG, 1884

Introduction

The family Prosthiostomidae is characterized by *i*) an elongated body with a ventral sucker posterior to the female gonopore, *ii*) a plicate tubular pharynx, and *iii*) paired prostatic vesicles. Monophyly of this family has been supported in previous molecular phylogenetic studies based on partial sequences of the 28S gene alone (Bahia et al. 2017, Tsunashima et al. 2017, Litavaitis et al. 2019) or in combination with the 18S gene (Dittmann et al. 2019a). Aguado et al. (2017) argued that Prosthiostomidae was not monophyletic, but this is probably due to the fast-evolving gene markers that they utilized (i.e., the mitochondrial 16S and COI genes). Prosthiostomidae currently includes five genera: *Enchiridium* Bock, 1913; *Enterogonimus* Hallez, 1911; *Euprosthiostomum* Bock, 1925; *Lurymare* Du Bois-Reymond Marcus and Marcus, 1968; and *Prosthiostomum* Quatrefages, 1845 (Faubel 1984).

The genus *Enchiridium sensu* Faubel (1984) contains eight species: *E. delicatum* (Palombi, 1939); *E. evelinae* Marcus, 1949; *E. gabriellae* (Marcus, 1949); *E. japonicum* Kato, 1943b; *E. magec* Cuadrado et al., 2017; *E. periommatum* Bock, 1913; *E. punctatum* Hyman, 1953; and *E. russoi* (Palombi, 1939). Members of this genus are distinguished from other prosthiostomids by having a muscle sheath (or bulb) that encloses just the two prostatic vesicles among other male reproductive organs; i.e., the seminal vesicle and the male atrium are not enclosed by the muscle sheath (Faubel 1984). Before starting my research, there was no record of *Enchiridium* from Japan (Kato 1944).

One of the genera, *Lurymare*, may be a junior synonym of *Prosthiostomum* (cf.

Dittmann et al. 2019a, Litvaitis et al. 2019), because the alleged morphological distinction between the two genera is based on a character that can vary ontogenetically (Prudhoe 1989), namely the presence/absence of a muscle bulb surrounding the seminal and prostatic vesicles (Faubel 1984). Indeed, Litvaitis et al. (2019) transferred two species formerly placed in *Lurymare* into *Prosthiostomum* primarily because their phylogenetic positions were nested within a clade comprising *Prosthiostomum* species. While the separation of *Lurymare* from *Prosthiostomum* based on this character alone (i.e., presence/absence of a muscle bulb) appears systematically unsubstantiated, a definitive taxonomic act to formally synonymize *Lurymare* with *Prosthiostomum* should not proceed until an analysis is performed using reliably identified prosthiostomid specimens, including those representing the type species of the two genera (*Prosthiostomum drygalskii* Bock, 1931 for *Lurymare*; *Planaria siphunculus* Delle Chiaje, 1828 for *Prosthiostomum*).

For the sake of conciseness, this *Prosthiostomum–Lurymare* complex is simply referred to as the genus *Prosthiostomum* in this thesis. It currently contains about 60 species worldwide, which are characterized by *i*) the seminal and prostatic vesicles that are occasionally (but usually not) surrounded by a common muscle bulb, *ii*) the main intestine accompanied with a frontal branch over the pharynx, and *iii*) the penis armed with a pointed tubular stylet (cf. Faubel 1984). Congeners are distinguished chiefly based on body color pattern and eyespot arrangement (Bock 1913, Hyman 1939b). In Japan, 21 species of *Prosthiostomum* have been reported (Kato 1944). Nineteen of these—all except for *P. purum* Kato, 1937b (Litvaitis et al. 2019 [Israel]) and *P. trilineatum* Yeri and Kaburaki, 1920 (Newman and Cannon 2003 [Australia]; Pitale et al. 2014 [India]; Litvaitis et al. 2019 [Guam])—have so far been found exclusively

along the Japanese coasts, and thus may be endemic to this area.

In this section, I provide morphological descriptions of a species of *Enchiridium* and two species of *Prosthiostomum* that turned out to be new to science during my research and five known *Prosthiostomum* species originated from Japan. In addition, I examine the generic placements of these species through molecular phylogenetic analysis using sequences of 28S and COI.

Material and Methods

Sampling and morphological observation

Specimens were collected from Misaki (Kanagawa), Shirahama (Wakayama), Kochi, Amakusa (Kumamoto), Kagoshima, and Okinawa. In Misaki, nine specimens were from kelp holdfasts at a depth of 2 m by SCUBA on February 19, 2019; the others were subtidally from branching coralline algae by snorkeling on March 25, 2019. In Shirahama, all specimens were collected intertidally. In Kochi, Kagoshima, and Okinawa, all polyclads were collected from undersurfaces of rocks in subtidal zone by SCUBA. In Amakusa, colonies of *Acropora* species were collected from a shallow reef habitat (1–5 m depth) under Kumamoto Prefectural Government Permits (No. 2956 for 2018; No. 2992 for 2019); coral colonies were carefully chiseled off substrate and transported in a container with fresh seawater, then living flatworms crawled out from the colonies and were found on the inner wall of the container. All worms were anesthetized in seawater containing menthol before fixation. The worms were photographed, fixed, and preserved in the same way in Chapter II-3; for DNA extraction, a posterior piece of the body was removed and stored in 99.5% ethanol. The methods of histological observation were almost accordance with those in Chapter II-1;

for only *P. torquatum*, sections were stained with not only HE but also MT. All examined specimens were deposited in the ICHUM or Aoi Tsuyuki's personal polyclad collection (AT).

DNA extraction, PCR amplification, and sequencing

Total DNA was extracted in the same way as mentioned in Chapter II-2 or using a silica-based method (Boom et al. 1990) after specimens were incubated overnight at 55°C in 180 µl of ATL buffer (Qiagen, Germany) with 20 µl of proteinase K (>700 U/ml; Kanto Chemical, Japan). A 585-bp fragment of the COI gene was amplified with primers Pros_COIF (5′-AGGTGTTTGAGCAGGTTTTATAGGTACAGG-3′) and Pros_COIR (5′-ATGGGATCTCCTCCTCCTGAAGGRTC-3′) for all species examined except for *P. ohshimai* and *P. sonorum*. In *P. torquatum*, the different region of COI from above (462 bp) was also amplified with the primer pair Hoso_COI_F (5′-ATGGACGTCCTTTGCGTGAT-3′) and Hoso_COI_R (5′-CAGGATGTGTTCTAGGAGAGCC-3′) to compare the region with the most closely related species. A fragment (ca. 1010 bp) of the 28S was amplified with primers fw1 and rev2 (Sonnenberg et al. 2007) for all species examined. PCR amplification and direct sequencing were done in the same way as mentioned in Chapter II-1. Sequences were checked and edited in the same way as mentioned in Chapter II-1. All edited sequences except for those of *P. ohshimai* and *P. sonorum* have been deposited in DDBJ/EMBL/GenBank.

Phylogenetic tree construction and genetic distance calculation

For a phylogenetic analysis, a concatenated dataset comprised of partial COI and 28S

sequences was prepared. In addition to the ones determined for the eight species, two partial COI sequence of *P. amri* Rodríguez et al., 2021 and *P. grande* Stimpson, 1857 as well as other 20 partial 28S sequences of 19 prosthiostomid species downloaded from GenBank were used for the analysis (Table 12). As outgroups, *Prostheceraeus crozieri* (Hyman, 1939a) (Eurylepidae) and *Pseudobiceros splendidus* (Lang, 1884) (Pseudocerotidae) were also downloaded (Table 12). Alignment of COI was done manually with MEGA ver. 7.0 (Kumar et al. 2016). The 28S sequences were aligned using MAFFT ver. 7.427 (Katoh et al. 2017), with L-INS-i strategy selected by the "Auto" option; ambiguous sites were trimmed using Clipkit ver. 1.0 via the "kpic" option (Steenwyk et al. 2020). A concatenated dataset (2,104 bp in total length, consisting of 583-bp COI and 1,521-bp 28S) was prepared also with MEGA ver. 7.0.

The phylogenetic analysis was performed with ML method by using IQtree ver. 1.6 (Nguyen et al. 2015) under a partition model. The optimal substitution models selected with PartitionFinder ver. 2.1.1 (Lanfear et al. 2016) under the AIC (Akaike 1974) using the greedy algorithm were GTR+I+G (28S, first and third codon positions in COI) and GTR+G (second codon position in COI). Nodal support within the ML tree was assessed by analyses of 1000 bootstrap pseudoreplicates.

Data treatment

Same as in Chapter II-1.

Results

Taxonomy

Family Prosthiostomidae Lang, 1884

5. Genus *Enchiridium* Bock, 1913 *sensu* Faubel (1984)

9. *Enchiridium daidai* Tsuyuki and Kajihara, 2020

[Japanese name: daidai-hoso-hiramushi]

(Figs 25–27)

Enchiridium daidai Tsuyuki and Kajihara, 2020: 19–26, figs 2–4 (Kagoshima, Okinawa).

Etymology. The specific name *daidai* is a Japanese noun, meaning the color orange. It was named after the thin marginal orange line surrounding the entire dorsal fringe.

Material examined. Holotype: ICHUM 5993, sagittal sections through reproductive structures, 22 slides (HE), along with the remaining unsectioned body (preserved in 70% ethanol), collected by A. Tsuyuki at 13–14 m depth off the coast of Bonomisaki (31.2542°N, 130.2150°E), Kagoshima, Japan, on 26 July 2018. Paratypes (2 specimens): ICHUM 5994, sagittal sections through head to reproductive structures, 9 slides (HE), collected by A. Tsuyuki at 5 m depth in Nago (26.6013°N, 127.9137°E), Okinawa, Japan, on 22 May 2019; ICHUM 5995, cross sections through reproductive structures, 21 slides (HE), collection data same as ICHUM 5994.

Type locality. Off the coast of Bonomisaki (31.2542°N, 130.2150°E), Kagoshima, Japan.

Description. Body elongated, tapered posteriorly, 28–77 mm long (77 mm in holotype) and 4.6–14 mm maximum width (14 mm in holotype) in living state (Fig. 25A); anterior margin rounded; mid-point of posterior margin acute. Tentacles absent. Dorsal surface smooth, translucent, fringed with thin marginal orange line (Fig. 25A). Ventral surface translucent, without color pattern. Pair of cerebral-eyespot clusters, each consisting of 20–52 eyespots (left 20 and right 23 in holotype); each cluster of an antero-posteriorly elongated spindle shape (Fig. 25B). Marginal-eyespot clusters forming single marginal band, extending to position of mouth (about anterior one-eighth of body) along margins on both sides; marginal eyespots abundant along anterior margin, diminishing posteriorly (Fig. 25B). Ventral eyespots absent. Intestine highly branched, spreading all over body. Plicated pharynx tubular in shape, about one-fifth of body length, located in anterior one-third of body (Fig. 25A). Mouth situated at anterior end of pharynx, behind brain. Male and female gonopores closely set, both situated behind posterior end of pharynx. Male copulatory apparatus consisting of large seminal vesicle, pair of prostatic vesicles, and armed penis papilla (Fig. 26A). Antero-posterior length of seminal vesicle more than twice as long as diameter of each prostatic vesicle. Spermiducal vesicles forming single row on each side of midline, separately entering into seminal vesicle. Ejaculatory duct with thick muscular layer, entering penis papilla. Prostatic ducts with muscular layer, connected to ejaculatory duct separately at proximal end of penis papilla. Pair of spherical prostatic vesicles coated within thin non-nucleated muscular wall, arranged anterodorsally to ejaculatory duct. Common muscular sheath enclosing two prostatic vesicles (Fig. 26B). Seminal vesicle oval, coated with thick muscular wall, narrowing anteriorly and forming ejaculatory duct; latter almost immediately penetrating common muscular sheath (Fig. 26C). Penis papilla armed with

pointed tubular stylet, enclosed in penis pouch, protruding into male atrium (Fig. 26C). Male atrium elongated anteriorly, lined with ciliated, muscularized epithelium (Fig. 26B). Female reproductive system immediately posterior to male reproductive system. Cement glands numerous, concentrated around vagina and releasing their contents in cement pouch (Fig. 26D). Vagina curving anteriorly, leading to two narrow lateral branches of uteri. Each branch of uteri turning laterally and then running backwards. Lang's vesicle absent. Sucker set on body center (Fig. 25A).

Distribution. To date, this species has been known from Bonomisaki (Kagoshima) and Nago (Okinawa).

Habitat. Subtidal (5–14 m depth), under rocks.

Variation. Specimens from Kagoshima and Okinawa differed in body size. The holotype from Kagoshima was 77 mm long and 15 mm wide, whereas the paratype specimens from Okinawa were 28–37 mm long and 4.6–7.4 mm wide (Fig. 27).

Diagnosis. Body elongated, usually rounded anteriorly; dorsal surface translucent, fringed by a thin marginal orange line; marginal eyespots present only anteriorly; plicated pharynx tubular in shape, about one-fifth of body length; pair of prostatic vesicles bound by common muscular sheath, the latter penetrated by ejaculatory duct.

Sequences. Partial COI (585 bp) and 28S (1,017 bp) sequences from three individuals: LC504240 (COI), LC504235 (28S) from ICHUM 5993 (holotype); LC504238 (COI), LC504236 (28S) from ICHUM 5994 (paratype); LC504239 (COI), LC504237 (28S) from ICHUM 5995 (paratype).

Genetic distances. The genetic distances (uncorrected *p*-values) for the COI sequences among three specimens of *E. daidai* were 0.2–1.2%. Genetic distances

between individuals from different localities (Kagoshima *vs.* Okinawa), 1.0–1.2%, were larger than that between individuals from the same locality (Okinawa), 0.2%.

Remarks. In spite of the noticeable difference in body size, specimens from Kagoshima and Okinawa—all having reached sexual maturity—were identified as conspecific. They shared the following morphological characteristics: *i*) body dorsally fringed with a thin orange line, *ii*) marginal-eyespot band extending to the position of the mouth (about anterior one-eighth of the body), *iii*) two prostatic vesicles covered by a common muscle sheath, and *iv*) common muscle sheath penetrated by ejaculatory duct. In addition, the COI *p*-distances among the specimens, 0.2–1.2%, fell in a range of intraspecific values, 0.00–2.00%, which was observed in four species of the acotylean leptoplanoid *Notocomplana* (Oya and Kajihara 2017), thus rendering support for my interpretation of conspecificity. Within Polycladida, remarkable intraspecific variation in body size has been reported for the acotylean stylochoid *Planocera reticulata* (Stimpson, 1855), which was recorded to vary by 10–80 mm in length and 6–45 mm in width (Yeri and Kaburaki 1918). Among the cotylean Prosthiostomidae, sexually matured individuals of *Prosthiostomum cyclops* (Verrill, 1901) have been reported to vary a great deal (> ×10) in size by locality: 75–90 mm long × 10–15 mm wide in the Bermuda Islands (Verrill 1901), whereas 6.5 mm long × 1.7 mm wide in the islands of Bonaire and Klein Bonaire (Du Bois-Reymond Marcus and Marcus 1968). These observations may imply that these polyclads undergo an indeterminate growth, in which growth is not terminated after reaching adulthood, although other factors—such as geographical and ecological ones—must also be taken into account.

Enchiridium daidai is distinguished from *E. evelinae*, *E. japonicum*, *E. periommatum*, and *E. punctatum* by the arrangement of the marginal eyespots; the

marginal-eyespot band in these four species completely encircles the periphery of the dorsal surface, whereas that of my specimens is present only along the anterior margin. The species herein is also easily distinguished from the other four congeners, *E. delicatum*, *E. gabriellae*, *E. magec*, and *E. russoi*, by the thin marginal orange line surrounding the entire dorsal fringe and by the lack of spots or maculae on the dorsal surface (Table 13).

Reaching 77 mm in body length, *Enchiridium daidai* is the largest species in the genus over *E. punctatum* (about 40 mm in body length; Hyman 1953, p. 386). Indeed, *E. daidai* is the second largest in the Prosthiostomidae after *P. cyclops*, which reaches 90 mm (Verrill 1901). Among about 80 species of prosthiostomids, only *E. daidai* and *P. cyclops* are known to exceed 70 mm in body length, while most of the other species are less than 30 mm long. Therefore, the present species is considered to be unusually big in body size for a prosthiostomid.

6. Genus *Prosthiostomum* Quatrefages, 1845

10. *Prosthiostomum auratum* Kato, 1937b

(Fig. 28)

Prosthiostomum auratum Kato, 1937b: 363–364, pl. 22, fig. 8, text-figs 23–24 (Misaki); Kato 1938a, 572 (Amakusa); Kato 1938b, 589, pl. 39, fig. 7 (Shirahama); Kato 1939b, 152 (Aomori); Kato 1944, 307 (Noto); Prudhoe 1985, 191; Hagiya and Gamô 1992, 18, pl. 1, fig. 9, pl. 2, fig. 9 (Manaduru); Tsuyuki et al. 2021, 5–7, fig. 1 (Misaki).

Euprosthiostomum auratum (Faubel, 1984): 234.

Material examined. ICHUM 6149, sagittal sections, 5 slides (HE), collected by T. Miura, K. Oguchi, and H. Kohtsuka in Arai-hama (35.1609°N, 139.6105°E), Misaki, Kanagawa, Japan, on March 25, 2019; ICHUM 6150, sagittal sections, 4 slides (HE), collection data same as above; AT2019033110, unsectioned, preserved in 70% ethanol, collection data same as above; AT2019022104–AT2019022110, unsectioned, preserved in 70% ethanol, collection data same as above except for date (February 19, 2019).

Type locality. Misaki, Kanagawa, Japan.

Description. Body elongated, tapered posteriorly, 7.3–12.0 mm long and 2.3–3.4 mm wide at its widest point while alive; anterior margin rounded; mid-point of posterior margin acute. Tentacles absent. Dorsal surface smooth, uniformly golden-yellow except cerebral-eyespot area; a little darker along midline; a few reddish-brown spots present in front of brain in one individual (Fig. 28A). Ventral surface translucent without color pattern (Fig. 28B, C). Pair of linear cerebral-eyespot clusters, each consisting of five to 10 eyespots; anterior end of cluster located at distance of 0.80 mm posterior to anterior margin of body (Fig. 28D). About 12 marginal eyespots arranged in single row along frontal margin, extending anterior to brain (Fig. 28D, E). One pair of ventral eyespots present near front end of brain (Fig. 28E). Anterior branch of main intestine short, extending to position 0.33 mm posterior from anterior margin of body (Fig. 28F, G). Plicated pharynx tubular in shape, 1.46 mm in length (about one-third of body), located in anterior half of body (Fig. 28B, F). Mouth situated at anterior end of pharynx, located at 1.10 mm posterior from anterior margin of body (Fig. 28B, F). Male copulatory apparatus consisting of large seminal vesicle, pair of prostatic vesicles, and

armed penis papilla, located immediately posterior to pharyngeal pocket (Fig. 28F). Pair of spermiducal vesicles forming single row on each side of midline, separately entering into seminal vesicle laterally (Fig. 28C, F). Ejaculatory duct with thick muscular layer, entering penis papilla. Prostatic ducts with thin muscular layer, separately connected to ejaculatory duct behind proximal end of penis papilla. Pair of spherical prostatic vesicles, each coated with 0.05-mm-thick, non-nucleated muscular wall, located on each side of ejaculatory duct. Seminal vesicle oval, coated with 0.04-mm-thick muscular wall. Diameter of prostatic vesicle (0.16 mm) as long as dorsoventral diameter of seminal vesicle (0.13 mm). Penis papilla armed with pointed tubular stylet (0.08 mm in length), enclosed in penis pouch, protruding into male atrium (Fig. 28F, H). Male atrium elongated anteriorly from gonopore to penis pouch (0.31 mm in length). Female gonopore situated at 0.25 mm behind male gonopore (Fig. 28B). Female copulatory apparatus posterior to male reproductive system. Female gonopore leading to vagina across cement pouch; proximal end of vagina anteriorly curved (Fig. 28F). Cement glands developed, concentrated around vagina and releasing their contents in cement pouch (Fig. 28H). Oviducts not observed. Sucker large (0.46 mm in diameter), situated at center of body (0.32 mm length from female atrium; 4.10 mm length from posterior extremity) (Fig. 28B).

Distribution. So far, this species has only been confirmed along Japanese coasts, from the northmost Honshu Island to the southwestern Kyushu: Yuno-shima near Asamushi, Aomori; Ohtsuchi, Iwate; Nanao, Noto, Ishikawa; Misaki, Kanagawa; Manazuru, Kanagawa; Suzaki, Shimoda, Shizuoka; Shirahama, Wakayama; and Tomioka, Amakusa, Kumamoto.

Habitat. In the original description, this species was found on the surfgrass

Phyllospadix in Misaki (Kato 1937b). In Shirahama, numerous specimens were obtained under stones (Kato 1938b). The present specimens were collected from the seaweed Corallinales spp. and holdfasts of the kelp *Eisenia bicyclis* subtidally in Misaki.

Sequences. Partial COI (585 bp) and 28S (1,011 bp) sequences from two individuals: LC625892 (COI) and LC625886 (28S) from AT2019033110; LC625893 (COI) from ICHUM 6149.

Remarks. Although *P. auratum* was once placed in *Euprosthiostomum* (Faubel 1984), my morphological examination of the present topotypes confirmed that it is part of *Prosthiostomum*, primarily due to the presence of a frontal branch of the main intestine, a character state that was not mentioned in the original description by Kato (1937b). My specimens are consistent with the original description in that *i*) the dorsal body is colored uniformly golden-yellow, *ii*) each cerebral-eyespot cluster is formed in a linear shape, and *iii*) a pair of prostatic vesicles are moderately large. No mention was made as to the ventral eyespots in the original description, but these were clearly present in a photograph of a specimen from Shirahama (Kato 1938b, pl. 39, fig. 7) as well as in my specimens (Fig. 28E).

As was shown in *P. auratum* based on topotypes, there is room for examination in the adequacy of classifying the other five species, *P. angustum* Bock, 1913, *P. bellum* Kato, 1939a, *P. laetum* Kato, 1938a, *P. matarazzoi* Marcus, 1950, and *P. pulchrum* Bock, 1913, in the genus *Euprosthiostomum*, because these were listed under the latter genus by Faubel (1984) without sound basis. The genus *Euprosthiostomum* was established by Bock (1925) based on *E. adhaerens* Bock, 1925, which was characterized by *i*) the location of the sucker relatively near the caudal end of the body and *ii*) the

absence of a frontal median branch of the intestine (Bock 1925, Marcus 1948, Hyman 1953). Subsequently, *E. viscosum* Palombi, 1936, *E. mortenseni* Marcus, 1948, and *E. pakium* Du Bois-Reymond Marcus and Marcus, 1968 were established in this genus. Also, *Prosthiostomum molle* Freeman, 1930 was transferred to *Euprosthiostomum* by Hyman (1953). Later, Faubel (1984) proposed the presence/absence of the frontal median branch of the intestine as a determination key to distinguish *Prosthiostomum* (present) from *Euprosthiostomum* (absent). As a result, Faubel (1984) transferred *P. angustum*, *P. auratum*, *P. bellum*, *Prosthiostomum exiguum* Hyman, 1959, *P. laetum*, *P. matarazzoi* (= *Lurymare matarazzoi*), and *P. pulchrum* to *Euprosthiostomum*. In fact, however, in the original descriptions of *P. angustum*, *P. auratum*, *P. bellum*, *P. laetum*, *P. matarazzoi*, and *P. pulchrum*, the presence/absence of this branch was not clearly shown (Bock 1913, Kato 1937b, 1938b, 1939a, Marcus 1950), although Faubel (1984) apparently assumed as if the frontal median branch was absent in these species. In the same work, Faubel (1984) categorized other 34 species for which the presence/absence of the frontal branch was unknown into *Prosthiostomum* (see Faubel 1984, p. 232). Among the six species which was transferred into *Euprosthiostomum* by Faubel (1984), *P. matarazzoi* was redescribed based on freshly collected material (Bahia 2016); a lectotype was subsequently designated for this species (Bahia and Schrödl 2018). Still, the presence/absence of the frontal branch in *P. matarazzoi* was not mentioned in these works (Bahia 2016, Bahia and Schrödl 2018).

9. ***Prosthiostomum hibana*** Tsuyuki, Kohtsuka, and Kajihara, 2021

[Japanese name: hibana-hoso-hiramushi]

(Figs 29–31)

Prosthiostomum hibana Tsuyuki, Kohtsuka, and Kajihara, 2021: 7–11, figs 2–4 (Misaki).

Etymology. The specific name *hibana* is a Japanese noun, meaning fire sparks. It was named after the dorsal color pattern of the orange maculae, which look like sparks flying.

Material examined. Holotype: ICHUM 6147, sagittal sections, 6 slides (HE), collected by T. Miura, K. Oguchi, and H. Kohtsuka in Arai-hama (35.1609°N, 139.6105°E), Misaki, Kanagawa, Japan, on March 25, 2019. Paratype: ICHUM 6148, paratype, 4 slides (HE), collection data same as holotype.

Type locality. Arai-hama, Misaki, Kanagawa, Japan.

Description of holotype. Body elongated, tapered posteriorly, 14 mm long and 3 mm wide at its widest point while alive (Fig. 29A); anterior margin rounded; mid-point of posterior margin acute. Tentacles absent. Dorsal surface smooth, translucent, uniformly covered with numerous orange maculae, some of which being agglutinated and forming larger maculae; the larger maculae scattered throughout (Fig. 29A); orange pigments more abundant medially. Ventral surface translucent, without color pattern (Fig. 29B, C). Pair of cerebral-eyespot clusters, each consisting of nine (left) and eight (right) eyespots; each cluster forming an antero-posteriorly elongated, curved line; anterior end of clusters located at distance of 0.85 mm posterior to anterior margin of body (Fig. 29D). About 20 marginal eyespots distributed antero-ventrally in front of brain (Fig. 29E, F). Four pairs of ventral eyespots, embedded in parenchyma (Fig. 29G); four eyespots on each side arranged at corner of parallelogram (Fig. 29E). Intestine

highly branched, spreading all over body; anterior branch of main intestine extending to position 0.4 mm posterior from anterior margin of body. Plicated pharynx tubular in shape, 4.1 mm in length (about two-sevenths of body), located in anterior half of body (Fig. 29A, B). Mouth situated at anterior end of pharynx, located at 1.04 mm posterior from anterior margin of body (Fig. 29B). Male gonopore, female gonopore, and sucker closely set on body center (Fig. 29B, C); distance between male and female gonopores being 0.34 mm; distance between female gonopore and sucker being 0.39 mm. Male copulatory apparatus consisting of large seminal vesicle, pair of prostatic vesicles, and armed penis papilla, located immediately posterior to pharyngeal pocket (Fig. 30A). Spermiducal vesicles forming single row on each side of midline, each running from posterior to anterior, then bending posteriorly and separately entering into seminal vesicle. Ejaculatory duct wide, with thick muscular layer, entering penis papilla. Prostatic ducts with muscular layer, connected to ejaculatory duct separately at proximal end of penis papilla. Pair of spherical prostatic vesicles coated within 0.05-mm-thick, non-nucleated muscular wall, located on both sides of ejaculatory duct (Fig. 30A, B). Seminal vesicle oval, coated with 0.11-mm-thick muscular wall; its lumen narrow and elongated in shape (Fig. 30A, C). Without common muscular bulb enclosing male copulatory apparatus. Seminal vesicle (long axis 0.34 mm, short axis 0.23 mm) more than twice as large as prostatic vesicle (0.14 mm in diameter) (Fig. 30A, B). Penis papilla armed with pointed tubular stylet (0.14 mm in length), enclosed in penis pouch, protruding into male atrium (Fig. 30D). Penis sheath present between penis pouch and male atrium (Fig. 30A, B). Male atrium elongated anteriorly from male gonopore to penis pouch (0.40 mm in length); inner wall deeply ruffled, lined with ciliated and muscularized epithelium (Fig. 30A, B). Immature female reproductive system

immediately posterior to male copulatory apparatus. Female gonopore leading to vagina across cement pouch (Fig. 30A, E); proximal end of vagina anteriorly curved (Fig. 30A). Cement glands and oviducts undeveloped and not observed. Lang's vesicle absent. Sucker large (0.40 mm in diameter; 2.9% of body length), situated immediately behind female gonopore (Fig. 30E), at 4.2 mm anterior from posterior margin of body.

Description of paratype. Body 7.8 mm long and 2.9 mm wide at its widest point when slightly contracted while alive. Body coloration almost same as holotype. Pair of cerebral-eyespot clusters, each consisting of seven (left) and eight (right) eyespots (Fig. 31A). About 20 marginal eyespots, distributed ventrally along anterior margin (Fig. 31B). Ventral eyespots, 3–4 pairs in number, embedded in parenchyma (Fig. 31B). Frontal branch of main intestine extending anterior to brain. Pharynx 2.82 mm in length. Male and female reproductive systems undeveloped. Sucker large (0.20 mm in diameter; 2.6% of body length), situated on body center (3.6 mm anterior from posterior margin of body).

Distribution. So far only from the type locality, Misaki, Kanagawa, Japan.

Habitat. Among branching coralline algae Corallinales spp.

Diagnosis. Body elongated; anterior margin rounded; dorsal surface translucent, covered with numerous orange maculae, some of which being agglutinated and forming larger maculae; pair of linear cerebral-eyespot clusters composed of relatively few eyespots; 3–4 pairs of ventral eyespots, embedded in parenchyma; marginal eyespots distributed antero-ventrally; inner wall of male atrium deeply ruffled; lumen of seminal vesicle narrow and elongated in shape; sucker large, occupying about 3% of body length, situated on body center.

Sequences. Partial COI (585 bp) and 28S (1,009 bp) sequences from two

individuals: LC625894 (COI) and LC625887 (28S) from the holotype (ICHUM 6147); LC625895 (COI) and LC625888 (28S) from the paratype (ICHUM 6148).

Remarks. Among ~60 species in *Prosthiostomum*, the species is unique in having 3–4 pairs of ventral eyespots (Figs 29E, 31B) and thus can easily be distinguished from the other congeners, where the ventral eyespots are mostly absent or at most single pair in number, if present. Only *P. bellum* has been known to possess two pairs of ventral eyespots (Kato 1939a), but it is quite different from *P. hibana* in the body coloration (white background with numerous brown spots scattered over the body in *P. bellum*; translucent with orange maculae in *P. hibana*) as well as the number of cerebral eyespots in each cluster (about 40 in *P. bellum*; 7–9 in *P. hibana*).

Nine other congeners are known to show a similar character state to that in *P. hibana* pertaining to either dorsal coloration or cerebral-eyespot arrangement (Table 14). *Prosthiostomum capense* Bock, 1931, *P. dohrnii* Lang, 1884, and *P. grande* resemble *P. hibana* in having yellow to orange maculae or spots scattered all over the body; *P. dohrnii* and *P. grande* are different from the species in the number and distribution of the cerebral eyespots; *P. capense* is separated from *P. hibana* by the size and position of the sucker (small, situated at four-fifths of the body in *P. capense*; large, situated at the middle of the body in *P. hibana*) (Table 14). The five species *P. auratum*, *P. cynarium* Marcus, 1950, *P. purum* Kato, 1937b, *P. siphunculus*, and *P. vulgare* Kato, 1937b have cerebral-eyespot arrangements similar to that in *P. hibana*, i.e., a pair of linear cerebral-eyespot clusters composed of relatively few (≤ 15) eyespots, but can be easily distinguished from *P. hibana* by the dorsal coloration (Table 14). *Prosthiostomum parvicelis* Hyman, 1939b also has this type of cerebral-eyespot arrangement; although the dorsal coloration is not known for this species, it can be distinguished from *P.*

hibana by the pyriform lumen of the seminal vesicle (Hyman 1939b), whereas the seminal-vesicle lumen is narrow and elongated in *P. hibana* (Fig. 30A, C).

Noticeably, in *P. hibana*, the inner wall of the male atrium is deeply ruffled (Fig. 30A, B). The morphology of the inner wall of the male atrium has so far attracted little attention as taxonomic features in Prosthiostomidae. This feature is not mentioned in the original descriptions or re-descriptions for most of the prosthiostomid species, but a slightly ruffled inner wall of the male atrium has been illustrated for *P. gilvum* Marcus, 1950, *P. latocelis* Hyman, 1953, and *P. ostreae* Kato, 1937b (Kato 1937b; Marcus 1950; Hyman 1953).

I was not able to obtain materials with the fully mature female reproductive organ. Further investigation should uncover the actual morphological characteristics of the organ.

12. *Prosthiostomum ohshimai* (Kato, 1938a)

(Figs 32, 33)

Amakusaplana ohshimai Kato, 1938a: pp. 573–575, Pl. XXXVII, figs 4, 5.

Prosthiostomum ohshimai: Faubel 1984, p. 232.

Material examined. ICHUM 6033, sagittal sections, 6 slides (HE), collected by S. Arakaki in Ushibuka (32.1701°N, 130.0366°E), Amakusa, Kumamoto, Japan, on June 15, 2018.

Type locality. Tomioka, the Amakusa islands, Kumamoto, Japan.

Description. Body oval, slightly tapered posteriorly, 10.7 mm long and 3.6 mm maximum width in living state (Fig. 32A); frontal margin of body slightly indented in

midline (Fig. 32A–C). Body very thin, 0.39 mm thick in fixed state. Tentacles absent. Dorsal surface smooth, translucent white in ground body color. Intestine highly branched, spreading all over body, appearing brownish-red color; numerous white specks filling gaps between intestinal branches (like apparent color pattern of host coral, *Acropora* spp.) on dorsal surface (Fig. 32A). Ventral surface translucent, without color pattern. Brain located at first fourteenth of body length. Cerebral-eyespot cluster scattered around dorsal midline in front of pharyngeal pouch, consisting of about 40 eyespots (Fig. 32B); pair of marginal-eyespot clusters spreading in ventral anterior region, each composed of 13–14 eyespots (Fig. 32C); cerebral eyespots denser than marginal ones (Fig. 32B, C). Plicate pharynx tubular in shape, very short, about one-eighth of body length (Fig. 32A); modified by shallow longitudinal cleft in ventral side. Mouth situated at anterior end of pharynx, behind brain. Male gonopore situated immediately behind base of pharynx. Male copulatory apparatus consisting of seminal vesicle, pair of prostatic vesicles, and armed penis papilla (Fig. 33A–C). Ejaculatory duct, with thick muscular layer, entering penis papilla. Prostatic ducts narrow with muscular layer, connected to ejaculatory duct separately at proximal end of penis papilla. Pair of spherical prostatic vesicles coated within thick non-nucleated muscular wall, located on both sides of ejaculatory duct. Seminal vesicle oval, coated with thick muscular wall (Fig. 33A). Penis papilla armed with pointed tubular stylet, enclosed in penis pouch (Fig. 33B). Male atrium extending posteriorly. Female gonopore widely separated from male gonopore (Fig. 33A). Cement glands well developed, spreading widely around vagina. Cement pouch not well observed due to too developed glands. Vagina extending anteriorly (Fig. 33D). Uterus located immediately posterior to seminal vesicle. Lang's vesicle absent. Sucker absent (Fig. 32A).

Distribution. This species is distributed in Magari-zaki, Tomioka, Amakusa (type locality). I collected *P. ohshimai* from Ushibuka, southern Shimoshima Island.

Habitat. Subtidal, found on colonies of *Acropora* spp.

Diagnosis. Thin body oval, slightly indented at anterior tip; dorsal surface translucent; intestinal branches appearing brownish-red color, spreading all over body; pair of marginal-eyespot clusters on ventral side; cerebral-eyespot cluster composed of about 40 eyespots; short plicated tubular pharynx with shallow longitudinal cleft; sucker absent.

Sequence. Partial 28S (1,010 bp) from the specimen (Appendix 1).

Remarks. Kato (1938a) originally described *Amakusaplana ohshimai* based on material collected from the body surface of madreporarian corals at Magari-zaki (Amakusa). My specimen from Ushibuka (Amakusa) is consistent with the original description in that *i*) the anterior margin of the body is slightly indented, *ii*) the intestinal branches appear brownish red, *iii*) the marginal eyespots are spread in front of the level of the brain; about 40 cerebral eyespots are scattered on either side of the midline anterior to the level of half the pharynx, and *iv*) the sucker is absent. Based on the phylogenetic position of the other congener *Amakusaplana acroporae* Rawlinson et al., 2011 being nested within *Prosthiostomum*, the genus *Amakusaplana* is now considered as a junior synonym of *Prosthiostomum* (Litvaitis et al. 2019).

In my observation, three morphological traits were newly found, which were not mentioned in the original description: *i*) a pair of marginal-eyespot clusters are present on the ventral side and the cerebral-eyespot cluster is on the dorsal side; *ii*) numerous white specks fill the gaps between the intestinal branches, and *iii*) the shallow longitudinal cleft is present on the ventral side of the plicated tubular pharynx like other

two coral-eating prosthiostomids, *P. acroporae* and *P. montiporae* Poulter, 1975 (Jokiel and Townsley 1974; Rawlinson et al. 2011).

Prosthiostomum ohshimai and *P. acroporae* are considered to be separated specifically based on the morphological and genetic differences: *i*) the number of eyespots in *P. ohshimai* is greater than that in *P. acroporae*, *ii*) the apparent dorsal coloration of *P. ohshimai* is brownish red on translucent white background whereas that of *P. acroporae* is brown on white background (Rawlinson et al. 2011).

13. *Prosthiostomum* cf. ***ostreae*** Kato, 1937b

(Fig. 34)

Prosthiostomum cf. *ostreae* Kato, 1937b: Tsuyuki et al. 2021, 11–14, fig. 5.

?*Prosthiostomum ostreae* Kato, 1937b: 365–366, pl. 22, figs 4–5, text-figs 25–27; Kato 1944, 308; Faubel 1984, 232; Prudhoe 1985, 192.

Material examined. ICHUM 6151, sagittal sections, 4 slides (HE), collected by T. Miura, K. Oguchi, and H. Kohtsuka in Arai-hama (35.1609°N, 139.6105°E), Misaki, Kanagawa, Japan, on February 19, 2019; ICHUM 6152, sagittal sections, 4 slides (HE), collection data same as above except for date (March 25, 2019); ICHUM 6153, sagittal sections, 8 slides (HE), collection data same as ICHUM 6152.

Description. Body elongated, tapered posteriorly, 9.0–13.0 mm long and 2.4–3.3 mm wide at its widest point when slightly contracted while alive; anterior margin rounded (Fig. 34A–D). Tentacles absent. Dorsal surface smooth, light brown, covered with numerous brown maculae (Fig. 34A). Brown pigments aggregating mid-dorsally to form posteriorly fading band, running from behind brain; non-pigmented specks

forming line along midline on brown band (Fig. 34A). Body margin translucent. Ventral surface translucent, without color pattern (Fig. 34B). Pair of cerebral-eyespot clusters, each consisting of 20–22 eyespots; each cerebral-eyespot cluster approaching each other on midline at three points; anterior end of clusters located at distance of 1.20 mm posterior to anterior margin of body (Fig. 34C, D). About 70 marginal eyespots irregularly scattered along anterior margin, extending to half position of cerebral-eyespot cluster (Fig. 34D). One pair of ventral eyespots present near front end of brain (Fig. 34D). Anterior branch of main intestine extending to position 0.52 mm posterior from anterior margin of brain. Plicated pharynx tubular in shape, 4.7 mm in length (about one-third of body), located in anterior half of body (Fig. 34B). Mouth situated at anterior end of pharynx, located at 1.53 mm posterior from anterior margin of body. Male gonopore, female gonopore, and sucker closely set on body center (Fig. 34B); distance between male and female gonopores being 0.34 mm; distance between female gonopore and sucker being 0.31 mm. Male copulatory apparatus consisting of large seminal vesicle, pair of prostatic vesicles, and armed penis papilla, located immediately posterior to pharyngeal pocket. Pair of spermiducal vesicles, running on each side of midline and curving posteriorly behind penis to separately enter into anteroventral end of seminal vesicle (Fig. 34E). Ejaculatory duct with thin muscular layer, entering penis papilla. Prostatic ducts with thin muscular layer, connected to ejaculatory duct separately at proximal end of penis papilla. Pair of spherical prostatic vesicles coated with 0.04-mm-thick, non-nucleated muscular wall, located on both sides of ejaculatory duct (Fig. 34E, F). Seminal vesicle oval, coated with 0.04-mm-thick muscular wall (Fig. 34E, F). Seminal vesicle (long axis 0.26 mm, short axis 0.17 mm) more than twice as large as prostatic vesicle (0.12 mm in diameter) (Fig. 34E). Penis papilla armed with

rather thick, pointed tubular stylet (0.13 mm in length), enclosed in penis pouch, protruding into male atrium (Fig. 34E, F). Male atrium elongated anteriorly from gonopore to penis pouch (0.27 mm in length); inner wall slightly ruffled, lined with ciliated and muscularized epithelium (Fig. 34F). Female copulatory apparatus posterior to male reproductive system (Fig. 34G, H). Cement glands concentrated around vagina and releasing their contents in cement pouch when developed (Fig. 34H). Oviducts not observed. Sucker large (0.26 mm in diameter), situated immediately behind female reproductive system (Fig. 34B, E, G), at 7.4 mm anterior from posterior margin of body.

Distribution. Arai-hama, Misaki, Kanagawa, Japan.

Habitat. Among branching coralline algae Corallinales spp. and holdfasts of the kelp *Eisenia bicyclis* subtidally in Misaki.

Sequences. Partial COI (585 bp) and 28S (1,013 bp) sequences from two individuals: LC625896 (COI) and LC625889 (28S) from ICHUM 6151; LC625897 (COI) and LC625890 (28S) from ICHUM 6152.

Remarks. I tentatively identified the specimens as *P.* cf. *ostreae*. Kato (1937b) originally described *P. ostreae* based on three specimens found on cultivated oyster shells from Moroiso, Misaki, Kanagawa, Japan. Unfortunately, the type series of *P. ostreae* is not extant (Kawakatsu 2004), and therefore I could not compare my samples to the type series. The dorsal body color pattern, the arrangements of cerebral and marginal eyespots, and the form of male copulatory apparatus in my specimens are largely consistent with those given by Kato (1937b). However, my specimens differ from the original description of *P. ostreae* by *i*) the body-margin coloration (translucent in my specimens; partly lemon-yellow in the original description) and *ii*) the frontal eyespots (absent in my specimens; four eyespots present in the original description). In

addition, the pair of the ventral eyespots were confirmed in my materials although they were not mentioned in the original description. My materials were collected from coralline algae and kelp holdfasts whereas the original specimens were found on oyster shells. Additional data are needed to test whether the two (possibly three) morphological differences between my specimens and the original description represent interspecific or intraspecific ones stemming from the habitat difference.

14. *Prosthiostomum sonorum* Kato, 1938a

(Figs 35, 36)

Prosthiostomum sonorum Kato, 1938a: 72, 573, pl. 36, figs 5, 6 (Kumamoto).

Material examined. ICHUM 6034, sagittal sections, 7 slides (HE), collected by S. Arakaki and M. Tokeshi in Yatagasone (32.5286°N, 130.0454°E), off the coast of Magari-zaki, Amakusa, Kumamoto, Japan, on June 5, 2019.

Type locality. Tomioka, the Amakusa islands, Kumamoto, Japan.

Description. Body elongated, tapered posteriorly, 13 mm long and 2.8 mm maximum width in living state (Fig. 35A). Body thin, 0.46 mm thick in fixed state. Tentacles absent. Dorsal surface smooth, translucent white, covered with numerous brownish-red maculae. Intestine highly branched, spreading all over body, appearing deep brownish red (Fig. 35A). Ventral surface translucent, without color pattern. Pair of cerebral-eyespot clusters, consisting of 26 (left) and 28 (right) eyespots; each cluster composed of 4–5 large eyespots in line anterior to brain and 21–24 small and large eyespot cluster around brain and mouth; pair of the latter clusters hardly separated each other (Fig. 35B). Pair of ventral eyespots present anterior to brain (Fig. 35C). Marginal

eyespots in roughly two lines, extending to approximate position of ventral eyespots along margins on both sides (Fig. 35B, C). Plicated pharynx tubular in shape, about one-sixth of body length (Fig. 35A); cleft not observed. Mouth situated at anterior end of pharynx, behind brain. Male gonopore located immediately behind base of pharynx. Male copulatory apparatus consisting of seminal vesicle, pair of prostatic vesicles, and armed penis papilla (Fig. 36A). Spermiducal vesicles forming single row on each side of midline, separately entering into seminal vesicle. Ejaculatory duct wide, with thick muscular layer, entering penis papilla. Prostatic ducts narrow with muscular layer, connected to ejaculatory duct separately at proximal end of penis papilla. Pair of spherical prostatic vesicles coated within thick non-nucleated muscular wall, located on both sides of ejaculatory duct. Seminal vesicle oval, coated with thick muscular wall (Fig. 36B). Penis papilla armed with tubular stylet, enclosed in penis pouch, protruding into male atrium (Fig. 36C). Penis sheath present between penis pouch and male atrium (Fig. 36C). Male atrium urn-shaped (Fig. 36A–C). Female reproductive system behind male reproductive system (Fig. 36A). Vagina forking into two branches at proximal end; one curving anteriorly and another posteriorly (Fig. 36D). Each branch of vagina connecting to oviducts, further forking into two branches running on each side of main intestine. Cement glands numerous, concentrated around vagina (Fig. 36D). Lang's vesicle absent. Sucker large, set on body center (Figs 35A, 36E).

Distribution. So far only from type locality.

Habitat. Subtidal, found on colonies of *Acropora pruinosa*.

Sequences. Partial 28S rDNA (1011 bp) from the specimen (Appendix 2).

Remarks. *Prosthiostomum sonorum* was originally described by Kato (1938a) based on a single specimen collected by dredging along with some corals from a depth

of about 18 m off Tomoe-zaki, Amakusa. The arrangements and number of cerebral eyespots are consistent with those given by Kato (1938a).

15. *Prosthiostomum torquatum* Tsuyuki, Oya, and Kajihara, 2019

(Figs 37–39)

Prosthiostomum torquatum Tsuyuki, Oya, and Kajihara, 2019: 138–142, figs 1–3 (Shirahama).

Etymology. The specific name *torquatum* is a Latin adjective, meaning "adorned with a neck chain or collar". It was named after the anterior transverse white line, bending backward at the mid-point.

Material examined. Holotype: ICHUM 5563, 13 slides (HE), collected by Y. Oya in Shirahama (33.6926°N, 135.3332°E), Wakayama, Japan, on August 22, 2017. Paratypes (4 specimens): ICHUM 5562, sections through reproductive structures (7 slides) and anterior part (4 slides) (HE), collected by N. Jimi in Shirahama, Wakayama, Japan, on May 16, 2015; ICHUM 5565, 9 slides (HE), collection data same as holotype; ICHUM 5566, 12 slides (HE), collection data same as holotype; ICHUM 5567, 13 slides (MT), collected by Y. Oya in Shirahama (33.6951°N, 135.3440°E), Wakayama, Japan, on August 23, 2017. Non-type specimens: ICHUM 5564, unsectioned, preserved in 70% ethanol, collection data same as holotype; ICHUM 6040, unsectioned, preserved in 70% ethanol, collected by A. Tsuyuki at 1–10 m depth in the beach in front of the Kuroshio Biology Research Institute (32.7789°N, 132.7322°E), Otsuki, Kochi, Japan, on April 10, 2019.

For comparison, I also examined digital photomicrographs of the male

copulatory apparatus in the holotype (AM W. 44692, MI QLD 2395) and paratype (AM W.44065, MI QLD 2351) of *Lurymare clavocapitata* Marquina et al., 2015 deposited at the Australian Museum, Sydney.

Type locality. Shirahama, Wakayama, Japan.

Description. Body elongated, anterior margin rounded, slightly tapered posteriorly, mid-point of posterior margin acute, 9–18 mm long (14 mm in holotype) and 2.5–5 mm maximum width (4 mm in holotype) in living state (Fig. 37A, B). Tentacles absent. Dorsal surface smooth, translucent, covered with numerous orange maculae and blue dots; orange maculae denser medially, blue dots uniformly scattered; each orange macula larger than single blue dot. Single transverse narrow dark-brown line running on dorsal surface of body in front of cerebral eyespots; its mid-point slightly arched backwards. Another transverse white line on dorsal surface, situated in short distance behind dark-brown line, likewise bending posteriorly at mid-point. Dark-brown pigments aggregating mid-dorsally to form incomplete, mesh-like, posteriorly-fading band, running from behind transverse white line (Fig. 37A). Body margin transparent. Ventral surface translucent, without color pattern. Intestine highly branched, spreading all over body. Pair of cerebral-eyespot clusters situated between transverse dark-brown and white lines near midline, each consisting of 7–13 eyespots (13 eyespots each in holotype); each cerebral-eyespot cluster approaching each other on midline at two or three points; two size categories among eyespots, larger one being more than twice the size of smaller one (Fig. 37C). Marginal eyespots sparsely anterior to transverse dark-brown line; marginal eyespots smaller than cerebral ones (Fig. 37C). Pair of ventral eyespots anterior to brain (Fig. 37D). Plicated pharynx tubular in shape, one third of body length, located in anterior half of body (Fig. 37B). Oral pore situated

at anterior end of pharynx, behind brain. Male gonopore, female gonopore, and sucker closely set on body center (Fig. 37B). Male copulatory apparatus consisting of large seminal vesicle, pair of prostatic vesicles, and armed penis papilla, located immediately posterior to pharynx (Fig. 38A). Spermiducal vesicles forming single row on each side of midline, separately entering into seminal vescle. Ejaculatory duct wide, with thick muscular layer, entering penis papilla. Prostatic ducts narrow, with muscular layer, attached to ejaculatory duct at proximal end of penis papilla. Pair of prostatic vesicles and seminal vesicle closely set to each other (Fig. 38B). Muscular bulb enclosing three vesicles not found (Fig. 38B). Pair of spherical prostatic vesicles coated with thin non-nucleated muscular wall, located on both sides of ejaculatory duct. Seminal vesicle oval, coated with thick muscular wall. Penis papilla armed with pointed tubular stylet, enclosed in penis pouch, protruding into male atrium (Fig. 38C, D). Penis sheath present between penis pouch and male antrum (Fig. 38C, D). Male atrium elongated anteriorly, lined with cilliated and muscularized epithelium (Fig. 38A). Female reproductive system immediately posterior to male reproductive system. Vagina short, leading from uterus to cement pouch (Fig. 38A, D). Cement glands numerous, concentrated around vagina and releasing their contents in cement pouch (Fig. 38A). Oviduct running on each side of main intestine, extending anteriorly and posteriorly to female copulatory apparatus; anterior and posterior branches of oviduct converging before joining proximal end of vagina. Lang's vesicle absent. Sucker large, situated at center of body (Figs 37B, 38D).

Variation. Specimens exhibited variation in the color pattern on the dorsal surface (Fig. 39). The body color in general appearance ranged from orange to white depending on the gut contents. In addition, the density and distribution of the dark-

brown pigments that form the mid-dorsal, mesh-like band were different among the specimens examined; the transverse narrow dark-brown line in front of cerebral eyespots was interrupted in some specimens; another transverse white line in short distance behind dark-brown line was not clear in the largest specimen (Fig. 39E).

Distribution. To date, this species has been known from Shirahama (Wakayama) and Otsuki (Kochi).

Habitat. From intertidal to subtidal, under rocks.

Diagnosis. Body elongated, usually rounded anteriorly; dorsal surface speckled with numerous orange maculae, blue dots, and dark-brown pigments, with dark-brown mesh-like band along median line; transverse dark-brown line running short distance in front of similar, transverse white line on anterior part of body; pair of free prostatic vesicles and seminal vesicle located close together.

Sequences. Partial COI (462 bp) from five individuals: LC429590 from the holotype (ICHUM 5563); LC429589 (COI) and LC429591 (COI) from two paratypes (ICHUM 5562, ICHUM 5565); and LC429592 (COI) and Appendix 3 (COI) from two non-type specimens (ICHUM 5567, ICHUM 6040). The four COI sequences from Shirahama (LC429589–LC429592) were completely identical to each other whereas those between Shirahama and Kochi were different (uncorrected *p*-distance, 0.6%).

For phylogenetic analysis, partial COI (585 bp) and 28S (946 bp): LC625899 (COI) and LC504234 (28S) from the holotype (ICHUM 5563).

Genetic distance. The uncorrected *p*-distance in terms of the 462-bp COI sequence between *P. torquatum* and the most similar-looking species *Lurymare clavocapitata* (GenBank MF371153) was 9.4% (see Remarks).

Remarks. *Prosthiostomum torquatum* was originally described from

Shirahama, Wakayama, Japan (Tsuyuki et al. 2019). Among about ~60 species of *Prosthiostomum*, this species is similar to *P. komaii* Kato, 1944, and *P. trilineatum* in the dorsal color pattern, which includes several transverse lines in the anterior part of the body and longitudinal stripes along the median line (Yeri and Kaburaki 1920, Kato 1944). However, *P. torquatum* can be easily distinguished from the two species by the orange maculae and blue dots scattered all over the dorsal surface. Considering all *Lurymare* species for comparison (see Introduction), *P. torquatum* is most similar to *L. clavocapitata* by a unique dorsal color pattern among prosthiostomids: *i*) a translucent white body covered with numerous orange maculae and blue dots, *ii*) a transverse dark-brown line in front of the cerebral eyespots, directing backwards at the mid-point, and *iii*) another transverse white line running slightly behind the dark-brown one, likewise sharpening posteriorly at the mid-point. However, *P. torquatum* differs from *L. clavocapitata* by their dorsal color pattern: this species has a mesh-like band along the mid-dorsal line formed by dark-brown pigments, although the density of the dark-brown pigments varies intraspecifically (Fig. 39); *L. clavocapitata* has two discontinuous longitudinal lines composed of dark-brown pigments, instead of a mesh-like band (Marquina et al. 2015, fig. 11A). The COI *p*-distance between the two species, 9.4%, is greater than the value of 4.5%, which was observed between two sympatric *Notocomplana* species morphologically distinguishable from each other (Oya and Kajihara 2017).

16. *Prosthiostomum vulgare* Kato, 1938b

(Fig. 40)

Prosthiostomum vulgaris [sic] Kato, 1938b: 589–590, pl. 39, figs 3–4 (Shirahama);

Kato 1938a, 578 (Amakusa); Kato 1944 (Noto; Sugashima Island), 308; Faubel 1984, 232; Prudhoe 1985, 192; Hagiya and Gamo 1992, 18, pl. 1, fig. 10, pl. 2, fig. 10 (Manaduru); Tsunashima et al. 2017, fig. 2B (Shimoda).

Prosthiostomum vulgare Kato, 1938b: Tsuyuki et al. 2021, 14–20, fig. 6 (Misaki).

Prosthiostomum siphunculus Delle Chiaje, 1828: Yeri and Kaburaki 1918, 41, pl. 2, fig. 13 (Misaki; Awa); Kato 1937a, 230 (Izu).

Material examined. ICHUM 6036, sagittal sections, 3 slides (HE), collected by T. Miura, K. Oguchi, and H. Kohtsuka in Arai-hama (35.1609°N, 139.6105°E), Misaki, Kanagawa, Japan, on March 25, 2019; ICHUM 6154, sagittal sections, 4 slides (HE), collection data same as above; ICHUM 6155, sagittal sections, 5 slides (HE), collection data same as above.

Type locality. Yuzaki, Shirahama, Wakayama, Japan.

Description. Body elongated, tapered posteriorly, 6.8–8.8 mm long and 1.4–2.1 mm wide at its widest point when slightly contracted while alive (n = 3); anterior margin rounded (Fig. 40A–D). Tentacles absent. Dorsal surface smooth, buffy; cinnamon pigments medially abundant, forming wide midline (Fig. 40A). Ventral surface translucent, without color pattern (Fig. 40B). Pair of cerebral-eyespot clusters, each consisting of seven eyespots; each cluster forming antero-posteriorly elongated line; anterior end of clusters located at distance of 0.58 mm posterior to anterior margin of body (Fig. 40C). Marginal eyespots distributed along frontal margin rather irregularly but largely arranged into two or three rows, extending backward to half position of brain (Fig. 40C). One pair of ventral eyespots present near front end of brain (Fig. 40D). Anterior branch of main intestine extending anterior to brain. Plicated pharynx tubular

in shape, 3.0 mm in length (about one-third of body), located in anterior half of body (Fig. 40B). Mouth situated at distance of 0.81 mm posterior to anterior margin of body (Fig. 40B). Male copulatory apparatus consisting of large seminal vesicle, pair of prostatic vesicles, and armed penis papilla, located immediately posterior to pharyngeal pocket (Fig. 40E–H). Pair of spermiducal vesicles forming single row on each side of midline, separately entering into seminal vesicle at point being close to proximal end of ejaculatory duct (Fig. 40E, G). Ejaculatory duct with thick muscular layer, entering penis papilla. Prostatic ducts with thin muscular layer, connected to ejaculatory duct separately posterior to proximal end of penis papilla. Pair of spherical prostatic vesicles coated with 0.03-mm-thick, non-nucleated muscular wall, located on both sides of ejaculatory duct (Fig. 40E, G, H). Seminal vesicle oval, coated with 0.009-mm-thin muscular wall (Fig. 40G, H). Seminal vesicle (long axis 0.17 mm, short axis 0.09 mm) twice as large as prostatic vesicle (0.09 mm in diameter) (Fig. 40E). Penis papilla armed with pointed tubular stylet, enclosed in penis pouch, protruding into male atrium (Fig. 40F). Male atrium elongated, lined with ciliated and muscularized epithelium (Fig. 40H). Female copulatory apparatus immature; only female gonopore developed, located at distance of 0.20 mm behind male gonopore (Fig. 40E, H). Sucker large (0.21 mm in diameter), situated immediately (0.19 mm in length) behind female gonopore, at distance of 3.47 mm anterior to posterior margin of body (Fig. 40E, H).

Distribution. This species was confirmed along Japanese coasts, from the Noto Peninsula of Honshu Island to the southwestern Kyushu: Nozaki, Noto, Ishikawa; Misaki, Kanagawa; Manazuru, Kanagawa; Suzaki, Shimoda, Shizuoka; Sugashima, Mie; Shirahama, Wakayama; and Tomioka, Amakusa, Kumamoto.

Habitat. The information about habitats of this species was not mentioned in

Yeri and Kaburaki (1918), Kato (1937a, 1938a, 1938b), or Hagiya and Gamô (1992). My specimens were collected from branching coralline algae Corallinales spp. in Misaki, Kanagawa, Japan.

Sequence. Partial 1008-bp 28S rRNA (LC625891) and 585-bp COI (LC 625898) gene sequences from ICHUM 6036.

Remarks. Kato (1938b) originally described this species from Shirahama, Wakayama, Japan. He also pointed out that the specimens from Misaki identified as *P. siphunculus* by Yeri and Kaburaki (1918) should represent *P. vulgare*, assuming that these would possess a pair of spermiducal vesicles that open into the seminal vesicle at its anterior part near the ejaculatory duct. With this character, Kato (1938b) speculated that *P. vulgare* could be differentiated from *P. siphunculus*. My specimens are consistent with the original description by Kato (1938b) in this characteristic position of the junction of the spermiducal vesicles into the seminal vesicle (Fig. 40E, G) in addition to the body coloration and the arrangement of the cerebral-eyespot clusters. I was not able to compare the specimens with Yeri and Kaburaki's (1918) and Kato's (1937a, 1938a, 1938b) specimens, which had been lost (Kawakatsu 2004).

Molecular phylogeny

The resulting tree (Fig. 41) showed the family Prosthiostomidae to be monophyletic (with full support). Within prosthiostomids, the genus *Enchiridium* was supported to be monophyletic (with 72% bootstrap [BS]) whereas the monophyly of *Prosthiostomum* was not well supported (with 61% BS). All remaining *Prosthiostomum* species except for *P. lobatum* formed a clade supported with a 78% BS value. Furthermore, except for an unidentified *Prosthiostomum* sp. in Litvaitis et al. (2019), the remaining

Prosthiostomum clade had 82% BS support. Included in this latter clade were all the species for which sequences were generated *de novo* in this section, i.e., *P. auratum*, *P. grande*, *P. hibana*, *P. ohshimai*, *P.* cf. *ostreae*, *P. sonorum*, *P. torquatum*, and *P. vulgare*. *Euprosthiostomum mortenseni*'s position as sister to the *Prosthiostomum* clade received medium nodal support (81% BS value).

Discussion

As for the taxon concept of *Enchiridium*, the results did not show a compatibility to Bock's (1913) original view on the genus. The genus *Enchiridium* was established by Bock (1913) for *E. periommatum* based on two characteristics: *i*) two prostatic vesicles enclosed in a common muscle sheath and *ii*) marginal eyespots completely surrounding the entire periphery of the dorsal surface. Subsequently, *E. evelinae*, *E. japonicum*, and *E. punctatum* were added to the genus (Kato 1943c, Marcus 1949, Hyman 1953) before Faubel (1984) re-defined *Enchiridium*. It was circumscribed so that "only the prostatic vesicles are bound into a common muscle bulb and oriented anterodorsal to the ejaculatory duct" (Faubel 1984, p. 231); namely, the encircling marginal eyespots were not regarded as a necessary condition for *Enchiridium*. At the same time, Faubel (1984) transferred three *Lurymare* species, *viz.*, *L. delicatum*, *L. gabriellae*, and *L. russoi*, into *Enchiridium*. As a result, seven species were included in *Enchiridium* in the taxonomic system of Faubel (1984). In contrast, Prudhoe (1985) supported Bock's (1913) taxon concept of *Enchiridium*, retaining four species, *E. evelinae*, *E. japonicum*, *E. periommatum*, and *E. punctatum*, in *Enchiridium* and three species, *L. delicatum*, *L. gabriellae*, and *L. russoi*, in *Lurymare*. On the other hand, Cuadrado et al. (2017) followed Faubel's (1984) redefinition when they established *E. magec*. The monophyly

of *Enchidirium sensu* Faubel (1984) was strongly supported in a molecular phylogenetic analysis based on partial 28S (Litvaitis et al 2019). In this study, *Enchidirium sensu* Faubel (1984) received 72% bootstrap support. Also, *Enchiridium* in the sense of Bock (1913) and Prudhoe (1985)—represented by *E. evelinae*, *E. japonicum*, *E. periommatum*, *Enchiridium* sp. 1 (cf. Bahia et al. 2017, table 2) in the analysis—was not monophyletic. Therefore, the taxonomy of *Enchiridium* should be revised with further molecular phylogenetic analyses as well as careful examination of morphological characters among the constituent members. At the moment, however, I adopt Faubel's (1984) redefinition and place *E. daidai* in the genus *Enchiridium* along with eight other species. I did so because the results indicated that the arrangement of the marginal eyespots should not be taken into account as generic diagnostic characters.

All the seven *Prosthiostomum* species for which I gave morphological accounts in this study—*P. auratum*, *P. hibana*, *P. ohshimai*, *P.* cf. *ostreae*, *P. sonorum*, *P. torquatum* and *P. vulgare*—were nested in the *Prosthiostomum* clade (Fig. 41), corroborating my morphology-based generic assignments although its monophyly was not well supported. While a different taxonomic view was once proposed in terms of the generic affiliation (see Remarks for *P. auratum*), *P. auratum* was more closely related to *P. siphunculus* (type species of *Prosthiostomum*) than to *Euprosthiostomum mortenseni* in my tree (Fig. 41). This result supports the placement of the species in *Prosthiostomum* based on my morphological observation, given that the *E. mortenseni* specimen sequenced by Litvaitis et al. (2019) was actually more closely related to *E. adhaerens* (type species of *Euprosthiostomum*) than to *Prosthiostomum* species.

As has been advocated previously (Hyman 1959, Faubel 1984, Litvaitis et al. 2019), my molecular phylogenetic analysis incorporating the type species

Amakusaplana ohshimai (=*Prosthiostomum ohshimai*) undoubtedly shows that *Amakusaplana* should indeed be synonymized with *Prosthiostomum*, unless the latter were left paraphyletic in terms of the former. There could have been other options to deal with this situation; one of such potential options would be to subdivide *Prosthiostomum* in the sense of this chapter into some genera (or subgenera) including *Amakusaplana*. However, this option sounds unreasonable considering the uncertain phylogeny within *Prosthiostomum* (Fig. 41), in which no apparent synapomorphic trait is at present recognizable for potential subtaxa except *Amakusaplana*.

Prosthiostomum katoi Poulter, 1975 was nested in the *Prosthiostomum* clade (Fig. 41), rendering further support for the taxonomic view that *Lurymare* is indeed a junior synonym of *Prosthiostomum* (cf. Dittmann et al. 2019a, Litvaitis et al. 2019). Being originally described as a member of the subgenus *Lurymare* within the genus *Prosthiostomum* (Poulter 1975), *P. katoi* was then transferred into the genus *Lurymare* by Faubel (1984). Since then, the generic affiliation of the species has been controversial in relation to the validity of *Lurymare* (Prudhoe 1985, Marquina et al. 2015, Dittmann et al. 2019a). The common muscle bulb enclosing prostatic and seminal vesicles has been used to distinguish *Lurymare* from *Prosthiostomum* (Faubel 1984). However, according to Prudhoe (1989), this trait could develop as maturity increases in several *Prosthiostomum* species. Also, some previous phylogenetic studies showed a skeptical view about the validity of *Lurymare* as a genus (Dittmann et al. 2019a, Litvaitis et al. 2019). Based on phylogenetic positions within *Prosthiostomum*, Litvaitis et al. (2019) supported the original affiliations of *P. cynarium* Marcus, 1950 and *P. utarum* Marcus, 1952, which had been formerly belonged to *Lurymare* (Du Bois-Reymond Marcus and Marcus 1968, Bahia and Schrödl 2018). Likewise, I adopt the

original generic placement of *P. katoi* because this species was nested in the *Prosthiostomum* clade (Fig. 41). The *Lurymare* in relation to *Prosthiostomum* requires a review in future studies with further investigation including not only phylogenetic analyses but also careful examinations of morphological characters that have been used to diagnose *Lurymare*.

II-6. PSEUDOCEROTIDAE LANG, 1884

Introduction

The family Pseudocerotidae contains nine valid genera: *Acanthozoon* Collingwood, 1876; *Bulaceros* Newman and Cannon, 1996a; *Monobiceros* Faubel, 1984; *Nymphozoon* Hyman, 1959; *Phrikoceros* Newman and Cannon, 1996b; *Pseudobiceros* Faubel, 1984; *Pseudoceros* Lang, 1884; *Thysanozoon* Grube, 1840; and *Yungia* Lang, 1884. A previous study supported the monophyly of this family including the eight of these genera except *Bulaceros* based on partial sequences of 28S (Cuadrado et al. 2021); however, confirmation of this family's monophyly incorporating *Bulaceros* species using molecular analysis is still needed. Morphologically, *Bulaceros* is characterized by: *i*) the presence of a single male copulatory apparatus; *ii*) a pair of pseudotentacles with developed distal knobs; *iii*) two clusters of cerebral eyespots; *iv*) scattered dorsal pseudotentacular eyes; *v*) a simply folded pharynx; and *vi*) reduced sclerotization of the stylet (Newman and Cannon 1996a). This genus currently contains two species, *B. porcellanus* Newman and Cannon, 1996a (type species) and *B. newcannorum* Dixit, 2021 in Dixit et al. (2021), both of which have been reported in the subtropical and tropical regions of the Indo-Pacific Ocean (Newman and Cannon 1996a, Dixit et al. 2021). In Japan, an unidentified species of *Bulaceros* has been reported from the Kerama Islands based on a photographic record, but this record has not been substantiated by actual voucher specimen(s) (Ono 2015).

In this section, I provide the first record of *B. porcellanus* in Japan based on specimens collected from Misaki, Kanagawa. This is the northernmost record of this species. In addition, I infer the phylogenetic position of the genus *Bulaceros* among

Pseudocerotidae from an analysis using partial 28S sequences from the pseudocerotid species currently available in public databases in addition to data obtained from the Misaki *B. porcellanus* specimens in my study.

Material and Methods

Sampling and morphological observation

Two polyclad specimens were collected by hand or skin diving by K. Oguchi and N. Hookabe in the intertidal and subtidal zones in Misaki, Miura, Kanagawa, Japan in 2019–2020. I took photographs of the worms alive, fixed them after anesthetization, and observed the internal morphology in the same way as mentioned in the Chapter II-1. A part of sections was stained with alcian blue and safranin O (AB-SO) or alcian blue and periodic acid-Schiff (AB-PAS) in addition to the HE. The two specimens were deposited in the ICHUM.

For comparison, I also examined digital images of the type series of *B. porcellanus*, which has been deposited at the Queensland Museum (QM), Australia.

DNA extraction, PCR amplification, and sequencing

Total DNA was extracted in the same way as mentioned in the Chapter II-4. A fragment (1,009 bp) of the 28S was amplified with the primers fw1 and rev2 (Sonnenberg et al. 2007). PCR amplification conditions were 94 °C for 5 min; 35 cycles at 94 °C for 30 s, 52.5 °C for 30 s, 72 °C for 1.5 min; and 72 °C for 7 min. The sequence was determined, checked, and edited by the same method mentioned in Chapter II-1. The sequence has been deposited in DDBJ/EMBL/GenBank.

Molecular phylogenetic analysis

In addition to the sequence determined in this study, other partial 28S sequences from 48 pseudocerotid species downloaded from GenBank were used in the phylogenetic analysis (Table 15). The prosthiostomid *Prosthiostomum siphunculus* and three species-group taxa of euryleptids (*Cycloporus papillosus* (Sars in Jensen, 1878), *Eurylepta cornuta melobesiarum* (Schmidtlein, 1880), and *Prostheceraeus vittatus* (Montagu, 1813)), were chosen as outgroups. The sequences were aligned using MAFFT ver. 7.427, with the FFT-NS-i strategy selected by the "Auto" option. The alignment was trimmed using a Clipkit ver. 1.0 using the "kpic" option. The optimal substitution models were selected using the jModelTest ver. 2.1.4 (Darriba et al. 2012) under the AIC, which were GTR+I+G. The phylogenetic analysis was performed using the ML method via RAxML ver. 8.2.10. Nodal support was assessed by analyzing 1000 bootstrap pseudoreplicates.

Data treatment

Same as in Chapter II-1.

Results

Taxonomy

Family Pseudocerotidae Lang, 1884

7. Genus *Bulaceros* Newman and Cannon, 1996a

Amended diagnosis. Pseudocerotidae with soft, oval, medially flat body; posterior of body slightly tapering; pair of erect pseudotentacles formed from anterior margin, well

developed, ear-like with distal knobs; dorsal surface translucent in background; cerebral eyespots in two clusters; dorsal pseudotentacular eyes few in number, scattered between pseudotentacle pairs, not forming clusters; ventral pseudotentacular eyespots more numerous than dorsal ones, extending medially; pharynx small, rounded, with several pairs of simple pharyngeal folds; mouth situated centrally in pharynx; main intestine narrow, extending posteriorly but ending prior to posterior margin; lateral branches of intestine not evident; single male copulatory apparatus consisting of seminal vesicle, prostatic vesicle, and penis papilla with sclerotized stylet.

17. *Bulaceros porcellanus* Newman and Cannon, 1996a

[Japanese name: yamayuri-nisetsuno-hiramushi]

(Figs 42, 43, 45)

Bulaceros porcellanus Newman and Cannon, 1996a: 481–483, figs 1A–D, 2, 8A (the Great Barrier Reef, Australia); Dixit et al. 2021, 7–8, fig. 6 (the Lakshadweep Islands, India); Tsuyuki et al. 2022a, 148–153, figs 1, 2, 5 (Misaki, Japan).

Material examined. ICHUM 6264, sagittal sections of the reproductive organs, 17 slides (HE), along with the remaining unsectioned body (preserved in 70% ethanol), collected by K. Oguchi in Arai-hama (35.1609°N, 139.6105°E), Koajiro, Misaki, Miura, Kanagawa, Japan, on August 21, 2019; ICHUM 6265, sagittal sections of the reproductive organs, 17 slides (the 8–9th slides, AB-SO; the 10–12th slides, AB-PAS; the other slides, HE), along with the remaining unsectioned body (preserved in 70% ethanol), collected by N. Hookabe intertidally in Hama-moroiso (35.1557°N,

139.6060°E), Moroiso, Misaki, Miura, Kanagawa, Japan, on August 18, 2020.

For comparison, I also examined two digital photographs of the holotype of *B. porcellanus* (QM G210662) in living state and digital photomicrographs of the copulatory apparatuses in two paratypes of *B. porcellanus* (QM G210663 and G210665).

Description. Body oval, 20.0–21.5 mm long and 7.4–8.1 mm wide at its widest point while alive (Fig. 42A, B). Pair of pseudotentacles well developed with knobs at tip (Fig. 42C). Dorsal surface translucent with opaque-white maculae; variously shaped, brown to black spots distributed all over dorsal surface except for margin, medially greater in size, but smaller along midline and sparser on both sides of midline; white maculae often absent around these dark spots; fine, unevenly blurred orange-brown markings distributed along both sides of midline on dorsal surface; narrow, orange marginal band surrounding dorsal surface slightly inside body periphery (Fig. 42A), continuously running on both pseudotentacles (Fig. 42D); numerous, opaque-white maculae with varying size and shape alternating with translucent portions along body margin outside orange marginal band (Fig. 42A, C). Orange-brown blotches forming rectangle anterior to cerebral eyespots; narrow, darker triangle present, with its acute corner pointing anteriorly, and its posterior half overlapping on the rectangle (Fig. 42C). Ventral surface translucent white, without any color pattern (Fig. 42B). Pair of cerebral-eyespot clusters, each consisting of about 30 eyespots (Fig. 42A, C). Dorsal pseudotentacular eyespots about 10 in number, sparsely distributed between pseudotentacles (Fig. 42D, E). Ventral pseudotentacular eyespots about 40 in number, extending medially from pseudotentacular tips, more concentrated at tips (Fig. 42F). Pharyngeal mouth, male gonopore, female gonopore, and sucker present along midline

on ventral side (Fig. 42B). Pharynx simply ruffled with several pairs of folds, 1.9–3.7 mm in length, located at anterior one-thirds of body (Fig. 42B). Mouth situated centrally in pharynx (Fig. 42B). Male gonopore located posterior to pharyngeal mouth. Male copulatory apparatus composed of large seminal vesicle, prostatic vesicle, and armed penis papilla (Fig. 43A, B). Seminal vesicle elongated (long axis 0.82 mm, short axis 0.18 mm), coated with 55-µm-thick muscular layer (Fig. 43A, B). Ejaculatory duct not coiled, entering penis papilla. Prostatic vesicle oval, lined with 34-µm-thick smooth granular epithelium and covered by muscular wall (Fig. 43C), connected to ejaculatory duct at proximal end of penis papilla. Penis papilla armed with tubular penial stylet (86 µm in length and 13 µm in width), enclosed in penis pouch, protruding into male atrium (Fig. 43D). Male atrium opening to exterior via male gonopore (Fig. 43A, B). Female gonopore situated at 6.58 mm posterior to male gonopore. Female copulatory apparatus consisting of cement pouch surrounded by numerous cement glands, vagina, and uteri (Fig. 43B, E). Pair of uteri entering vagina separately. Vagina leading to female atrium across cement pouch (Fig. 43B, E). Female atrium opening to exterior via female gonopore. Sucker large, 1.04 mm in diameter, located at 12.6 mm anterior from posterior margin of body (Fig. 42B).

Distribution. The Great Barrier Reef, Australia (Newman and Cannon 1996a); the Marshall Islands, Republic of the Marshall Islands (Newman and Cannon 2005); the Lakshadweep Islands, India (Dixit et al. 2021); and Miura Peninsula, Japan (present study) (Fig. 44).

Sequence. Partial 28S sequence from one individual (1,009 bp): LC660222 from ICHUM 6264.

Remarks. I amended the diagnosis of *Bulaceros* by Newman and Cannon

(1996a) so that the histological feature of the penial stylet was removed and that a body coloration of translucent background was added. Newman and Cannon (1996a) pointed out that the reduced sclerotization of the penial stylet was available as a key character that distinguished *Bulaceros* from *Pseudoceros*. However, my reexamination of QM G210663, a paratype specimen of *B. porcellanus* (Fig. 45A), revealed that the penial stylet of *B. porcellanus* was as much sclerotized as that of *Pseudoceros* species. A translucent background was newly recognized as a key feature of *B. porcellanus*, *B. newcannorum*, and *Pseudoceros harrisi* (Bolaños et al., 2007) as compared to other pseudocerotid species (cf. Newman and Cannon 1994, 1996a, Bolaños et al. 2007, Dixit et al. 2021); the last species was transferred from *Pseudoceros* into *Bulaceros* based on my phylogenetic results (see Discussion).

Newman and Cannon (1996a) originally described *Bulaceros porcellanus* specimens from Lizard Island Lagoon, Australia. The following morphological characteristics observed in my specimens correspond to the diagnostic body color pattern of *B*. *porcellanus* provided by the original description: *i*) translucent with mottled opaque-white spots; and *ii*) evenly spaced brown to black spots (Newman and Cannon 1996a). In my materials from Misaki, and in the Indian specimen by Dixit et al. (2021), the coloration of the narrow marginal band seems to be slightly different from the original description in terms of the absence of a brown inner part (see Newman and Cannon 1996a, fig. 8A). However, this color variation should represent intraspecific because the re-examined holotype material of *B. porcellanus* appears to have the same color pattern as mine (Fig. 45B). In my materials, there are other three morphological differences from the original description: *i*) the number of the dorsal pseudotentacular eyespots (about 10 in the present material; about 30–40 in the original description), *ii*)

the ventral pseudotentacular-eyespot arrangement (the medial cluster, absent in mine; present in the original description), and *ii*) the penial stylet proportion (the length to width ratio, 6.6:1 in mines; 4:1 in the original description) (Newman and Cannon 1996a). These variations should be evaluated by comparison with genetic information among morphologically different specimens in a future study.

Molecular phylogeny

In the resulting tree, *Bulaceros porcellanus* (ICHUM 6264) from Japan was nested with the other pseudocerotid species with 76% bootstrap (BS) support (Fig. 46). Within this clade, *B. porcellanus* and *Pseudoceros harrisi* (Bolaños et al., 2007) formed a clade with a 90% BS value. This was a sister clade to all the other species within this family that were included in this analysis. All the remaining ingroup taxa, except for *B. porcellanus* and *B. harrisi*, formed a clade supported with an 84% BS value. Except for *P. harrisi* (= *B. harrisi*), the *Pseudoceros* species were monophyletic with 96% BS support. All the remaining pseudocerotid genera, except for *Bulaceros* and *Pseudoceros*, formed a highly supported clade (91% BS value). The genera *Phrikoceros*, *Pseudobiceros*, *Pseudoceros*, *Monobiceros*, and *Thysanozoon* were not recovered as monophyletic.

Discussion

This study provides the first record of *Bulaceros porcellanus* from Japanese waters. This species shows a relatively wide distribution in the Indo-Pacific region, and has thus far been recorded in the Great Barrier Reef (Australia), the Marshall Islands (Republic of

the Marshall Islands), and the Lakshadweep Islands (India). The specimens from Misaki, Kanagawa, Japan are the first records of this species in warm-temperate waters (Fig. 44). Although the geographical distribution of *B. porcellanus* have thus far been limited to only a few areas of the Pacific Ocean, recent studies (Dixit et al. 2021, Tsuyuki et al. 2022a) are revealing its broader distribution range. Further investigation will help to understand the actual distribution of this species.

Given that my species/generic identification was correct, *Bulaceros harrisi* (formerly *Pseudoceros harrisi*) should be transferred to the genus *Bulaceros*, and the key features separating *Bulaceros* and *Pseudoceros* require a revision. In the phylogenetic tree, *B. harrisi* formed a clade with my *B. porcellanus* (the type species of *Bulaceros*; Fig. 46). This clade was separated from a monophyletic group composed of 19 other *Pseudoceros* species, which included *P. velutinus* (Blanchard, 1847) (originally *Proceros velutinus* Blanchard, 1847; the type species of *Pseudoceros*) (Fig. 46). The genera *Bulaceros* and *Pseudoceros* share morphological characteristics in having a single male copulatory apparatus and a sclerotized penial stylet, but they are distinguished by the following four morphological traits: *i*) pseudotentacle form (with developed distal knobs in *Bulaceros*; simple folds in *Pseudoceros*); *ii*) the arrangement of cerebral eyespots (separated into two clusters in *Bulaceros*; horseshoe-shaped in one cluster in *Pseudoceros*); *iii*) the arrangement of pseudotentacular eyespots (scattered in *Bulaceros*; arranged in rows along the margin in *Pseudoceros*); and *iv*) the pharyngeal folds (simple in *Bulaceros*; complex in *Pseudoceros*) (Newman and Cannon 1996a, Dixit et al. 2021, Tsuyuki et al. 2022a). *Bulaceros harrisi* was described based on only one damaged specimen from Panama. This species was included in *Pseudoceros* based on having *i*) the simple folds of pseudotentacles; and *ii*) one cluster of cerebral eyespots,

but these characteristics are not clearly shown in the photograph of a living animal (Bolaños et al. 2007, fig. 7A). In addition, I cannot evaluate the character state of the pseudotentacular eyespots and pharyngeal folds based on the original description (cf. Bolaños et al. 2007, p. 14). Also, *P. harrisi* is unique among *Pseudoceros* species in having a translucent body (Bolaños et al. 2007). This coloration is more similar to *B. porcellanus* and *B. newcannorum* than the other *Pseudoceros* species (cf. Newman and Cannon 1994, 1996a, Dixit et al. 2021). Based on the phylogenetic and morphological closeness, *B. harrisi* should be in *Bulaceros* with amendment of the *Bulaceros* diagnosis; I provided an amended diagnosis to include the translucent background (see Amended diagnosis). At present, I retain *i*) the pseudotentacles with distal knobs, *ii*) the cerebral eyespots in two clusters, *iii*) the scattered pseudotentacular eyespots, and *iv*) the simple pharyngeal folds, as the diagnostic characters of *Bulaceros* although it is uncertain whether *B. harrisi* shares these traits with *B. porcellanus*. Further studies with morphological trait re-observation of *B. harrisi* may make certain of its morphology-based generic assignment of the species by examining these characters

II-7. THEAMATIDAE MARCUS, 1949

Introduction

The family Theamatidae is exclusively composed of interstitial polyclad species (Marcus 1949, Sopott-Ehlers and Schmidt 1975, Bulnes and Faubel 2003, Curini-Galletti et al. 2008, Tsuyuki et al. 2022b). This family is currently monotypic, consisting of a single genus, *Theama* Marcus, 1949, which is morphologically characterized by *i*) a narrow and elongated body without any tentacles, *ii*) the interpolated prostatic vesicle with tall inner glandular epithelium developed to form radial folds, and *iii*) the penis papilla directed backward, housed within a tube-shaped penis sheath (cf. Faubel 1983, Prudhoe 1985, Curini-Galletti et al. 2008). At present, this genus contains four species: *T. evelinae* Marcus, 1949 from Brazil; *T. forrestensis* (Bulnes and Faubel 2003) from Australia; *T. mediterranea* Curini-Galletti et al., 2008 from the Mediterranean Sea; and *T. occidua* Sopott-Ehlers and Schmidt, 1975 from the Galápagos Islands. So far, there has been no record of Theamatidae from the Northwest Pacific Ocean.

During a faunal survey of polyclads in sandy interstitial habitats in this study, I collected specimens representing an undescribed species of *Theama* from eight localities in the Japanese archipelago. In this section, I provide a morphology-based formal taxonomic description of the species.

Material and Methods

Sampling, specimen processing, and morphological examination

A total of 21 polyclad specimens were collected at eight localities in six prefectures on

three Japanese main islands: Oshoro and Shiriuchi (Hokkaido); Noto (Ishikawa, Honshu); Tateyama (Chiba, Honshu); Enoshima and Misaki (Kanagawa, Honshu); Kushimoto (Wakayama, Honshu); and Yasu (Kochi, Shikoku). The sampling campaign in Noto was conducted during the 22nd Japanese Association for Marine Biology (JAMBIO) Coastal Organism Joint Survey.

At each locality, sediment samples were collected intertidally on beaches with coarse sand. To extract animals, each sediment sample (about 500 ml) was placed in a bucket with *i*) tap water or *ii*) a $MgCl_2$ solution prepared with tap water, or *iii*) sea water and gently agitated for up to 15 s. The supernatant was immediately filtered with a dip net of 32-µm or ca. 1-mm mesh size. The separated material was quickly transferred into seawater; this extraction procedure was repeated for up to three times for a single sediment sample as mentioned in Chapter II-1. At one occasion, a single specimen was found and directly picked up from under a rock on a beach (see Habitat below).

Of the 21 specimens collected, one was fixed directly in 99.5% ethanol without anesthetization; this specimen was later used for DNA extraction. The remaining 20 worms were anesthetized, and then photographed as mentioned in Chapter II-1. Of these 20 specimens, one was fixed in 10% formalin–seawater for whole-mount preparation. For the remaining 19 specimens, a part of the body was removed, fixed, and preserved in 99.5% ethanol for DNA extraction; the rest of the body was fixed in Bouin's solution or 10% formalin–seawater for 24–72h, and then preserved in 70% ethanol. Of these 19 specimens, nine were used for histological preparation and the remaining 10 have been left unsectioned.

For histological examination, eight specimens were cut sagittally and one transversally. Tissues were dehydrated in an ethanol series, cleared in xylene, embedded

in paraffin wax, and serially sectioned at 4 μm. Sections were mounted on glass slides, stained with HE, and embedded in Entellan New under cover slips on glass slides.

For whole-mount preparation, the body was gently compressed between two glass slides while dehydrated in an ethanol series and cleared in xylene, before being mounted on another glass slides and sealed in Entellan New under a cover slip.

The serial sections and the whole-mount specimen were observed and photographed as mentioned in Chapter II-1. All specimens were deposited in the ICHUM.

DNA extraction, PCR, and sequencing

Total DNA was extracted in the same way as in Chapter II-1. Partial sequence of COI (613 bp) and 28S (1,007 bp) were determined in the same way as in Chapter II-1. The primer pairs Theama_COIF (5′-CCGGTTTGGTAGGAACTGCATTTAG-3′) and Theama_COIR (5′-TTAAGATATACACCTCAGGATGACC-3′) were used for COI in addition to those listed in Table 2 for 28S. PerlPrimer ver. 1.1.21 (Marshall 2004) was used to design the primers Theama_COIF and Theama_COIR *de novo*. PCR amplification procedure was as follows: 94°C for 1 min; 35 cycles of 94°C for 30 s, 50°C (COI) or 52.5°C (28S) for 30s, and 72°C for 1 min (COI) or 1.5 min (28S); and 72°C for 7 min. PCR products were purified and the sequences were determined in the same way as in Chapter II-1. All edited sequences have been deposited in DDBJ/EMBL/GenBank (Table 16).

Molecular analyses

Uncorrected *p*-distances were calculated using MEGA ver. X (Kumar et al. 2018) for

COI and 28S sequences. To see if there was any amino-acid variation in the COI dataset (613 bp from 20 specimens), the nucleotide sequences were translated according to the flatworm mitochondrial code (Telford et al. 2000) using MEGA ver. X.

Data treatment

Same as in Chapter II-1.

Results

Taxonomy

Family Theamatidae Marcus, 1949

8. Genus *Theama* Marcus, 1949

18. *Theama* sp.

(Figs 47–49)

Material examined. Twenty-one specimens (Table 16).

Description. Body slender and elongated, tapered posteriorly, 3.62–10.2 mm long (6.13 mm in holotype) and 0.47–1.11 mm wide (0.65 mm in holotype) in anesthetized state (Fig. 47A, B). Dorsal surface smooth, translucent, without color pattern (Fig. 47A). Ventral surface translucent (Fig. 47B, C). Two pairs of cerebral eyespots present; two eyespots lying close to each other on both sides (Fig. 47D). Precerebral (= “frontal” in Bulnes and Faubel (2003); “marginal” in Curini-Galletti et al. (2008)) eyespots, four to six in number (four in holotype), distributed on both sides anterior to brain (Fig. 47D). Pharynx ruffled, 0.54–1.44 mm long (0.91 mm in

holotype), lying on body center (Fig. 47B, C). Mouth situated in center of pharynx. Epidermis ciliated; cilia slightly longer dorsally than ventrally (Fig. 48C, D). Dorsal epidermis columnar, about 11 μm in long axis. Ventral epithelium cubical, about 2.4 μm in longest axis (Fig. 48D). Rhabdites more numerous and longer dorsally than ventrally. Male gonopore situated behind pharynx. Male copulatory apparatus consisting of seminal vesicle, interpolated prostatic vesicle, and penis papilla (Figs 47E, 48A). Pair of sperm ducts running on each side of midline, separately leading to common sperm duct, forming spermiducal vesicle filled with sperm, then entering into seminal vesicle (Fig. 48A, B). Seminal vesicle oval (148 μm long; 80 μm high in holotype), running parallel to horizontal plane of body, with about 23-μm-thick, non-nucleated muscle fibers, leading to ejaculatory duct (Fig. 48A, B). Ejaculatory duct 16 μm thick and 55 μm long in holotype, opening into prostatic vesicle (Fig. 48A). Prostatic vesicle 141 μm long; 71 μm high in holotype; inner lining of prostatic vesicle formed by tall, glandular epithelium with radial folds (Fig. 48A, B, E–H). Muscle wall (16 μm thick) of prostatic vesicle, fusing with penis papilla, forming pyriform penis bulb. Several 4-μm-thick extra-vesicular gland's canals piercing prostatic vesicle muscle wall; a few fine granular secretions running through canals (Fig. 48A, E, G). Eosinophilic glands accumulated in distal half of inner ventral part of prostatic vesicle (Fig. 48A, E–G, I). Penis papilla conical, 14 μm thick (holotype), bent dorsally (Fig. 48A, B), protruding into male atrium for about 50.2 μm (holotype); innermost distal portion of ejaculatory duct sclerotized (Fig. 48A). Penis sheath differentiated into two portions: proximal one fused with parenchymatic tissue housing prostatic vesicle; distal one with cylindrical distal rim pierced by eosinophilic glands discharging their contents at tip, surrounding penis papilla; inner angular fold present on dorsal side (Fig. 48A, B, E–I); dorsal side of penis

sheath shorter than ventral one (about half length) (Fig. 48A, B). Penis bulb housed within tube-shaped penis sheath (206 μm long and 153 μm thick in holotype). Male atrium lined with ciliated epithelium, opening to exterior via male gonopore. Female gonopore located immediately posterior to male gonopore. Pair of oviducts running laterally, entering into near distal end of uterus (uterine/uterus vesicle). Uterus filled with eggs in several specimens (Fig. 49A–C). Vagina ciliated, leading to female atrium; latter opening to exterior via female gonopore (Fig. 49A, D). Cement glands concentrated around female reproductive systems. Lang's vesicle absent.

Type locality. Ikarikai Parking Park Beach (41.5357°N, 140.4297°E), Shiriuchi, Hokkaido, Japan.

Distribution. To date, confirmed from Hokkaido via Honshu to Shikoku, Japan: Oshoro and Shiriuchi (Hokkaido), Noto (Ishikawa, Honshu), Tateyama (Chiba, Honshu), Enoshima and Misaki (Kanagawa, Honshu), Kushimoto (Wakayama, Honshu), and Yasu (Kochi, Shikoku).

Habitat. Intertidal, on the surf zone in coarse sands and/or gravel, usually mixed with shell fragments. A single large specimen (ICHUM 8421) was collected from under a rock on a beach in Shiriuchi (type locality).

Sequences. Partial COI (613 bp; from 20 specimens) and 28S (1,007 bp; from two specimens) sequences were determined (Table 16). There were two variable sites within 204 amino-acid residues translated from the 613-bp COI nucleotide sequence among 20 specimens.

Genetic distances. Uncorrected *p*-distances among 28S sequences representing four species of *Theama* are shown in Table 17. The minimum value was 2.57% observed between my *Theama* sp. and *Theama* sp. 1 of Litvaitis et al. (2019).

Intraspecifically, uncorrected *p*-distances of COI were 0.00–1.47% within 20 specimens of *Theama* sp. collected from eight localities, Oshoro, Shiriuchi, Noto, Enoshima, Misaki, Tateyama, Kushimoto, and Yasu (Table 18). These values are encompassed within the intraspecific variations (0.00–2.00%) observed in a *Notocomplana* species for COI (Oya and Kajihara 2017).

Remarks. The specimens are assigned to *Theama* since they have the following characteristics: *i*) the narrow and elongated body without tentacles, *ii*) the prostatic vesicle interpolated, with the inner tall glandular epithelium developed to form radial folds, and *iii*) the penis papilla, directed backward, housed within a tube-shaped penis sheath (cf. Faubel 1983, Prudhoe 1985). *Theama* sp. is easily distinguished from *T. forrestensis* by having separated genital pores (Table 19). The species herein can be differentiated from *T. occidua* by *i*) the ratio of the dorsal/ventral ciliary lengths (longer dorsally than ventrally in *Theama* sp.; shorter dorsally than ventrally in *T. occidua*) and *ii*) the characteristics of the penis papilla (bent dorsally with its tip being a sclerotized cylindrical sheath in *Theama* sp.; straight and not sclerotized in *T. occidua*). *Theama* sp. is also different from *T. evelinae* by *i*) the precerebral-eyespot number (2–3 on each side in *Theama* sp.; 6–10 on each side in *T. evelinae*), *ii*) the position of the mouth in the pharyngeal pouch (centrally in *Theama* sp.; posteriorly in *T. evelinae*), and *iii*) the sclerotization of the penis papilla (only distal part in *Theama* sp.; along the entire ejaculatory duct in *T. evelinae*). Comparing the eyespot number, the ratio of dorsal/ventral ciliary lengths, and the sclerotization of the penis papilla, my species is most similar to *T. mediterranea*; however, they can be distinguished by *i*) the shape of the penis papilla (bent up in *Theama* sp.; straight in *T. mediterranea*), *ii*) the distal portion of the penis sheath (an evident inner angular fold present only on the dorsal side

in *Theama* sp.; without any inner folds in *T. mediterranea*), and *iii*) the position of the eosinophilic glands in the prostatic vesicle (in the distal half of the ventral region in *Theama* sp.; in the distal 1/3 of both the dorsal and ventral regions in *T. mediterranea*). The penis papilla could be distorted due to fixation process, but it can be a diagnostic character that distinguishes *Theama* sp. from *T. mediterranea* when I compare specimens fixed after careful anesthetization; in *T. mediterranea*, the penis papilla would always be straight when specimens were thus treated (Curini-Galletti, pers. comm.), whereas it was always bent dorsally in *Theama* sp. The uncorrected *p*-distance for the 28S between *Theama* sp. and *T. mediterranea* (3.43%) supports that they are genetically distinct because the value is greater than 1.69%, a value observed between two boniniids, *Boninia antillata* (GenBank MH700282) and *B. neotethydis* (MH700283), a pair of species that are apparently different from each other.

III. CONCLUSIONS

The suborder Cotylea is composed of more than 400 species of marine flatworms that are characterized by having the ventral adhesive organ located posterior to the female reproductive organ (Faubel 1983, Prudhoe 1985). In Japan, 72 species had been recorded before my study. During my Master's and Ph.D. courses, I investigated cotylean fauna around Japan including Hokkaido (Oshoro, Akkeshi, and Shiriuchi), Ishikawa, Chiba, Kanagawa, Shizuoka, Wakayama, Kochi, Kumamoto, Kagoshima, Okinawa (Okinawa Island and Ishigaki Island), and the Ogasawara Islands, based on morphological and molecular data of specimens collected in 2015–2022. This thesis is compiled from Tsuyuki and Kajihara (2020) and Tsuyuki et al. (2019, 2020a, b, 2021, 2022a, b, c).

In Chapter I, I provided an overview of Polycladida, reviewing the systematics of Cotylea from morphological and phylogenetic perspectives. Also, taxonomic problems of Cotylea in Japan were addressed.

In Chapter II, I discussed evolutionary routes of *Boninia* species as to colonization onto different microhabitats (interstitial/epibenthic) using an ancestral-state reconstruction analysis based on molecular phylogenetic results (Tsuyuki et al. 2022b). The results showed a habitat shift from the interstitial to epibenthic marine realm in the evolutionary history of flatworms based on molecular phylogenetic evidence with statistical support; such a route seems to be rare among Animalia because it has been reported only in acochilidian slugs in the clade Hedylopsacea so far (Jörger et al. 2014).

In the same chapter, I gave morphological accounts on 18 species in eight genera and seven families based on material from the intertidal and subtidal zones along

Japanese coasts. Of the 18, eight were established as new species (*Boninia uru* Tsuyuki et al., 2022b; *B. yambarensis* Tsuyuki et al., 2022b; *Enchiridium daidai* Tsuyuki and Kajihara, 2020; *Pericelis flavomarginata* Tsuyuki et al., 2020a; *Pe. lactea* Tsuyuki et al., 2022c; *Pe. maculosa* Tsuyuki et al., 2022c; *Prosthiostomum hibana* Tsuyuki et al., 2021; *Pr. torquatum* Tsuyuki et al., 2019), two turned to be undescribed ones (*Eucestoplana* sp. and *Theama* sp.), and three were newly recorded from Japan (*Bulaceros porcellanus* Newman and Cannon, 1996a (Tsuyuki et al. 2022a); *Eucestoplana* cf. *cuneata* (Sopott-Ehlers and Schmidt, 1975); *Stylostomum ellipse* (Dalyell, 1853) (Tsuyuki et al. 2020b)), respectively, during my Ph.D. course; for the remaining five (*Prosthiostomum auratum* Kato, 1937b; *Pr. ohshimai* (Kato, 1938a); *Pr.* cf. *ostreae* Kato, 1937b; *Pr. sonorum* Kato, 1938a; *Pr. vulgare* Kato, 1938b), I gave taxonomic re-descriptions because these had been insufficiently known (Tsuyuki et al. 2021). The following taxa (one family and three genera) were discovered in Japanese waters for the first time: Theamatidae, *Bulaceros* (Tsuyuki et al. 2022a), *Enchiridium* (Tsuyuki and Kajihara 2020), and *Eucestoplana*.

In Chapter II, I also performed molecular phylogenetic analyses. Integrating morphology and molecular phylogeny, I amended diagnoses of the two genera *Bulaceros* (Tsuyuki et al. 2022a) and *Pericelis* (Tsuyuki et al. 2022c), which resulted in transfer of the nominal species *Pseudoceros harrisi* Bolaños et al., 2007 and *Marcusia alba* Cuadrado et al., 2021 into respective genera, each yielding a new combination of the generic and specific names. My integrative approach (Tsuyuki and Kajihara 2020) upheld the concept of *Enchiridium* by Faubel (1984), instead of Bock (1913) or Prudhoe (1985), one of long-standing controversies in the history of polyclad systematics. Likewise, this approach provided support for regarding *Amakusaplana* as a junior

synonym of *Prosthiostomum*, something that had been in dispute between two camps of pro (Hyman 1959, Faubel 1984, Litvaitis et al. 2019) and con (Kato 1938a, Prudhoe 1985, Rawlinson et al. 2011) among polyclad specialists for more than 80 years.

Overall, my graduate research increased the number of cotylean taxa in Japanese waters from 72 species, 16 genera, 8 families to 85 species, 19 genera, 9 families.

REFERENCES

Aguado MT, Noreña C, Alcaraz L, Marquina D, Brusa F, Damborenea C, Almon B, Bleidorn C, Grande C (2017) Phylogeny of Polycladida (Platyhelminthes) based on mtDNA data. Organisms Diversity & Evolution 17: 767–778.

Akaike H (1974) A new look at the statistical model identification. IEEE Transactions on Automatic Control 19: 716–723.

Altekar G, Dwarkadas S, Huelsenbeck JP, Ronquist F (2004) Parallel Metropolis coupled Markov chain Monte Carlo for Bayesian phylogenetic inference. Bioinformatics 20: 407–415.

Andrade SC, Strand M, Schwartz M, Chen H, Kajihara H, von Döhren J, Sun S, Junoy J, Thiel M, Norenburg JL, Turbeville JM, Giribet G, Sundberg P (2012) Disentangling ribbon worm relationships: multi-locus analysis supports traditional classification of the phylum Nemertea. Cladistics 28: 141–159.

Ang HP, Newman LJ (1998) Warning colouration in pseudocerotid flatworms (Platyhelminthes, Polycladida). A preliminary study. Hydrobiologia 383: 29–33.

Anker A, Murina F-V, Lira C, Caripe JAV, Palmer AR, Jeng M-S (2005) Macrofauna associated with Echiuran Burrows: a review with new observations of the innkeeper worm, *Ochetostoma erythrogrammon* Lauckart and Rüppel, in Venezuela. Zoological Studies 44: 157–190.

Ax P (1984) Das Phylogenetische System: Systematisierung der lebenden Natur aufgrund ihrer Phylogenese. Gustav Fischer, Stuttgart.

Bahia J (2016) First records of polyclads (Platyhelminthes, Polycladida) associated with *Nodipecten nodosus* (Linnaeus 1758) aquaculture. Marine Biodiversity 46: 911–915.

Bahia J, Padula V (2009) First record of *Pseudoceros bicolor* and *Pericelis cata* (Platyhelminthes: Polycladida) from Brazil. Marine Biodiversity Records 2: 1–5.

Bahia J, Padula V, Correia MD, Sovierzoski HH (2015) First records of the order Polycladida (Platyhelminthes, Rhabditophora) from reef ecosystems of Alagoas

State, north-eastern Brazil, with the description of *Thysanozoon alagoensis* sp. nov. Journal of Marine Biological Association of the United Kingdom 8: 1653–1666.

Bahia J, Padula V, Lavrado HP, Quiroga S (2014) Taxonomy of Cotylea (Platyhelminthes: Polycladida) from Cabo Frio, southeastern Brazil, with the description of a new species. Zootaxa 3873: 495–525.

Bahia J, Padula V, Schrödl M (2017) Polycladida phylogeny and evolution: integrating evidence from 28S rDNA and morphology. Organisms Diversity & Evolution 17: 653–678.

Bahia J, Schrödl M (2018) Brazilian Polycladida (Rhabditophora: Platyhelminthes): rediscovery of Marcus' type material and general revision. Zootaxa 4490: 1–121.

Bassindale R, Barrett JH (1957) The Dale Fort marine fauna. Proceedings of the Bristol Naturalists' Society 29: 227–328.

Bergendal D (1890) Studien über nordische Turbellarien und Nemertinen. Vorläufige Mittheilung. Öfversigt af Kongl. Vetenskaps-Akademiens Förhandlingar Stockhorm 6: 323–328.

Blanchard E (1847) Recherches sur l'organisation des vers. Annales des Sciences Naturelles (3) Zoologie 8: 119–149, 271–275.

Bock S (1913) Studien über Polycladen. Zoologische Beiträge aus Uppsala 2: 31–344.

Bock S (1922) Two new cotylean genera of polyclads from Japan and remarks on some other cotyleans. Arkiv för Zoologi 14: 1–31.

Bock S (1923) *Boninia*, a new polyclad genus from the Pacific. Nova Acta Regiae Societatis Scientiarum Upsaliensis (4) 6: 1–32.

Bock S (1925) Papers from Dr. Th. Mortensen's Pacific Expedition 1914–16. XXV. Planarians, Pts. I–III. Videnskabelige Meddelelser Dansk Naturhistorisk Forening 79: 1–84.

Bock S (1931) Die Polycladen der deutschen Südpolar-Expedition 1901–1903. Deutsche Südpolar-Expedition 20 Zoologie: 259–304.

Bolaños DM, Quiroga SY, Litvaitis MK (2007) Five new species of cotylean flatworms (Platyhelminthes: Polycladida) from the wider Caribbean. Zootaxa 1650: 1–23.

Boom R, Sol CJ, Salimans MM, Jansen CL, Wertheim-van Dillen PM, van der Noordaa J (1990) Rapid and simple method for purification of nucleic acids. Journal of Clinical Microbiology 28: 495–503.

Brenzinger B, Haszprunar G, Schrödl M (2013) At the limits of a successful body plan – 3D microanatomy, histology and evolution of *Helminthope* (Mollusca: Heterobranchia: Rhodopemorpha), the most worm-like gastropod. Frontiers in Zoology 10: 37.

Bresslau E (1928–33) Turbellaria. In: Kükenthal W, Krumbach T (Eds) Handbuch der Zoologie: eine Naturgeschichte der Stämme des Tierreiches 2 (1). Walter de Gruyter, Berlin and Leipzig, 52–319.

Browne ET, Thompson IC, Gamble FW, Herdman WA, Cunningham JT, Beaumont WI, Weiss FE (1898) The Fauna and Flora of Valencia Harbour on the West Coast of Ireland. Proceedings of the Royal Irish Academy (1889–1901) 5: 667–854.

Bucklin A, Steinke D, Blanco-Bercial L (2011) DNA barcoding of marine metazoan. Annual Review of Marine Science 3: 471–508.

Bulnes VN, Faubel A (2003) *Eutheama forrestensis* n. sp. (Acotylea, Polycladida, Plathelminthes) from Australia. Zootaxa 220: 1–8.

Cannon LRG (1990) *Apidioplana apluda*, new species, a turbellarian symbiote of gorgonian corals from the Great Barrier Reef, with a review of the family Apidioplanidae (Polycladida: Acotylea). Memoirs of the Queensland Museum 28: 435–442.

Carus JV (1885) Vennes Polycladidea. In: Carus JV (Ed.) Prodromus faunae mediterraneae, sive descriptio animalium maris Mediterranei incolarum, quam comparata silva rerum quatenus innotuit, adiectis locis et nominibus vulgaribus eorumque auctoribus in commodum zoologorum 1. E. Schweizerbart, Stuttgart, 148–158.

Castresana J (2002) Gblocks. Version 0.91b. Online version. [accessed 2021 September 7]. http://molevol.cmima.csic.es/castresana/Gblocks_server.html

Cerca J, Purschke G, Struck TH (2018) Marine connectivity dynamics: clarifying cosmopolitan distributions of marine interstitial invertebrates and the meiofauna paradox. Marine Biology 165: 123.

Çinar ME (2014) Checklist of the phyla Platyhelminthes, Xenacoelomorpha, Nematoda, Acanthocephala, Myxozoa, Tardigrada, Cephalorhyncha, Nemertea, Echiura, Brachiopoda, Phoronida, Chaetognatha, and Chordata (Tunicata, Cephalochordata, and Hemichordata) from the coasts of Turkey. Turkish Journal of Zoology 38: 698–722.

Collingwood C (1876) On thirty-one species of marine planarians, collected partly by the late Dr Kelaart, F.L.S., at Trincomalee, and partly by Dr Collingwood, F.L.S. in the eastern seas. Transactions of the Linnean Society of London, 2nd Series, Zoology 1: 83–98.

Crothers JH (1966) Dale Fort Marine Fauna, 2nd Edition. Field Studies, London.

Cuadrado D, Moro L, Noreña C (2017) The Polycladida (Platyhelminthes) of the Canary Islands. New genus, species and records. Zootaxa 4312: 38–68.

Cuadrado D, Rodríguez J, Moro L, Grande C, Noreña C (2021) Polycladida (Platyhelminthes, Rhabditophora) from Cape Verde and related regions of Macaronesia. European Journal of Taxonomy 736: 1–43.

Curini-Galletti M, Campus P (2007) *Boninia neotethydis* sp. nov. (Platyhelminthes: Polycladida: Cotylea)—the first lessepsian flatworm. Journal of the Marine Biological Association of the United Kingdom 87: 435–442.

Curini-Galletti M, Campus P, Delogu V (2008) *Theama mediterranea* sp. nov. (Platyhelminthes, Polycladida), the first interstitial polyclad from the Mediterranean. Italian Journal of Zoology 75: 77–83.

Dalyell J (1853) The Powers of the Creator Displayed in the Creation, or, Observations on Life Amidst the Various Forms of the Humbler Tribes of Animated Nature: With Practical Comments and Illustrations 2. John Van Voorst, London.

Darriba D, Taboada GL, Doallo R, Posada D (2012) jModelTest 2: more models, new heuristics and parallel computing. Nature Methods 9: 772.

Deiss WA, Manning RB (1981) The fate of the invertebrate collections of the North Pacific Exploring Expedition, 1853–1856. Archives of Natural History 1981: 79–85.

Delle Chiaje S (1828) Memorie sulla storia e notomia degli animali senza vertebre del regno di Napoli. Vol. III. Fratelli Fernandes, Napoli.

Diesing KM (1862) Revision der Turbellarien. Abtheilung: Dendrocoelen. Sitzungsberichte der Kaiserlichen Akademie der Wissenschaften Wien 44: 485–578.

Dittmann IL, Cuadrado D, Aguado MT, Noreña C, Egger B (2019a) Polyclad phylogeny persists to be problematic. Organisms Diversity & Evolution 19: 585–608.

Dittmann IL, Dibiasi W, Noreña C, Egger B (2019b) Description of the snail-eating flatworm in marine aquaria, *Pericelis tectivorum* sp. nov. (Polycladida, Platyhelminthes). Zootaxa 4565: 383–397.

Dixit S, Manjebrayakath H, Saravanane N (2021) A rare polyclad genus *Bulaceros* (Platyhelminthes: Polycladida: Pseudocerotidae): new species and new record from Indian coral atolls. Marine Biology Research 16: 632–642.

Du Bois-Reymond Marcus E (1957) On Turbellaria. Anais da Academia Brasileira de Ciências 29: 153–191.

Du Bois-Reymond Marcus E, Marcus E (1966) Systematische Übersicht der Polykladen. Zoologische Beiträge 12: 319–343.

Du Bois-Reymond Marcus E, Marcus E (1968) Polycladida from Curaçao and faunistically related regions. Studies on the Fauna of Curaçao and other Caribbean Islands 101: 1–133.

Dujardin F (1851) Sur un petit animal marin, l'Echinodére, formant un type intermédiaire entre les Crustacés et les Vers. Annales des Sciences Naturelles 3: 158–160.

Eales NB (1961) The Littoral Fauna of the British Isles: a Handbook for Collectors by N. B. Eales with a Forward by the Late Stanley Kemp, 3rd Edition. Cambridge University Press, London.

Egger B, Lapraz F, Tomiczek B, Müller S, Dessimoz C, Girstmair J, Škunca N, Rawlinson KA, Cameron CB, Beli E, Todaro MA, Gammoudi M, Noreña C, Telford MJ (2015) A transcriptomic-phylogenomic analysis of the evolutionary relationships of flatworms. Current Biology 25: 1347–1353.

Ehrenberg CG (1831) Phytozoa Turbellaria africana et asiatica. In: Hemprich and Ehrenberg "Symbolae physicae." Animalia Evertebrata Exclusis Insectis Recensuit Dr. CG Ehrenberg. Series Prima Cum Tabularum Decade Prima. Berolini, Fol. Phytozoa Turbellaria folia a-d, T4-5.

Evans AC (1967) Syntypes of Decapoda described by William Stimpson and James Dana in the collections of the British Museum (Natural History). Journal of Natural History 1: 399–411.

Faasse M, Ligthart M (2007) De Nederlandse polyclade platwormen (Platyhelminthes: Turbellaria: Polycladida): IV. *Stylostomum ellipse* en *Imogine necopinata* (en *Euplana gracilis*). Het Zeepaard 67: 44–47.

Farran GP (1915) Results of a biological survey of Blacksod Bay, Co. Mayo. Fisheries Ireland Scientific Investigations 1914 3: 1–72.

Faubel A (1983) The Polycladida, Turbellaria. Proposal and establishment of a new system. Part I. The Acotylea. Mitteilungen aus dem Hamburgischen Zoologischen Museum und Institut 80: 17–121.

Faubel A (1984) The Polycladida, Turbellaria. Proposal and establishment of a new system. Part II. The Cotylea. Mitteilungen aus dem Hamburgischen Zoologischen Museum und Institut 81: 189–259.

Faubel A, Warwick RM (2005) The marine flora and fauna of the Isles of Scilly: free-living Plathelminthes (‘Turbellaria’). Journal of Natural History 39: 1–45.

Felsenstein J (1985) Confidence limits on phylogenies: an approach using the bootstrap. Evolution 39: 783–791.

Fenchel TM (1978) The ecology of micro-and meiobenthos. Annual Review of Ecology and Systematics 9: 99–121.

Freeman D (1930) Three polyclads from the region of Point Firmin, San Pedro, California. Transactions of the American Microscopical Society 49: 334–341.

Fujiwara Y, Urabe J, Takeda S (2014) Host preference of a symbiotic flatworm in relation to the ecology of littoral snails. Marine Biology 161: 1873–1882.

Galleni L, Puccinelli I (1981) Karyological observation on polyclads. Hydrobiologia 84: 31–44.

Gamble FW (1893a) Contributions to a knowledge of British marine Turbellaria. Quarterly Journal of Microscopical Science 34: 433–528.

Gamble FW (1893b) The Turbellaria of Plymouth Sound and the neighbourhood. Journal of the Marine Biological Association of the United Kingdom 3: 30–47.

Gamble FW (1893c) Report on the Turbellaria of the L.M.B.C. district. Proceedings and Transactions of the Liverpool Biological Society 7: 148–174.

Gammoudi M, Noreña C, Tekaya S, Prantl V, Egger B (2011) Insemination and embryonic development of some Mediterranean polyclad flatworms. Invertebrate Reproduction & Development 56: 272–286.

Gammoudi M, Tekaya S, Noreña C (2009) Contribution to the knowledge of acotylean polyclads (Platyhelminthes, Polycladida) from Tunisian coasts. Zootaxa 2195: 43–60.

Grube E (1840) Actinien, Echinodermen und Würmer des Adriatischen- und Mittelmeers, nach eigenen Sammlungen beschrieben. Verlag von J.H. Bon, Königsberg.

Ha TM (2016) Adaptation of ostracods (Arthropoda:Crustacea) from sediment surface to interstitial environment: an example of leptocytherid species inferred from morphological and molecular phylogeny. D. Sc. Thesis, Shizuoka University

Hagiya M, Gamô S (1992) Polyclads (Platyhelminthes) collected from the intertidal rocky shore at Manazuru, Sagami Bay. Reports of the Manazuru Marine Laboratory

for Science Education, Faculty of Education, Yokohama University 8: 13–24. (Japanese with English abstract)

Hallez P (1893) Catalogue des turbellariés (Rhabdocoelides, Triclades et Polyclades) du Nord de la France et de la côte Boulonnaise. Revue biologique du nord de la France 5: 1–239.

Hallez P (1894) Catalogue des Rhabdocelides, Triclades & Polyclades du Nord de la France, 2nd edition. L. Danel, Lille.

Hallez P (1905) Note préliminaire sur les polyclades recueillis dans l'Expédition antarctique du 'Français'. Bulletin de la Société zoologique de France 30: 124–127.

Hallez P (1907) Vers polyclades et triclades maricoles. In: Charcot J (Ed.) Expédition antarctique française (1903–1905). Masson et C^{ie}, Paris, 1–26.

Hallez P (1911) Double fonction des ovaires de quelques polyclades. Comptes-rendus de l'Académie des Sciences de Paris 153: 141–143.

Hallez P (1913) Vers polyclades et triclades maricoles. In: Charcot J (Ed.) Deuxième Expédition Antarctique Française (1908–1910). Masson et C^{ie}, Paris, 1–70.

Heath H, McGregor EA (1913) New polyclads from Monterey Bay, California. Proceedings of the Academy of Natural Sciences of Philadelphia 64: 455–488.

Hebert PDN, Gregory TR (2005) The promise of DNA barcoding for taxonomy. Systematic Biology 54: 852–859.

Hendelberg J (1974) Polyclader yid svenska väskusten. Zoologisk Revys 36: 3–18.

Holleman JJ (1972) Marine turbellarians of the Pacific Coast 1. Proceedings of the Biological Society of Washington 85: 405–412.

Holleman JJ (2001) A review of the genus *Stylostomum* Lang, 1884 (Platyhelminthes, Polycladida) and the description of a new species. Belgian Journal of Zoology (Supplement) 131: 227–229.

Hyman LH (1939a) Acoel and polyclad Turbellaria from Bermuda and the Sargassum. Bulletin of the Bingham Oceanographic Collection 7(Art I): 1–26.

Hyman LH (1939b) Polyclad worms collected on the Presidential cruise of 1938. Smithsonian Miscellaneous Collections 98: 1–13.

Hyman LH (1951) The Invertebrates: Platyhelminthes and Rhynchocoela. The Acoelomate Bilateria. McGraw-Hill Book Company, New York.

Hyman LH (1953) The polyclad flatworms of the Pacific coast of North America. Bulletin of the American Museum of Natural History 100: 269–391.

Hyman LH (1955a) A further study of the polyclad flatworms of the West Indian region. Bulletin of Marine Science 5: 259–268.

Hyman LH (1955b) Some polyclad flatworms from the West Indies and Florida. Proceedings of the United States National Museum 104: 115–150.

Hyman LH (1959) A further study of Micronesian polyclad flatworms. Proceedings of the United States National Museum 108: 543–597.

Iwase F, Uchida H, Nomura K, Fukuda T, Misaki H (1990) Okinawa Kaichu Seibutsu Zukan [Illustrated Guide to Marine Life in Okinawa]. (Shinsei Zukan Series; vol. 11). Sazan Press, Okinawa. (Japanese)

Jensen OS (1878) Turbellaria ad litora norvegiae occidentalia. Turbellarier ved Norges Vestkyst. Bergens Museums Skrifter 1: 1–98.

Jie W-B, Kuo S-C, Wu S-C, Lee K-S (2013) Unreported predatory behavior on crustaceans by *Ilyella gigas* (Schmarda, 1859) (Polycladida: Ilyplanidae), a newly-recorded flatworm from Taiwan. Platax 10: 57–71.

Johnston G (1865) A catalogue of the British non-parasitical worms in the collection of the British Museum. British Museum, London.

Jokiel PL, Townsley SJ (1974) Biology of the Polyclad *Prosthiostomum* (*Prosthiostomum*) sp., a new coral parasite from Hawaii. Pacific Science 28: 361–373.

Jörger KM, Brenzinger B, Neusser TP, Martynov AV, Wilson NG, Schrödl M (2014) Panpulmonate habitat transitions: tracing the evolution of Acochlidia

(Heterobranchia, Gastropoda). BioRxiv [Preprint]. Available from: https://www.biorxiv.org/content/10.1101/010322v1.

Kaburaki T (1918) Zoological results of a tour in the far east. Brackish-water polyclads. Memoirs of the Asiatic society of Bengal 6: 185–192.

Kaburaki T (1923) Notes on Japanese polyclad Turbellarians. Annotationes Zoologicae Japonenses 10: 191–201.

Kato K (1934) Polyclad turbellarians from the neighborhood of the Mitsui Institute of Marine Biology. Japanese Journal of Zoology 6: 123–138.

Kato K (1935) *Stylochoplana parasitica* sp. nov., a polyclad parasitic in the pallial groove of the chiton. Annotationes Zoologicae Japonenses 15: 123–129.

Kato K (1937a) Polyclads collected in Idu, Japan. Japanese Journal of Zoology 7: 211–232.

Kato K (1937b) Thirteen new polyclads from Misaki. Japanese Journal of Zoology 7: 347–371.

Kato K (1937c) Three polyclads from northern Japan. Annotationes Zoologicae Japonenses 16: 35–38.

Kato K (1938a) Polyclads from Amakusa, southern Japan. Japanese Journal of Zoology 7: 559–576.

Kato K (1938b) Polyclads from Seto, Middle Japan. Japanese Journal of Zoology 7: 577–593.

Kato K (1939a) Polyclads in Onagawa and vicinity. Science reports of the Tohoku Imperial University 14: 65–79.

Kato K (1939b) Report of the biological survey of Mutsu Bay. Science reports of the Tohoku Imperial University 14: 141–153.

Kato K (1943a) A new polyclad with anus. Bulletin of the Biogeographical Society of Japan 13: 47–53.

Kato K (1943b) Polyclads from Formosa. Bulletin of the Biogeographical Society of Japan 13: 69–77.

Kato K (1943c) Polyclads from Palao. Bulletin of the Biogeographical Society of Japan 13: 79–90.

Kato K (1944) Polycladida of Japan. Journal of Sigenkagaku Kenkyusyo 1: 257–319.

Kato M (2018) Restoration of the collection information for an Australian mammal skeletal specimen stored in the National Museum of Nature and Science, Japan. Proceedings of the Japanese Society of Systematics Zoology 45:61–72. (Japanese with English abstract)

Katoh K, Rozewicki J, Yamada KD (2017) MAFFT online service: multiple sequence alignment, interactive sequence choice and visualization. Briefings in Bioinformatics 20: 1160–1166.

Kawakatsu M (2004) [The status of management for type series of Japanese turbellarians (Platyhelminthes: "Turbellaria")—especially Tricladida]. In: Ohtaka A (ed) [Promotion of appropriate management of important specimens in the taxonomy of freshwater invertebrates in Japan]. Report from the River Foundation 16-1-10-1, Tokyo, pp. 5–6. (Japanese)

Kumar S, Stecher G, Li M, Knyaz C, Tamura K (2018) MEGA X: molecular evolutionary genetics analysis across computing platforms. Molecular Biology and Evolution 35: 1547–1549.

Kumar S, Stecher G, Tamura K (2016) MEGA7: molecular evolutionary genetics analysis version 7.0 for bigger datasets. Molecular biology and evolution 33: 1870–1874.

Laidlaw FF (1902) The marine Turbellaria, with an account of the anatomy of some of the species. The Fauna and Geography of the Maldive and Laccadive Archipelagoes 1: 282–312.

Laidlaw FF (1903a) On a collection of Turbellaria Polycladida from the Straits of Malacca. (Skeat Expedition, 1899–1900). Proceedings of the Zoological Society of London 1: 301–318.

Laidlaw FF (1903b) Suggestions for a revision of the classification of the polyclad Turbellaria. Memoirs and Proceedings of the Manchester Literary & Philoshophical Society 48: 1–16.

Laidlaw FF (1906) On the marine fauna of the Cape Verde Islands, from collections made in 1904 by Mr C. Crosslan—The polyclad Turbellaria. Proceedings of the Zoological Society of London 2: 705–719.

Lanfear R, Calcott B, Ho SYW, Guindon S (2012) PartitionFinder: combined selection of partitioning schemes and substitution models for phylogenetic analyses. Molecular Biology and Evolution 29: 1695–1701.

Lanfear R, Frandsen PB, Wright AM, Senfeld T, Calcott B (2016) PartitionFinder 2: new methods for selecting partitioned models of evolution for molecular and morphological phylogenetic analyses. Molecular Biology and Evolution 34: 772–773.

Lang A (1884) Die Polycladen (Seeplanarien) des Golfes von Neapel und der angrenzenden Meeresabschnitte. Eine Monographie. Wilhelm Engelmann, Leipzig.

Lapraz F, Rawlinson KA, Girstmair J, Tomiczek B, Berger J, Jékely G, Telford MJ, Egger B (2013) Put a tiger in your tank: the polyclad flatworm *Maritigrella crozieri* as a proposed model for evo-devo. EvoDevo 4: 29.

Laumer CE, Giribet G (2014) Inclusive taxon sampling suggests a single, stepwise origin of ectolecithality in Platyhelminthes. Biological Journal of the Linnean Society 111: 570–588.

Laumer CE, Hejnol A, Giribet G (2015) Nuclear genomic signals of the 'microturbellarian' roots of platyhelminth evolutionary innovation. eLife 4: e05503.

Laverack MS, Blackler M (1974) Fauna and Flora of St. Andrews Bay. Scottish Academic Press, Edinburgh and London.

Leasi F, Andrade SC, Norenburg J (2016) At least some meiofaunal species are not everywhere. Indication of geographic, ecological and geological barriers affecting the dispersion of species of *Ototyphlonemertes* (Nemertea, Hoplonemertea). Molecular Ecology 25: 1381–1397.

Lee K, Beal MA, Johnston EL (2006) A new predatory flatworm (Platyhelminthes, Polycladida) from Botany Bay, New South Wales, Australia. Journal of Natural History 39: 3987–3995.

Leuckart R (1859) Bericht über die wissenschaftlichen Leistungen in der Naturgeschichte der niederen Thiere während des Jahres 1858. Archiv für Naturgeschichte 25: 97–255.

Litvaitis MK, Bolaños DM, Quiroga SY (2010) When names are wrong and colours deceive: unravelling the *Pseudoceros bicolor* species complex (Turbellaria: Polycladida). Journal of Natural History 44: 829–845.

Litvaitis MK, Bolaños DM, Quiroga SY (2019) Systematic congruence in Polycladida (Platyhelminthes, Rhabditophora): are DNA and morphology telling the same story? Zoological Journal of the Linnean Society 186: 865–891.

Lo Bianco S (1888) Notizie biologiche riguardanti specialmente il periodo di maturita sessuale degli animali del Golfo di Napoli. Mitteilungen aus der Zoologischen Station zu Neapel 8: 385–440.

Lovén S (1844) *Chaetoderma*, ett nytt maskslägte n.g. Öfversigt af Kongl. Vetenskaps-akademiens förhandlingar 1: 116, pl. 112.

Lytwyn MW, McDermott JJ (1976) Incidence, reproduction and feeding of *Stylochus zebra*, a polyclad turbellarian symbiont of hermit crabs. Marine Biology 38: 365–372.

Marcus E (1948) Turbellaria do Brasil. Boletim da Faculdade de Filosofia, Ciências e Letras, Universidade de São Paulo, Zoologia 13: 111–243.

Marcus E (1949) Turbellaria Brasileiros (7). Boletim da Faculdade de Filosofia, Ciências e Letras, Universidade de São Paulo, Zoologia 14: 7–155.

Marcus E (1950) Turbellaria brasileiros (8). Boletim da Faculdade de Filosofia, Ciências e Letras, Universidade de São Paulo, Zoologia 15: 5–191.

Marcus E (1954) Reports of the Lund University Chile Expedition 1948–1949. 11. Turbellaria. Lunds Universitets Årsskrift. Ny Följd 49: 1–115.

Marquina D, Aguado MT, Noreña C (2015) New records of Cotylea (Polycladida, Platyhelminthes) and one new species from Lizard Island (Australia), with remarks on the distribution of the *Pseudoceros* Lang, 1884 and *Pseudobiceros* Faubel, 1984 species of the Indo-Pacific marine region. Zootaxa 4019: 354–377.

Marshall OJ (2004) PerlPrimer: cross-platform, graphical primer design for standard, bisulphite and real-time PCR. Bioinformatics 20: 2471–2472.

McIntosh WC (1874) On the invertebrate marine fauna and fishes of St. Andrews. Annals and Magazine of Natural History, Series 4 14: 144–155.

McIntosh WC (1875) The marine invertebrates and fishes of St. Andrews. Adam and Charles Black, Edinburgh.

Meixner A (1907) Polycladen von der Somaliküste, nebst einer Revision der Stylochinen. Zeitschrift für wissenschaftliche Zoologie 88: 385–498.

Merory M, Newman LJ (2005) A new stylochid flatworm (Platyhelminthes, Polycladida) from Victoria, Australia and observations on its biology. Journal of Natural History 39: 2581–2589.

Michiels NK, Newman LJ (1998) Sex and violence in hermaphrodites. Nature 391: 647–647.

Micoletzky H (1910) Die Turbellarienfauna des Golfes von Triest. Arbeiten aus dem Zoologischen Institut der Universität Wien 18: 167–182.

Montagu G (1813) Description of several new or rare animals, principally marine, found on the south coast of Devonshire. Transactions of the Linnean Society of London 11: 1–26.

Neusser TP, Jörger KM, Lodde-Bensch E, Strong EE, Schrödl M (2016) The unique deep sea—land connection: interactive 3D visualization and molecular phylogeny of *Bathyhedyle boucheti* n. sp. (Bathyhedylidae n. fam.)—the first panpulmonate slug from bathyal zones. PeerJ 4: e2738.

Newman LJ (2002) A new euryleptid flatworm (Platyhelminthes, Polycladida) associated with a colonial ascidian from the Great Barrier Reef. Memoirs of the Queensland Museum 48: 169–172.

Newman LJ, Cannon LRG (1994) *Pseudoceros* and *Pseudobiceros* (Platyhelminthes, Polycladida, Pseudocerotidae) form eastern Australia and Papua New Guinea. Memoirs of the Queensland Museum 37: 205–266.

Newman LJ, Cannon LRG (1996a) *Bulaceros*, new genus, and *Tytthosoceros*, new genus, (Platyhelminthes: Polycladida) from the Great Barrier Reef, Australia and Papua New Guinea. Raffles Bulletin of Zoology 44: 479–492.

Newman LJ, Cannon LRG (1996b) New genera of pseudocerotid flatworms (Platyhelminthes: Polycladida) from Australian and Papua New Guinean coral reefs. Journal of Natural History 30: 1425–1441.

Newman LJ, Cannon LRG (2000) A new genus of euryleptid flatworm (Platyhelminthes, Polycladida) from the Indo-Pacific. Journal of Natural History 34: 191–205.

Newman LJ, Cannon LRG (2003) Marine Flatworms: the World of Polyclad Flatworms. CSIRO Publishing, Collingwood.

Newman LJ, Cannon LRG (2005) Fabulous Flatworms: a Guide to Marine Polyclads. Version 1. ABRS & CSIRO Publishing, Clayton. CD-ROM.

Newman LJ, Cannon LRG, Brunckhorst DJ (1994) A new flatworm (Platyhelminthes: Polycladida) which mimics a Phyllidiid Nudibranch (Mollusca, Nudibranchia). Zoological Journal of the Linnean Society 110: 19–25.

Newman LJ, Norenburg JL, Reed S (2000) Taxonomic and biological observations on the tiger flatworm, *Maritigrella crozieri* (Hyman, 1939), new combination (Platyhelminthes, Polycladida, Euryleptidae) from Florida waters. Journal of Natural History 34: 799–808.

Nguyen LT, Schmidt HA, Von Haeseler A, Minh BQ (2015) IQ-TREE: a fast and effective stochastic algorithm for estimating maximum-likelihood phylogenies. Molecular Biology and Evolution 32: 268–274.

Noodt W (1974) Anpassung an interstitielle Bedingungen: ein Faktor in der Evolution höherer Taxa der Crustacea? Faunistisch-ökologische Mitteilungen 4: 445–452.

Noren M, Jondelius U (2002) The phylogenetic position of the Prolecithophora (Rhabditophora, 'Platyhelminthes'). Zoologica Scripta 31: 403–414.

Noreña C, Marquina D, Perez J, Almon B (2014) First records of Cotylea (Polycladida, Platyhelminthes) for the Atlantic coast of the Iberian Peninsula. ZooKeys 404: 1–22.

Okada Y, Uchida S, Uchida T (1965) New Illustrated Encyclopedia of the Fauna of Japan. Vol. 1. Hokuryu-kan Publishing, Tokyo. (Japanese)

Okuno J, Naruse T (2013) First records of five flatworms belonging to the genus *Pseudoceros* Lang (Turbellaria: Polycladida) from Japanese waters. Biological Magazine Okinawa 51: 57–66. (Japanese with English abstract)

Ono A (2015) Flatworms Illustrated. Seibundoshinkosha, Tokyo. (Japanese)

Ooishi S (1970) Marine invertebrate fauna of the Ogasawara and Volcano Islands collected by S. Ooishi, Y. Tomida, K. Izawa and S. Manabe. In: Toba Aquarium and Asahi Shinbun Publishing Company (Ed.), Report on the Marine Biological Expedition to the Ogasawara (Bonin) Islands, 1968. Asahi Shinbun Publishing Company, Tokyo, 75–95. (Japanese)

Oya Y, Kajihara H (2017) Description of a new *Notocomplana* species (Platyhelminthes: Acotylea), new combination and new records of Polycladida from the northeastern Sea of Japan, with a comparison of two different barcoding markers. Zootaxa 4282: 526–542.

Oya Y, Kajihara H (2019) A new bathyal species of *Cestoplana* (Polycladida: Cotylea) from the West Pacific Ocean. Marine Biodiversity 49: 905–911.

Oya Y, Kajihara H (2020) Molecular phylogenetic analysis of Acotylea (Platyhelminthes: Polycladida). Zoological Science 37: 271–279.

Oya Y, Nakajima H, Kajihara H (2022) A new symbiotic relationship between a polyclad flatworm and a mantis shrimp: description of a new species of

Emprosthopharynx (Polycladida: Acotylea) associated with *Lysiosquilla maculata* (Crustacea: Stomatopoda). Marine Biodiversity 52: 46.

Palombi A (1924) Diagnosi di nuove specie di polycladi della R.N. “Liguria”. Note preliminaire. Bolletino della Societá di Sciencia Naturale di Napoli 35: 33–37.

Palombi A (1928) Report on the Turbellaria. Cambridge Expedition to Suez Canal, 1924. Transations of the Zoological Society of London 22: 579–631.

Palombi A (1936) Policladi liberi e commensali raccoliti sulle coste del Sud Africa, della Florida e del golfo di Napoli. Archivio Zoologico Italiano 23: 1–45.

Palombi A (1939) Turbellaria del Sud Africa. Policladi di East London. Terzo contributo. Archivio Zoologico Italiano 28: 123–149.

Palumbi S, Martin A, Romano S, McMillan WO, Stice L, Grabowski G (1991) The Simple Fools Guide to PCR. Ver. 2. Department of Zoology and Kewalo Marine Laboratory, University of Hawaii, Honolulu.

Pearse AS (1938) Zoological Names. A List of Phyla, Classes, and Orders, Prepared for Section F, American Association for the Advancement of Science. Duke University Press, United, Durham.

Pérez-García P, Herrero-Barrencua A, Noreña C, Cervera JL (2020) Marine flatworms in the Gulf of Guinea: a description of a new species of *Pseudobiceros* (Platyhelminthes; Polycladida) from Principe Island. Bulletin of Marine Science 96: 753–764.

Pitale R, Apte D (2019) Intertidal euryleptid polyclads and description of a new *Stylostomum* Lang, 1884 from Maharashtra, India. Zootaxa 4652: 317–339.

Pitale R, Bhave V, Apte D (2014) First record of family Prosthiostomidae and *Prosthiostomum trilineatum* (Platyhelminthes: Polycladida) from the west coast of India. Marine Biodiversity Records 7: 1–6.

Plehn M (1896) Neue Polycladen, gesammelt von Herrn Kapitän Chierchia bei der Erdumschiffung der Korvette Vettor Pisani, von Herrn Prof. Dr Kükenthal im

nördlichen Eismeer und von Herrn Prof. Dr Semon in Java. Jenaische Zeitschrift für Naturwissenschaft 30: 137–176.

Poche F (1926) Das System der Platodaria. Archiv für Naturgeschichte A: 1–458.

Poulter JL (1974) A new species of the genus *Pericelis*, a polyclad flatworm from Hawaii. In: Riser NW, Morse MP (Eds) Biology of the Turbellaria. McGraw-Hill, New York, 93–107.

Poulter JL (1975) Hawaiian polyclad flatworms: Prosthiostomids. Pacific Science 29: 317–339.

Prudhoe S (1944) On some polyclad turbellarians from the Cayman Islands. Annals and Magazine of Natural History 11: 322–334.

Prudhoe S (1982a) British polyclad turbellarians. In: Kermack DM, Barnes RSK (Eds) Synopses of the British Fauna (New Series) 6. The Linnean Society of London and the Estuarine and Brackish-water Sciences Association, Cambridge University Press, Cambridge, 1–77.

Prudhoe S (1982b) Polyclad flatworms. In: Shepherd SA, Thomas IM (Eds) Marine Invertebrates of Southern Australia. Handbook of the Flora and Fauna of South Australia. Part I: South Australian Government, Adelaide, 220–227.

Prudhoe S (1982c) Polyclad turbellarians from the southern coasts of Australia. Records of the South Australian Museum (Adelaide) 18: 361–384.

Prudhoe S (1985) A Monograph on Polyclad Turbellaria. Oxford University Press, Oxford.

Prudhoe S (1989) Polyclad turbellarians recorded from African waters. Bulletin of the British Museum (Natural History) Zoology 55: 47–96.

Quatrefages A de (1845) Études sur les types inférieurs de l'embranchement des annelés: mémoire sur quelques planairées marines appartenant aux genres *Tricelis* (Ehr.), *Polycelis* (Ehr.), *Prosthiostomum* (Nob.), *Proceros* (Nob.), *Eolidiceros* (Nob.), et *Stylochus* (Ehr.). Annales des Sciences Naturelles (3) Zoologie 4: 129–184.

Quiroga SY, Bolaños DM, Litvaitis MK (2006) First description of deep-sea polyclad flatworms from the North Pacific: *Anocellidus* n. gen. *profundus* n. sp. (Anocellidae, n. fam.) and *Oligocladus voightae* n. sp. (Euryleptidae). Zootaxa 1317: 1–19.

Ramos-Sánchez M, Bahia J, Bastida-Zavala JR (2020) Five new species of cotylean flatworms (Platyhelminthes: Polycladida: Cotylea) from Oaxaca, southern Mexican Pacific. Zootaxa 4819: 49–83.

Rawlinson KA, Bolaños DM, Liana MK, Litvaitis MK (2008) Reproduction, development and parental care in two direct-developing flatworms (Platyhelminthes: Polycladida: Acotylea). Journal of Natural History 42: 2173–2192.

Rawlinson KA, Gillis JA, Billings RE, Borneman EH (2011) Taxonomy and life history of the *Acropora*-eating flatworm *Amakusaplana acroporae* nov. sp. (Polycladida: Prosthiostomidae). Coral Reefs 30: 693–705.

Remane A (1933) Verteilung und organisation der benthonischen Mikrofauna der Kieler Bucht. Wissenschaftliche Meeresuntersuchungen 21: 161–221.

Ritson-Williams R, Yotsu-Yamashita M, Paul VJ (2006) Ecological functions of tetrodotoxin in a deadly polyclad flatworm. Proceedings of the National Academy of Sciences 103: 3176–3179.

Rodríguez J, Hutchings PA, Williamson JE (2021) Biodiversity of intertidal marine flatworms (Polycladida, Platyhelminthes) in southeastern Australia. Zootaxa 5024: 1–63.

Ronquist F, Huelsenbeck JP (2003) MrBayes 3: Bayesian phylogenetic inference under mixed models. Bioinformatics 19: 1572–1574.

Schmarda LK (1859) Neue wirbellose Thiere beobachtet und gesammelt auf einer Reise um die Erde 1853 bis 1857. Vol. 1. Bd. I. Turbellarien, Rotatorien und Anneliden. Wilhelm Engelmann, Leipzig.

Schmidtlein R (1880) Vergleichende Übersicht über das Erscheinen grösserer pelagisher Thiere und Bermerkungen über Fortpflanzungsverhältnisse einiger Seethiere im Aquarium. Mitteilungen aus der Zoologischen Station zu Neapal 2: 162–175.

Sonnenberg R, Nolte AW, Tautz D (2007) An evaluation of LSU rDNA D1-D2 sequences for their use in species identification. Frontiers in Zoology 4: 1–12.

Sopott-Ehlers B, Schmidt P (1975) Interstitielle Fauna von Galapagos XIV. Polycladida (Turbellaria). Mikrofauna des Meeresbodens 54: 193–222.

Southern R (1936) Turbellaria of Ireland. Proceedings of the Royal Irish Academy 43 (B): 43–72.

Soutullo P, Cuadrado D, Noreña C (2021) First study of the Polycladida (Rhabditophora, Platyhelminthes) from the Pacific Coast of Costa Rica. Zootaxa 4964: 363–381.

Stamatakis A (2014) RAxML version 8: a tool for phylogenetic analysis and post-analysis of large phylogenies. Bioinformatics 30: 1312–1313.

Steenwyk JL, Buida TJ, Li Y, Shen X-X, Rokas A (2020) ClipKIT: a multiple sequence alignment trimming software for accurate phylogenomic inference. PLOS Biology 18: e3001007.

Steinböck O (1932) Die Turbellarian des arktischen Gebietes. In: Römer F, Schaudinn FR (Eds) Fauna Arctica 6: 295–342.

Steinböck O (1933) Die Turbellarienfauna der Umgebung von Rovingno. Thalassia 1: 1–33.

Stimpson W (1855) Descriptions of some of the new marine Invertebrata from the Chinese and Japanese seas. Proceedings of the Academy of Natural Sciences of Philadelphia 7: 375–384.

Stimpson W (1857) Prodromus descriptionis animalium evertebratorum quae in expeditione ad Oceanum, Pacificum Septentrionalem a Republica Federata missa, Johanne Rodgers Duce observavit et descripsit. Pars. I. Tubellaria Dendrocoela. Proceedings of the Academy of Natural Sciences of Philadelphia 9: 19–31.

Strand E (1926) Miscellanea nomenclatorial zoologica. Archiv für Naturgeschichte 92: 30–75.

Struck TH, Golombek A, Weigert A, Franke FA, Westheide W, Purschke G, Bleidorn C, Halanych KM (2015) The evolution of annelids reveals two adaptive routes to the interstitial realm. Current Biology 25: 1993–1999.

Stummer-Traunfels RR von (1902) Eine Süßwasser-Polyclade aus Borneo. Zoologischer Anzeiger 26: 159–161.

Stummer-Traunfels R (1933) Polycladida (continued). In: Bronn HG (Ed.) Klassen und Ordnungen des Tier-Reichs IV. (Vermes). Akademische Verlagsgesellschaft, Leipzig, 3485–3596.

Tajika K-I, Raj U, Horiuchi S, Koshida Y (1991) Polyclad turbellarians collected on the Osaka University Expedition to Viti Levu, Fiji, in 1985, with remarks on distribution and phylogeny of the genus *Discoplana*. Hydrobiologia 227: 333–339.

Telford MJ, Herniou EA, Russell RB, Littlewood DTJ (2000) Changes in mitochondrial genetic codes as phylogenetic characters: two examples from the flatworms. Proceedings of the National Academy of Sciences 97: 11359–11364.

Tong SJW, Ong RSL (2020) Mating behavior, spawning, parental care, and embryonic development of some marine pseudocerotid flatworms (Platyhelminthes: Rhabditophora: Polycladida) in Singapore. Invertebrate Biology 139: e12293.

Tsunashima T, Hagiya M, Yamada R, Koito T, Tsuyuki N, Izawa S, Kosoba K, Itoi S, Sugita H (2017) A molecular framework for the taxonomy and systematics of Japanese marine turbellarian flatworms (Platyhelminthes, Polycladida). Aquatic Biology 26: 159–167.

Tsuyuki A, Kajihara H (2020) A giant new species of *Enchiridium* (Polycladida, Prosthiostomidae) from southwestern Japan. ZooKeys 918: 15–28.

Tsuyuki A, Kohtsuka H, Kajihara H (2021) Description of a new species of the marine flatworm *Prosthiostomum* (Platyhelminthes: Polycladida) and its three known congeners from Misaki, Japan, with inference of their phylogenetic positions within Prosthiostomidae. Zoological Studies 60: 1–20.

Tsuyuki A, Kohtsuka H, Hookabe N, Kajihara H (2022a) First record of *Bulaceros porcellanus* Newman & Cannon, 1996 (Platyhelminthes, Polycladida, Cotylea) from

Japanese waters, with a revision of the generic diagnosis based on morphology and molecular phylogeny. Plankton and Benthos Research 17: 147–155.

Tsuyuki A, Oya Y, Jimi N, Kajihara H (2020a) Description of *Pericelis flavomarginata* sp. nov. (Polycladida: Cotylea) and its predatory behavior on a scaleworm. Zootaxa 4894: 403–412.

Tsuyuki A, Oya Y, Kajihara K (2019) A new species of *Prosthiostomum* (Platyhelminthes: Polycladida) from Shirahama, Japan. Species Diversity 24: 137–143.

Tsuyuki A, Oya Y, Kajihara H (2020b) First record of *Stylostomum ellipse* (Dalyell, 1853) (Platyhelminthes, Polycladida) from the Pacific Ocean. Check List 16: 773–779.

Tsuyuki A, Oya Y, Kajihara H (2022b) Reversible shifts between interstitial and epibenthic habitats in evolutionary history: molecular phylogeny of the marine flatworm family Boniniidae (Platyhelminthes: Polycladida: Cotylea) with descriptions of two new species. PLoS ONE 17: e0276847.

Tsuyuki A, Oya Y, Kajihara H (2022c) Two new species of the marine flatworm *Pericelis* (Platyhelminthes: Polycladida) from southwestern Japan with an amendment of the generic diagnosis based on phylogenetic inference. Marine Biology Research 17: 946–959.

Tyler S, Schilling S, Hooge M, Bush LF (2006–2022) Turbellarian taxonomic database, version 2.07. URL: http://turbellaria.umaine.edu Accessed 18 November 2022.

Vaillant L (1890) Lombriciniens, hirudiniens, bdellomorphes, térétulariens et planariens. In: Quatrefages A de (Ed.) Histoire Naturelle des Annelés Marins et d'eau Douce 3(2). Librairie encyclopédique de Roret, Paris, 341–768.

Velasquez X, Bolaños DM, Benayahu Y (2018) New records of cotylean flatworms (Platyhelminthes: Polycladida: Rhabditophora) from coastal habitats of Israel. Zootaxa 4438: 237–260.

Verrill AE (1901) Additions to the fauna of the Bermudas from the Yale Expedition of 1901, with notes on other species. Transactions of the Connecticut Academy of Arts and Sciences 11: 15–62.

Westblad E (1952) Turbellaria (excl. Kalyptorhynchia) of the Swedish South Polar Expedition 1901–1903. Further Zoological Results of the Swedish Antarctic Expedition 1901–1903 4: 1–55.

Westheide W (1982) *Microphthalmus hamosus* sp.n. (Polychaeta, Hesionidae)—an example of evolution leading from the interstitial fauna to a macrofaunal interspecific relationship. Zoologica Scripta 11: 189–193.

Westheide W (1987) Progenesis as a principle in meiofauna evolution. Journal of Natural History 21: 843–854.

Wilson NG, Jörger KM, Brenzinger B, Schrödl M (2017) Phylogenetic placement of the enigmatic worm-like Rhodopemorpha slugs as basal Heterobranchia. Journal of Molluscan Studies 83: 399–408.

Woodworth WM (1898) Some planarians from the Great Barrier Reef of Australia. Bulletin of the Museum of Comparative Zoölogy at Harvard College 32: 61–67.

Worsaae K, Giribet G, Martínez A (2018) The role of progenesis in the diversification of the interstitial annelid lineage Psammodrilidae. Invertebrate Systematics 32: 774–793.

Worsaae K, Kerbl A, Domenico MD, Gonzalez BC, Bekkouche N, Martínez A (2021) Interstitial Annelida. Diversity 13: 1–77.

Worsaae K, Kristensen RM (2005) Evolution of interstitial Polychaeta (Annelida). In: Bartolomaeus T, Purschke G (Eds), Morphology, molecules, evolution and phylogeny in Polychaeta and related taxa. Developments in Hydrobiologia. Springer, Dordrecht, 319–340.

Worsaae K, Sterrer W, Kaul-Strehlow S, Hay-Schmidt A, Giribet G (2012) An anatomical description of a miniaturized acorn worm (Hemichordata, Enteropneusta) with asexual reproduction by paratomy. PLoS ONE 7: e48529.

Yeri M, Kaburaki T (1918) Description of some Japanese polyclad Turbellaria. Journal of the College of Science, Tokyo Imperial University 39: 1–54.

Yeri M, Kaburaki T (1920) Notes on two new species of Japanese polyclads. Annotationes Zoologicae Japonenses 9: 591–598.

Yu Y, Blair C, He X (2020) RASP 4: ancestral state reconstruction tool for multiple genes and characters. Molecular Biology and Evolution 37: 604–606.

Yu Y, Harris AJ, Blair C, He X (2015) RASP (Reconstruct Ancestral State in Phylogenies): a tool for historical biogeography. Molecular Phylogenetics and Evolution 87: 46–49.

FIGURES

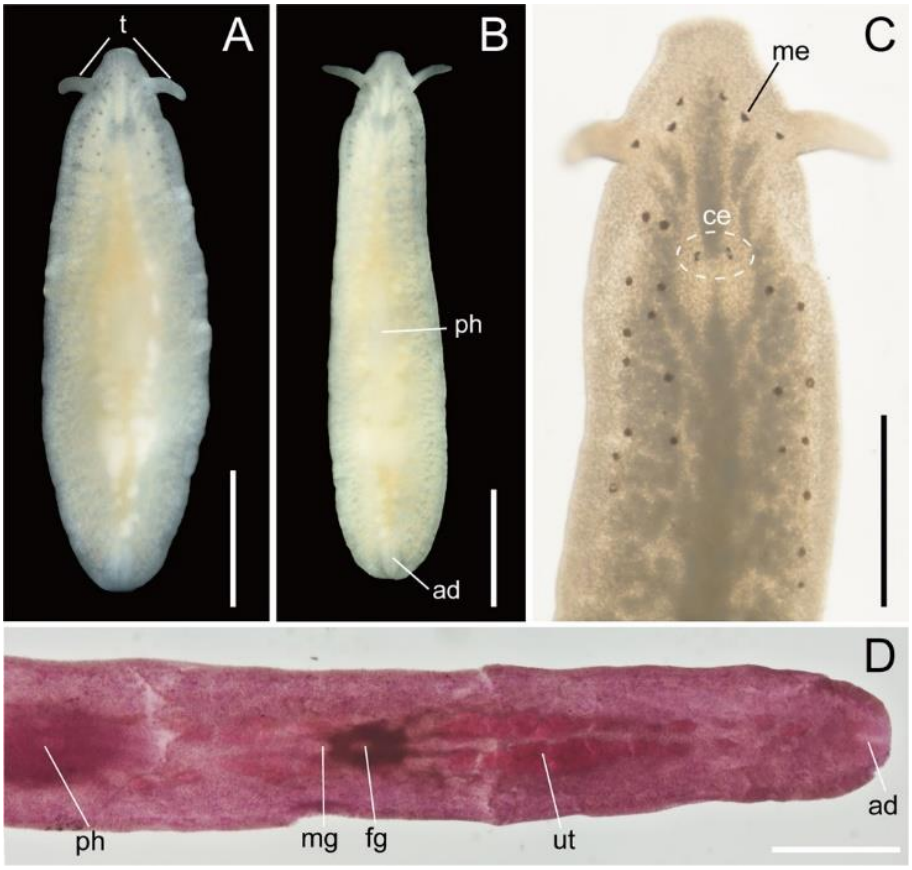

Fig. 1. *Boninia uru* Tsuyuki et al., 2022b, ICHUM 8278, photographs of living and fixed specimens (Chapter II-1). A, Entire animal, living state, dorsal view; B, entire animal, living state, ventral view; C, magnification of anterior body, living state; D, posterior body showing reproductive organs, fixed state, stained with acid fuchsin and cleared in xylene, ventral view. Abbreviations: ad, adhesive organ; ce, cerebral eyespots; fg, female gonopore; me, marginal eyespot; mg, male gonopore; ph, pharynx; t, tentacles; ut, uterus. Scale bars: 1 mm (A, B), 0.5 mm (C, D). After Tsyuyuki et al. (2022b, fig. 1).

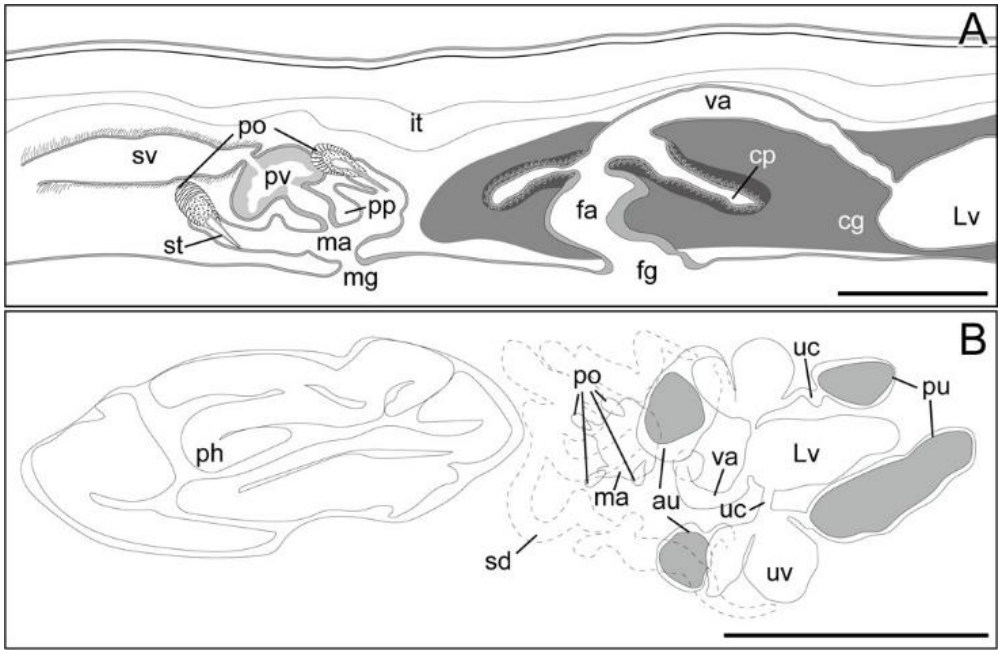

Fig. 2. *Boninia uru* Tsuyuki et al., 2022b, schematic diagrams of sagittal (A) and horizontal (B) sections (anterior to the left) (Chapter II-1). A, ICHUM 8278 (holotype), copulatory complex; B, ICHUM 8283 (paratype), pharynx, male and female copulatory apparatuses. Abbreviations: au, anterior dilations of uteri; cg, cement glands; cp, cement pouch; fa, female atrium; fg, female gonopore; it, intestine; Lv, Lang's vesicle; ma, male atrium; mg, male gonopore; ph, pharynx; po, prostatoid organ(s); pp, penis papilla; pu, posterior dilations of uteri; pv, prostatoid vesicle; sd, sperm duct; st, stylet; sv, seminal vesicle; uc, uterine canal; uv, uterine vesicle; va, vagina. Scale bars: 100 μm (A), 300 μm (B). After Tsuyuki et al. (2022b, fig. 2).

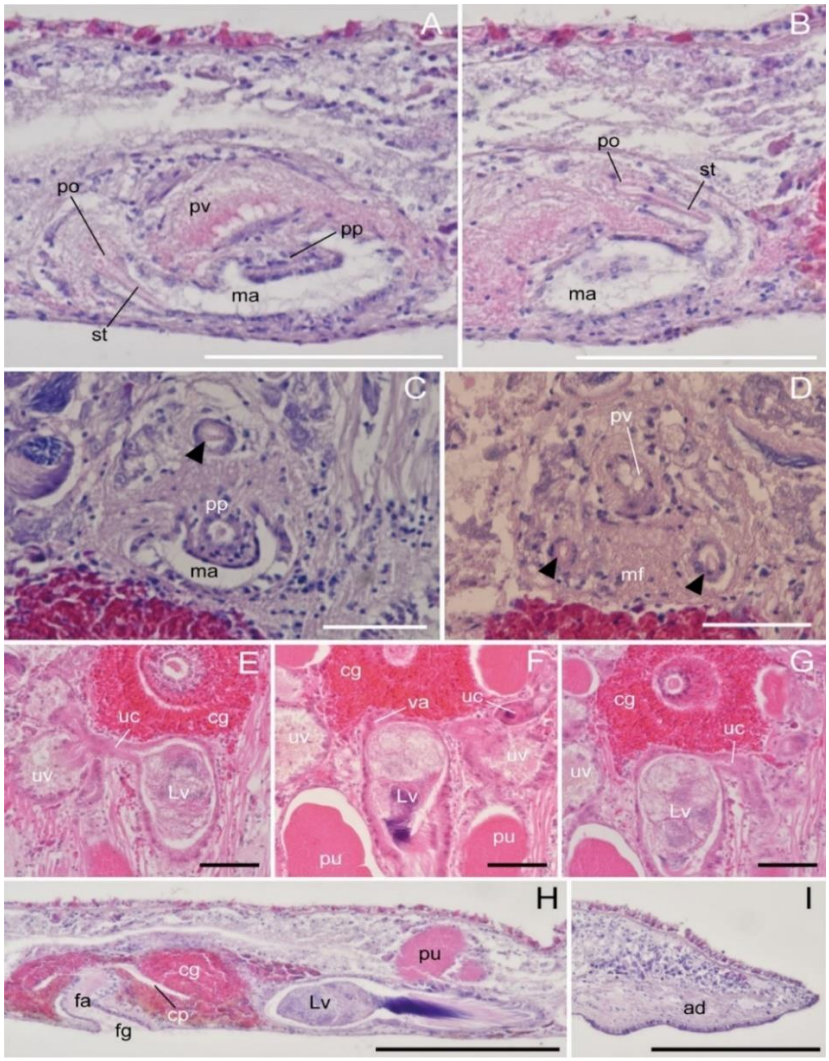

Fig. 3. *Boninia uru* Tsuyuki et al., 2022b, photomicrographs of sagittal (A, B, H, I) and horizontal (C–G) sections (Chapter II-1). A, B, ICHUM 8278 (holotype), male copulatory apparatus, anterior to the left; C, D, ICHUM 8279 (paratype), male copulatory apparatus, with stylet of the prostatoid organ indicated by arrowheads; E–G, ICHUM 8283 (paratype), connection between uterine canal and Lang's vesicle; H, ICHUM 8278 (holotype), female copulatory complex, anterior to the left; I, ICHUM 8278 (holotype), adhesive organ, anterior to the left. Abbreviations: ad, adhesive organ; cg, cement glands; cp, cement pouch; fa, female atrium; fg, female gonopore; Lv, Lang's vesicle; ma, male atrium; mf, muscle fiber; po, prostatoid organ(s); pp, penis papilla; pu, posterior dilations of uteri; pv, prostatoid vesicle; st, stylet; uc, uterine canal; uv, uterine vesicle. Scale bars: 100 µm (A, B), 50 µm (C–G), 200 µm (H, I). After Tsuyuki et al. (2022b, fig. 3).

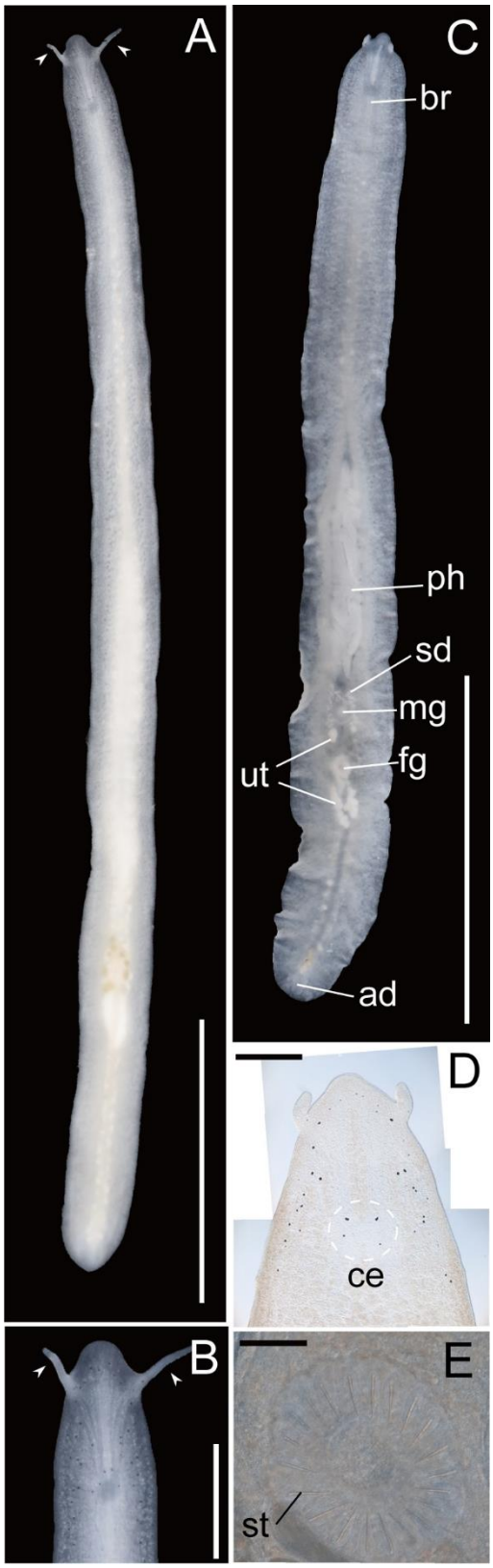

Fig. 4. *Boninia yambarensis* Tsuyuki et al., 2022b, photographs taken in the living state (Chapter II-1). A, ICHUM 8284, dorsal view; B, ICHUM 8284, magnification of the anterior body, dorsal view; C, ICHUM 8288, ventral view; D, ICHUM 8289, magnification of anterior body (squeezed); E, ICHUM 8289, arrangement of prostatoid organs (squeezed). Pointed tentacles are shown by arrowheads (A, B). Abbreviations: ad, adhesive organ; br, brain; ce, cerebral eyespots; fg, female gonopore; mg, male gonopore; ph, pharynx; sd, sperm duct; st, stylet; ut, uteri. Scale bars: 5 mm (A, C), 1 mm (B), 500 µm (D), 300 µm (E). After Tsuyuki et al. (2022b, fig. 4).

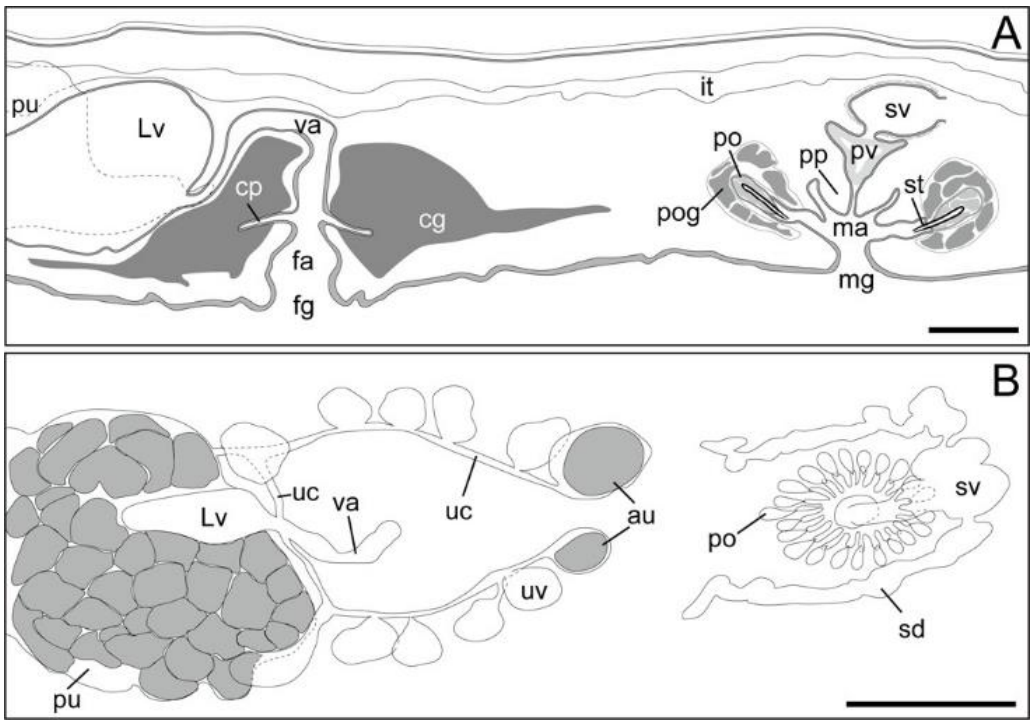

Fig. 5. *Boninia yambarensis* Tsuyuki et al., 2022b, schematic diagrams of sagittal (A) and horizontal (B) sections (anterior to the right) (Chapter II-1). A, ICHUM 8284 (holotype), sagittal view of copulatory complex; B, ICHUM 8285 (paratype), histological view of copulatory complex. Abbreviations: au, anterior dilation of uterus; cg, cement glands; cp, cement pouch; fa, female atrium; fg, female gonopore; it, intestine; Lv, Lang's vesicle; ma, male atrium; mg, male gonopore; po, prostatoid organ; pog, prostatoid organ glands; pp, penis papilla; pu, posterior dilation of uterus; pv, prostatoid vesicle; sd, sperm duct; st, stylet; sv, seminal vesicle; uc, uterine canal; uv, uterine vesicle; va, vagina. Scale bars: 100 μm (A), 300 μm (B). After Tsuyuki et al. (2022b, fig. 5).

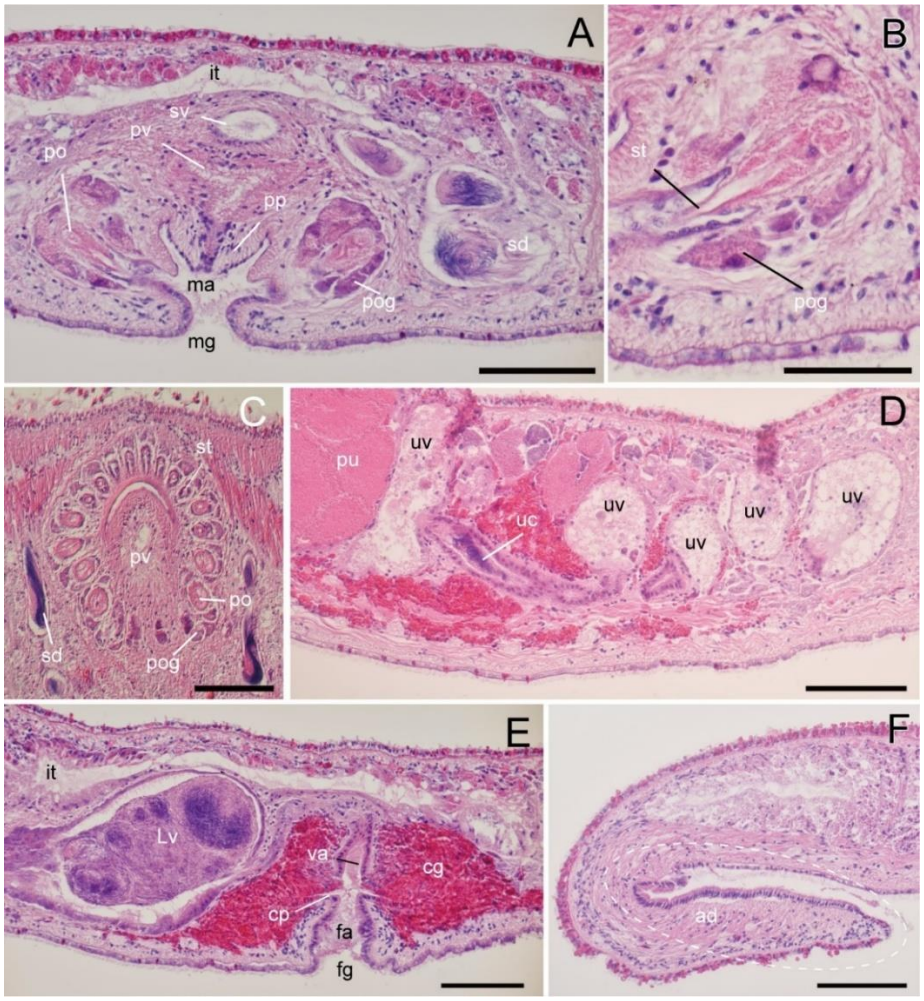

Fig. 6. *Boninia yambarensis* Tsuyuki et al., 2022b, photomicrographs of sagittal (A, B, D–G) and horizontal sections (C) (Chapter II-1). A, ICHUM 8284 (holotype), male copulatory apparatus, anterior to the right; B, ICHUM 8284 (holotype), prostatoid organ, anterior to the right; C, ICHUM 8285 (paratype), arrangement of prostatoid organs; D, ICHUM 8284 (holotype), uterine vesicles, anterior to the right; E, ICHUM 8284 (holotype), female copulatory apparatus, anterior to the right; F, ICHUM 8284 (holotype), adhesive organ. Abbreviations: ad, adhesive organ; au, anterior dilation of uterus; cg, cement glands; cp, cement pouch; fa, female atrium; fg, female gonopore; it, intestine; Lv, Lang's vesicle; ma, male atrium; mg, male gonopore; po, prostatoid organ; pog, prostatoid organ glands; pp, penis papilla; pu, posterior dilation of uterus; pv, prostatoid vesicle; sd, sperm duct; st, stylet; sv, seminal vesicle; uc, uterine canal; uv, uterine vesicle; va, vagina. Scale bars: 100 µm (A, C–F), 50 µm (B). After Tsuyuki et al. (2022b, fig. 6).

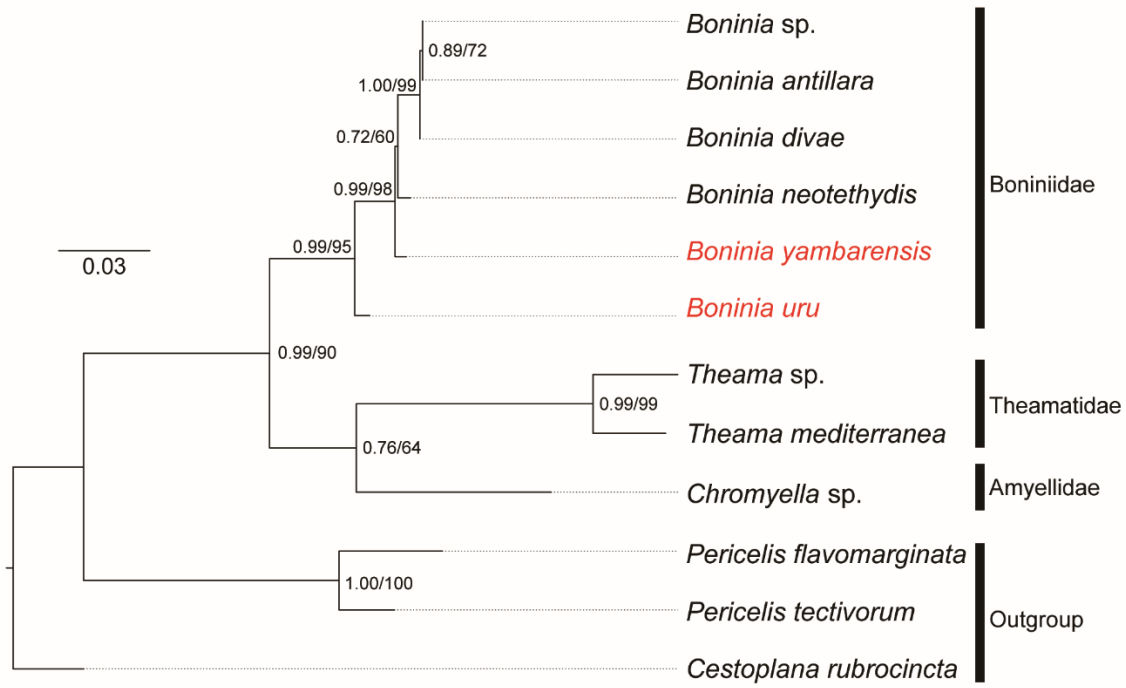

Fig. 7. ML tree based on a concatenated dataset of partial 18S and 28S (Chapter II-1). Numbers near nodes are posterior probability and bootstrap values, respectively. Modified from Tsuyuki et al. (2022b, fig. 7).

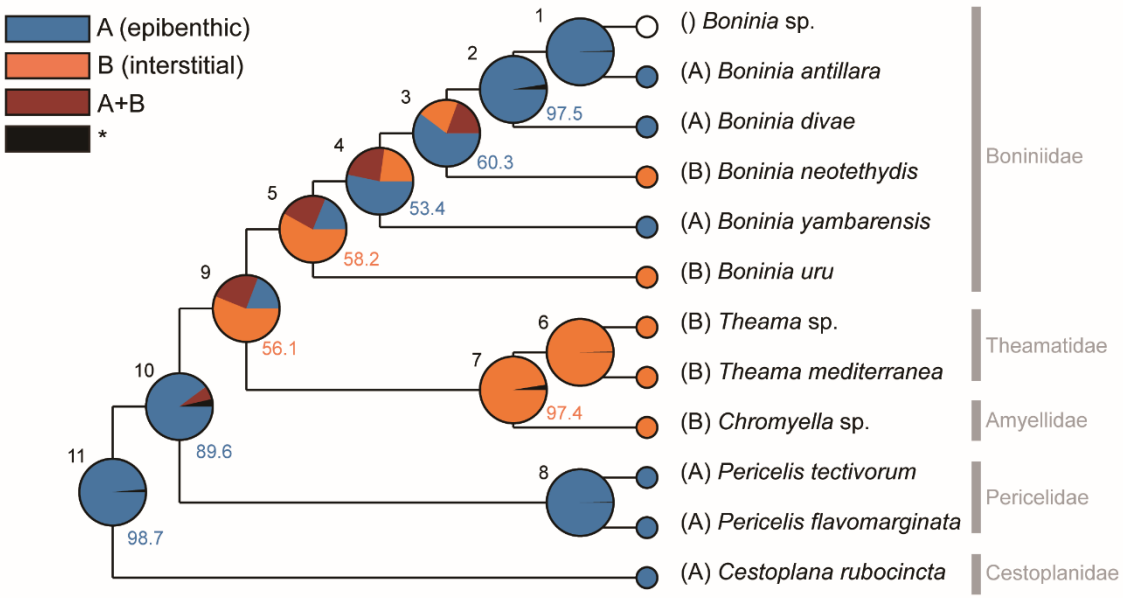

Fig. 8. Ancestral reconstruction of habitats produced using Bayesian Binary Markov chain Monte Carlo analysis (Chapter II-1). Nodes are numbered. Pie charts on nodes show the probabilities of possible ancestral states with numbers representing the highest probabilities (%). *, ancestral state with a relative probability <5%. After Tsuyuki et al. (2022b, fig. 8).

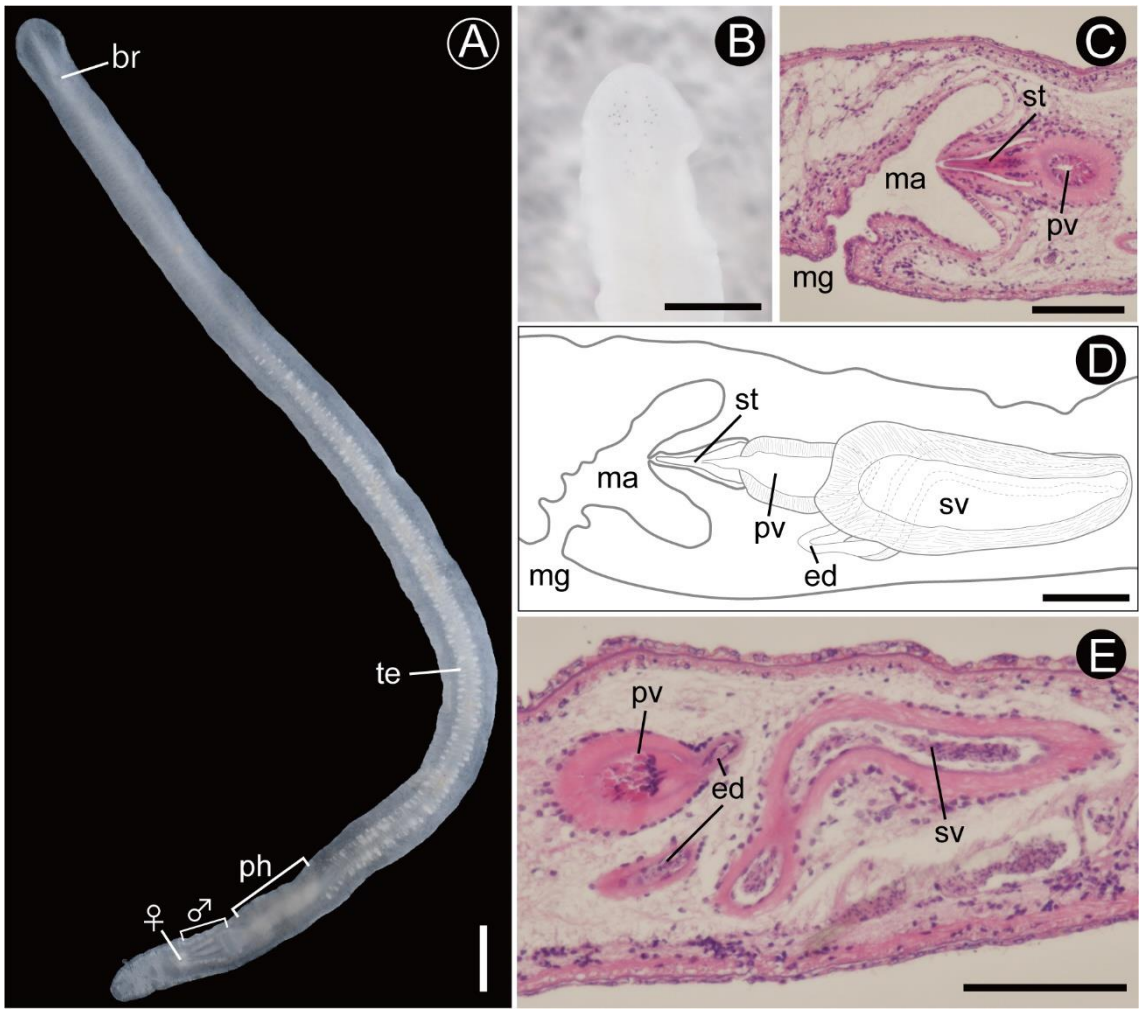

Fig. 9. *Eucestoplana* cf. *cuneata* (Sopott-Ehlers and Schmidt, 1975) (Chapter II-2). A, ICHUM 8442, whole animal in living state, dorsal view; B, ICHUM 8442, magnification of anterior body in living state, dorsal view, showing eyespot distribution; C, E, ICHUM 8440, photomicrographs of sagittal sections, anterior to the left, showing male copulatory apparatus; D, ICHUM 8440, schematic diagram of male copulatory apparatus in sagittal view, anterior to the left. Abbreviations: br, brain; ed, ejaculatory duct; ma, male atrium; mg, male gonopore; ph, pharynx; pv, prostatic vesicle; st, stylet; sv, seminal vesicle; te, testicular follicle; ♀, female copulatory apparatus; ♂, male copulatory apparatus. Scale bars: 1 mm (A, B), 100 μm (C–E).

Fig. 10. *Eucestoplana* sp., ICHUM 8443 (Chapter II-2). A, Whole animal in living state, dorsal view; B, magnification of anterior body, dorsal view, showing eyespot distribution; C, photomicrograph of sagittal section (anterior to the left), showing pharynx and mouth. Abbreviations: mo, mouth; ph, pharynx; te, testicular follicle; ♀, female copulatory apparatus; ♂, male copulatory apparatus. Scale bars: 1 mm (A), 0.5 mm (B), 100 µm (C).

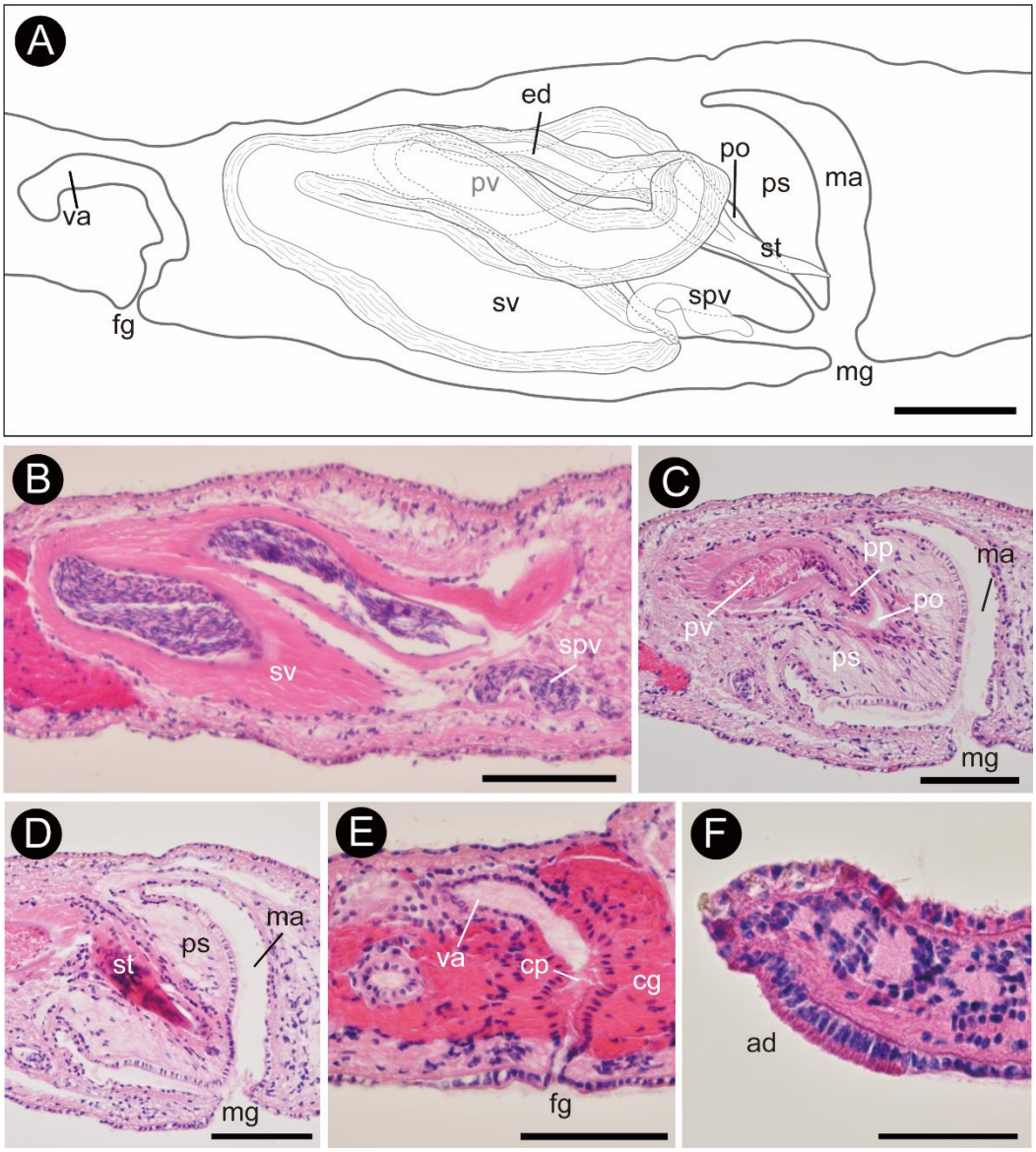

Fig. 11. *Eucestoplana* sp., schematic diagram (A) and photomicrographs of sagittal sections (B–F) (anterior to the right) (Chapter II-2). A, ICHUM 8443, male and female copulatory apparatuses; B–D, ICHUM 8443, male copulatory apparatus; E, ICHUM 8444, female copulatory apparatus; F, ICHUM 8444, adhesive organ. Abbreviations: ad, adhesive organ; cg, cement glands; cp, cement pouch; ed, ejaculatory duct; fg, female gonopore; ma, male atrium; mg, male gonopore; po, penis pouch; pp, penis papilla; pv, prostatic vesicle; ps, penis sheath; spv, spermiducal vesicle; st, stylet; sv, seminal vesicle; va, vagina. Scale bars: 100 μm (A–F).

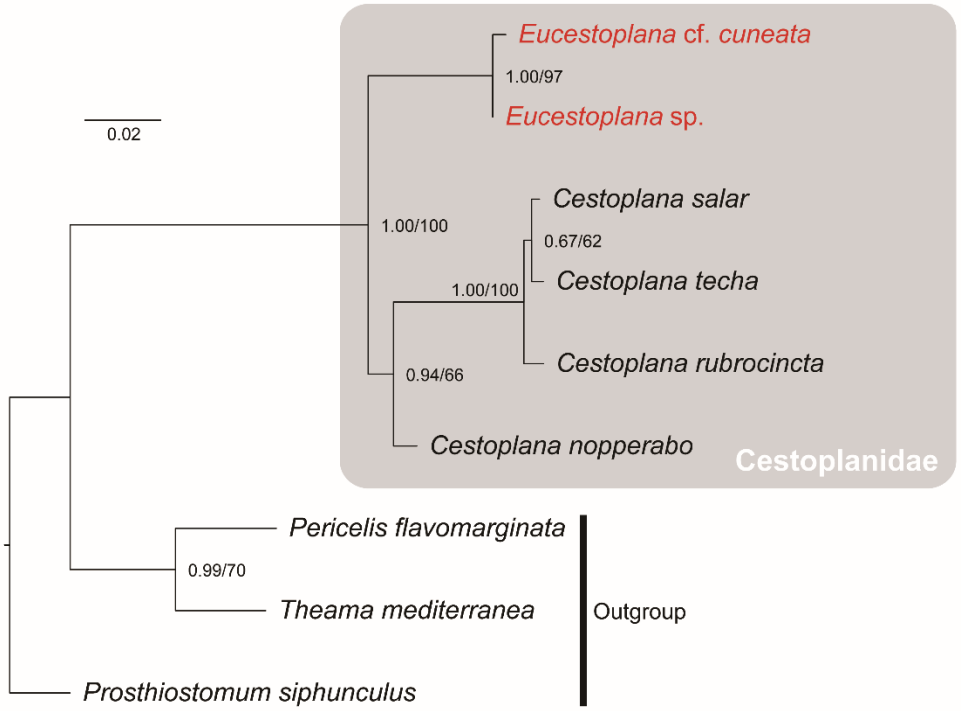

Fig. 12. ML phylogenetic tree based on a concatenated dataset of partial 18S and 28S rDNA sequences (Chapter II-2). Numbers near nodes are posterior probabilities and bootstrap values, respectively. The species name of which sequences are newly determined in this study are indicated in the red.

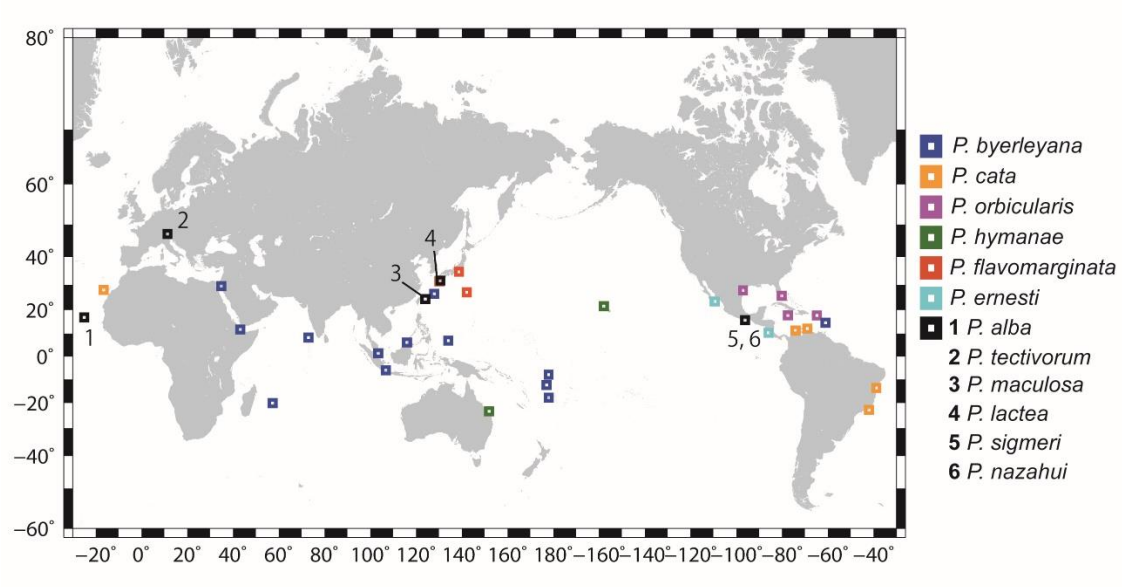

Fig. 13. Map showing updated distributions of *Pericelis* species (Chapter II-3).

After Tsuyuki et al. (2022c, fig. 1).

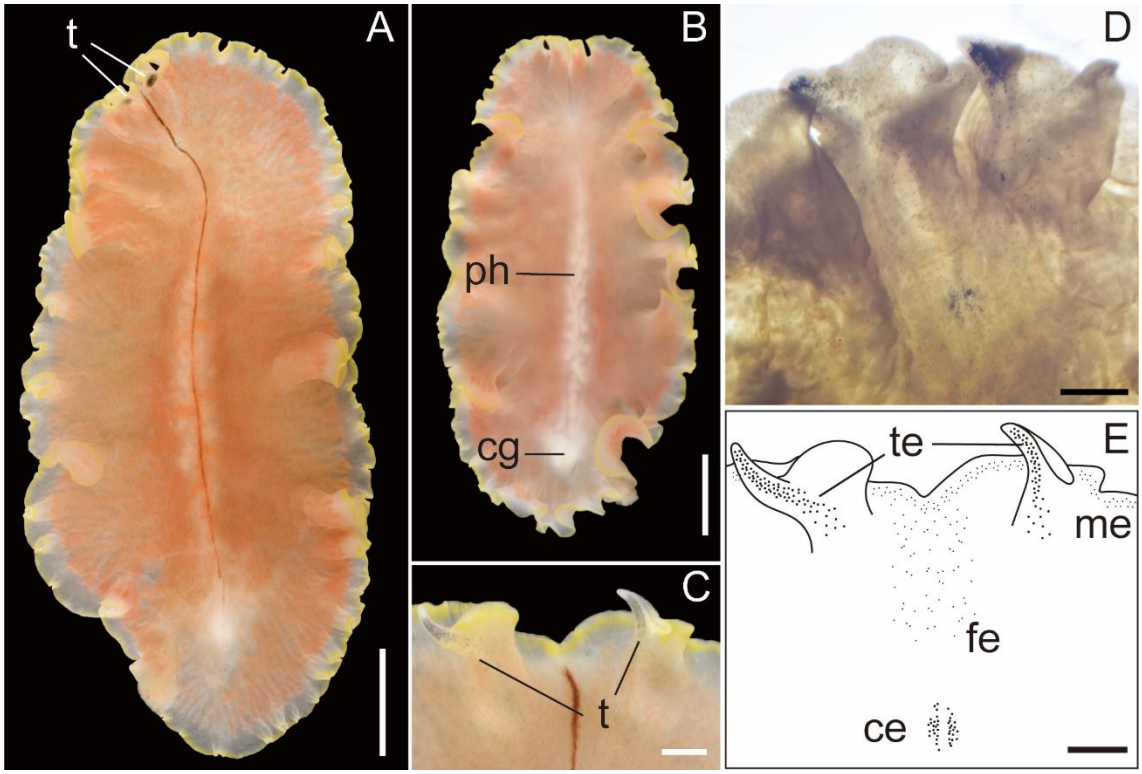

Fig. 14. ***Pericelis flavomarginata*** **Tsuyuki et al., 2020a, photographs of a living specimen (A–C) and a specimen after being cleared in xylene (D); sketch of eyespot distribution (E) (Chapter II-3).** A, ICHUM 6116 (holotype), entire animal, dorsal view; B, ICHUM 6116 (holotype), entire animal, ventral view; C, ICHUM 6122 (paratype), magnification of tentacles; D, ICHUM 6122 (paratype), magnification of anterior body; E, cerebral, frontal, marginal, and tentacular eyespots distribution. Abbreviations: ce, cerebral eyespots; cg, cement glands; fe, frontal eyespots; me, marginal eyespots; ph, pharynx; t, marginal tentacles; te, tentacular eyespots. Scale bars: 5 mm (A, B), 1 mm (C–E). After Tsuyuki et al. (2020a, fig. 2).

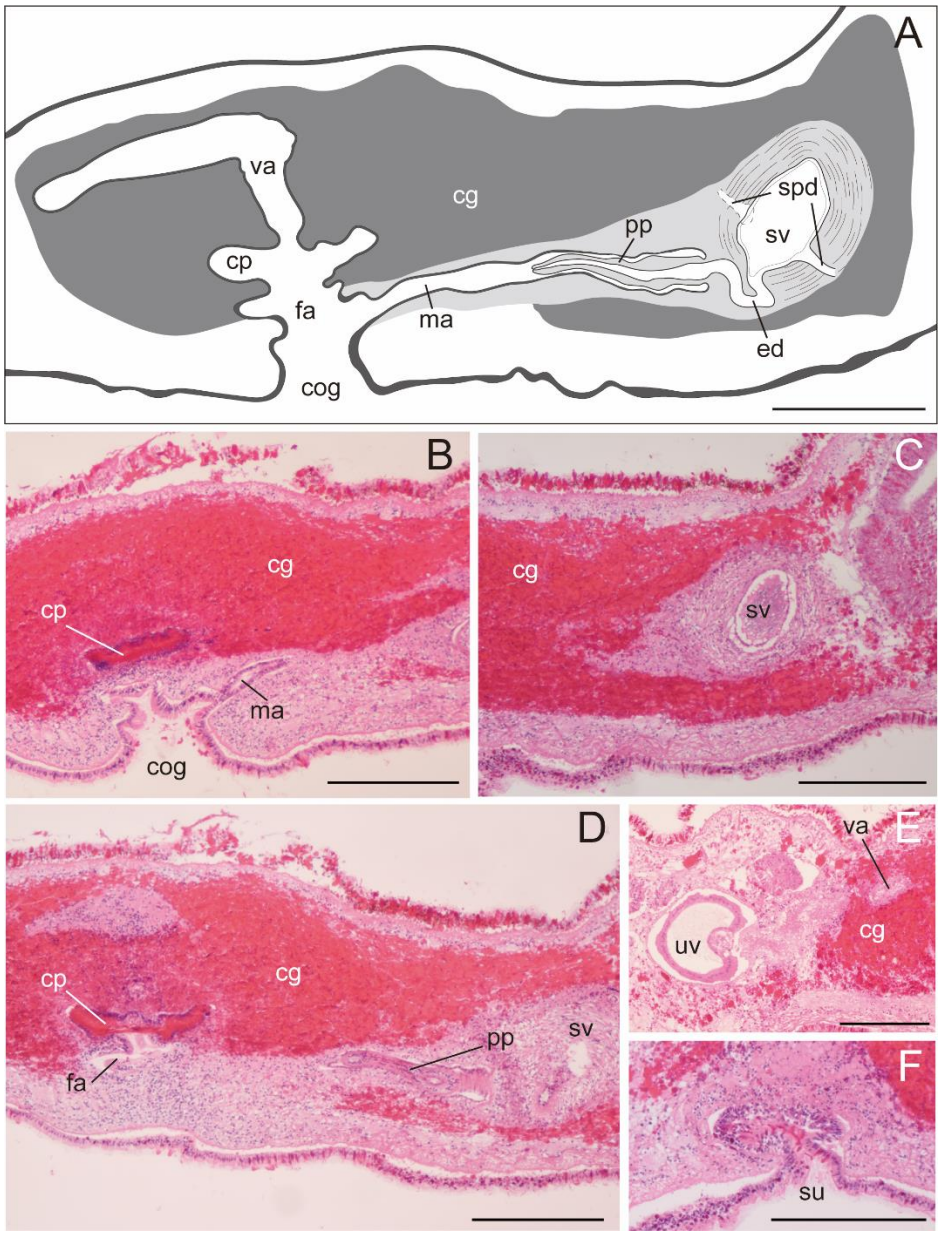

Fig. 15. *Pericelis flavomarginata* Tsuyuki et al., 2020a, ICHUM 6116 (holotype), schematic diagram (A) and photomicrographs of sagittal sections (B–F) (anterior to the right) (Chapter II-3). A, Copulatory complex; B, common gonopore of male and female atriums; C, seminal vesicle; D, penis papilla and female copulatory apparatus; E, uterine vesicle; F, sucker. Abbreviations: cg, cement glands; cog, common gonopore; cp, cement pouch; ed, ejaculatory duct; fa, female atrium; ma, male atrium; pp, penis papilla; spd, sperm duct; su, sucker; sv, seminal vesicle; uv, uterine vesicle; va, vagina. Scale bars: 300 μm. After Tsuyuki et al. (2020a, fig. 3).

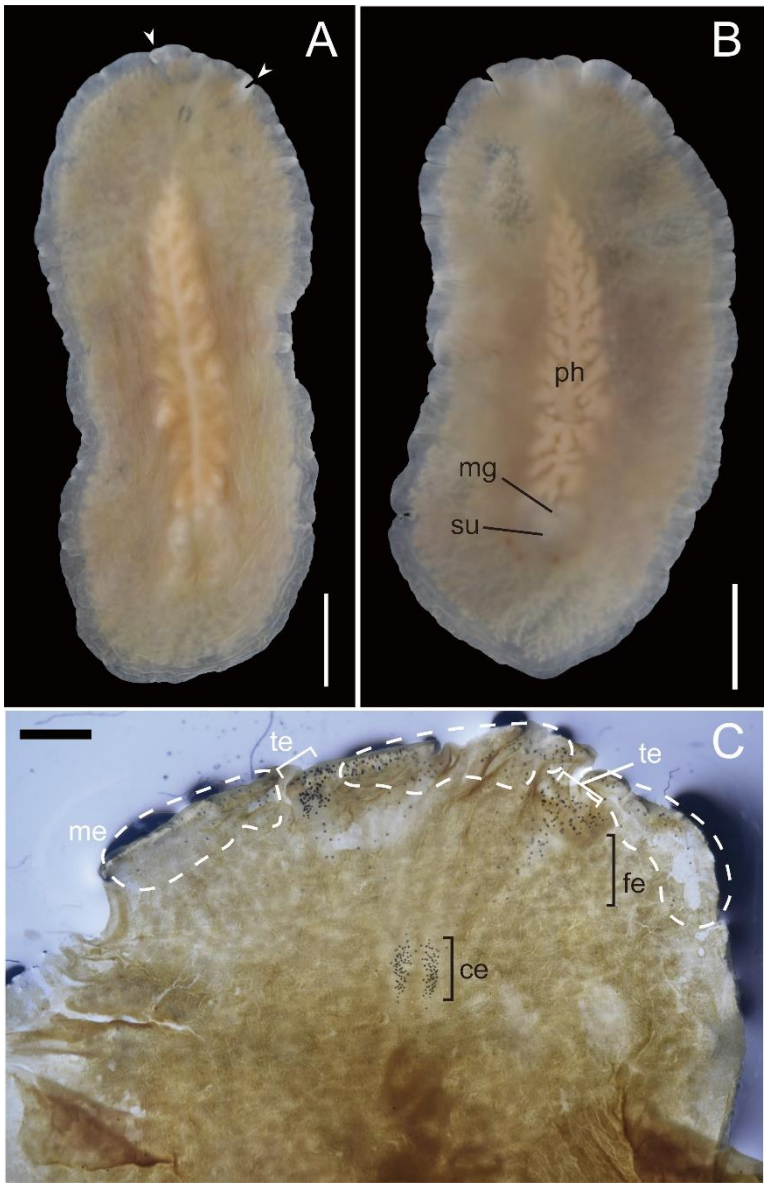

Fig. 16. *Pericelis lactea* Tsuyuki et al., 2022c, holotype (ICHUM 6288) (Chapter II-3). A, Living animal, dorsal view, marginal tentacles shown with arrowheads; B, living animal, ventral view; C, magnification of anterior body in fixed state, cleared in xylene. Abbreviations: ce, cerebral eyespots; fe, frontal eyespots; me, marginal eyespots; mg, male gonopore; ph, pharynx; te, tentacular eyespots; su, sucker. Scale bars: 5 mm (A, B), 1 mm (C). After Tsuyuki et al. (2022c, fig. 2).

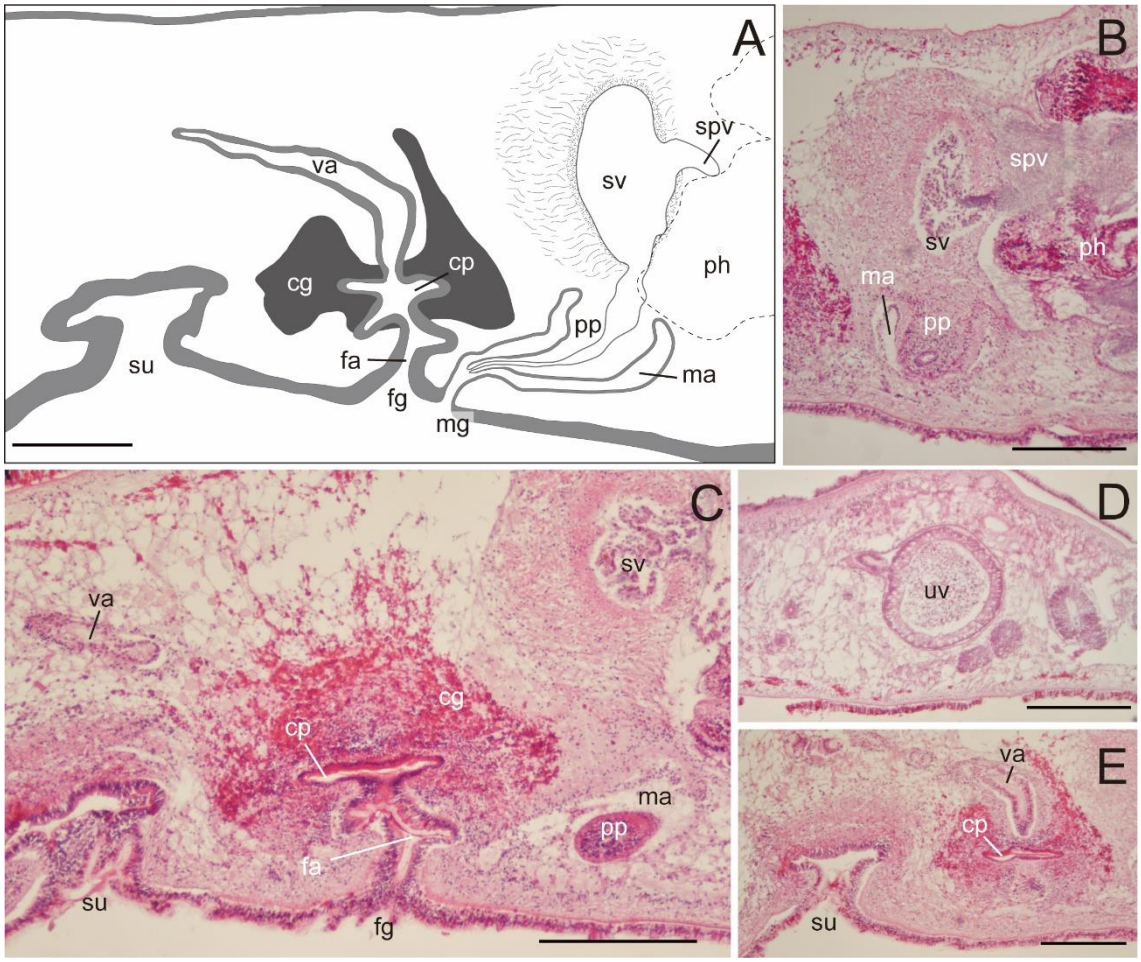

Fig. 17. *Pericelis lactea* Tsuyuki et al., 2022c, ICHUM 6288 (holotype), schematic diagram (A) and photomicrographs of sagittal sections (B–E) (anterior to the right) (Chapter II-3). A, Male and female copulatory apparatuses; B, male copulatory apparatus; C, female copulatory apparatus; D, uterine vesicle; E, female copulatory apparatus and sucker. Abbreviations: cg, cement glands; cp, cement pouch; fg, female gonopore; ma, male atrium; mg, male gonopore; ph, pharynx; pp, penis papilla; spv, spermiducal vesicle; su, sucker; sv, seminal vesicle; uv, uterine vesicle; va, vagina. Scale bars: 300 µm (A–E). After Tsuyuki et al. (2022c, fig. 3).

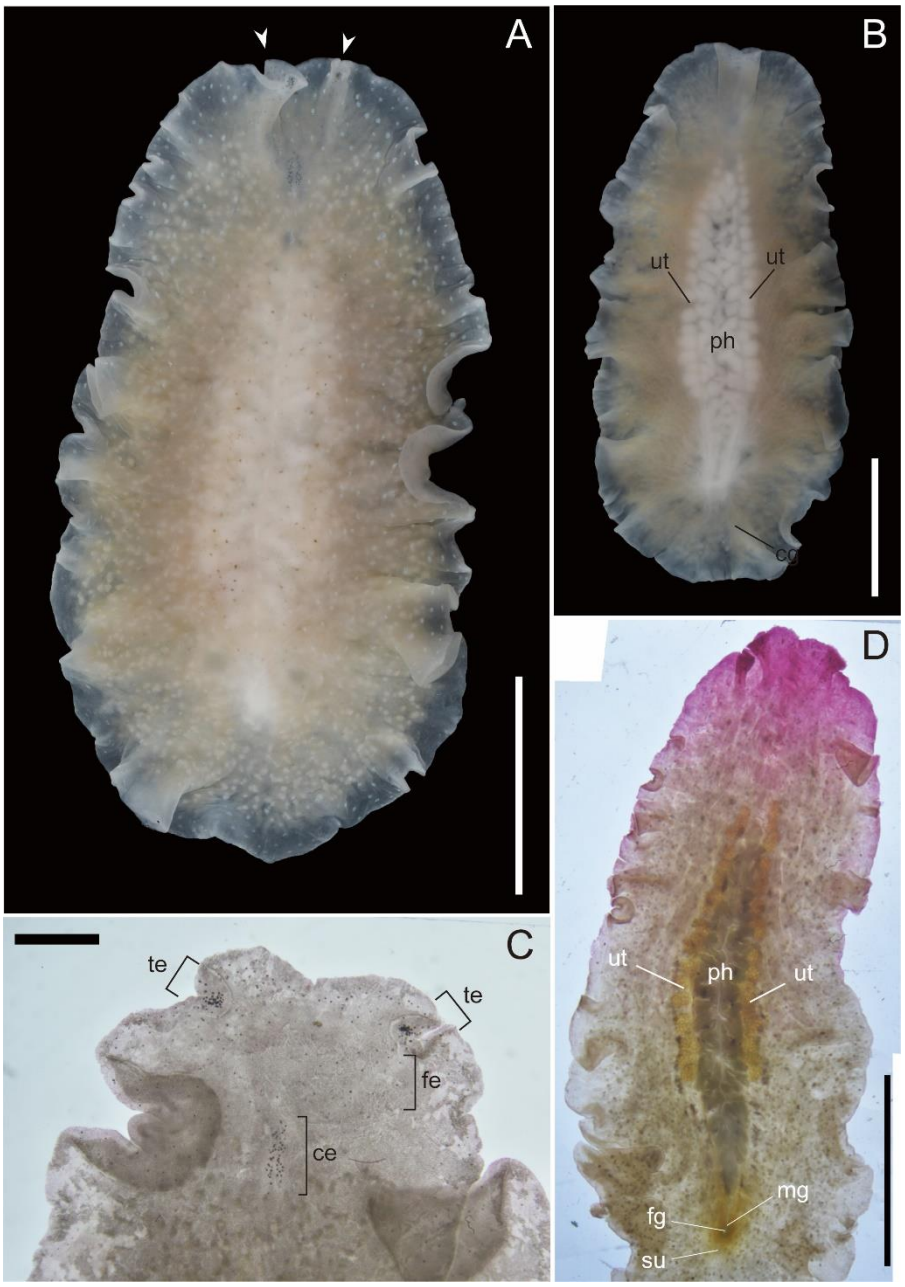

Fig. 18. *Pericelis maculosa* Tsuyuki et al., 2022c (A–C) ICHUM 6290 (holotype); (D) ICHUM 6292 (paratype) (Chapter II-3). A, Living animal, dorsal view, marginal tentacles shown with arrowheads; B, living animal, ventral view; C, magnification of anterior body in fixed state, cleared in xylene; D, entire animal in fixed state, cleared in xylene, ventral view (anterior portion pre-stained with acid fuchsin), anterior to the right. Abbreviations: ce, cerebral eyespots; cg, cement glands; fe, frontal eyespots; fg, female gonopore; mg, male gonopore; ph, pharynx; su, sucker; te, tentacular eyespots; ut, uterus. Scale bars: 5 mm (A, B, D), 1 mm (C). After Tsuyuki et al. (2022c, fig. 4).

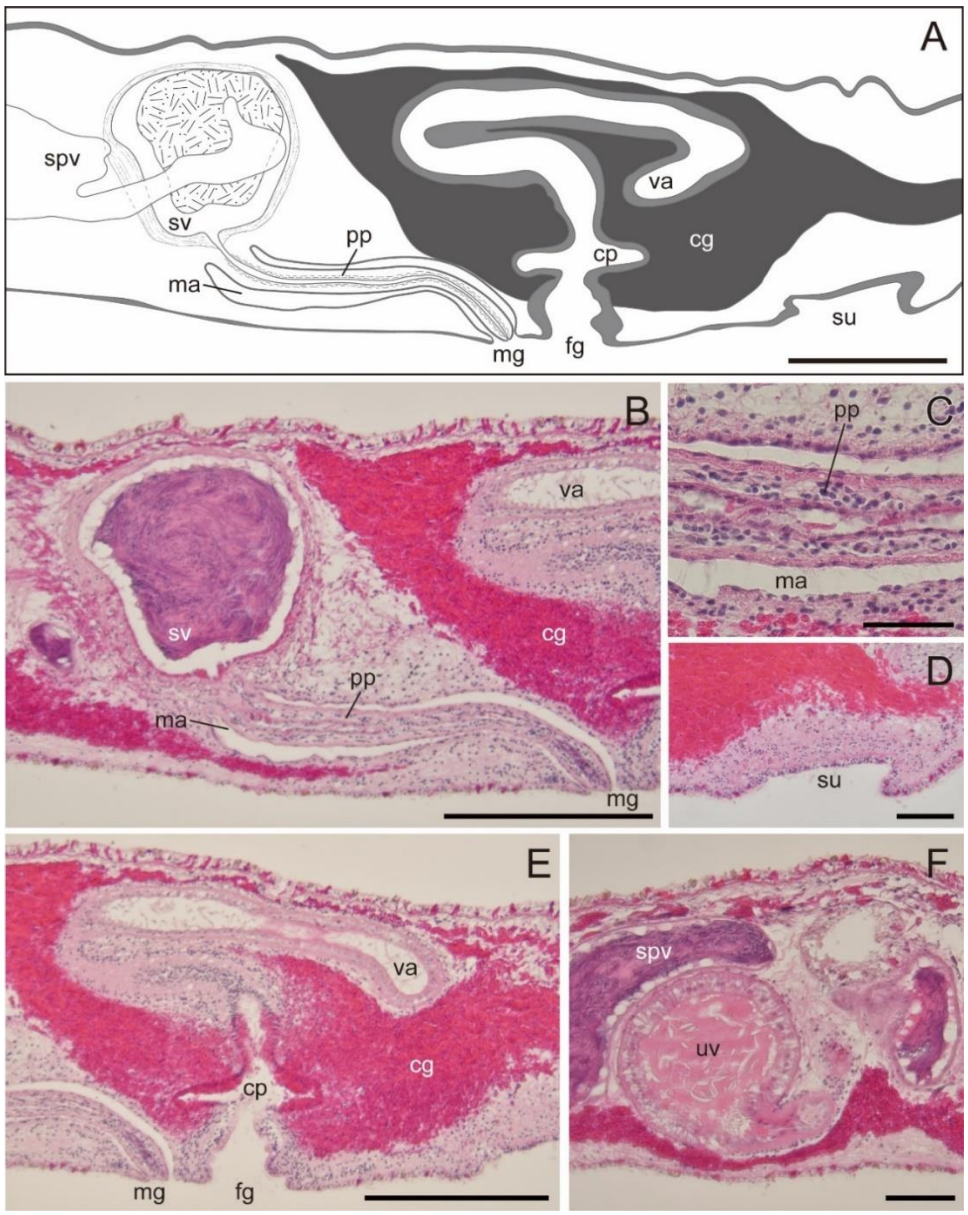

Fig. 19. *Pericelis maculosa* Tsuyuki et al., 2022c, ICHUM 6290 (holotype), schematic diagram (A) and photomicrographs of sagittal sections (B–F) (anterior to the left) (Chapter II-3). A, Male and female copulatory apparatuses; B, male copulatory apparatus; C, penis papilla; D, sucker; E, female copulatory apparatus; F, uterine vesicle. Abbreviations: cg, cement glands; cp, cement pouch; fg, female gonopore; ma, male atrium; mg, male gonopore; pp, penis papilla; spv, spermiducal vesicle; su, sucker; sv, seminal vesicle; uv, uterine vesicle; va, vagina. Scale bars: 300 µm (A, B, E), 50 µm (C), 100 µm (D, F). After Tsuyuki et al. (2022c, fig. 5).

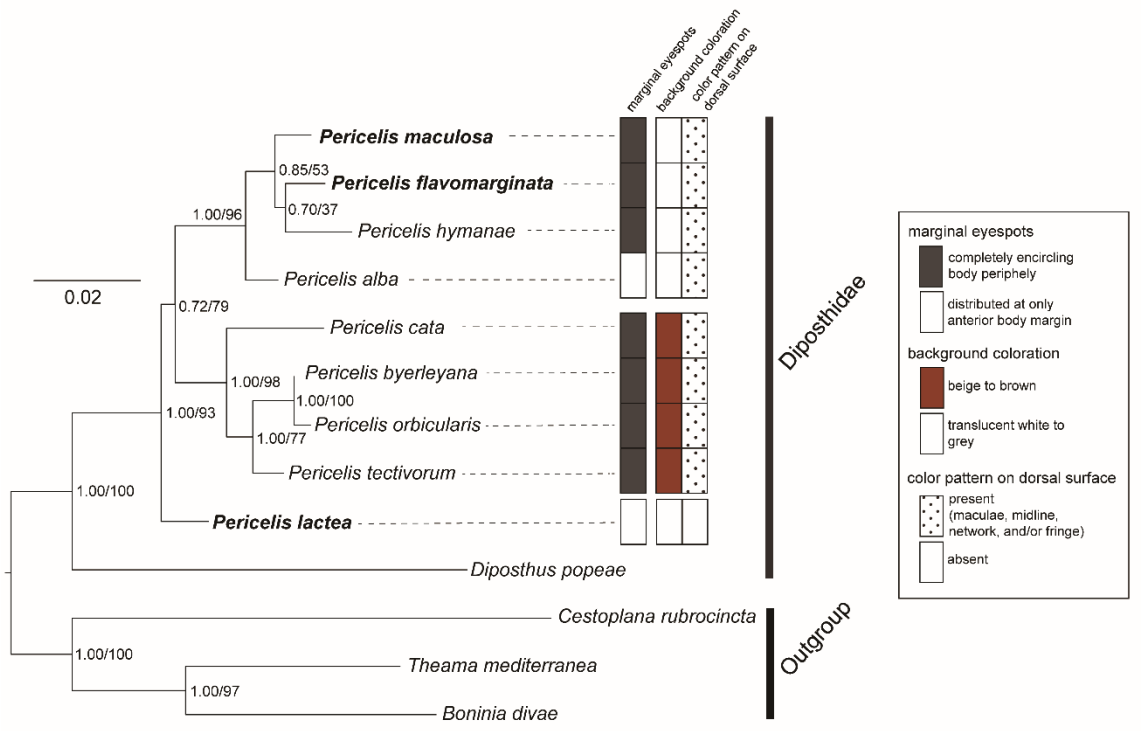

Fig. 20. ML phylogenetic tree based on a concatenated dataset (2,934 bp) of partial 18S (1,756 bp) and 28S rDNA (1,178 bp) (Chapter II-3). Numbers near nodes are posterior probabilities and bootstrap values, respectively. The morphological characteristics of *i*) marginal eyespots, *ii*) background coloration, and *iii*) color pattern on dorsal surface are plotted along the terminal taxa of *Pericelis*. The species name of which sequences determined here are shown in bold face. Modified from Tsuyuki et al. (2022c, fig. 6).

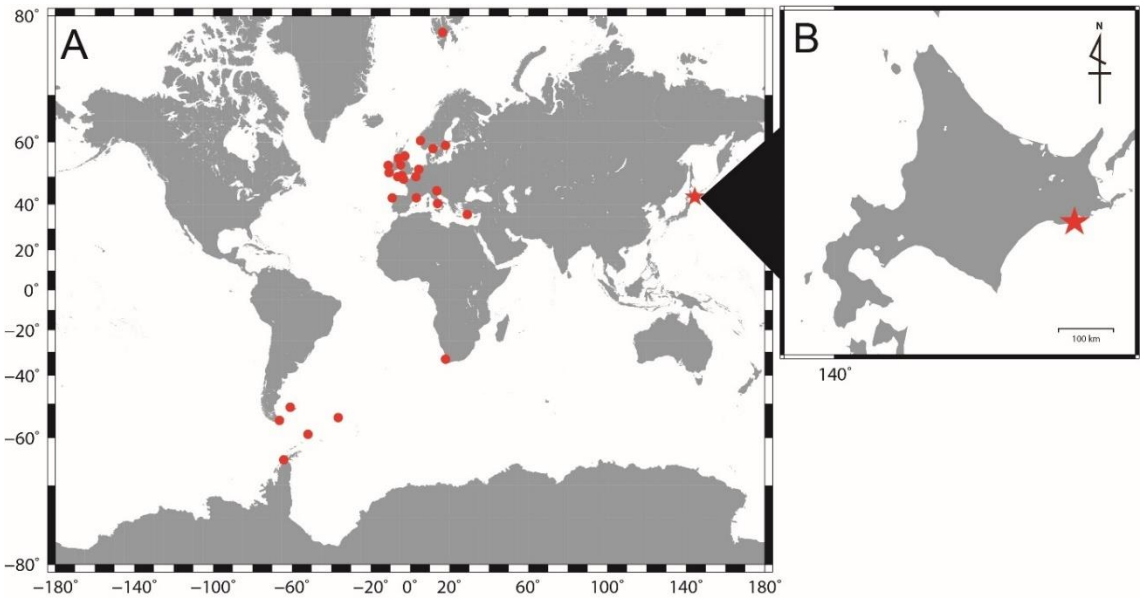

Fig. 21. Distribution of *Stylostomum ellipse* (Dalyell, 1853) (Chapter II-4). Stars indicate new distributions in this paper. A, Previous reports around the Atlantic Ocean and the new report in this paper; B, magnification of Hokkaido, showing the sampling site in this study. After Tsuyuki et al. (2020b, fig. 1).

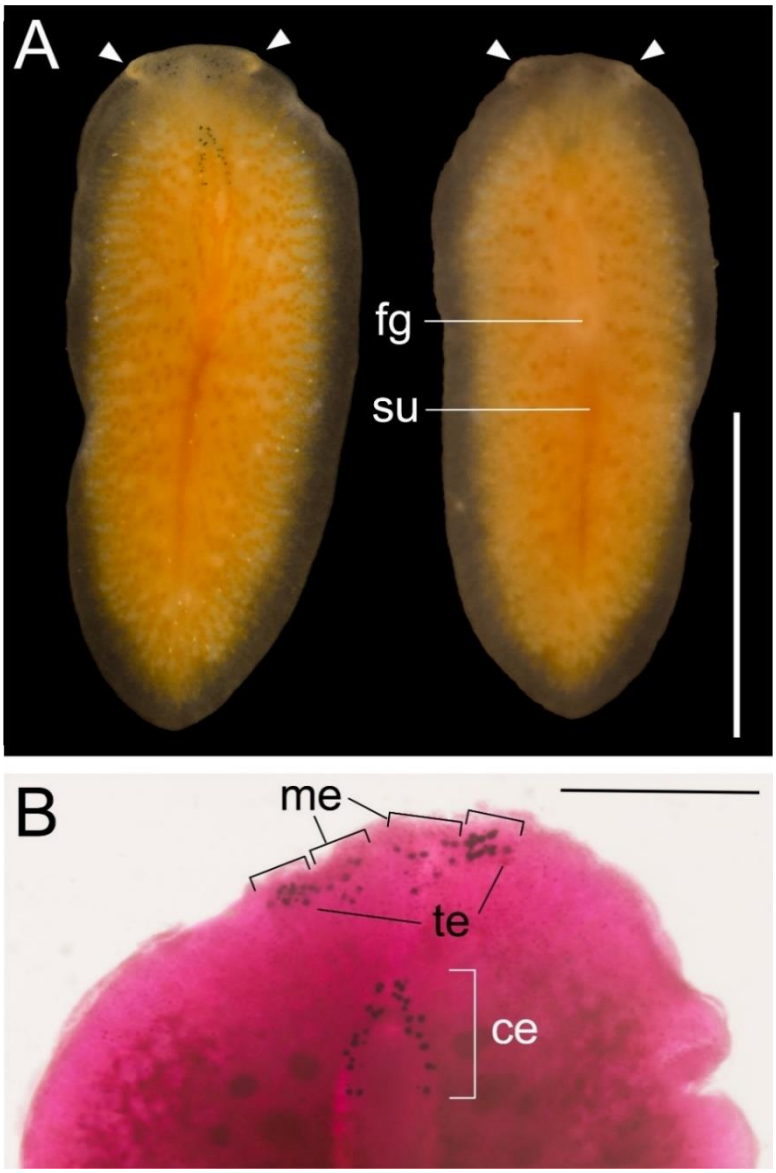

Fig. 22. *Stylostomum ellipse* (Dalyell, 1853), ICHUM 6003, from Japan (Chapter II-4). A, Entire animal in anaesthetized living state, dorsal (left) and ventral (right) views, showing marginal tentacles (indicated by arrow heads); B, magnification of anterior body in fixed state after cleared in xylene, dorsal view, showing position and arrangement of cerebral and marginal eyespots. Abbreviations: ce, cerebral eyespots; fg, female gonopore; me, marginal eyespots; su, sucker; te, tentacle eyespots. Scale bars: 5 mm (A), 1 mm (B). After Tsuyuki et al. (2020b, fig. 2).

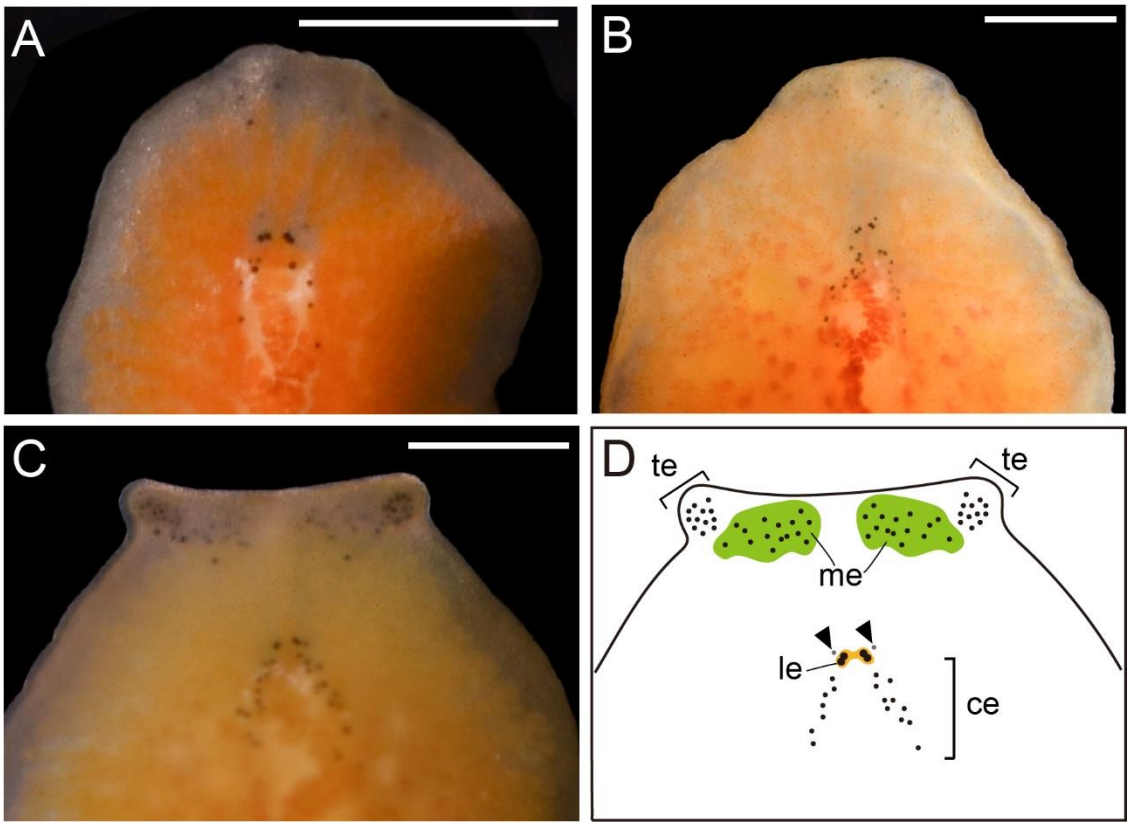

Fig. 23. *Stylostomum ellipse* (Dalyell, 1853), variations of the arrangement of eyespots (Chapter II-4). A, ICHUM 6006; B, ICHUM 6001; C, ICHUM 6007; D, distribution of eyespots, showing positions of small cerebral eyespots embedded in parenchyma (indicated by arrowheads). Abbreviations: ce, cerebral eyespots; le, pair of two large cerebral eyespots; me, marginal eyespots; te, tentacular eyespots. Scale bars: 500 µm (A–C). After Tsuyuki et al. (2020b, fig. 3).

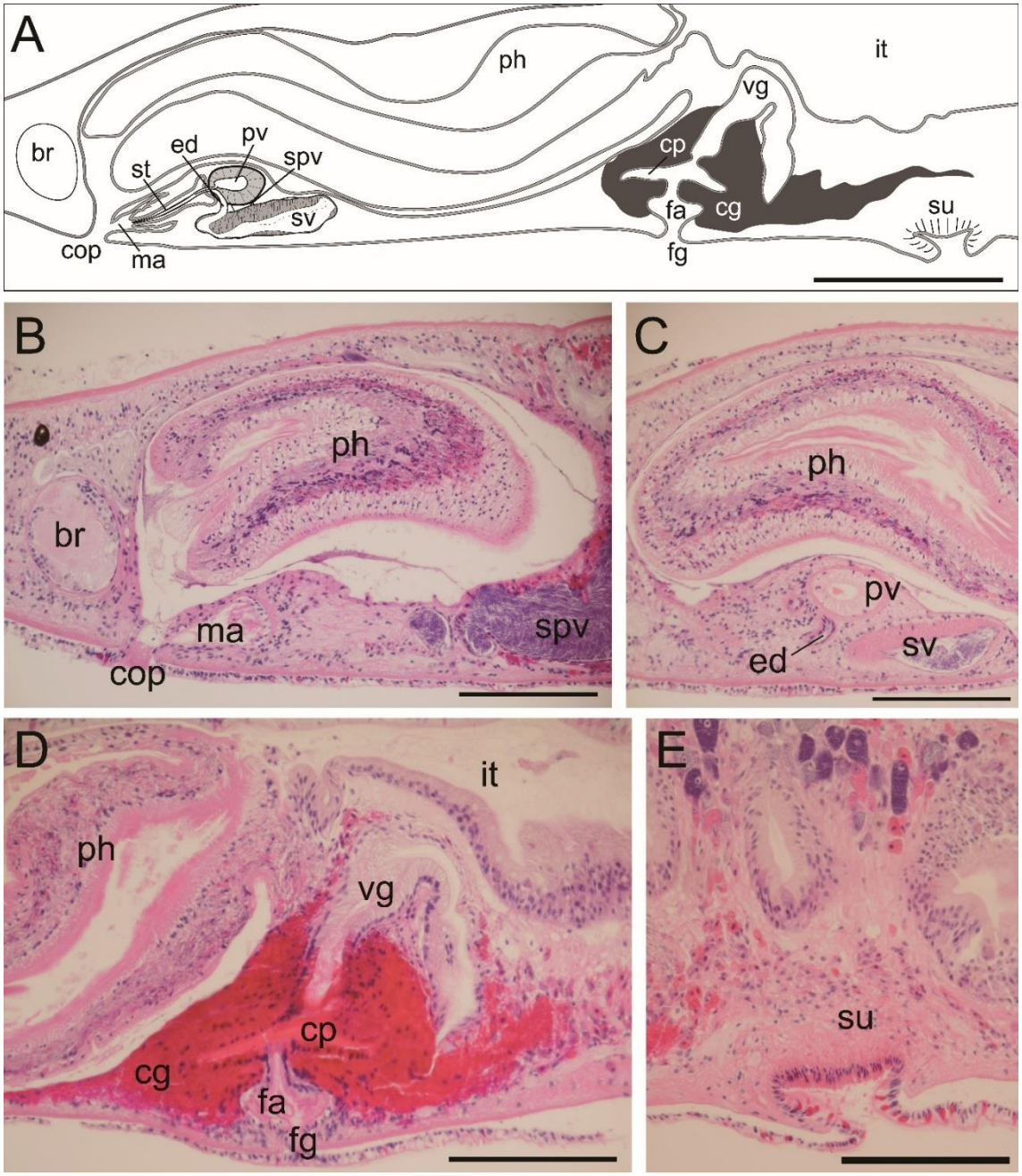

Fig. 24. *Stylostomum ellipse* (Dalyell, 1853), sagittal sections, head to the left, ICHUM 6003 (Chapter II-4). A, Diagrammatic reconstruction of copulatory complex; B, common pore including mouth and male gonopore; C, prostatic vesicle and seminal vesicle; D, female reproductive organ; E, sucker. Abbreviations: br, brain; cg, cement gland; cop, common pore; cp, cement pouch; ed, ejaculatory duct; fa, female atrium; fg, female gonopore; it, intestine; ma, male atrium; ph, pharynx; pv, prostatic vesicle; spv, spermiducal vesicle; st, stylet; sv, seminal vesicle; su, sucker; vg, vagina. Scale bars: 500 µm (A), 300 µm (B–E). After Tsuyuki et al. (2020b, fig. 4).

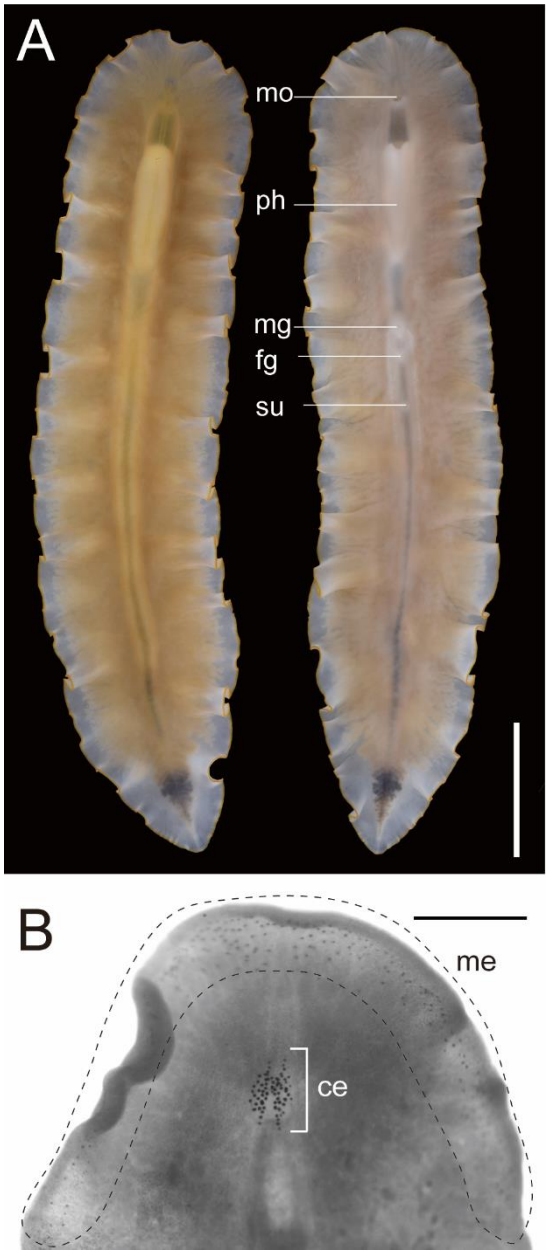

Fig. 25. *Enchiridium daidai* Tsuyuki and Kajihara, 2020, photograph taken in life and eyespots observed in fixed state after cleared in xylene (Chapter II-5). A, ICHUM 5993 (holotype), entire animal, dorsal view (left) and ventral view (right); B, ICHUM 5994 (paratype), magnification of anterior body, showing arrangements of cerebral and marginal eyespots. Abbreviations: ce, cerebral eyespots; fg, female gonopore; me, marginal eyespots; mg, male gonopore; mo, mouth; ph, pharynx; su, sucker. Scale bars: 10 mm (A), 1 mm (B). After Tsuyuki and Kajihara (2020, fig. 2).

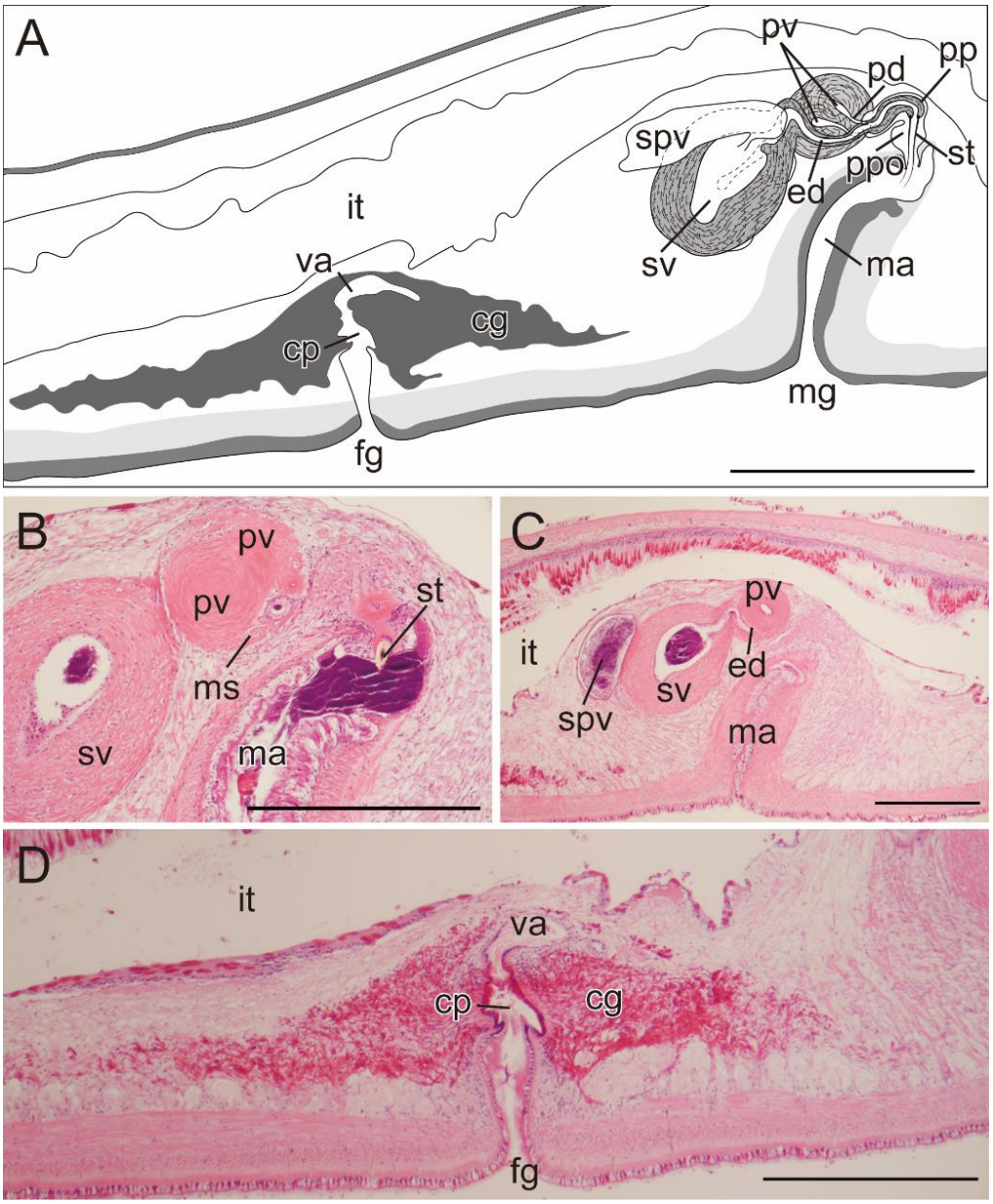

Fig. 26. *Enchiridium daidai* Tsuyuki and Kajihara, 2020, ICHUM 5993 (holotype), schematic diagram (A) and sagittal sections (B–D), anterior to the right (Chapter II-5). A, Schematic diagram of copulatory complex; B, a common muscle sheath/bulb enclosing two prostatic vesicles and penis stylet; C, ejaculatory duct penetrating a common muscles sheath/bulb; D, female copulatory apparatus. Abbreviations: cg, cement glands; cp, cement pouch; ed, ejaculatory duct; fg, female gonopore; it, intestine; ma, male atrium; mg, male gonopore; ms, muscle sheath/bulb; pd, prostatic duct; pp**,** penis papilla; ppo, penis pouch; pv, prostatic vesicle; spv, spermiducal vesicle; st, stylet; sv, seminal vesicle; va, vagina. Scale bars: 500 µm. After Tsuyuki and Kajihara (2020, fig. 3).

Fig. 27. Difference in mature body size among *Enchiridium daidai* Tsuyuki and Kajihara, 2020 (Chapter II-5). A, ICHUM 5993 (holotype), from Kagoshima; B, ICHUM 5995 (paratype), from Okinawa; C, ICHUM 5994 (paratype), from Okinawa. Scale bar: 10 mm. After Tsuyuki and Kajihara (2020, fig. 4).

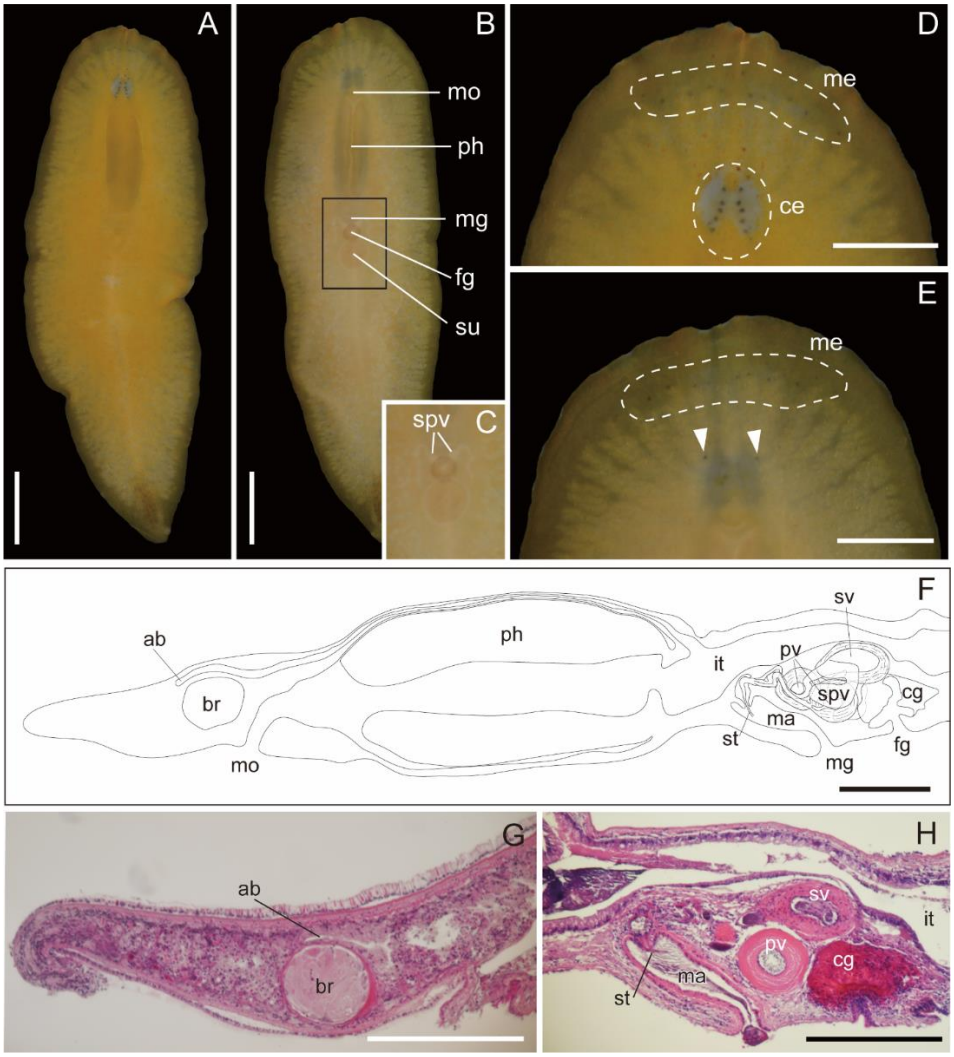

Fig. 28. ***Prosthiostomum auratum*** **Kato, 1937b, photographs taken in life (ICHUM 6150) (A–E), schematic diagram (F), and photomicrographs of sagittal sections (anterior to the left) (ICHUM 6149) (G, H) (Chapter II-5).** A, Entire body, dorsal view; B, entire body, ventral view; C, magnification of the black edged area on B; D, magnification of head, dorsal view; E, magnification of head, ventral view, showing ventral eyespots (arrowheads); F, anterior half of the body, lateral view, anterior to the left; G, anterior end of body; H, middle portion of body, showing male and female copulatory apparatuses. Abbreviations: ab, anterior branch of main intestine; br, brain; ce, cerebral eyespots; cg, cement glands; fg, female gonopore; it, intestine; ma, male atrium; me, marginal eyespots; mg, male gonopore; mo, mouth; ph, pharynx; pv, prostatic vesicle; spv, spermiducal vesicle; st, stylet; su, sucker; sv, seminal vesicle. Scale bars: 1 mm (A, B), 100 µm (D, E), 300 µm (F–H). After Tsuyuki et al. (2021, fig. 1).

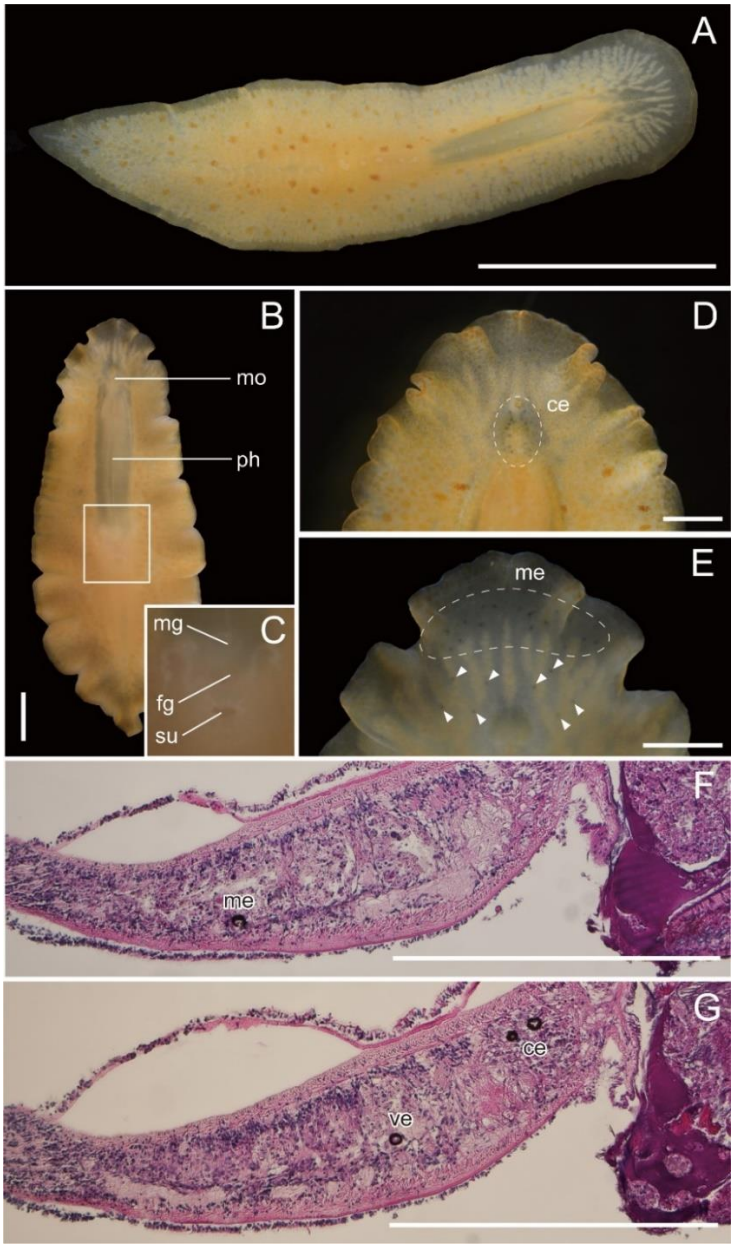

Fig. 29. ***Prosthiostomum hibana*** **Tsuyuki et al., 2021, ICHUM 6147 (holotype); photographs taken in life (A–E) and photomicrographs showing eyespots observed in sagittal sections (anterior to the left) (F, G) (Chapter II-5).** A, entire body, dorsal view; B, entire body, ventral view; C, magnification of the white edged area on B; D, magnification of head, dorsal view; E, magnification of head, ventral view (ventral eyespots indicated by arrowheads); F, anterior portion of body, showing marginal eyespot; G, anterior portion of body, showing cerebral and frontal eyespots. Abbreviations: ce, cerebral eyespots; fg, female gonopore; me, marginal eyespot(s); mg, male gonopore; mo, mouth; ph, pharynx; su, sucker; ve, ventral eyespot. Scale bars: 5 mm (A), 1 mm (B), 500 μm (D–G). After Tsuyuki et al. (2021, fig. 2).

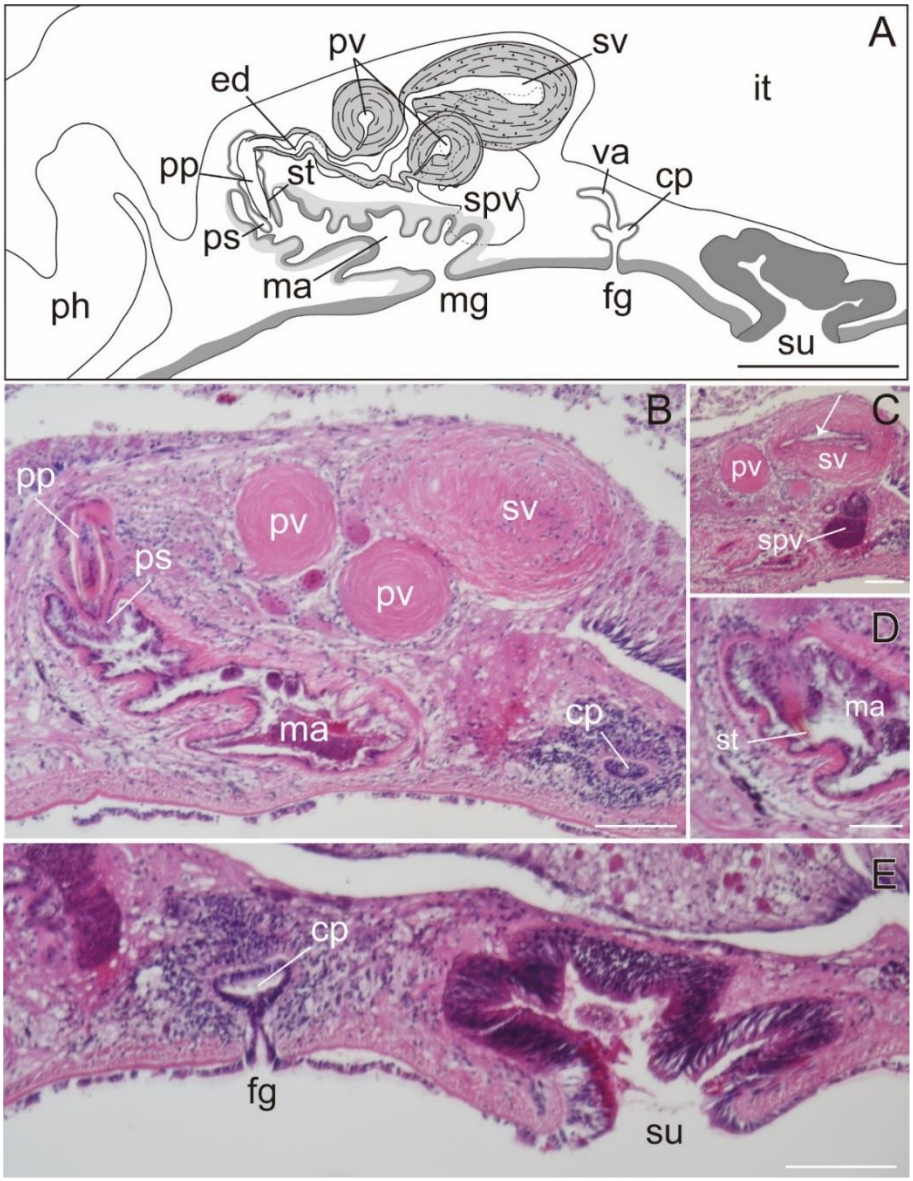

Fig. 30. ***Prosthiostomum hibana*** **Tsuyuki et al., 2021, ICHUM 6147 (holotype), schematic diagram (A) and photomicrographs of sagittal sections (anterior to the left) (B–D) (Chapter II-5).** A, Copulatory complex and sucker; B, male copulatory apparatus through male atrium lumen; C, male copulatory apparatus through seminal vesicle lumen, indicated by arrow; D, proximal portion of male atrium; E, female gonopore and sucker. Abbreviations: cp, cement pouch; ed, ejaculatory duct; fg, female gonopore; it, intestine; ma, male atrium; mg, male gonopore; ph, pharynx; pp, penis papilla; ps, penis sheath; pv, prostatic vesicle; spv, spermiducal vesicle; st, stylet; su, sucker; sv, seminal vesicle; va, vagina. Scale bars: 300 µm (A), 100 µm (B, C, E), 50 µm (D). After Tsuyuki et al. (2021, fig. 3).

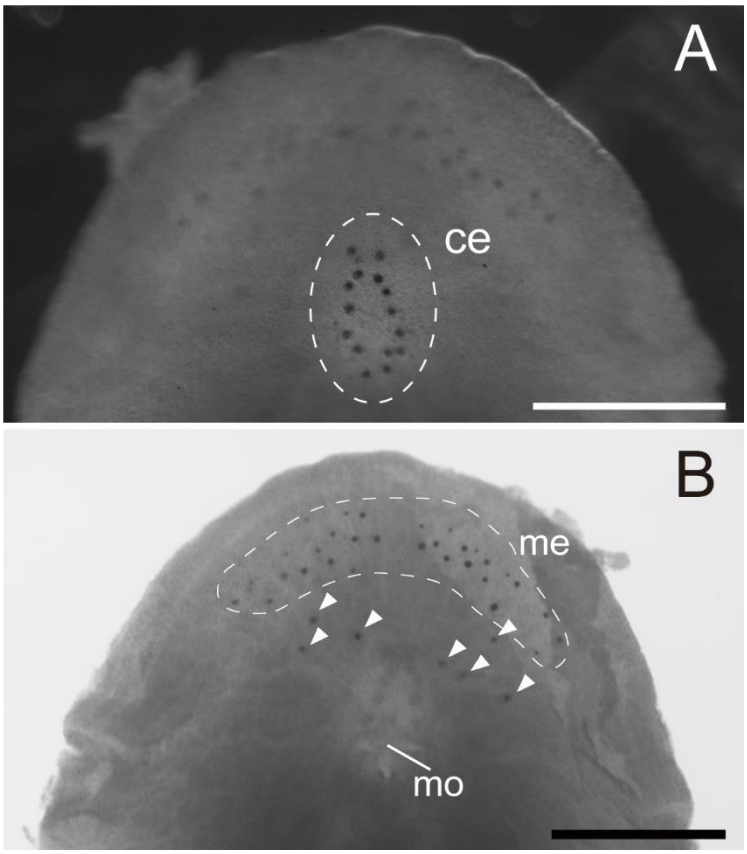

Fig. 31. ***Prosthiostomum hibana*** **Tsuyuki et al., 2021, ICHUM 6148 (paratype); photographs taken after being cleared in xylene (Chapter II-5).** A, magnification of head, dorsal view; B, magnification of head, ventral view (ventral eyespots indicated by arrowheads). Abbreviations: ce, cerebral eyespots; me, marginal eyespots; mo, mouth. Scale bars: 500 μm. After Tsuyuki et al. (2021, fig. 4).

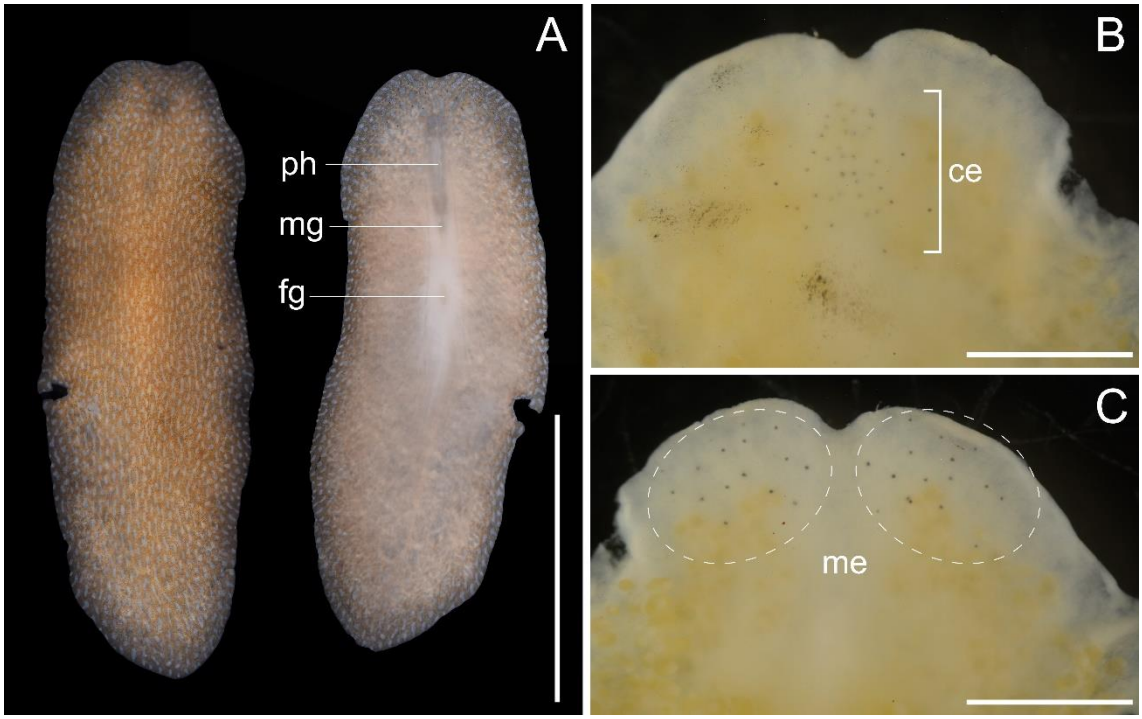

Fig. 32. *Prosthiostomum ohshimai* (Kato, 1938), photographs taken in life (A) and eyespots observed in fixed state (B, C), ICHUM 6033 (Chapter II-5). A, Entire animal, dorsal view (left) and ventral view (right); B, magnification of anterior body, dorsal view, showing position and arrangement of cerebral eyespots; C, magnification of anterior body, ventral view, showing position and arrangement of marginal eyespots. Abbreviations: ce, cerebral eyespots; fg, female gonopore; me, marginal eyespots; mg, male gonopore; ph, pharynx. Scale bars: 5 mm (A), 1 mm (B, C).

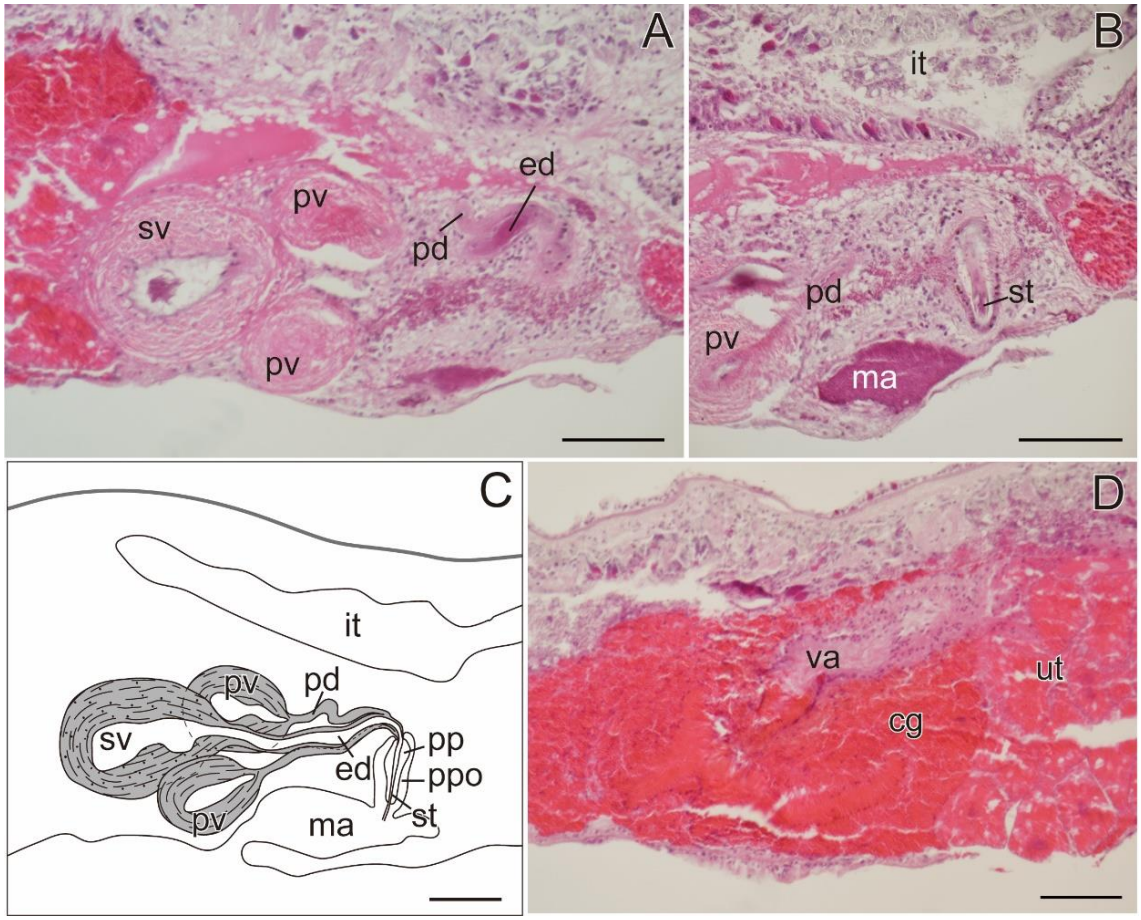

Fig. 33. *Prosthiostomum ohshimai* (Kato, 1938), sagittal sections, head to the right, A, B, D, ICHUM 6033 (Chapter II-5). A, Seminal vesicle and paired prostatic vesicles; B, penis stylet; C, diagrammatic reconstruction of male copulatory complex; D, vagina, cement grand, and uterus. Abbreviations: cg, cement glands; ed, ejaculatory duct; it, intestine; ma, male atrium; pd, prostatic duct; ph, pharynx; pp, penis papilla; ppo, penis pouch; pv, prostatic vesicle; st, stylet; sv, seminal vesicle; ut, uterus; va, vagina. Scale bars: 100 µm.

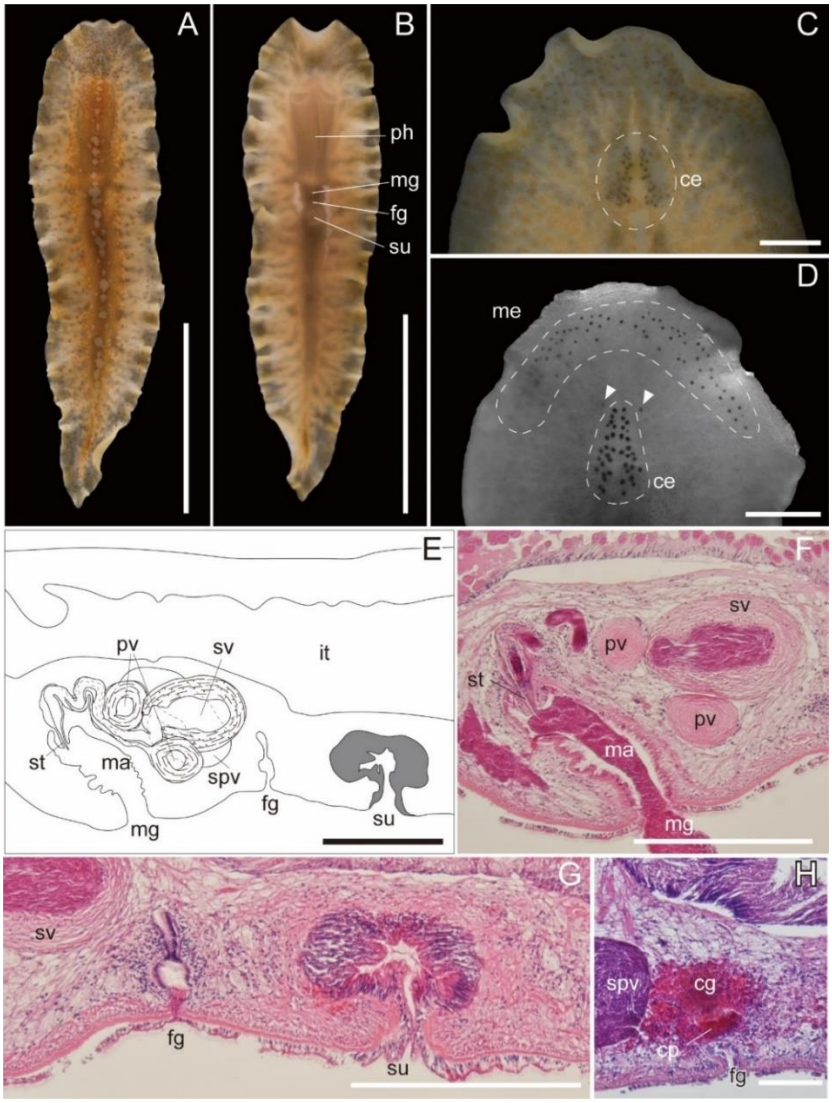

Fig. 34. ***Prosthiostomum*** **cf.** ***ostreae*** **Kato, 1937b, ICHUM 6153 (A, B, H), ICHUM 6151 (C, E–G), ICHUM 6152 (D); photographs taken in life (A–C) and after being cleared in xylene (D), schematic diagram (E), and photomicrographs of sagittal sections (F–H) (anterior to the left) (Chapter II-5).** A, Entire body, dorsal view; B, entire body, ventral view; C, magnification of head, dorsal view; D, magnification of head, dorsal view, showing ventral eyespots (arrowheads); E, copulatory organs and sucker; F, male copulatory apparatus; G, female gonopore and sucker; H, cement glands. Abbreviations: ce, cerebral eyespots; cg, cement glands; cp, cement pouch; fg, female gonopore; it, intestine; ma, male atrium; me, marginal eyespots; mg, male gonopore; ph, pharynx; pv, prostatic vesicle; spv, spermiducal vesicle; st, stylet; su, sucker; sv, seminal vesicle. Scale bars: 5 mm (A, B), 1 mm (C, D), 300 µm (E–G), 100 µm (H). After Tsuyuki et al. (2021, fig. 5).

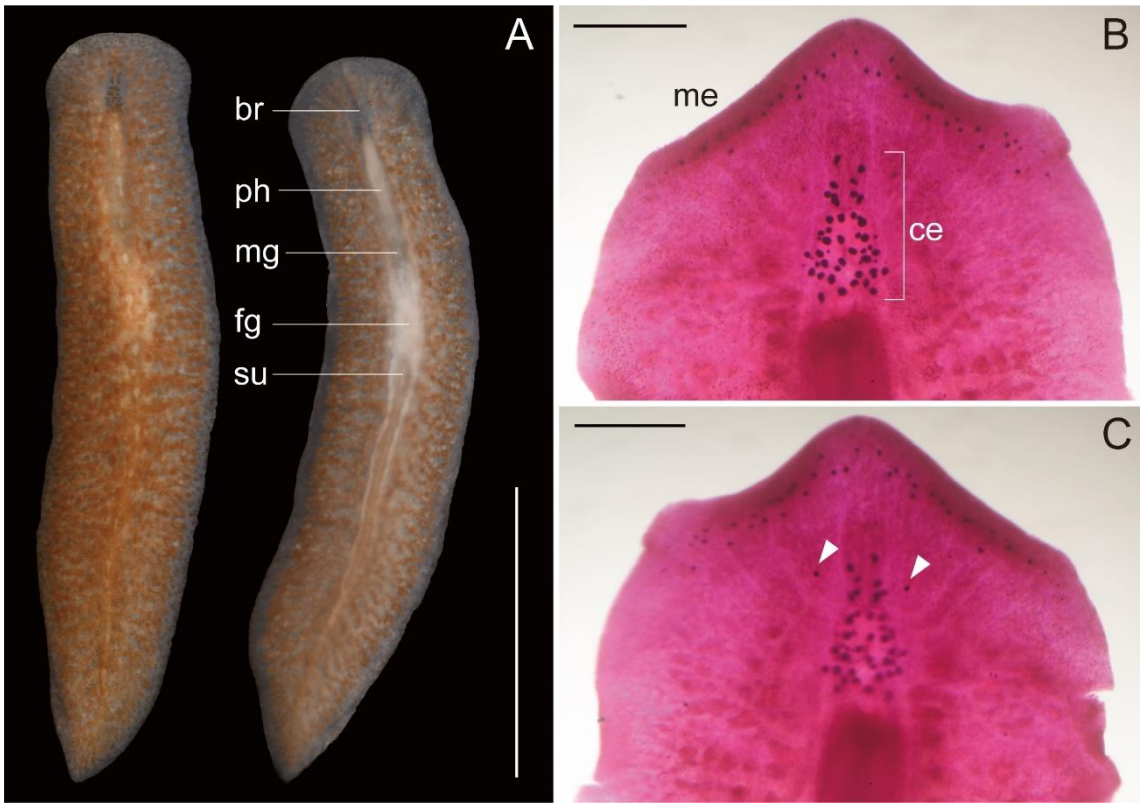

Fig. 35. *Prosthiostomum sonorum* Kato, 1938, photographs taken in life (A) and eyespots observed in fixed state after being cleared in xylene (B, C), ICHUM 6034 (Chapter II-5). A, Entire animal, dorsal view (left) and ventral view (right); B, magnification of anterior body, dorsal view, showing position and arrangement of cerebral and marginal eyespots; C, magnification of anterior body, ventral view, showing position of ventral eyespots, indicated by arrowheads. Abbreviations: br, brain; ce, cerebral eyespots; fg, female gonopore; me marginal eyespots; mg, male gonopore; ph, pharynx; su, sucker. Scale bars: 5 mm (A), 0.5 mm (B, C).

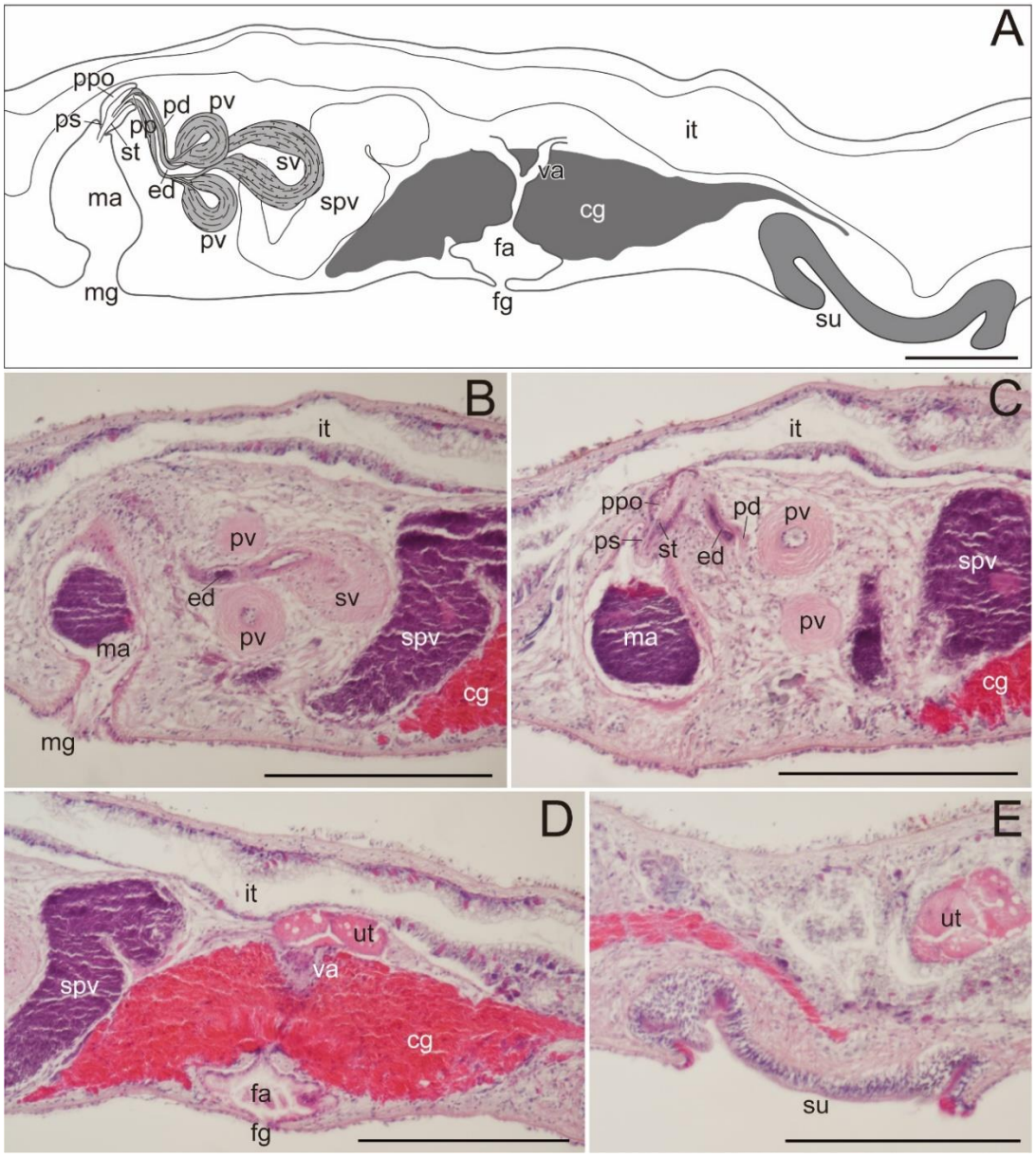

Fig. 36. *Prosthiostomum sonorum* Kato, 1938, sagittal sections, head to the left, B–E, ICHUM 6034 (Chapter II-5). A, Diagrammatic reconstruction of copulatory complex; B, seminal vesicle and paired prostatic vesicles; C, penis papillae, penis pouch, and penis stylet; D, female copulatory apparatus; E, sucker. Abbreviations: cg, cement glands; fa, female atrium; fg, female gonopore; ed, ejaculatory duct; it, intestine; ma, male atrium; mg, male gonopore; pd, prostatic duct; ph, pharynx; pp, penis papilla; ppo, penis pouch; ps, penis sheath; pv, prostatic vesicle; spv, spermiducal bulb; st, stylet; su, sucker; sv, seminal vesicle; ut, uterus; va, vagina. Scale bars: 300 µm.

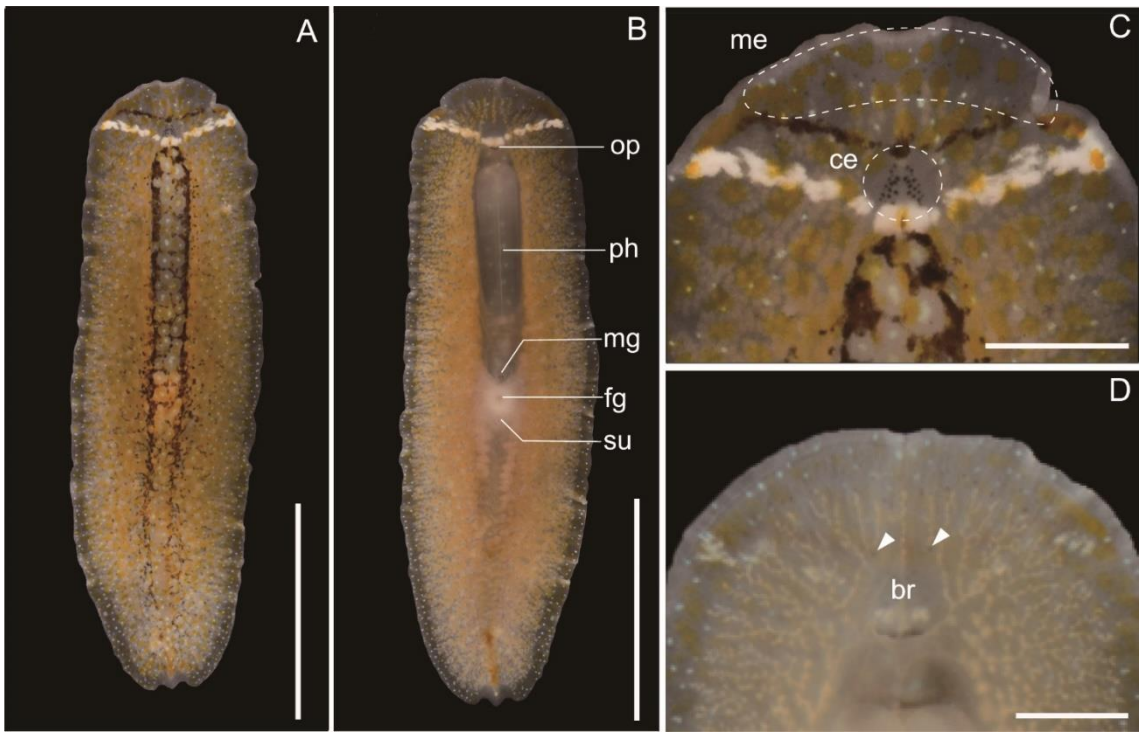

Fig. 37. *Prosthiostomum torquatum* Tsuyuki et al., 2019, photographs taken in anaesthetised living state. A–C, ICHUM 5563 (holotype); D, ICHUM 5562 (paratype) (Chapter II-5). A, Entire animal, dorsal view; B, entire animal, ventral view; C, magnification of anterior body, dorsal view, showing position and arrangement of cerebral and marginal eyespots; D, magnification of anterior body, ventral view, showing position of ventral eyespots (indicated by arrowheads). Abbreviations: br, brain; ce, cerebral eyespots; fg, female gonopore; me, marginal eyespots; mg, male gonopore; op, oral pore; ph, pharynx; su, sucker. Scale bars: 5 mm (A, B), 1 mm (C, D). After Tsuyuki et al. (2019, fig. 1).

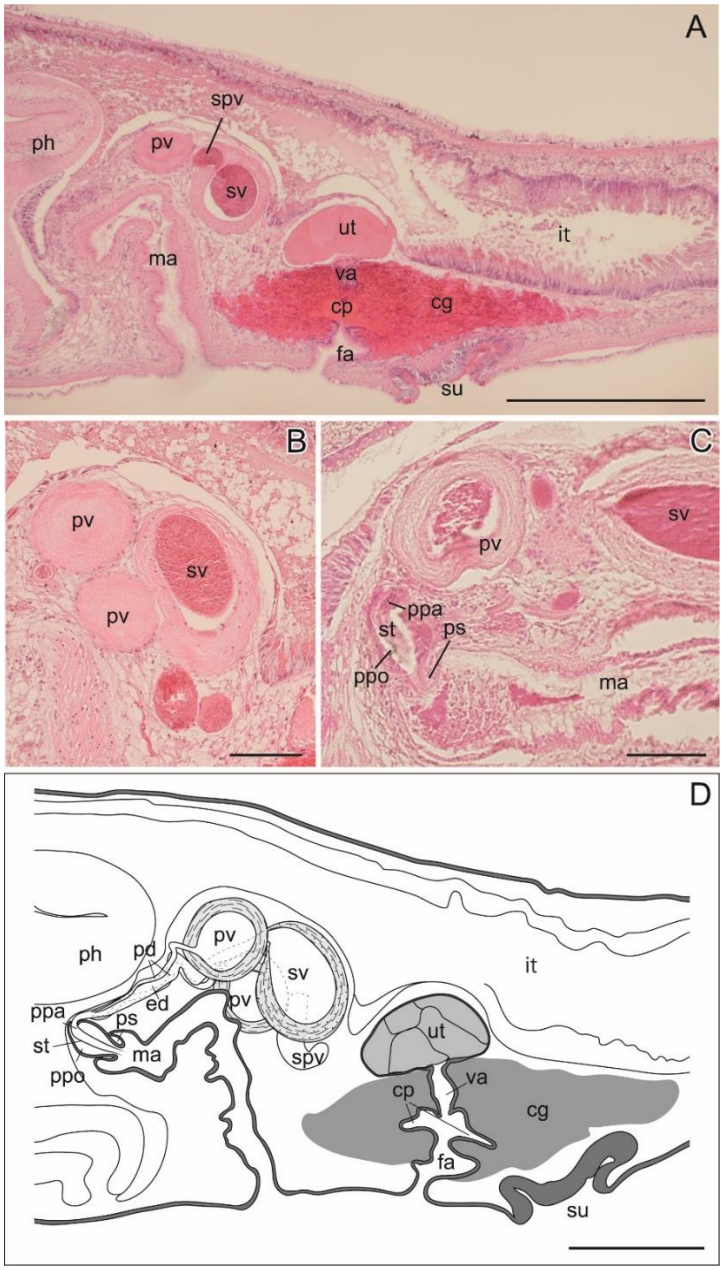

Fig. 38. *Prosthiostomum torquatum* Tsuyuki et al., 2019, sagittal sections, head to the left. A, B, ICHUM 5563 (holotype); C, ICHUM 5566 (paratype) (Chapter II-5). A, Copulatory complex; B, seminal vesicle and paired prostatic vesicles; C, penis pouch; D, diagrammatic reconstruction of copulatory complex. Abbreviations: cg, cement glands; cp, cement pouch; ed, ejaculatory duct; fa, female atrium; it, intestine; ma, male atrium; pd, prostatic duct; ph, pharynx; ppa, penis papilla; ppo, penis pouch; ps, penis sheath; pv, prostatic vesicle; spv, spermiducal vesicle; st, stylet; su, sucker; sv, seminal vesicle; ut, uterus; va, vagina. Scale bars: 500 µm (A), 100 µm (B, C), 300 µm (D). After Tsuyuki et al. (2019, fig. 2).

Fig. 39. Dorsal colour pattern variation in *Prosthiostomum torquatum* Tsuyuki et al., 2019 (Chapter II-5). A, ICHUM 5563 (holotype); B, ICHUM 5565 (paratype); C, ICHUM 5566 (paratype); D, ICHUM 5564 (non-type); E, ICHUM 5562 (paratype); F, ICHUM 6040 (non-type). Scale bar: 5 mm. After Tsuyuki et al. (2019, fig. 3).

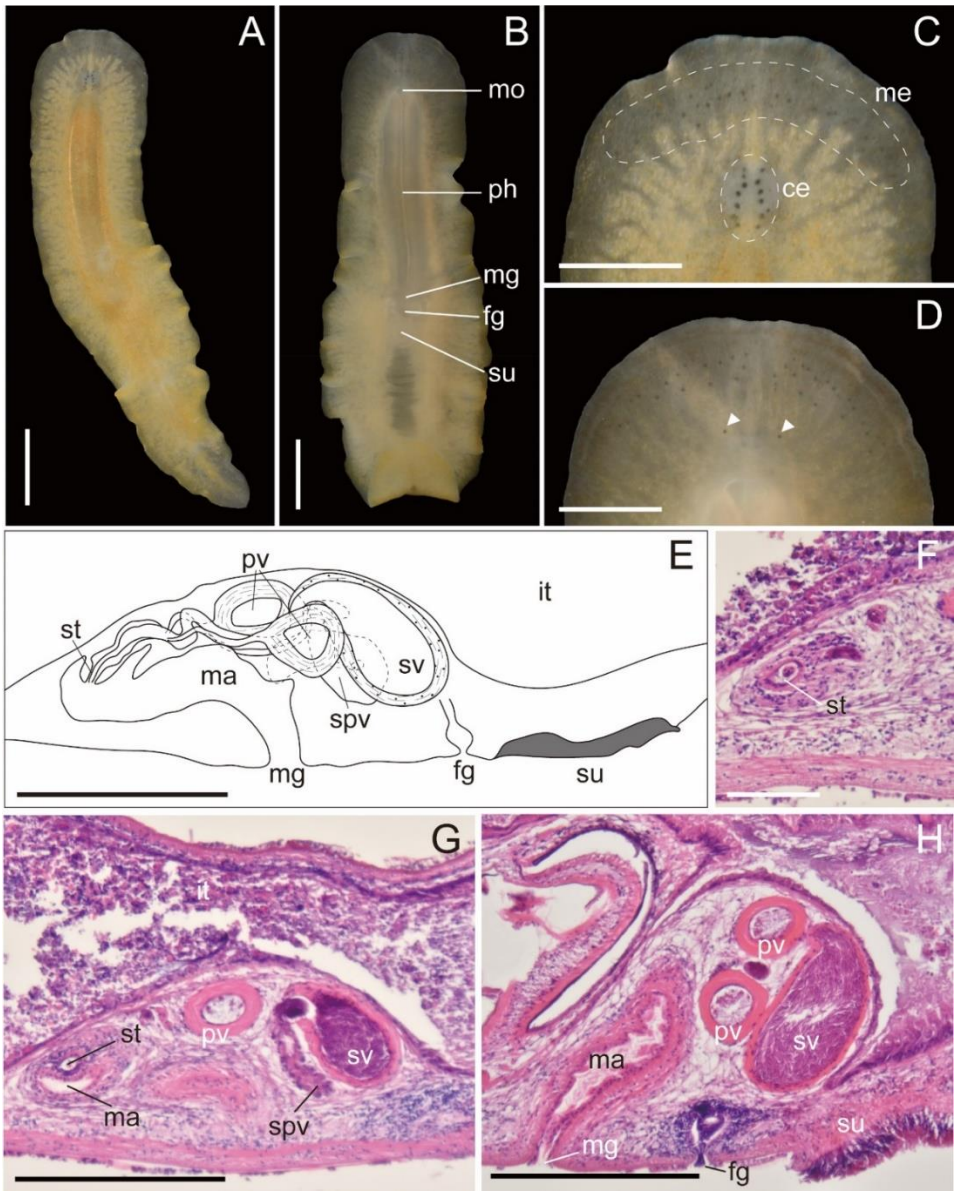

Fig. 40. ***Prosthiostomum vulgare*** **Kato, 1938b, ICHUM 6036 (A, C), ICHUM 6154 (B, D, H), ICHUM 6155 (E–G); photographs taken in life (A–D), schematic diagram (E), and photomicrographs of sagittal sections (anterior to the left) (F–H) (Chapter II-5).** A, Entire body, dorsal view; B, entire body, ventral view; C, magnification of head, dorsal view; D, magnification of head, ventral view, showing ventral eyespots (arrowheads); E, copulatory complex and sucker; F, stylet; G, male copulatory apparatus; H, copulatory complex and sucker. Abbreviations: ce, cerebral eyespots; fg, female gonopore; it, intestine; ma, male atrium; me, marginal eyespots; mg, male gonopore; mo, mouth; ph, pharynx; pv, prostatic vesicle; spv, spermiducal vesicle; st, stylet; su, sucker; sv, seminal vesicle. Scale bars: 1 mm (A, B); 0.5 mm (C, D); 300 µm (E, G, H); 100 µm (F). After Tsuyuki et al. (2021, fig. 6).

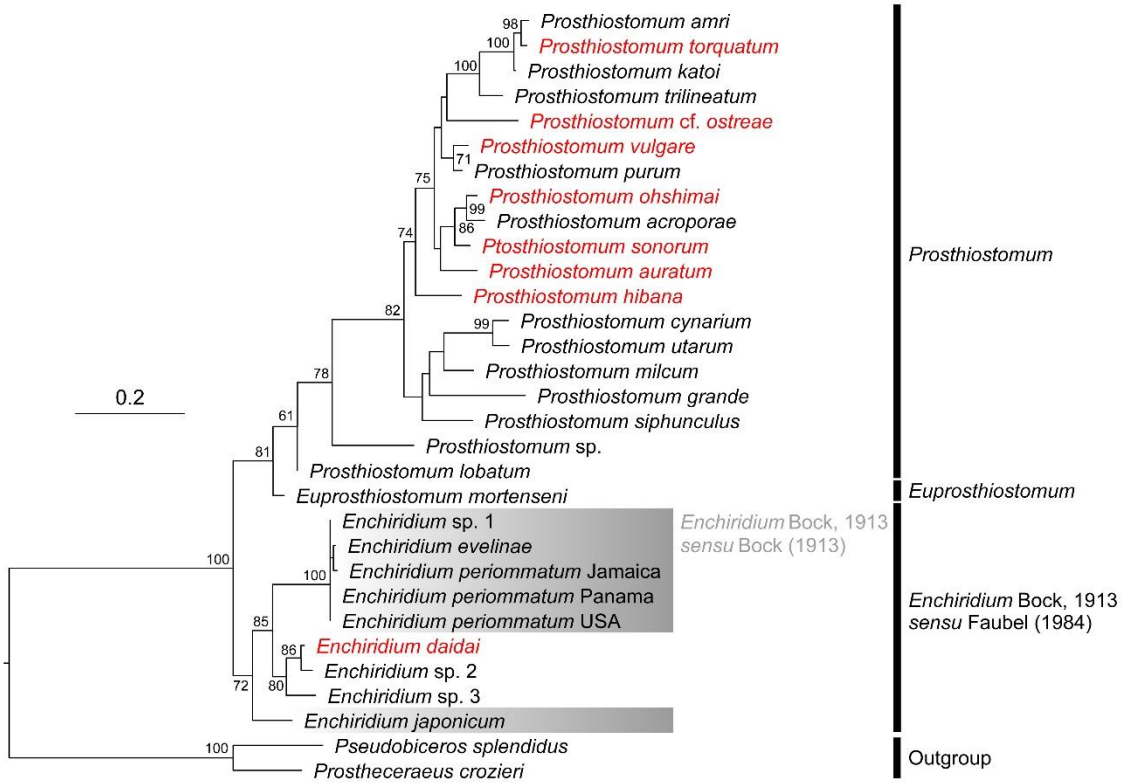

Fig. 41. Maximum likelihood phylogenetic tree based on the concatenated 2,104-bp dataset composed of 28S (1,521 bp) and COI (583 bp) sequences (Chapter II-5). Numbers near nodes are the bootstrap values (≥60) (%). The names of species for which morphological description are provided in this study are indicated in red. Modified from Tsuyuki et al. (2021, fig. 7).

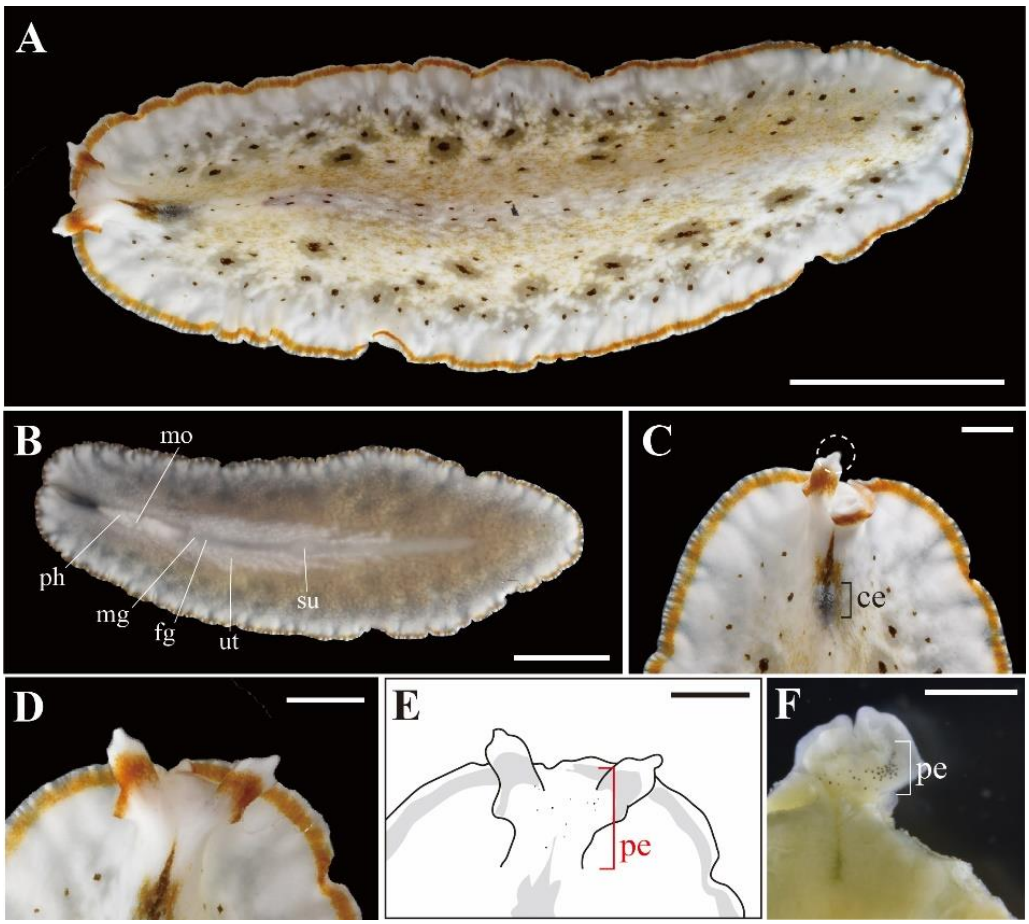

Fig. 42. *Bulaceros porcellanus* Newman and Cannon, 1996, ICHUM 6265, photographs taken in living (A–D) and fixed states (F); a diagram of eyespot distribution (E) (Chapter II-6). A, Entire body, dorsal view; B, entire body, ventral view; C, magnification of anterior body, dorsal view, showing arrangement of cerebral eyespots and pseudotentacle form, a distal knob of the pseudotentacle indicated by circle with a white broken line; D, E, magnification of anterior body, dorsal view, showing arrangement of pseudotentacular eyespots; F, magnification of anterior body, ventral view, showing arrangement of pseudotentacular eyespots. Abbreviations: ce, cerebral eyespots; fg, female gonopore; mg, male gonopore; mo, mouth; ph, pharynx; su, sucker; pe, pseudotentacular eyespots; ut, uterus. Scale bars: 5 mm (A, B), 1 mm (C–F). After Tsuyuki et al. (2022a, fig. 1).

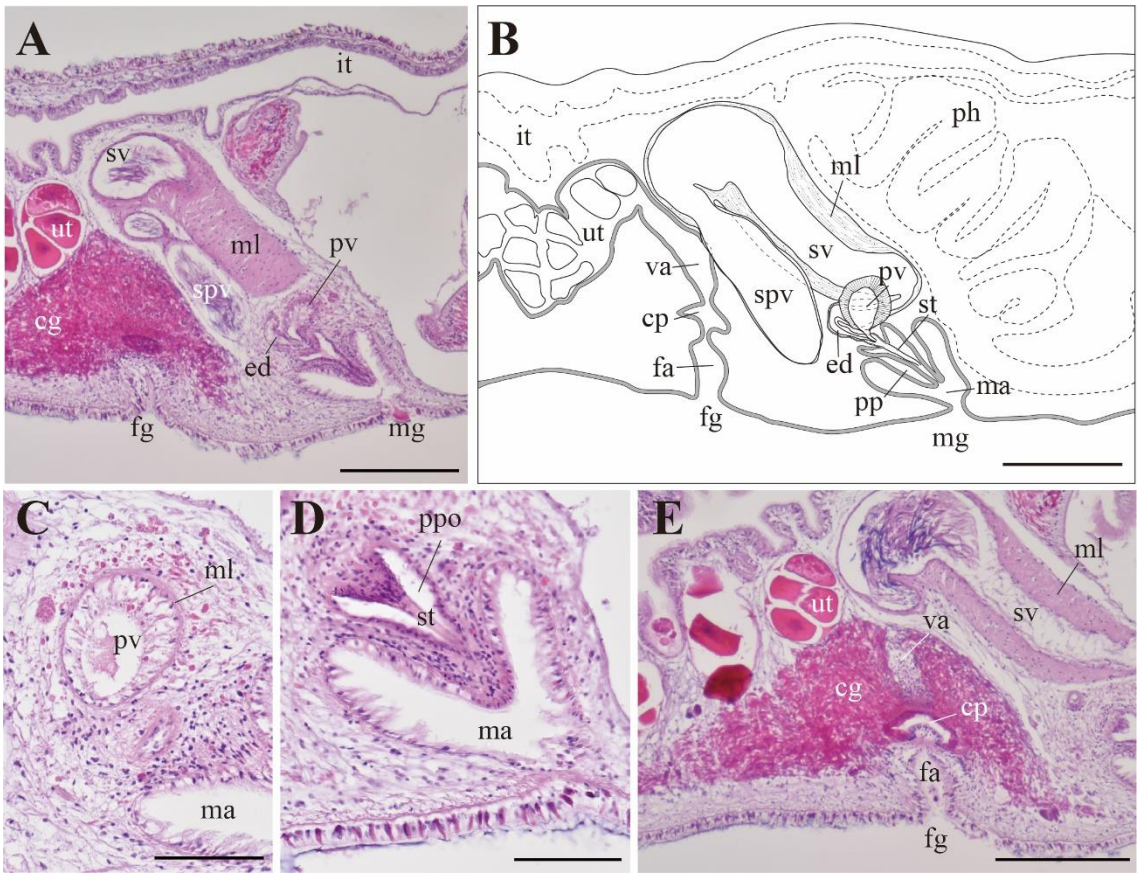

Fig. 43. *Bulaceros porcellanus* Newman and Cannon, 1996, ICHUM 6264, photomicrographs (A, C–E) and schematic diagram (B) of sagittal sections, head to the right (Chapter II-6). A, Male and female copulatory apparatuses; B, diagrammatic reconstruction of copulatory complex; C, prostatic vesicle; D, penial stylet enclosed in penis pouch; E, female copulatory apparatus. Abbreviations: cg, cement glands; cp, cement pouch; ed, ejaculatory duct; fa, female atrium; fg, female gonopore; it, intestine; ma, male atrium; mg, male gonopore; ml, muscular layer (we judged the fibers as muscular ones according to Faubel (1984)); ph, pharynx; pp, penis papilla; ppo, penis pouch; pv, prostatic vesicle; st, stylet; spv, spermiducal vesicle; sv, seminal vesicle; ut, uterus; va, vagina. Scale bars: 300 µm (A, B, E), 100 µm (C–D). After Tsuyuki et al. (2022a, fig. 2).

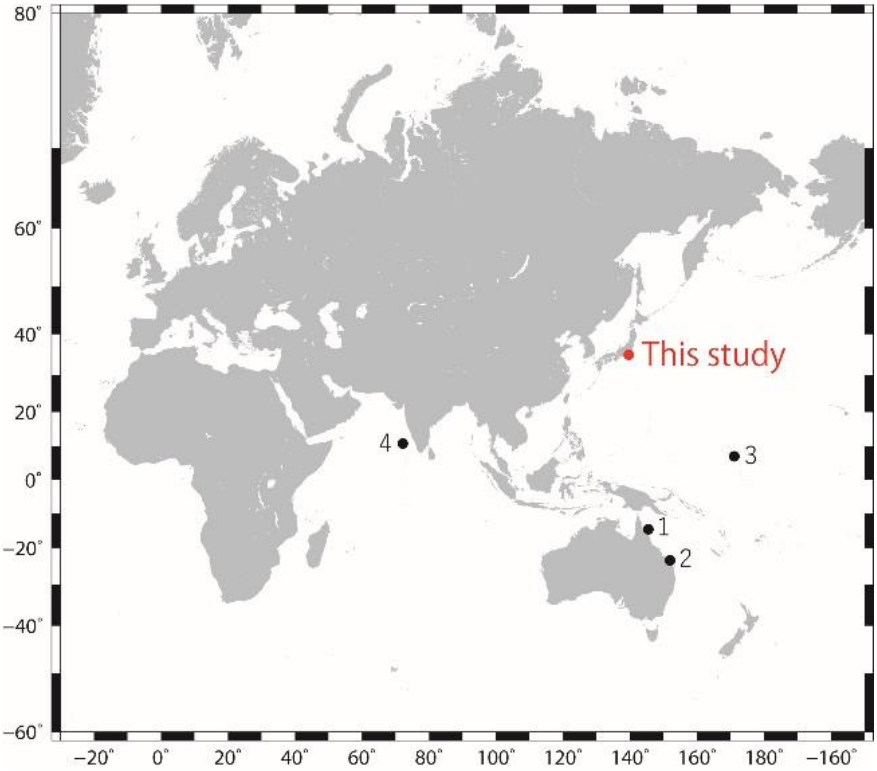

Fig. 44. Updated distribution map of *Bulaceros porcellanus* Newman and Cannon, 1996a (Chapter II-6). The red point shows the new record from Misaki, the Pacific coast of Japan. Black points show previously known localities: 1. Lizard Island, Australia (Newman and Cannon 1996a); 2. Heron Island, Australia (Newman and Cannon 1996a); 3. the Marshall Islands (Newman and Cannon 2005); 4. the Lakshadweep Islands, India (Dixit et al. 2021). After Tsuyuki et al. (2022a, fig. 3).

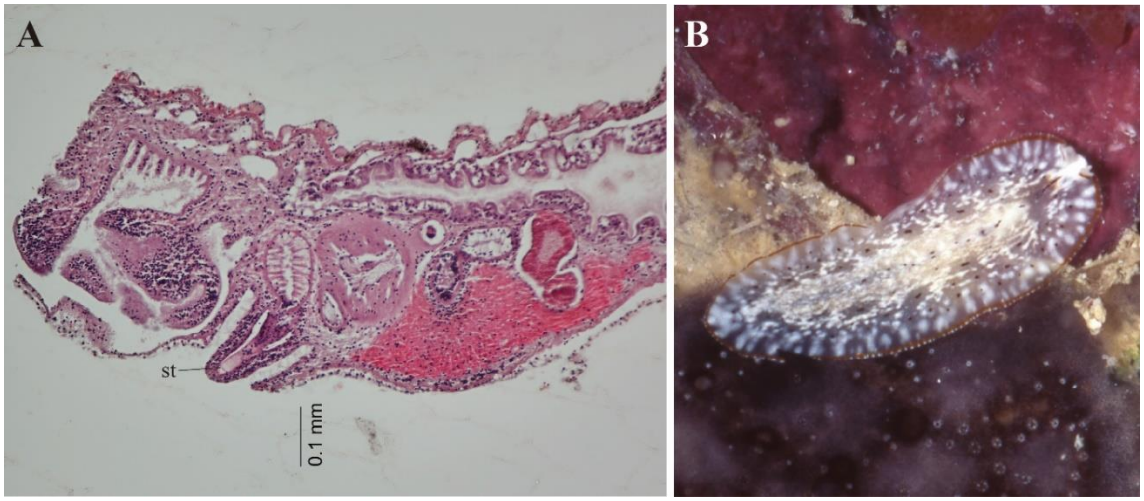

Fig. 45. *Bulaceros porcellanus* Newman and Cannon, 1996a, photographs deposited in the Queensland Museum, Southbank (Chapter II-6). A, Sagittal section of paratype QM G210663, showing a sclerotized penis stylet (st), head to the left; B, living state of holotype (QM G210662), taken on April 5, 1995, under rubble (2 m in depth). After Tsuyuki et al. (2022a, fig. 5).

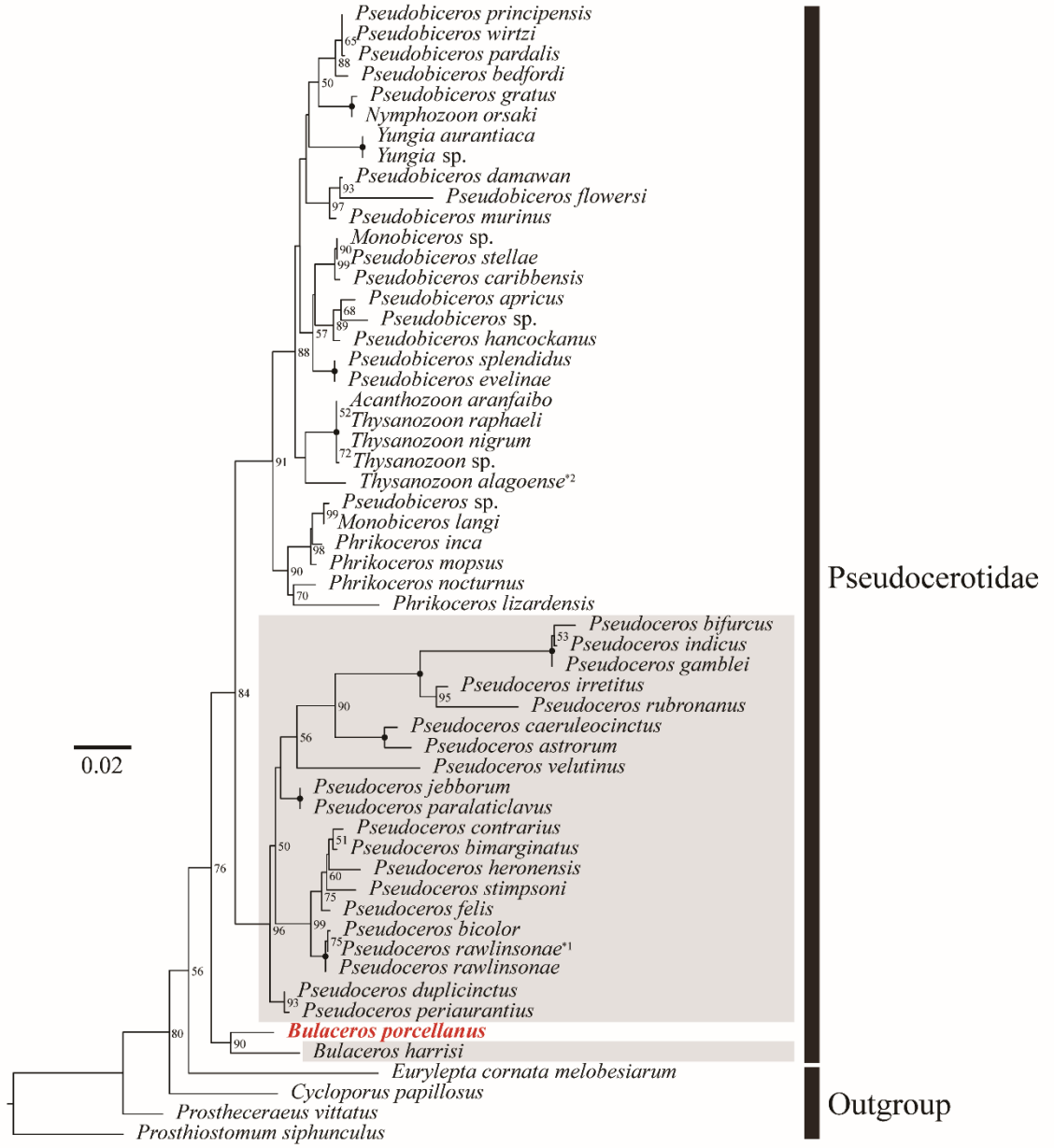

Fig. 46. ML phylogenetic tree based on 28S (1,433 bp). Bootstrap support values (≥50) are indicated near nodes (Chapter II-6). Nodes with full support (BS 100) are indicated by black circles. *Bulaceros porcellanus* from this study is indicated in red bold face. The members of *Pseudoceros* before this study are displayed with a gray background. Modified from Tsuyuki et al. (2022a, fig. 4).

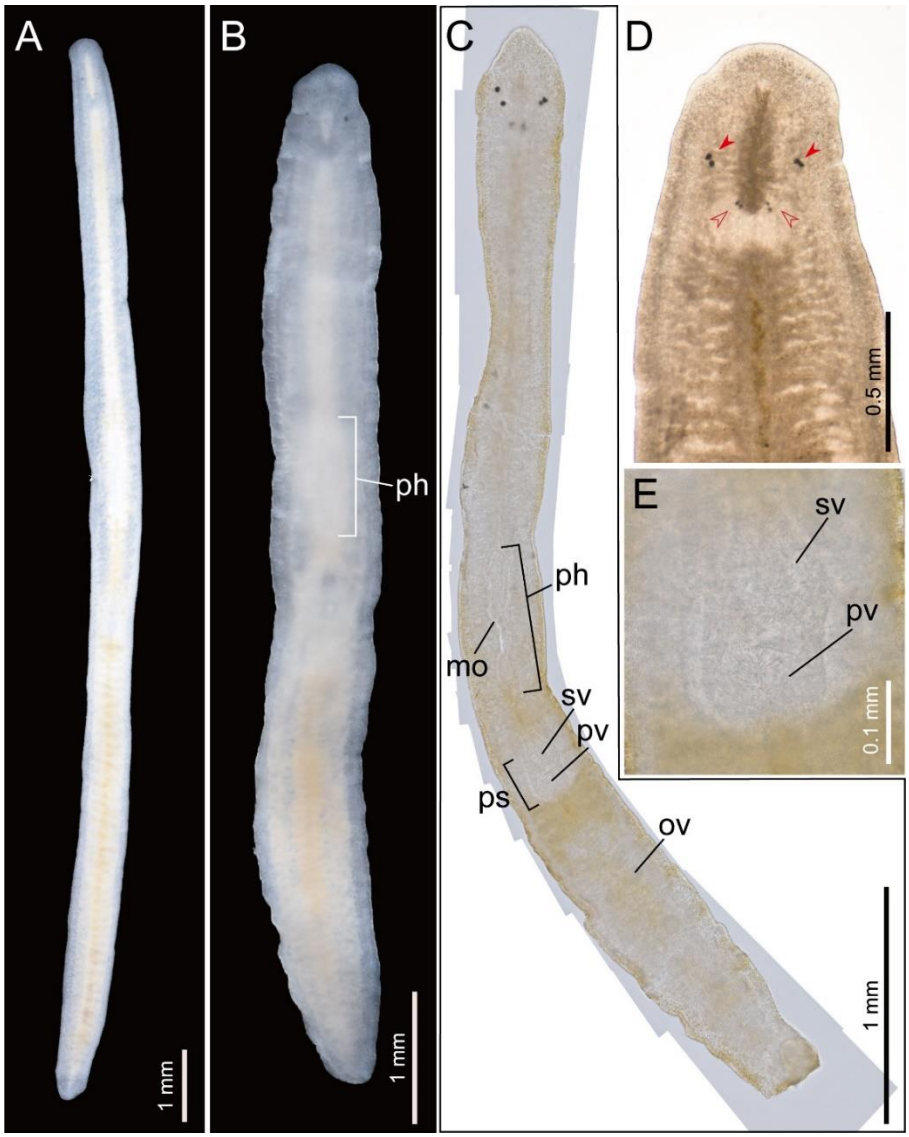

Fig. 47. *Theama* sp., photographs of living specimens (A, B, and D) and a whole mount (C, E). (A, D) ICHUM 8426. (B) ICHUM 8420. (C, E) ICHUM 8425 (Chapter II-7). A, whole animal, dorsal view; B, C, whole animal, ventral view; D, magnification of anterior body, showing precerebral (solid arrows) and cerebral eyespots (open arrows); E, magnification of male copulatory apparatus. Abbreviations: mo, mouth; ov, ovary; ph, pharynx; ps, penis sheath; pv, prostatic vesicle; sv, seminal vesicle.

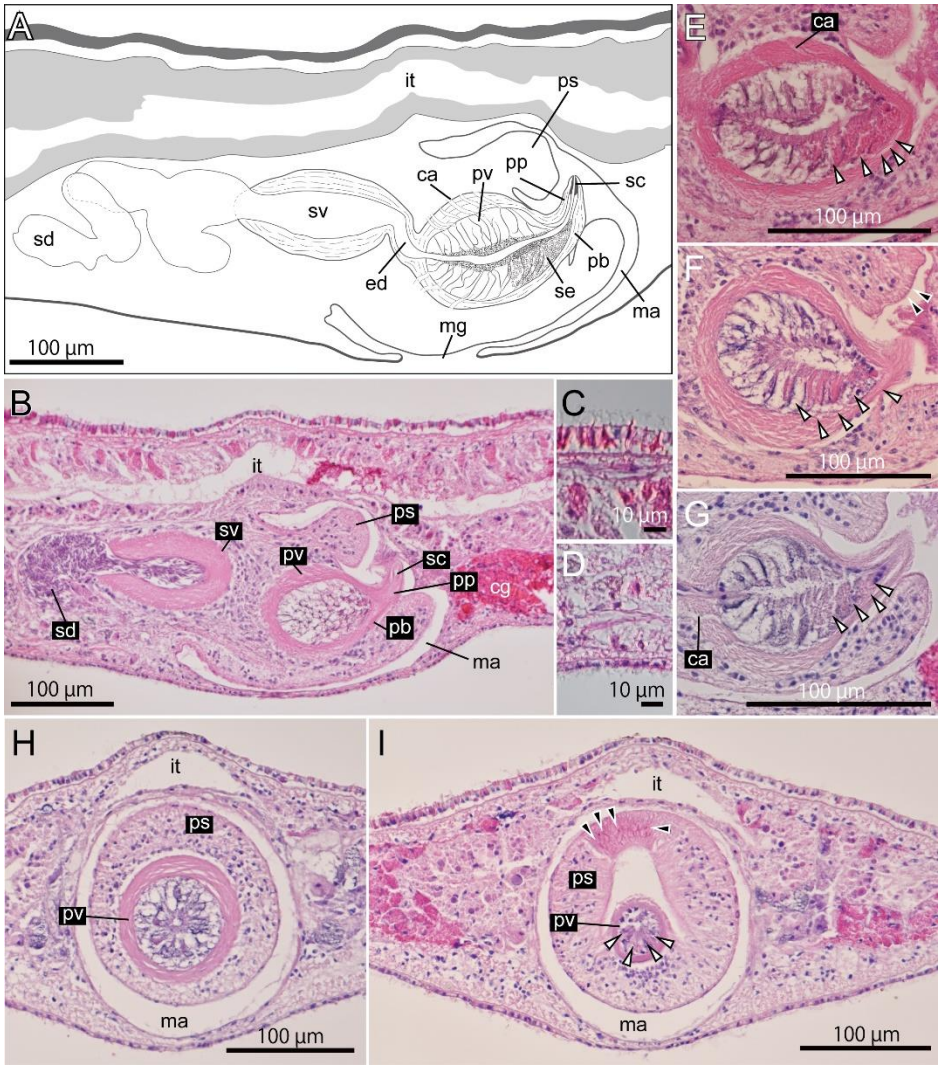

Fig. 48. *Theama* sp., schematic diagram (A) and photomicrographs of sagittal (B–G) (anterior to the left) and cross (H, I) sections. (A–E) ICHUM 8419. (F) ICHUM 8421. (G) ICHUM 8422. (H, I) ICHUM 8424 (Chapter II-7). A, Male copulatory apparatus; B, male and female copulatory apparatuses; C, dorsal epidermis; D, ventral epidermis; E–G, magnification of prostatic vesicle, arrows showing distributions of prostatic glands; H, prostatic vesicle and penis sheath; I, distal end of prostatic vesicle. White arrows showing distributions of prostatic glands; black arrows showing eosinophilic glands, piercing the distal rim of penis sheath. Abbreviations: ca, extra-vesicular gland's canal; cg, cement glands; ed, ejaculatory duct; it, intestine; ma, male atrium; mg, male gonopore; pb, penis bulb; pp, penis papilla; ps, penis sheath; pv, prostatic vesicle; sc, sclerotized epithelium; sd, sperm duct; se, eosinophilic secretion glands; sv, seminal vesicle.

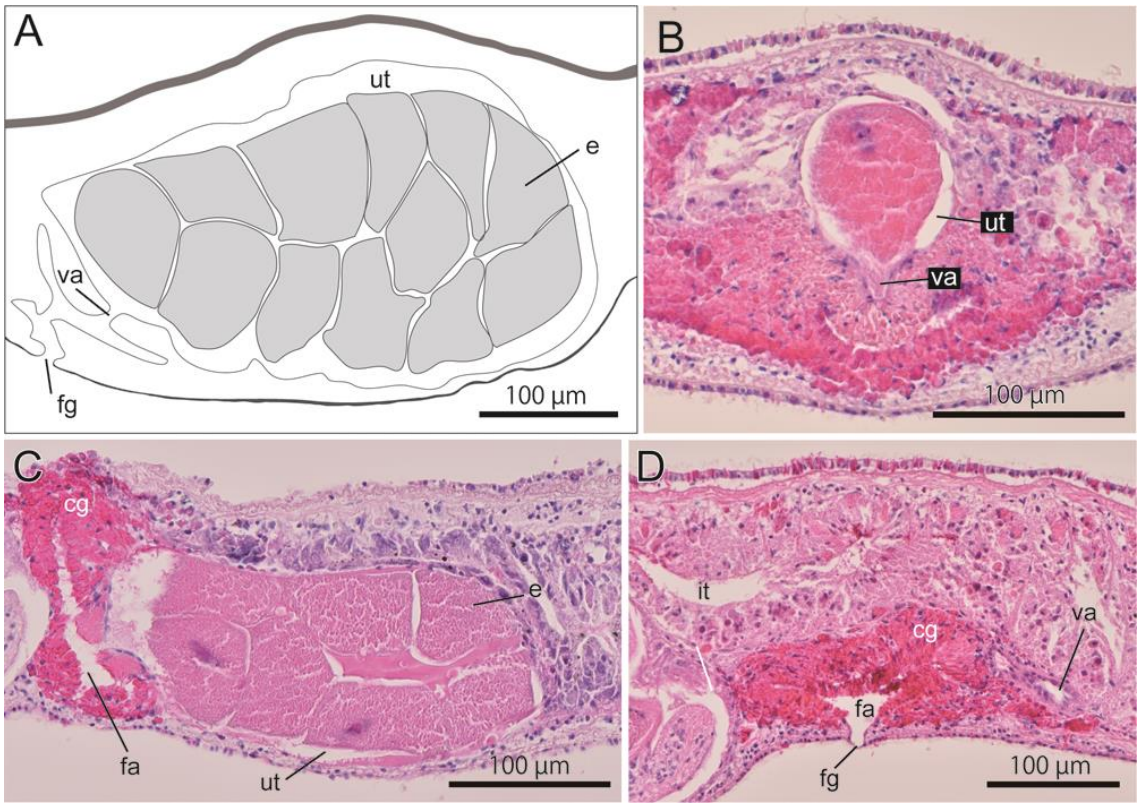

Fig. 49. *Theama* sp., schematic diagram (A) and photomicrographs of cross (B) and sagittal (C, D) sections (Chapter II-7). A, ICHUM 8423, female copulatory apparatus; B, ICHUM 8424, uterus; C, ICHUM 8422, uterus; D, ICHUM 8419, female atrium and gonopore. Abbreviations: cg, cement glands; e, egg; fa, female atrium; fg, female gonopore; it, intestine; ut, uterus; va, vagina.

TABLES

Table 1. Comparison of taxon concepts as to superfamily/family in Cotylea in the selected previous studies (Chapter I).

Family	Faubel (1984)	Bahia et al. (2017)	Dittmann et al. (2019a)	Litvaitis et al. (2019)
Amyellidae	In Pseudocerotoidea	In Chromoplanoidea	In Boninioidea	Amyellidae
Anonymidae	In Pseudocerotoidea	—	In Anonymoidea	—
Boniniidae	In Pseudocerotoidea	In Chromoplanoidea	In Boninioidea	Boniniidae
Chromoplanidae	In Pseudocerotoidea	In Chromoplanoidea	In Anonymoidea	to Amyellidae
Dicteroidae	In Pseudocerotoidea	—	—	—
Diposthidae	In Pseudocerotoidea	—	—	Diposthidae
Euryleptidae	In Euryleptoidea	In Pseudocerotoidea	Euryleptidae	Euryleptidae
Euryleptididae	In Euryleptoidea	—	—	—
Laidlawiidae	In Euryleptoidea	—	—	—
Opisthogeniidae	In Opisthogeniioidea	—	—	—

Pericelidae	In Pseudocerotoidea	In Periceloidea	In Periceloidea	to Diposthidae
Prosthiostomidae	In Euryleptoidea	In Prosthiostomoidea	In Prosthiostomoidea	Prosthiostomidae
Pseudocerotidae	In Pseudocerotoidea	In Pseudocerotoidea	Pseudocerotidae	Pseudocerotidae
Stylochoididae	In Pseudocerotoidea	—	—	—
Cestoplanidae	In Leptoplanoidea (Acotylea)	In Cestoplanoidea	In Cestoplanoidea	Cestoplanidae
Theamatidae	In Leptoplanoidea (Acotylea)	In Chromoplanoidea	In Boninioidea	Theamatidae
Stylostomidae[a]	—	—	Stylostomidae	—

[a]I consider the family Stylostomidae as invalid in this thesis (see **Systematic and phylogenetics** under **Suborder Cotylea** in **Chapter I**).

Table 2. List of protocols for fixation and GenBank accession numbers of the sequences of materials (Chapter II-1). After Tsuyuki et al. (2022b, table 1).

Species	ICHUM number	Protocol for fixation	Type status	Sequence data		
				COI	18S	28S
Boninia uru	ICHUM 8278	i	holotype	LC699268	—	LC699275
Boninia uru	ICHUM 8279	ii	paratype	—	—	—
Boninia uru	ICHUM 8280	ii	paratype	—	—	—
Boninia uru	ICHUM 8281	iii	paratype	LC699269	LC699274	LC699276
Boninia uru	ICHUM 8282	iii	paratype	LC699270	—	LC699277
Boninia uru	ICHUM 8283	ii	paratype	—	—	—
Boninia yambarensis	ICHUM 8284	i	holotype	LC699271	LC699273	LC699278
Boninia yambarensis	ICHUM 8285	i	paratype	—	—	LC699279
Boninia yambarensis	ICHUM 8286	i	paratype	—	—	LC699280
Boninia yambarensis	ICHUM 8287	i	paratype	LC699272	—	LC699281

Boninia yambarensis	ICHUM 8288	i	paratype	—	—	LC699282
Boninia yambarensis	ICHUM 8289	iv	paratype	—	—	—

The fixation protocols (i–iv) are: (i) a part of the body was removed and preserved in 99.5% ethanol for DNA extraction and the rest of the body was fixed in Bouin's solution for 24 h and subsequently preserved in 70% ethanol; (ii) the whole body was fixed in Bouin's solution for 24 h and subsequently preserved in 70% ethanol; (iii) the whole body was preserved in 99.5% ethanol for DNA extraction; and (iv) the whole body was mounted on a glass slide, squeezed under a cover slip, and preserved in 10% formaldehyde solution in seawater.

Table 3. List of primers used in this study (Chapter II-1). After Tsuyuki et al. (2022b, table 2).

Gene	Primer name	Sequence	Application	Reference
COI	Acotylea_COI_F	ACTTTATTCTACTAATCATAAGGATATAGG	amplification and sequencing	Oya and Kajihara (2017)
COI	Acotylea_COI_R	CTTTCCTCTATAAAATGTTACTATTTGAGA	amplification and sequencing	Oya and Kajihara (2017)
18S	hrms18S_F	ATCCTGCCAGTAGTCATATGC	amplification and sequencing	Oya and Kajihara (2020)
18S	hrms18S_Fi1	GCCGCGGTAATTCCAGCTCC	sequencing	Oya and Kajihara (2020)
18S	hrms18S_Fi2	GGGTTCCGGGGGAAGTATG	amplification and sequencing	Oya and Kajihara (2020)
18S	hrms18S_R	CTACGGAAACCTTGTTACGAC	amplification and sequencing	Oya and Kajihara (2020)
18S	hrms18S_Ri1	CTTTAATATACGCTATTGGAGCTGG	sequencing	Oya and Kajihara (2020)
18S	hrms18S_Ri2	CTATTTAGTGGCTAGAGTCTCGTTCG	sequencing	Oya and Kajihara (2020)
28S	fw1	AGCGGAGGAAAAGAAACTA	amplification and sequencing	Sonnenberg et al. (2007)
28S	hrms_fw2	AGAAGTACCGCGAGGGAARGTTG	sequencing	Oya and Kajihara (2020)
28S	rev4	GTTAGACTYCTTGGTCCGTG	sequencing	Sonnenberg et al. (2007)
28S	rev2	ACGATCGATTTGCACGTCAG	amplification and sequencing	Sonnenberg et al. (2007)

Table 4. List of species used for the molecular phylogenetic analysis, and their respective collection localities and habitats, GenBank accession numbers, and references (Chapter II-1). After Tsuyuki et al. (2022b, table 3).

Species	Collection locality	Habitat	GenBank accession		Reference
			18S rDNA	28S rDNA	
Amyellidae					
Chromyella sp.	Bocas del Toro, Panama	interstitial (sandy sediments)	KC869795	KC869848	Laumer and Giribet (2014); Laumer pers. comm.
Boniniidae					
Boninia uru	Okinawa Island, Okinawa, Japan	interstitial (among course gravelly sediments)	LC699274	LC699276	Tsuyuki et al. (2022b)
Boninia antillara	Great Lameshure Bay, St. John, US Virgin Islands	epibenthic (under rocks)	—	MH700282	Litvaitis et al. (2019)
Boninia divae[a]	Playa Santa Cruz, Curaçao	epibenthic (under rocks)	—	MH700280	Litvaitis et al. (2019)
Boninia neotethydis	Eilat, Israel	interstitial (course sediments)	—	MH700283	Litvaitis et al. (2019)
Boninia yambarensis	Okinawa Island, Okinawa, Japan	epibenthic (under rocks)	LC699273	LC699278	Tsuyuki et al. (2022b)
Boninia sp.[b]	Bocas del Toro, Panama	—[c]	KC869793	KC869846	Laumer and Giribet (2014); Laumer pers. comm.

Theamatidae					
Theama mediterranea	Rovinj, Croatia	interstitial (sandy sediments)	—	MN384705	Dittmann et al. (2019a)
Theama sp.	Bocas del Toro, Panama	interstitial (sandy sediments)	KC869792	KC869845	Laumer and Giribet (2014); Laumer pers. comm.
Outgroup					
Cestoplana rubrocincta	Naples, Italy	epibenthic (under rocks)	MN384689	MN334198	Dittmann et al. (2019a)
Pericelis flavomarginata	Kagoshima, Japan	epibenthic (under rocks)	LC672041	LC568535	Tsuyuki et al. (2020b, 2021)
Pericelis tectivorum	Aquaria Innsbruck, Austria	epibenthic (under rocks or other objects)	MK181525	MK181524	Dittmann et al. (2019a, b)

[a]The specimen is currently registered as *B. antillara* based on the taxon concept of Litvaitis et al. (Litvaitis et al. 2019) in that *B. divae* should be synonymized with *B. antillara*, but it was originally identified as *B. divae* based on the morphology (Litvaitis et al. 2019).

[b]In the GenBank database, the specimen was assigned to *Boninia divae*, but it should be "*Boninia* sp." because it was unidentifiable due to its juvenile state (cf. https://mczbase.mcz.harvard.edu/guid/MCZ:IZ:132897).

[c]Although the specimen was collected from an interstitial habitat, I treated the habitat of *Boninia* sp. as indeterminate in this paper because I cannot evaluate the habitat in adult state due to its juvenile state (see Introduction).

Table 5. Comparison of selected characters among *Boninia* species (Chapter II-1). After Tsuyuki et al. (2022b, table 4).

Species	*B. antillara*	*B. divae*	*B. mirabilis*	*B. neotethydis*	*B. oaxaquensis*	*B. uru*	*B. yambarensis*	*Boninia* sp.
Body size Length = L Width = W	8 mm (L), 2 mm (W)[a]; 16 mm (L), 3.3, 3.5, and 3.9 mm (W)[b]	30–50 mm (L), 2–4 mm (W)[d]	29 mm (L), 4.5 mm (W) (preserved state)	60 mm (L), 5 mm (W)	3–11 mm (L), 1–3 mm (W)	3–4.5 mm (L); 0.65–0.9 mm (W)	13.9–22.4 mm (L); 0.93–1.25 mm (W)	?
Marginal eyespot number	about 40[a]	numerous[d]	numerous, present dorsally and ventrally	10–18 (3–8 per side)	36–126	21–29, only dorsally	19–42, only dorsally	?
Cerebral eyespot number	ca. 30[a]	numerous (arranged in two long bands)[d]	13 (arranged in 2 separate clusters)	4 (2 pairs, each pair lying close to each other)	14–66	4 (two pairs, each pair lying close to each other)	6–7 (3–4 pairs; 2 eyespots lying close to each other whereas 1 or 2 eyespots located posteriorly)	?
Relative diameter of eyespots Marginal eyespot: M Cerebral eyespots: C	M:C = 40:25 (μm)[b]	M:C = 23:23 (μm)[d]	M:C = 20:20 (μm)	?	almost the same diameter between M and C (fig. 2D)	M:C = 55:24 (μm)	M:C = (8–23):14 (μm)	?

Pharynx length (mm)	4.5–5 (ca. 1/3 body length)[b]	12.5 (ca. 1/2 body length)[d]	?	? (ca. 1/3 body length)	1.2	0.5–1.1 (ca. 1/4 body length)	2.6–6.6 (ca. 1/3 body length)	?
Prostatoid organ number	25[a]; <30[b]	>50[d]	ca. 40	10–18	16–24	2–4	21–22	3, 7
Girdle	triple[a, c]	triple[e]	double	single	single	single	single	single
Uterine vesicle number	several[b]	8–10 in each[d]	5 in each	several	?	2 in each	5 in each	?
Inner wall of Lang's vesicle	non-ciliated[c]	ciliated[e]	ciliated	partly ciliated	?	lined with cilia; elongated in posterior region	lined with cilia; elongated in posterior region	non-ciliated
Connection point of uterine canals	vagina immediately anterior to the entrance of Lang's vesicle[b]	vagina immediately anterior to the entrance of Lang's vesicle[d]	vagina immediately anterior to the entrance of Lang's vesicle	vagina at its junction with Lang's vesicle	?	lateral to Lang's vesicle	vagina immediately anterior to the entrance of Lang's vesicle	?
Habitat	under stones at high water line; beach-rock[b]	under stones at highwater line[d]	under stones near the highwater limit	coarse sediments (shell and madrepore fragments)	under littoral to sublittoral rocks	interstitial coarse sand	under intertidal rocks	?
Distribution	Charotte Amalie, St. Thomas, Virgin Islands	Piscadera Baai, St. Michels Baai,	Haha-jima and Chichi-jima (Ogasawara Islands), Japan	Eilat, Israel (Red Sea); Akko, Shiqmona,	Agua Blanca, San Agustinillo, Panteón,	Nagahama Beach, Okinawa Island, Japan	Nagahama Beach, Okinawa Island, Japan	Samboanga, Philippines

	(USA)[a]; Curaçao[b]; Kralendijk, near Pasanggrahan, Bonaire[b]	Vaerssen Baai, Curaçao[d]		Israel (Mediterranean Sea)	Estacahuite, Dos Hermanas beaches, Cacaluta Bay, Oaxaca			
Reference	[a]Hyman (1955b) [b]Du Bois-Reymond Marcus and Marcus (1968) [c]Curini-Galletti and Campus (2007)	[d]Du Bois-Reymond Marcus and Marcus (1968) [c]Curini-Galletti and Campus (2007)	Bock (1923), Curini-Galletti and Campus (2007)	Curini-Galletti and Campus (2007)	Ramos-Sánchez et al. (2020)	Tsuyuki et al. (2022b)	Tsuyuki et al. (2022b)	Curini-Galletti and Campus (2007)

Table 6. List of species used for the molecular phylogenetic analysis, GenBank accession numbers, and references, respectively (Chapter II-2).

Species	GenBank accession		Reference
	18S rDNA	28S rDNA	
Cestoplanidae			
Eucestoplana cf. *cuneata*	LC740491	LC740493	this study
Eucestoplana sp.	LC740492	LC740495	this study
Cestoplana nopperabo	LC745668	LC322284	Oya and Kajihara (2019); this study
Cestoplana rubrocincta	MW376751	MW377504	Rodríguez et al. (2021)
Cestoplana salar	—	KY263653.2	Bahia et al. (2017)
Cestoplana techa	—	KY263654.2	Bahia et al. (2017)
Outgroup			
Pericelis flavomarginata	LC672041	LC568535	Tsuyuki et al. (2020b, 2022c)
Prosthiostomum siphunculus	MZ292836	MZ292816	Rodríguez et al. (unpub.)
Theama mediterranea	MN384707	MN384705	Dittmann et al. (2019a)

Table 7. Comparison of the selected characteristics among the known *Eucestoplana* species including the undetermined species in the present study (Chapter II-2).

Species	*E.* cf. *cuneata*	*E. meridionalis*	*Eucestoplana* sp.
Body length (mm)	10	20	26
Body width (mm)	?(slender, ribbon-shaped)	3	0.7
Anterior body shape	rounded	slightly pointed	rounded
Eyespots	35–40, only anterior to the brain	numerous, distributed around brain	about 20–30, only anterior to the brain
Dorsal coloration	?	chocolate-brown	translucent white
Dorsal color pattern	?	absent	absent
Mouth position	?	in posterior region of pharyngeal cavity	near posterior end of pharynx
Seminal vesicle	elongate-oval	elongate-oval	elongated, bending 180° at position posterior to female reproductive organ
Stylet	70-µm long; wedge-shaped	present	131-µm long; wedge-shaped
Penis sheath	cone-like shape	cone-like shape	dome-like shape
Cilia along inner wall of male atrium	surrounding the whole male atrium	?	only present along the outside of the penis sheath
Adhesive organ	present	absent	present
Distribution	the Galápagos Islands; Fiji; the Okinawa Islands, Japan	South Australia	the Okinawa Islands, Japan

Reference	Sopott-Ehlers and Schmidt (1975); Tajika et al. (1991); this study	Prudhoe (1982a, b)	this study

Table 8. Interspecific uncorrected *p*-distances for the 28S gene fragments between cestoplanid species of which sequences are available in public database (Chapter II-2).

	C. nopperabo	*C. rubrocincta*	*C. salar*	*C. techa*	*Eucestoplana* sp.
C. nopperabo LC322284.1					
C. rubrocincta MW377504.1	0.05980				
C. salar KY263653.2	0.05094	0.01772			
C. techa KY263654.2	0.04873	0.01883	0.00664		
Eucesoplana sp.	0.04430	0.06755	0.06091	0.05759	
Eucestoplana cf. *cuneata*	0.04651	0.06977	0.06312	0.05980	0.01107

Table 9. List of GenBank accession numbers of the sequences determined for three species of *Pericelis* (Chapter II-3). Modified from Tsuyuki et al. (2022c, table 1).

Species	ICHUM number	28S rDNA	18S rDNA (1748 bp)	COI (712 bp)
Pericelis flavomarginata	6116 (holotype)	LC568536 (1008 bp)	—	LC568540
Pericelis flavomarginata	6117 (paratype)	LC568535 (2117 bp)	LC672041	—
Pericelis flavomarginata	6118 (paratype)	—	—	LC568539
Pericelis flavomarginata	6119 (paratype)	LC56853 (1008 bp)	—	LC568541
Pericelis lactea	6288 (holotype)	LC699189 (1008 bp)	LC699193	LC699195
Pericelis lactea	6289 (paratype)	—	—	LC699196
Pericelis maculosa	6290 (holotype)	LC699190 (1008 bp)	LC699194	LC699197
Pericelis maculosa	6293 (paratype)	LC699191 (1008 bp)	—	LC699198
Pericelis maculosa	6294 (paratype)	LC699192 (1008 bp)	—	LC699199

Table 10. List of species used for the molecular phylogenetic analysis, respective collection localities, GenBank accession numbers (18S and 28S rDNA), and sources (Chapter II-3). Modified from Tsuyuki et al. (2022c, table 2).

Species	Collection locality	18S	28S	Source
Diposthidae				
Diposthus popeae	Playa Kalki, Curaçao	—	MH700294	Litvaitis et al. (2019)
Pericelis alba	Cape Verde	—	MK299354	Cuadrado et al. (2021)
Pericelis byerleyana	Inter University Institute for Marine Sciences, Eilat, Israel	—	MH047291	Velasquez et al. (2018)
Pericelis cata	Cape Verde, San Vicente	—	MK299373	Cuadrado et al. (2021)
Pericelis flavomarginata	Kagoshima, Japan	LC672041	LC568535	Tsuyuki et al. (2020a, 2022c)
Pericelis hymanae	North Heron Island, Great Barrier Reef, Australia	—	MH700339	Litvaitis et al. (2019)
Pericelis lactea	Kagoshima, Japan	LC699193	LC699189	Tsuyuki et al. (2022c)
Pericelis maculosa	Ishigaki Island, Japan	LC699194	LC699190	Tsuyuki et al. (2022c)
Pericelis orbicularis	Reef Bay, St. John, US Virgin Islands	—	MH700340	Litvaitis et al. (2019)
Pericelis tectivorum	Commercial seawater aquarium Alpenriff in Innsbruck (Tirol; Austria)	MN334202	MK181525	Dittmann et al. (2019a, b)
Outgroup				
Boniniidae				
Boninia sp.	Bocas del Toro, Panama	KC869793	KC869846	Laumer and Giribet (2014)

Cestoplanidae				
Cestoplana rubrocincta	Naples, Italy	MN334198	MN384689	Dittmann et al. (2019a)
Theamatidae				
Theama mediterranea	Rovinj, Croatia	MN384707	MN384705	Dittmann et al. (2019a)

Table 11. Comparison of selected characters among *Pericelis* species (Chapter II-3). Modified from Tsuyuki et al. (2022c, table 3).

Species	*P. alba*	*P. byerleyana*	*P. cata*	*P. ernesti*	*P. flavomarginata*	*P. hymanae*
Body coloration	ivory white, darker along body center	light brown, darker along midline	beige	black, gray, brown or olive	translucent	translucent or gray
Color pattern on dorsal surface	amber dots and thin brushstroke-like lines; a thin, dark stripe extending along midline	well-defined roundish cream circles forming reticulate pattern; spaced ring smaller and more numerous toward margin	white and dark mottles with dense black dots; black and brown random mottles	white spots or dark brown or olive-tan splotches	lemon-yellow margin; narrow brown midline extending from anterior edge of body to posterior end of pharynx	dark brown dorsal midline
Marginal tentacles	delicate marginal folds, pointed	small, simply folded	marginal subtle folds of margin, 4 mm apart from each other	much folded	apparent; tip of tentacles extending and tapering	tiny V-shaped extensions with slight upward crease down center
Marginal eyespots distribution	only anteriorly	completely encircling body periphery	completely encircling body periphery	completely encircling body periphery	completely encircling body periphery	completely encircling body periphery

Tentacular eyespots	scarce and dispersed over the tentacles	numerous at tip	densely disposed; >100 eyespots	wanting	abundant at tip, scattered posteriorly	crowded in mid-region of tentacles
Frontal eyespots	absent	few in number	two broad and loose tracts	scattered in front of cerebral eyespots; fan out anteriorly to marginal tentacles	scattered between tentacles	scattered in front of cerebral eyespots; fan out anteriorly and laterally toward tentacular eyespots
Cerebral eyespots	two drop-shaped clusters	two elongated and separated clusters	45–55; not distinctly separated in midline	two elongated clusters of 40–50 eyespots	two elongated clusters, lateral to brown midline	two elongated, oval clusters of 35–50 eyespots
Gonopore(s)	common	separated (Laidlaw 1902; Velasquez et al. 2018); common (Meixner 1907; Kato 1943)	separated	common	common	separated
Penis papilla shape; length/width (L/W)	spherical; L/W: about 1	cylindric conical cone; L/W: 4–5	conical; L/W: 1–2	conical; L/W: about 4	cylindrical: L/W: 6–7	cylindrical; L/W: about 4

Internal glandular epithelium	present in entire penis papilla	? present in central penis papilla	present in entire penis papilla	present in ejaculatory duct*	absent	absent
Uterine vesicle number	?	?	about 10	?	4–5 pairs	>10
Reference	Cuadrado et al. (2021)	Laidlaw (1902); Meixner (1907); Kato (1943c); Velasquez et al. (2018)	Du Bois-Reymond Marcus and Marcus (1968); Bahia and Padula (2009); Bahia et al. (2014)	Hyman (1953); Soutullo et al. (2021)	Tsuyuki et al. (2020a)	Poulter (1974)

*The separation between the ejaculatory duct and the penis papilla is ambiguous in the specimen of *P. ernesti* provided by Soutullo et al. (2021) (cf. Soutullo et al. 2021, fig. 6D).

Table 11. continued.

Species	*P. lactea*	*P. maculosa*	*P. nazahui*	*P. orbicularis*	*P. sigmeri*	*P. tectivorum*
Body coloration	translucent	translucent	brown-dark, brownish-green, brown-pink or purple	light brown, brown-red or brown-olive	beige-light, brown	brown
Color pattern on dorsal surface	nothing	white dots scattered all over body; sparce brown speckles distributed centrally	pharyngeal region slightly grayish, whitish or beige; marginal and brain region whitish, from which slightly faint line directed towards tentacles	dark brown branches; reddish-brown network	white and light brown mottles; black dots concentrated in pharyngeal region	white ovals denser along margin
Marginal tentacles	shallowly folded	shallowly folded	slightly prominent	folded	folded	thin
Marginal eyespots	completely encircling the body periphery	only anteriorly	105–943; completely encircling body periphery	completely encircling body periphery	238–304; completely encircling body periphery	completely encircling body periphery

Tentacular eyespots	abundant at tip	abundant at tip	85–166	two wedge-formed clusters (Schmarda 1859; Stummer-Traunfels 1933); not well separated into two clusters (Hyman 1955)	35–87	especially dense at the tip
Frontal eyespots	scattered in front of cerebral-eyespot cluster, fanning out anteriorly, leading to marginal and tentacular eyespots	sparsely distributed between anterior margin and cerebral-eyespot cluster; absent around midline	two broad and loose tracts oriented towards anterior body	spreading to anterior margin in fan-like manner (Hyman 1955)	two broad and loose tracts oriented towards anterior body	merged from cerebral eyespots, extending in fan-like shape anteriorly
Cerebral eyespots	two clusters of 66–69 eyespots	two clusters of 17–54 eyespots	91–195	two elongated clusters of 50–60 eyespots (Hyman 1955)	54–77	two elongated, oval clusters

Reproductive gonopore	separated	separated	common	common (Hyman 1955); separated (Stummer-Traunfels 1933)	common	separated
Penis papilla shape; length/width (L/W)	conical; L/W: 2–3	cylindrical; L/W: >10	conical; L/W: 1–2	conical or mammiform; L/W: 1–2	cylindrical; L/W: about 9	cylindrical, U-shaped, or pointing posteriorly; L/W: ?
Internal glandular epithelium	absent	absent	present in entire penis papilla	absent	present in entire penis papilla	?
Uterine vesicle number	3 pairs	2 pairs	3–8	numerous	7–10	about 6
Reference	Tsuyuki et al. (2022c)	Tsuyuki et al. (2022c)	Ramos-Sánchez et al. (2020)	Schmarda (1859); Stummer-Traunfels (1933); Hyman (1955); Du Reymond Marcus and Marcus (1968)	Ramos-Sánchez et al. (2020)	Dittmann et al. (2019b)

Table 12. List of species used for the molecular phylogenetic analysis, sample locations, and DDBJ/EMBL/GenBank accession numbers (Chapter II-5). After Tsuyuki et al. (2021, table 1).

Species	location	GenBank Accession		Reference
		COI	28S	
Enchiridium daidai	Bonotsu, Kagoshima, Japan	LC504240	LC504235	Tsuyuki and Kajihara (2020)
Enchiridium evelinae	Brazil	—	KY263683	Bahia et al. (2017)
Enchiridium japonicum	Eilat, Israel	—	MH700298	Litavaitis et al. (2019)
Enchiridium periommatum	St. Ann's Bay, Jamaica	—	MH700299	Litavaitis et al. (2019)
Enchiridium periommatum	Crawl Cay, Bocas del Toro, Panama	—	MH700300	Litavaitis et al. (2019)
Enchiridium periommatum	Tavemier Key, Florida, USA	—	MH700301	Litavaitis et al. (2019)
Enchiridium sp. 1	Santa Heleria Island	—	KY263665	Bahia et al. (2017)
Enchiridium sp. 2	New South Wales, Australia	—	MH700302	Litavaitis et al. (2019)
Enchiridium sp. 3	Lizard Island, Australia	—	MN384686	Dittmann et al. (2019a)
Euprosthiostomum mortenseni	St. Ann's Parish, Jamaica	—	MH700304	Litavaitis et al. (2019)
Prosthiostomum amri	New South Wales, Australia	MW375900	MW377496	Rodríguez et al. (2021)
Prosthiostomum acroporae	Victocille, California, USA	—	HQ659011	Rawlinson et al. (2011)
Prosthiostomum auratum	Misaki, Kanagawa, Japan	LC625892	LC625886	Tsuyuki et al. (2021)
Prosthiostomum cynarium	St. John, US Virgin Islands	—	MH700371	Litavaitis et al. (2019)
Prosthiostomum grande	Sakurajima, Kagoshima, Japan	LC625900	LC635089	Tsuyuki et al. (2021)
Prosthiostomum hibana	Misaki, Kanagawa, Japan	LC625894	LC625887	Tsuyuki et al. (2021)
Prosthiostomum katoi	Lizard Island, Australia	—	MN384694	Dittmann et al. (2019a)

Prosthiostomum lobatum	Missouri Key, Florida, USA	—	MH700372	Litavaitis et al. (2019)
Prosthiostomum milcum	Long Key, Florida, USA	—	MH700373	Litavaitis et al. (2019)
Prosthiostomum ohshimai	Amakusa, Kumamoto, Japan	—	Appendix 3	Tsuyuki et al. (unpub.)
Prosthiostomum cf. *ostreae*	Misaki, Kanagawa, Japan	LC625896	LC625889	Litavaitis et al. (2019)
Prosthiostomum purum	Gulf of Aqaba, northern Red Sea	—	MH700374	Litavaitis et al. (2019)
Prosthiostomum siphunculus	Asturias, Spain	—	MN384697	Dittmann et al. (2019a)
Prosthiostomum sonorum	Amakusa, Kumamoto, Japan	—	Appendix 4	Tsuyuki et al. (unpub,)
Prosthiostomum torquatum	Shirahama, Wakayama, Japan	LC625899	LC504234	Tsuyuki and Kajihara (2020)
Prosthiostomum trilineatum	Guam	—	MH700376	Litavaitis et al. (2019)
Prosthiostomum utarum	Piscadera Baai, Curacao	—	MH700377	Litavaitis et al. (2019)
Prosthiostomum vulgare	Misaki, Kanagawa, Japan	LC625898	LC625891	Tsuyuki et al. (2021)
Prosthiostomum sp.	Eilat, Israel	—	MH700375	Litavaitis et al. (2019)
Outgroup				
Prostheceraeus crozieri	Long Key, Florida, USA	—	HQ659013	Rawlinson et al. (2011)
Pseudobiceros splendidus	North Heron Island, Australia	—	MH700388	Litavaitis et al. (2019)

Table 13. Comparison of characters between five *Enchiridium* species in which marginal eyespots are distributed only anteriorly (Chapter II-5). After Tsuyuki et al. (2020, table 2).

	E. daidai	*E. delicatum*	*E. gabriellae*	*E. magec*	*E. russoi*
Type locality	off the coast of Bonomisaki, Kagoshima, Japan	East London, South Africa	São Sebastião Island, São Paulo, Brazil	north of El Balito, Tenerife, Canary Islands, Spain	Shelley Beach, East London, South Africa
Dorsal coloration/ pattern:					
Background color	translucent	light yellow milky	transparent	whitish to cream	greyish yellow
Spots or maculae scattered all over the dorsal surface	none	none	none	brown caramel spots, arranged more densely in the central region	brown pigments spread especially in the central part
Median line	none	two yellow bands	none	a band composed of brown caramel spots	a band composed of brown pigments
Fringed line	a thin orange line	none	none	none	none
Reference	Tsuyuki and Kajihara (2020)	Palombi (1939)	Marcus (1949)	Cuarado et al. (2017)	Palombi (1939)

Table 14. Comparison of selected characters between *P. hibana* and nine other species of *Prosthiostomum*, which share either body coloration or cerebral-eyespot arrangement; species for which body coloration in life is unknown are also listed (Chapter II-5) (after Tsuyuki et al. 2021, table 2).

Species	*P. auratum*	*P. capense*	*P. cynarium*	*P. dohrnii*	*P. grande*
Body size	7.3–12 mm in length; 2.3–3.4 mm in width	about 6 mm in length; 1–1.5 mm in width	5 mm in length	25 mm in length; 6 mm in width	22 mm in length; 5 mm in width
Dorsal coloration	uniformly golden yellow except for cerebral-eyespot area	with yellow or brown spots	ivory-colored or grayish	soft bright orange yellow, with darker orange-yellow spots scattered over the body especially denser along midline	buffy ground color, with numerous small spots of ochraceous color distributed all over body
Cerebral eyespots	single pair of linear clusters composed of 5–10 eyespots	single pair of roughly linear clusters composed of about 15 eyespots	single pair of linear clusters composed of 4–10 eyespots	single pair of oval clusters composed of numerous eyespots	single pair of wedge clusters composed of about 25 eyespots
Marginal eyespots	about 12 eyespots in single row along frontal margin; distributed anterior to brain	about 40 in number; distributed anterior to brain	5–15 in number; distributed anterior to brain	numerous; elongated to the level behind brain	two irregular rows along the anterior margin
Ventral eyespots	single pair	none	single pair	single pair	none
Male atrium	elongated; inner wall smooth	?	elongated; inner wall smooth	?	?
Seminal vesicle	oval; lumen oval	?	spherical; lumen spherical	?	spherical; lumen shape unknown

Position of the junction of the spermiducal vesicles into the seminal vesicle	at the anterior corner of the seminal vesicle	?	middle portion of the seminal vesicle	?	?
Sucker	0.46 mm in diameter; located on body center	0. 11 mm in diameter; located at the four-fifths of body	0.35 mm in diameter; located on body center	present; details not described	about 4% of body length in size; located slightly behind body center
Distribution	Japan (Honshu and Kyushu)	South Africa (Simons Bay, Cape Town)	Brazil (São Sebastião Island)	Italy (60–80 m depth, Secca di Gajola in the Gulf of Naples)	Japan (Noto, Misaki, Shimoda, Shirahama, Amakusa, Amami-Oushima)
Reference	Kato (1937b); Tsuyuki et al. (2021)	Bock (1931)	Marcus (1950); Bahia and Schrödl (2018)	Lang (1884)	Stimpson (1857); Yeri and Kaburaki (1918); Tsuyuki (personal observation)

Table 14. continued.

Species	*P. hibana*	*P. parvicelis*	*P. purum*	*P. siphunculus*	*P. vulgare*
Body size	14 mm in length; 3 mm in width	6 mm in length	15–20 mm in length; about 1 mm in width	8–11 mm in length (Lang 1884); 10–18 mm in length, 4–6 mm in width (Noreña et al. 2014)	6.8–8.8 mm in length; 1.4–2.1 mm in width
Dorsal coloration	translucent, uniformly covered with numerous orange maculae, some of which being agglutinated and forming larger maculae; the larger maculae scattered throughout	?	translucent milky white without any color pattern	dirty white, beige to yellow; without spots or dots	light buffy, cinnamon pigments medially abundant
Cerebral eyespots	single pair of linear clusters composed of 6–9 eyespots	single pair of linear clusters composed of 7–8 eyespots; a pair of eyespots, each located at the level of the anterior end of the cerebral cluster	single pair of linear clusters composed of 6–8 eyespots	single pair of linear clusters composed of 10–14 eyespots; a pair of eyespots, each located at the level of the anterior end of the cerebral cluster	single pair of linear clusters composed of 7 eyespots
Marginal eyespots	about 25 in number; distributed ventrally along anterior margin in front of	obviously a few in number, elongated to the half position of	about 40 in number; elongated to the half position of the brain	about 40 in number; distributed anterior to brain; eyeless on midline	about 40 in number; distributed anterior to brain

	the brain	the brain			
Ventral eyespots	3–4 pairs	none	none	none	single pair
Male atrium	elongated; inner wall deeply ruffled	?	elongated; inner wall smooth	elongated; inner wall smooth	elongated; inner wall smooth
Seminal vesicle	oval; lumen narrow and elongated	oval; lumen pyriform	oval; lumen oval	oval to elongated; lumen fusiform	oval; lumen oval
Position of the junction of the spermiducal vesicles into the seminal vesicle	middle portion of the seminal vesicle	middle portion of the seminal vesicle	middle portion of the seminal vesicle	at the posterior corner of the seminal vesicle	at the anterior corner of the seminal vesicle
Sucker	0.40 mm in diameter; located on body center	located on body center	small; located immediately posterior to female gonopore	located on body center	0.21 mm in diameter; located on body center
Reference	Tsuyuki et al. (2021)	Hyman (1939b)	Kato (1937b)	Lang (1884); Noreña et al. (2014)	Kato (1938a); Tsuyuki et al. (2021)
Distribution	Japan (Misaki, Kanagawa)	Galápagos Islands	Japan (Misaki, Kanagawa)	European Atlantic coasts, the Mediterranean Sea, the Tyrrhenian Sea, North and South Africa, Somalia, and Vietnam	Japan (Noto, Misaki, Susaki, Suga-shima Island, Shirahama, Amakusa)

Table 15. List of species used for the molecular phylogenetic analysis and respective GenBank accession numbers (Chapter II-6). After Tsuyuki et al. (2022a, table 1).

Species	Accession number	Source
Pseudocerotidae		
Acanthozoon aranfaibo	MK299362	Cuadrado et al. (2021)
Bulaceros harrisi	EF514802	Bolaños et al. (2007)
Bulaceros porcellanus	LC660222	Tsuyuki et al. (2022a)
Nymphozoon orsaki	KY263697.2	Bahia et al. (2017)
Monobiceros langi	KY263710.2	Bahia et al. (2017)
Phrikoceros inca	MH700357	Litvaitis et al. (2019)
Phrikoceros lizardensis	MH700358	Litvaitis et al. (2019)
Phrikoceros mopsus	MH700359	Litvaitis et al. (2019)
Phrikoceros nocturnus	MH700362	Litvaitis et al. (2019)
Pseudocbiceros apricus	MH700379	Litvaitis et al. (2019)
Pseudobiceros bedfoldi	MH700380	Litvaitis et al. (2019)
Pseudobiceros caribbensis	MK299378	Cuadrado et al. (2021)
Pseudobiceros damawan	MH700381	Litvaitis et al. (2019)
Pseudobiceros evelinae	KY263719.2	Bahia et al. (2017)
Pseudobiceros flowersi	MN384698	Dittmann et al. (2019a)
Pseudobiceros gratus	MH700382	Litvaitis et al. (2019)
Pseudobiceros hancockanus	MN384699	Dittmann et al. (2019a)
Pseudobiceros murinus	MH700385	Litvaitis et al. (2019)
Pseudobiceros pardalis	KY263723.2	Bahia et al. (2017)
Pseudobiceros principensis	MT569345	Pérez-García et al. (2020)
Pseudobiceros splendidus	MH700389	Litvaitis et al. (2019)
Pseudobiceros stellae	MH047293	Velasquez et al. (2018)
Pseudobiceros wirtzi	KY263725	Bahia et al. (2017)
Pseudobiceros sp.	MK299359	Cuadrado et al. (2021)
Pseudoceros astrorum	KY263737	Bahia et al. (2017)
Pseudoceros bicolor	MH700391	Litvaitis et al. (2019)
Pseudoceros bifurcus	MH700392	Litvaitis et al. (2019)
Pseudoceros bimarginatus	MN384700	Dittmann et al. (2019a)
Pseudoceros caeruleocinctus	MH700394	Litvaitis et al. (2019)
Pseudoceros contrarius	KY263728.2	Bahia et al. (2017)
Pseudoceros duplicinctus	MH047292	Velasquez et al. (2018)
Pseudoceros felis	MH700399	Litvaitis et al. (2019)

Pseudoceros gamblei	MH700400	Litvaitis et al. (2019)
Pseudoceros heronensis	MH700401	Litvaitis et al. (2019)
Pseudoceros indicus	MH700402	Litvaitis et al. (2019)
Pseudoceros irretitus	MH700403	Litvaitis et al. (2019)
Pseudoceros jebborum	MN384701	Dittmann et al. (2019a)
Pseudoceros paralaticlavus	MH700405	Litvaitis et al. (2019)
Pseudoceros periaurantius	MN384702	Dittmann et al. (2019a)
Pseudoceros rawlinsonae	MH700406	Litvaitis et al. (2019)
Pseudoceros rawlinsonae[*1]	MK299357	Cuadrado et al. (2021)
Pseudoceros rubronanus	MH700407	Litvaitis et al. (2019)
Pseudoceros stimpsoni	MN384703	Dittmann et al. (2019a)
Pseudoceros velutinus	KY263740.2	Bahia et al. (2017)
Thysanozoon alagoense[*2]	KY263747.2	Bahia et al. (2017)
Thysanozoon nigrum	MH700417	Litvaitis et al. (2019)
Thysanozoon raphaeli	EF514810	Bolaños et al. (2007)
Thysanozoon sp.	MH700418	Litvaitis et al. (2019)
Yungia aurantiaca	MK299386	Litvaitis et al. (2019)
Yungia sp.	HQ659018	Rawlinson et al. (2011)
Outgroup		
Euryleptidae		
Cycloporus papillosus	MH700291	Litvaitis et al. (2019)
Eurylepta cornuta melobesiarum	MK299350	Cuadrado et al. (2021)
Prostheceraeus vittatus	AJ315647	Noren and Jondelius (2002)
Prosthiostomidae		
Prosthiostomum siphunculus	MN421934	Dittmann et al. (2019a)

[*1]As "*Pseudoceros rawlinsonae* var. *galaxy*" in Cuadrado et al. (2021).

[*2]The specific name "*alagoensis*" in Bahia et al. (2015) is herein corrected to read "*alagoense*" for gender agreement.

Table 16. List of material examined. Museum catalog number, type status, collection information, and DDBJ/EMBL/GenBank accession numbers for the specimens of *Theama* sp. (Chapter II-7).

Specimen number	Preservation state	Locality	Date	GenBank accession number			Collector	Maturity
				COI	18S	28S		
ICHUM 8419	Sagittal sections, 3 slides	Ikarikai, Shiriuchi, Hokkaido, Japan (41.5357°N, 140.4297°E)	27 Jun 2021	LC740188	—	—	A. Tsuyuki and Y. Oya	Mature
ICHUM 8420	Sagittal sections, 3 slides	Ikarikai, Shiriuchi, Hokkaido, Japan (41.5357°N, 140.4297°E)	26 Jun 2021	LC740189	LC740208	—	A. Tsuyuki and Y. Oya	Mature
ICHUM 8421	Sagittal sections, 7 slides	Ikarikai, Shiriuchi, Hokkaido, Japan (41.5357°N, 140.4297°E)	21 Jul 2020	LC740190	—	LC740209	A. Tsuyuki and Y. Oya	Mature
ICHUM 8422	Sagittal sections, 2 slides	Shioya Beach, Yasu, Kochi, Japan (33.5200°N, 133.7555°E,)	10 Jun 2021	LC740191	—	—	Y. Oya	Mature
ICHUM 8423	Sagittal sections, 3 slides	Enoshima, Kanagawa, Japan (35.2974°N, 139.4802°E)	15 May 2022	LC740192	—	—	Y. Oya	Mature
ICHUM 8424	Cross sections, 11 slides	Enoshima, Kanagawa, Japan (35.2974°N, 139.4802°E)	15 May 2022	LC740193	—	—	Y. Oya	Mature

ICHUM 8425	Whole mount	Enoshima, Kanagawa, Japan (35.2974°N, 139.4802°E)	15 May 2022	—	—	—	Y. Oya	Mature
ICHUM 8426	Unsectioned, 70% EtOH	Ikarikai, Shiriuchi, Hokkaido, Japan (41.5357°N, 140.4297°E)	27 Jun 2021	LC740194	—	—	A. Tsuyuki and Y. Oya	Mature
ICHUM 8427	Unsectioned, 70% EtOH	Ikarikai, Shiriuchi, Hokkaido, Japan (41.5357°N, 140.4297°E)	26 Jun 2021	LC740195	—	—	A. Tsuyuki and Y. Oya	Mature
ICHUM 8428	Sagittal sections, 2 slides	Noto, Ishikawa, Japan (137.2069°N, E)	19 Nov 2019	LC740196	—	—	N. Jimi, N. Hookabe, and S. Fujimoto	Immature
ICHUM 8429	Sagittal sections, 2 slides	Oshoro, Hokkaido, Japan (43.2100°N, 140.8578°E)	19 Oct 2020	LC740197	—	—	A. Tsuyuki	Immature
ICHUM 8430	Unsectioned, 70% EtOH	Oshoro, Hokkaido, Japan (43.2100°N, 140.8578°E)	19 Oct 2020	LC740198	—	—	A. Tsuyuki	Immature
ICHUM 8431	Unsectioned, 70% EtOH	Misaki, Kanagawa, Japan (35.1604°N, 139.6107°E)	17 Nov 2020	LC740199	—	—	N. Hookabe	Immature
ICHUM 8432	Unsectioned, 70% EtOH	Misaki, Kanagawa, Japan (35.1604°N, 139.6107°E)	17 Nov 2020	LC740200	—	—	N. Hookabe	Immature
ICHUM 8433	Sagittal sections, 2 slides	Misaki, Kanagawa, Japan (35.1604°N, 139.6107°E)	17 Nov 2020	LC740201	—	—	N. Hookabe	Immature
ICHUM 8434	Unsectioned, 70% EtOH	Misaki, Kanagawa, Japan (35.1604°N, 139.6107°E)	17 Nov 2020	LC740202	—	—	N. Hookabe	Immature

ICHUM 8435	Unsectioned, 70% EtOH	Okinoshima, Tateyama, Chiba, Japan (34.9909°N, 139.8232°E)	12 Jan 2021	LC740203	—	—	S. Fujimoto and M. Kiyomoto	Immature
ICHUM 8436	Unsectioned, 70% EtOH	Okinoshima, Tateyama, Chiba, Japan (34.9909°N, 139.8232°E)	12 Jan 2021	LC740204	—	—	S. Fujimoto and M. Kiyomoto	Immature
ICHUM 8437	Unsectioned, 70% EtOH	Enoshima, Kanagawa, Japan (35.2974°N, 139.4802°E)	15 May 2022	LC740205	—	—	A. Tsuyuki and Y. Oya	Mature
ICHUM 8438	Unsectioned, 70% EtOH	Enoshima, Kanagawa, Japan (35.2974°N, 139.4802°E)	15 May 2022	LC740206	—	—	A. Tsuyuki and Y. Oya	Mature
ICHUM 8439	99.5% EtOH	Shionomisaki, Kushimoto, Wakayama, Japan (33.4451°N, 135.7564°E)	16 May 2022	LC740207	—	LC740210	N. Jimi and N. Hookabe	?

Table 17. Interspecific uncorrected *p*-distances (%) for 28S fragments (934 bp) between the selected four *Theama* species (Chapter II-7).

	Theama sp. Japan	*Theama mediterranea*	*Theama* sp. 1
Theama sp. Japan	—	—	—
Theama mediterranea	3.43	—	—
Theama sp. 1 (MH700411)	2.57	3.96	—
Theama sp. 2 (KC869845)	7.28	6.42	7.17

Table 18. Intraspecific uncorrected *p*-distances (%) within 20 specimens of *Theama* sp. in terms of 613-bp partial sequences of the mitochondrial COI (Chapter II-7).

	1	2	3	4	5	6	7	8	9	10	11	12	13	14	15	16	17	18	19
1. ICHUM 8419																			
2. ICHUM 8420	0.65																		
3. ICHUM 8421	0.16	0.82																	
4. ICHUM 8422	0.16	0.49	0.33																
5. ICHUM 8423	0.49	0.49	0.65	0.33															
6. ICHUM 8424	0.49	0.82	0.65	0.33	0.65														
7. ICHUM 8426	0.65	0.98	0.82	0.49	0.82	0.82													
8. ICHUM 8427	0.49	0.82	0.65	0.33	0.65	0.65	0.82												
9. ICHUM 8428	0.33	0.98	0.49	0.49	0.82	0.49	0.98	0.82											
10. ICHUM 8429	0.82	1.14	0.98	0.65	0.98	0.98	1.14	0.98	1.14										
11. ICHUM 8430	0.33	0.65	0.49	0.16	0.49	0.49	0.65	0.49	0.65	0.82									
12. ICHUM 8431	0.33	0.65	0.49	0.16	0.49	0.33	0.65	0.49	0.65	0.82	0.33								
13. ICHUM 8432	0.82	1.14	0.98	0.65	0.98	0.65	1.14	0.98	1.14	1.31	0.82	0.65							
14. ICHUM 8433	0.98	1.31	1.14	0.82	1.14	0.82	1.31	1.14	1.31	1.47	0.98	0.82	0.16						
15. ICHUM 8434	0.33	0.65	0.49	0.16	0.49	0.49	0.65	0.49	0.65	0.82	0.33	0.33	0.82	0.98					
16. ICHUM 8435	0.33	0.65	0.49	0.16	0.49	0.49	0.65	0.49	0.65	0.82	0.33	0.33	0.82	0.98	0.33				
17. ICHUM 8436	0.33	0.33	0.49	0.16	0.49	0.49	0.65	0.49	0.65	0.82	0.33	0.33	0.82	0.98	0.33	0.33			
18. ICHUM 8437	0.33	0.65	0.49	0.16	0.49	0.49	0.65	0.49	0.65	0.82	0.33	0.33	0.82	0.98	0.33	0.33	0.33		
19. ICHUM 8438	0.49	0.82	0.65	0.33	0.65	0.65	0.82	0.65	0.82	0.98	0.49	0.49	0.65	0.82	0.49	0.49	0.49	0.49	
20. ICHUM 8439	0.16	0.49	0.33	0.00	0.33	0.33	0.49	0.33	0.49	0.65	0.16	0.16	0.65	0.82	0.16	0.16	0.16	0.16	0.33

Table 19. Comparison of the selected characteristics among the five species of *Theama* (Chapter II-7).

	T. evelinae	*T. forrestensis*	*T. mediterranea*	*T. occidua*	*Theama* sp.
Body size	5–7 mm long	up to 5 mm long; 0.3 mm wide	15–16 mm long; about 2.5 mm wide	6–7 mm long	3.62–10.2 mm long; 0.47–1.11 mm wide
Cerebral eyespots	4 on right; 5 on left	2 per side	2 per side	2 per side	2 per side
Marginal eyespots	6–10 per side	12	2–4 per side	5–6 per side	2–3 per side
Ciliary length	?	shorter dorsally than ventrally	about 10 µm, slightly longer dorsally than ventrally	shorter dorsally than ventrally	slightly longer dorsally than ventrally
Pharynx	very short length (0.4 mm); mouth open near the posterior end of pharynx	140 µm long; mouth opening centrally	length unknown; mouth open at a position slightly anterior to center	length and position of mouth unknown	about 1.0 mm; mouth opening in center of the pharynx
Genital pore	separate	common	separate	separate	separate
Seminal vesicle	ellipse; 100 µm long and 80 µm wide	86 µm long and 30 µm wide	oval; 130 µm long; 50 µm wide (ranging 80–185 µm; 50–80 µm, respectively); 45° tilted from horizontal plane	elongated	oval; 148 µm long and 80 µm wide; running parallel to whole body's horizontal plane
Prostatic vesicle	rounded	oval	oval	rounded	oval

Penis papilla	markedly pointed; with overall sclerotized inner lining	straight and short; without sclerotized inner lining	straight; with tip sclerotized cylindrical sheath	straight; without sclerotized inner lining; projected out of penis sheath	bent up; with tip sclerotized cylindrical sheath
Penis sheath	tube-shaped; with inner, angular fold; pieced by eosinophilous glands at edges	tube-shaped; distally, bordered with small papillae discharging fine granulated mucus	tube-shaped; without inner, angular fold; pieced by a few eosinophilous glands	rounded; without inner, angular fold; with fine-grained glands	tube-shaped; with inner angular fold on dorsal side; secretion glands not well developed
Prostatic glands	cyanophyll secretion produced by glands located in parenchyma; eosinophilous secretion accumulated in distal part	extravesicular glandular cells concentrated proximally around intervesicular ejaculatory duct	fine granular secretion in the proximal 2/3; much coarser eosinophilous secretion in the distal third	extracapsular secretion glands entering prostatic vesicle via muscular wall	fine granular secretion in the proximal part; much coarser eosinophilous secretion in the disto-ventral part
Distribution	Southern Brazil	Australia	Mediterranean; Red Sea	the Galapagos Islands	Japan
Reference	Marcus (1949); Curini-Galletti et al. (2008)	Bulnes and Faubel (2003)	Curini-Galletti et al. (2008); Gammoudi et al. (2009)	Sopott-Ehlers and Schmidt (1975)	this study

Appendices

Appendix 1. Partial 28S rDNA (1,010 bp) determined in this study from the specimen of *Prosthiostomum ohshimai* (Kato, 1938a) (ICHUM 6033).

ACAAGGATTCCACTAGTAACGGCGAGCGAAGGTGGAAAAGCCCAACACCGAATCCTTCACCGTACTGGTGACAGGAAATGTG
GTGTTTAGGCCGTACCTTGTGCTGACACGTCTCTCCTCAAGTCCACTTGATTGTGGCCTCAGGCCCAGAGAGGGTGTAAGGCCC
GTGGAGGCGAGATGTTCAGTTCCCGGTGCGTCCTTAGAGTCGGGTTGTTTGGGAATGCAGCCCTAAGCGGGTGGTAAACTCCA
TCCAAGGCTAAATACTAGCACGAGTCCGATAGCGAAGAAGTACCGTGAGGGAAAGTTGAAAAGAACTTTGAAGAGAGAGTTC
AAGAGTACGTGAAACCGCTGAGAGGCAAACTGGTGGAGCTGAAATGGCTTAGAGGAATTCAGCCGTTGGTTTCGTCATAATCA
GTGTTGTATCTGATCTCACGACAGTGCATCCGGTTAACGGCGTTGCCATAGGTGCACTTTCCTCTTTAGCCCAACCACGACCGG
TATACACTTGATTGTCCATCTTATCTGGAAGGTAGCGCCGGCTTCGGTCAGCGTATTATAGACAGATTTATGGAGCGATTGGTG
TACTGGAACATAATGCCTGCCTTCATGGCTCATACGTTGGCTGTTTTGTGAATGTATTCTGGTTTCACTACTTCGGTAGGGGAGT
CGGAGTCATTTGCTTTACGGTTGGCCTCTGTGATTGGCATTGATACAGTCTGTGGTTGTGAAGTAGGTAGTCCACCTGACCCGT
CTTGAAACACGGACCAAGGAGTCTAACATGTGCGCGAGTCATTGGGTTCTACGAAACCTAGAGGCGCAGTGAAGGTAAAGATT
CACATTGGTGAATTGAGGTGGGATATTGGGTTACGTGCTCAATCGCACCACCGGCCCGTTCCATTTGTATCTCAAAGGAGCGGA
GCAAGAGCGTACACGTTGGGACCCGAAAGATGGTGAACTATGCTTGCGCAGGATGAAGCCAGAGGAAACTCTGGTGGAAGTC
CGTAGCGATT

Appendix 2. Partial 28S rDNA (1011 bp) determined in this study from the specimen of *Prosthiostomum sonorum* Kato, 1938a (ICHUM 6034).

ACAAGGATTCCACTAGTAACGGCGAGCGAAGGTGGAAAAGCCCAACACCGAATCCTTCACCGTATTGGTGACAGGAAATGTG
GTGTTTAGGCCGTACCTTGTGCTGATACGTCTCTCCTCAAGTCCACTTGATTGTGGCCTCAGGCCCAGAGAGGGTGTAAGGCCC
GTGGAGGCGAGATGTTCAGTTCCCGGTGCGTCCTTAGAGTCGGGTTGTTTGGGAATGCAGCCCTAAGCGGGTGGTAAACTCCA
TCCAAGGCTAAATACTAGCACGAGTCCGATAGCGAAGAAGTACCGTGAGGGAAAGTTGAAAAGAACTTTGAAGAGAGAGTTC
AAGAGTACGTGAAACCGCTGAGAGGCAAACTGGTGGAGCTGAAATGGCTTGGAGGAATTCAGCCGTTGGAATGCGTCATAAT
CAGTGTTGTATCTGATCTCACGACAGTGCAGCCGGTTAACGTCGTTTCCATAGGTGCACTTCCCTCTTTAGCCCAACCACGACC
GGTATTCACTTGATTGTCCATCTTATCTGGAAGGTAGCGCCGGCTTCGGTCAGCGTATTATAGACAGATTTATGGAGCGATTGG
TGTACTGGAACATAATGCCTGCCTTCATGGCTCATACGTTGGCTGTTTTGTGAATGTATTCTGATTTCACTACTTCGGTAGGGGA
GTTGGAGTCATTTGCTTTACAGTTGGCCTCTGTGATTGGCGTTGATACAGTCTGTGGTTGTGAAGTAGGTAGTCCACCTGACCC
GTCTTGAAACACGGACCAAGGAGTCTAACATGTGCGCGAGTCATTGGGTTCTACGAAACCTAGAGGCGCAGTGAAGGTAAAG
ATTCACATTGGTGAATTGAGGTGGGATATTGGGTTACGTGCTCAATCGCACCACCGGCCCGTTCCAGTTGTATTTCAAAGGAGC
GGAGCAAGAGCGTACACGTTGGGACCCGAAAGATGGTGAACTATGCTTGCGCAGGATGAAGCCAGAGGAAACTCTGGTGGAA
GTCCGTAGCGATT

Appendix 3. Partial COI (462 bp) determined in this study from the specimen of *Prosthiostomum torquatum* Tsuyuki et al., 2019 (ICHUM 6040).

TTA AAT GAA GTT CCG GCA GCT ATT TGA TCT TTG GGT TTT GTA TTT TTA TTT ACT ATA GGG GGT TTA ACT GGT GTG GTT TTA GCT AGT GCT AGT TTA GAT ATA TGT TTA CAT GAC ACC TAT TAT GTA GTG GCT CAT TTT CAT TAT GTT TTA TCT ATG GGG GCT GTT TTC AGT ATT TTT GCT GGT ATA GTA CAT TGG TGA CCT TTA TTT ACA GGA GTG GCA TTA AAT ACA AAA ATG GTA ATT GCA CAC TTT TGA ATT ATG TTT ACA GGG GTA AAA ATT ACA TTT TTT CCT CAA CAT TTT TTA GGT TTA GCC GGT ATG CCT CGT CGC TAT AGT GAT TTT CCA GAT GGA TTT GCT TAT TTA AAT AGT ATT TCC AGT TAC GGA TCA TTA ATG TCT GTT GTA GGA GTA GTT TTC TTT ATG TTA ACT ATA TGA GAA GCT TTG GTT AGT GAA CGC AAG GTT ATA TAT GTT